UNIVERSIDADE DE LISBOA
FACULDADE DE FARMÁCIA


**Ana Sofia Gregório Fernandes**

# MODULATION OF OXIDATIVE STRESS BY SUPEROXIDE DISMUTASE MIMETICS

**DOUTORAMENTO EM FARMÁCIA**

(Toxicologia)

**2010**

UNIVERSIDADE DE LISBOA
FACULDADE DE FARMÁCIA


**Ana Sofia Gregório Fernandes**

# MODULATION OF OXIDATIVE STRESS BY SUPEROXIDE DISMUTASE MIMETICS

**DOUTORAMENTO EM FARMÁCIA**

(Toxicologia)

**Supervisor:** Professor Doutor Nuno Oliveira

**Co-supervisor:** Professora Doutora Judite Costa

**2010**

## Preface

Toxicology, once said to be the science of poisons, is presently defined by The Society of Toxicology as "the study of the adverse effects of chemical, physical or biological agents on living organisms and the ecosystem, including the prevention and amelioration of such adverse effects". It is therefore an inherently multidisciplinary subject that encompasses many areas, such as chemistry, biology and pharmacology.

Free radical toxicology is a very relevant and emerging field in Toxicology. During the past three decades, a remarkable rise of new information implicating reactive species in the mechanisms of action of many toxicants and pathological phenomena has driven an increasing interest of this scientific area. This thesis, by aiming at developing and studying antioxidant compounds, gathers concepts of chemistry and biology towards the discovery of novel approaches to overcome toxicity of oxidative stress-related conditions. Carrying out my PhD thesis in such a multidisciplinary area of research was very motivating, absorbing and challenging since the very beginning. The results presented herein contribute to the understanding of superoxide dismutase mimetics, representing a further step towards a potential clinical use of these promising antioxidants.

**Acknowledgments**

I want to express my deepest gratitude to my supervisor Professor Nuno Oliveira. Thank you for your mentorship, commitment, tireless, availability and scientific rigor. Our numerous broad scientific discussions were invaluable. More than just a supervisor, you have been a present and caring friend. Thank you for your support and friendship. It has been a pleasure to work under your guidance and I am looking forward to continue this fruitful partnership in future years.

I also want to thank my co-supervisor Professor Judite Costa. Thank you for giving me the opportunity to work with this research group, by joining your project POCTI/49114/QUI/2002. I want to thank all your support during this fellowship, as well as during these four years of my PhD. Thank you so much for your friendship, help and guidance.

My deepest gratitude to Professor Matilde Castro, who invited me to join her scientific studies when I was still an undergraduate student. Thank you for believing in me. I fell deeply honored in working in your group and in being mentored by someone who I profoundly admire personally and professionally. Even in your hardest moments, you are always there, caring and encouraging. Thanks for your leadership, vision, support, and constant help. And, most of all, thank you for your friendship.

I want to thank the colleagues of the Chemical Biology and Toxicology group. A special word to Professor Fátima Cabral: thank you for your constant availability and precious help. I also want to thank Ana Francisca for her friendship and permanent help. It has been a pleasure to work next to you. I remember gladly our trips to scientific meetings, as well as the simple moments we have shared in the Lab. Also to Joana Miranda, who recently joined the group, thank you for contributing to the nice and friendly environment of the Lab.

I want to express my acknowledgments to all the colleagues from Centro de Investigação em Genética Molecular Humana. A special word to Professor José Rueff, coordinator of this institute. Thank you for receiving me in your Lab and for providing what I needed to carry out my work. Your vision and vast knowledge were precious contributions for this research. I want to highlight the very important help of Professor Jorge Gaspar. Thank you for your support, assistance, and for the many fruitful

scientific discussions. I also want to acknowledge Michel Kranendonk for helping me in the DNA strand break analysis.

I would like to thank to all the other researchers that somehow were involved in this work. To Rita Guedes and Daniel dos Santos from the Medicinal Chemistry group of iMed.UL, thank you for carrying out the theoretical calculations on the copper(II) complexes. My acknowledgment to Professor Ines Batinic-Haberle, from the Department of Radiation Oncology of Duke University Medical School. Thank you for giving me the opportunity to study your *ortho*-substituted manganese(III) porphyrins, and thanks for the very constructive scientific discussions that we had. I also want to thank Octávia Gil and Vanda Martins from Instituto Tecnológico Nuclear who are now involved in the studies of radioprotection with the manganese(III) porphyrins.

I want to express my gratitude to Professors Teresa Chaveca and Ana Rita Conde for their support and friendship. Thank you for giving me the opportunity to integrate your pedagogical activities at Faculdade de Farmácia. I also want to thank my colleagues from Universidade Lusófona and from Escola Superior de Saúde Ribeiro Sanches for their contribution to my pedagogical development.

Being surrounded by such a group of extraordinary people made my scientific work a pleasant activity. But beyond science, I have the privilege to have very special friends, always helpful and enthusiastic… I want to thank all of you, and specially Ana, Andrea, Mafalda, Mara and Cátia, for enriching my life with happiness and great moments.

To my dear family, especially to my parents, sister and grandma… thank you for your constant support, encouragement, and most of all thank you so much for you unconditional love. I owe you everything.

A very special thank to Pedro, for being always by my side, walking with me every step of this way. Thank you for your love, attention, understanding and constant encouragement. Thank you for making our home a very special, warm and happy place. I also want to thank my little Rodrigo who, right from his *in utero* life, had to share his mother's attention with this thesis. Thank you for the joy that you brought to my life.

Finally, I want to acknowledge Fundação para a Ciência e a Tecnologia that financially supported the work presented in this thesis, through the Project POCTI/49114/QUI/2002 and through my PhD fellowship (SFRH/BD/28773/2006).

**Abstract**

Superoxide anion, along with other reactive species, is involved in many toxicological processes, as well as in a number of pathophysiological phenomena. Superoxide dismutase mimetics (SODm), i.e., synthetic compounds that mimic the functional properties of superoxide dismutase converting $O_2^{\bullet-}$ to $H_2O_2$ and $O_2$, have thus emerged as prospective pharmaceutical candidates to overcome toxicity in oxidative stress-related conditions. Several metal-containing compounds were previously shown to possess SOD-like activity. This thesis is focused on two promising classes of macrocyclic complexes: manganese(III) porphyrins (MnPs) and macrocyclic copper(II) complexes.

The effects of MnTM-4-PyP, a *para*-substituted MnP, against the cell injury induced by three different oxidants were evaluated in V79 cells. This MnP protected against the cytotoxicity and increase in intracellular $O_2^{\bullet-}$ levels induced by the xanthine-xanthine oxidase system (XXO; an extracellular $O_2^{\bullet-}$ generator) and by *tert*-butylhydroperoxide (TBHP; an analogue of lipid hydroperoxides). However, MnTM-4-PyP did not show considerable protection against the anticancer drug doxorubicin (Dox) that, among other mechanisms of cytotoxicity, generates $O_2^{\bullet-}$ intracellularly. The effects of MnTM-4-PyP were not observed at the cell division level, as shown by the mitotic index analysis. The results of this well established SODm in XXO- and TBHP-treated cells permitted the validation of cell-based models of oxidative stress to be used in the evaluation of the macrocyclic copper(II) complexes developed within the scope of this thesis.

Two optimized *ortho*-substituted MnPs, MnTE-2-PyP and MnTnHex-2-PyP, were also studied in this thesis and their role against TBHP-induced cell injury was evaluated. The two MnPs, even at low concentrations, counteracted remarkably the effects of TBHP in cell viability and intracellular $O_2^{\bullet-}$ levels. While the exposure of V79 cells to TBHP resulted in a significant depletion of total and reduced glutathione and in an increase in GSSG, MnPs augmented markedly the total and reduced glutathione contents in TBHP-treated cells.

Two sets of macrocyclic copper(II) complexes, without (CuL1-CuL5) or with a pyridine ring in the macrocyclic backbone (CuL6-CuL9), were synthesized and

evaluated *in vitro* for their $O_2^{\bullet-}$ scavenging ability. The complexes were chemically characterized in order to correlate their biochemical activity with thermodynamic, structural and electrochemical features. The complexes CuL3, CuL4 and CuL8 were selected to be further evaluated in cell-based assays since they presented high thermodynamic stability and effective ability to scavenge $O_2^{\bullet-}$, and were devoid of significant cytotoxicity. These complexes did not show considerable antioxidant activities in the oxidative stress models previously validated (XXO and TBHP). CuL3, CuL4 and CuL8 were also studied as redox modulators of anticancer drugs. The three complexes were shown to undergo Fenton chemistry *in vitro*. However, CuL3 and CuL4 did not potentiate the cytotoxicity of Dox in breast carcinoma (MCF7) cells. Conversely, CuL8 was shown to improve the therapeutic window of Dox, and especially of oxaliplatin, by both protecting non-tumoral human mammary cells (MCF10A) and boosting the cytotoxic effects in breast carcinoma cells.

The results presented in this thesis contribute to the comprehension of SODm as promising pharmaceutical agents both for antioxidant and cancer therapies, reinforcing the high therapeutic potential of this type of compounds.

**Keywords:** superoxide dismutase mimetics, manganese(III) porphyrins, macrocyclic copper(II) complexes, oxidative damage, antioxidant protection, chemotherapy sensitizers.

**Resumo**

A produção de espécies reactivas, nomeadamente de $O_2^{\bullet-}$, está associada a diversos fenómenos toxicológicos e fisiopatológicos. Entre estes, destacam-se os processos de lesão tecidular e inflamação, os quais são factores etiológicos chave num grande número de patologias, incluindo isquémia-reperfusão, aterosclerose, cancro, lesão por radiação, doenças neurodegenerativas, doenças inflamatórias pulmonares, intestinais e cardiovasculares, entre outras. A remoção de $O_2^{\bullet-}$ pode ser assim uma via importante para modular um vasto número de fenómenos patológicos. As enzimas superóxido dismutases (SOD), que catalizam a reacção de dismutação do $O_2^{\bullet-}$ em $H_2O_2$ e $O_2$, são metaloproteínas com um papel fulcral na defesa contra o excesso de espécies reactivas. Estudos pré-clínicos e clínicos com SOD têm demonstrado protecção contra os efeitos nocivos de várias situações de stress oxidativo. No entanto, a utilização clínica da enzima nativa apresenta diversas limitações. Tendo em conta que a remoção de $O_2^{\bullet-}$ permite minorar fenómenos inflamatórios, e de modo a ultrapassar as limitações do uso da SOD nativa, têm sido desenvolvidos nos últimos anos compostos de baixo peso molecular com a capacidade de mimetizar as propriedades funcionais da SOD. Estes compostos designam-se usualmente por SOD miméticos (SODm). Várias classes de SODm têm sido desenvolvidas, tendo demonstrado efeitos benéficos notáveis em diferentes modelos de stress oxidativo, quer em cultura de células, quer em modelos animais. A maioria destes compostos contém um ião metálico no seu centro activo, habitualmente Mn(III), Mn(II), Cu(II) ou Fe(III), o qual é estabilizado por coordenação com um ligando. A utilização de ligandos macrocíclicos tem revelado vantagens em termos de estabilidade termodinâmica e actividade catalítica. Neste âmbito, a presente tese incide sobre duas classes de complexos macrocíclicos com actividade mimética da SOD: porfirinas de Mn(III) (MnPs) e complexos macrocíclicos de Cu(II).

A classe das MnPs contém os SODm mais potentes e estáveis desenvolvidos até ao momento. Apesar de serem amplamente estudados, os efeitos ao nível celular destes compostos ainda não são totalmente conhecidos. A porfirina *para*-substituída MnTM-4-PyP é um SODm de eficácia bem estabelecida, disponível comercialmente, que tem vindo a ser estudado em vários modelos de situações fisiopatológicas. Os papel deste SODm face à toxicidade induzida por três oxidantes, cujos mecanismos de toxicidade diferem nas espécies reactivas envolvidas e no local de formação destas, foi avaliado em

células V79, uma linha celular de fibroblastos de pulmão de hamster chinês. Os sistemas oxidantes estudados foram: xantina-xantina oxidase (XXO), um gerador extracellular de $O_2^{\bullet-}$; *tert*-butilhidroperóxido (TBHP), um análogo de cadeia curta dos hidroperóxidos lipídicos; e o fármaco citotóxico Doxorrubicina (Dox) que, entre outros mecanismos, gera $O_2^{\bullet-}$ intracelularmente. A porfirina MnTM-4-PyP demonstrou efeitos protectores muito significativos face à XXO e ao TBHP, quer em termos de viabilidade celular (avaliada através dos ensaios MTT e Violeta cristal), quer no que respeita aos níveis intracelulares de $O_2^{\bullet-}$ (avaliados por fluorimetria, com a sonda dihidroetídio - DHE). No entanto, a análise do índice mitótico demonstrou que o efeito protector da MnP não foi observado ao nível da divisão celular. Relativamente à Dox, não se verificaram efeitos protectores consideráveis na presença de MnTM-4-PyP. Através dos resultados obtidos para os sistemas TBHP e XXO, estabeleceram-se protocolos para avaliar os possíveis efeitos antioxidantes dos complexos macrocíclicos de cobre(II) desenvolvidos no âmbito desta tese.

Estudos de relação estrutura-actividade anteriormente realizados na Duke University deram origem aos compostos MnTE-2-PyP e MnTnHex-2-PyP, duas MnPs optimizadas substituídas na posição *orto*, que apresentam uma elevada actividade catalítica. O efeito destas MnPs em células V79 expostas a TBHP foi avaliado. Ambas as MnPs, mesmo em concentrações muito baixas, revelaram uma capacidade notável para reverter o decréscimo de viabilidade celular induzido por este oxidante. Em relação aos níveis intracelulares de $O_2^{\bullet-}$, o efeito protector das MnPs foi também muito significativo. Foram ainda estudados os efeitos destas MnPs ao nível do glutationo. Em células expostas a TBHP observou-se uma depleção acentuada de glutationo total (quantificado pelo ensaio DTNB) e reduzido (avaliada por fluorimetria, usando a sonda monoclorobimano). Observou-se ainda um aumento considerável da proporção de glutationo na forma oxidada (pelo método DTNB). Em culturas simultaneamente tratadas com TBHP e MnTE-2-PyP ou MnTnHex-2-PyP, registou-se um aumento muito significativo nos níveis de glutationo total, assim como da forma reduzida, restabelecendo-se o equilíbrio do estado redox das células.

A segunda parte da presente tese é dedicada ao desenvolvimento e estudo de complexos macrocíclicos de cobre(II) com actividade mimética da SOD. Apesar de terem sido já estudados muitos complexos de Cu(II) para este fim, a descoberta de

novos complexos com elevada estabilidade e actividade, juntamente com baixa toxicidade constitui ainda um desafio. Foram assim sintetizados dois tipos de complexos macrocíclicos de cobre(II), contendo ou não um grupo piridínico no anel macrocíclico. Para o primeiro grupo de complexos (CuL1-CuL5), os respectivos ligandos foram sintetizados pelo método de Richman e Atkins, seguido da remoção dos grupos protectores por cisão reductiva. No caso do segundo tipo de complexos (CuL6-CuL9), contendo um grupo piridínico no anel macrocíclico, recorreu-se a um processo de ciclização assistida por ião metálico para a obtenção dos ligandos. Os ligandos sintetizados foram caracterizados por ressonância magnética nuclear ($^{1}$H-RMN e $^{13}$C-RMN). A estabilidade termodinâmica dos respectivos complexos de cobre(II) foi avaliada por técnicas potenciométricas. Foram ainda realizados estudos estruturais (ressonância paramagnética electrónica e absorção na região do visível) e electroquímicos (por voltametria cíclica), com o objectivo de correlacionar as propriedades químicas dos complexos com a respectiva capacidade de degradar $O_2^{\bullet-}$. A avaliação desta actividade sequestradora de $O_2^{\bullet-}$ dos complexos foi realizada *in vitro*, por dois métodos diferentes: a redução do NBT e a oxidação do DHE. Com base nestes estudos seleccionaram-se os complexos com elevada estabilidade termodinâmica, actividade sequestradora de $O_2^{\bullet-}$ efectiva e baixa citotoxicidade, para serem estudados mais aprofundadamente em ensaios celulares. As capacidades antioxidantes dos complexos CuL4, CuL5 e CuL8, foram então avaliadas nos dois modelos de *stress* oxidativo previamente validados (XXO e TBHP). No entanto, não se observaram efeitos protectores consideráveis face a estes sistemas oxidantes.

Os compostos com actividade mimética da SOD têm-se também revelado promissores adjuvantes em quimio- e radioterapia, quer por poderem potenciar a acção antitumoral destes regimes, quer pela possibilidade de protegerem o tecido não tumoral dos seus efeitos adversos. Assim, foram realizados estudos no sentido de avaliar uma possível utilização dos complexos CuL3, CuL4 e CuL8 no contexto do cancro da mama. Muitos dos complexos de cobre(II), para além de dismutarem o $O_2^{\bullet-}$, podem reagir com o $H_2O_2$ formado produzindo $HO^{\bullet}$, o que poderá ter vantagens na supressão da proliferação de células tumorais. Os três complexos foram assim avaliados pelo ensaio de clivagem do DNA plasmídico, tendo demonstrado capacidade de gerar $HO^{\bullet}$. No entanto, os complexos CuL3 e CuL4 não potenciaram a citotoxicidade da Dox em células humanas de carcinoma da mama (MCF7). Por outro lado, o complexo CuL8

revelou a capacidade de modulação redox dos efeitos da Dox e, sobretudo da oxaliplatina, em células mamárias humanas. Este complexo exerceu um efeito citoprotector em células mamárias não tumorais (MCF10A) e potenciou o efeitos dos fármacos citotóxicos nas células tumorais MCF7. O complexo CuL8, ao melhorar a janela terapêutica dos fármacos antitumorais Dox e oxaliplatina, poderá ser útil como adjuvante em regimes quimioterápicos e deverá ser mais estudado neste sentido.

Em suma, o desenvolvimento de SODm é uma área em grande expansão, dadas as múltiplas oportunidades terapêuticas destes compostos. Os resultados descritos na presente tese contribuem para um conhecimento mais aprofundados dos efeitos dos SODm quer em terapêutica antioxidante, quer em terapêutica antitumoral, reforçando o elevado potencial farmacoterapêutico destes compostos.

**Palavras-chave:** miméticos da superóxido dismutase, porfirinas de manganês(III), complexos macrocíclicos de cobre(II), lesão oxidativa, protecção antioxidante, sensibilizadores em quimioterapia.

**List of publications and communications**

From the results presented in this thesis, the following full papers were published in international refereed journals:

1. Protective role of *ortho*-substituted Mn(III) *N*-alkylpyridylporphyrins against the oxidative injury induced by *tert*-butylhydroperoxide
   **A.S. Fernandes**, J. Gaspar, M.F. Cabral, J. Rueff, M. Castro, I. Batinic-Haberle, J. Costa, N.G. Oliveira
   Free Radical Research (2010) 44, 430-440.

2. Oxidative injury in V79 Chinese hamster cells: protective role of the superoxide dismutase mimetic MnTM-4-PyP
   **A.S. Fernandes**, J. Serejo, J. Gaspar, M.F. Cabral, A.F. Bettencourt, J. Rueff, M. Castro, J. Costa, N.G. Oliveira
   Cell Biology and Toxicology (2010) 26, 91–101.

3. Macrocyclic copper(II) complexes: superoxide scavenging activity, structural studies and cytotoxicity evaluation
   **A.S. Fernandes**, J. Gaspar, M.F. Cabral, C. Caneiras, R. Guedes, J. Rueff, M. Castro, J. Costa, N.G. Oliveira
   Journal of Inorganic Biochemistry (2007) 101, 849-858.

Also, the following full-length paper was submitted and is being revised:

Two macrocyclic pentaaza compounds containing pyridine evaluated as novel chelating agents in copper(II) and nickel(II) overload
**A.S. Fernandes**, M.F. Cabral, J. Costa, M. Castro, R. Delgado, M.G.B. Drew, V. Félix
Journal of Inorganic Biochemistry (2010), *under final revision*.

In addition, two full papers are being prepared for submission:

1. Pyridine-containing macrocyclic copper(II) complexes with superoxide scavenging activity: CuPy[15]ane$N_5$ as a novel chemotherapy sensitizer for breast cancer
   **A.S. Fernandes**, J. Costa, J. Gaspar, J. Rueff, M.F. Cabral, M. Castro, N.G. Oliveira, *to be submitted*.

2. Macrocyclic copper(II) complexes as superoxide scavengers: Insights from a DFT study
   J.M. Matxain, D.J.V.A. dos Santos, **A.S. Fernandes**, M.F. Cabral, J. Costa, M. Castro, N.G. Oliveira, R.C. Guedes, *to be submitted*.

This thesis also contains data and methods published in the following paper:

Cytotoxicity and chromosomal aberrations induced by acrylamide in V79 cells: Role of glutathione modulators
N.G. Oliveira, M. Pingarilho, C. Martins, **A.S. Fernandes**, S. Vaz, V. Martins, J. Rueff, J.F. Gaspar
Mutation Research (2009) 676, 87–92.

Within the scope of this thesis, the following oral communications were presented in scientific meetings:

1. Macrocyclic copper(II) complexes as superoxide scavengers: Insights from a DFT study
   J.M. Matxain, D.J.V.A. dos Santos, **A.S. Fernandes**, M.F. Cabral, J. Costa, M. Castro, N.G. Oliveira, R.C. Guedes
   9º Encontro Nacional de Química-Física, 2009, Portugal.

2. Modulação do stress oxidativo por compostos miméticos da superóxido dismutase
   **A.S. Fernandes**
   III Conferências de Biologia Molecular da Escola Superior de Saúde Egas Moniz, 2008, Portugal.

3. Development and evaluation of novel copper(II) complexes with superoxide scavenger activity
   **A.S. Fernandes**, M.F. Cabral, J. Serejo, A.F. Bettencourt, C. Caneiras, R. Guedes, D. dos Santos, J. Rueff, J. Gaspar, J. Costa, N.G. Oliveira, M. Castro
   First Internal Meeting of iMed.UL, 2008, Portugal.

The results obtained in this thesis were also presented in scientific meetings in the following poster communications:

1. The superoxide scavenger Cu(py[15]ane$N_5$) is a novel oxaliplatin sensitizer for breast cancer
   **A.S. Fernandes**, J. Costa, J. Gaspar, J. Rueff, M.F. Cabral, M. Castro, N.G. Oliveira
   Society for Free Radical Research - Europe Meeting 2010, Norway; awarded with an Early Career Investigator Prize.

2. Role of the superoxide dismutase mimetic MnTMPyP on the modulation of the oxidative injury induced by *tert*-butylhydroperoxide
   **A.S. Fernandes**, J. Serejo, J. Gaspar, M.F. Cabral, A.F. Bettencourt, J. Rueff, M. Castro, J. Costa, N.G. Oliveira
   SFRR-E Free Radical Summer School, 2008, Greece.

3. Evaluation of the protective effect of superoxide scavengers on the cytotoxicity induced by *tert*-butylhydroperoxide
   **A.S. Fernandes**, J. Serejo, J. Gaspar, M.F. Cabral, A.F. Bettencourt, J. Rueff, M. Castro, J. Costa, N.G. Oliveira
   AOAC Europe Section International Workshop / II Encontro Nacional de Bromatologia, Hidrologia e Toxicologia, 2008, Portugal.

4. Evaluation of the protective effect of MnTMPyP on the cytotoxicity induced by different oxidant agents
   **A.S. Fernandes**, J. Gaspar, M.F. Cabral, A.F. Bettencourt, C. Caneiras, J. Rueff, M. Castro, J. Costa, N.G. Oliveira
   14$^{th}$ Annual Meeting of the Society for Free Radical Biology & Medicine, 2007, USA.

5. Pyridine-containing macrocyclic copper(II) complexes: studies on their potential role as superoxide scavengers
   **A.S. Fernandes**, N.G. Oliveira, J. Gaspar, M.F. Cabral, C. Caneiras, J. Rueff, M. Castro, J. Costa
   Society for Free Radical Research - Europe Meeting 2007, Portugal.

6. Novel copper(II) macrocyclic complexes with superoxide scavenging activity
   **A.S. Fernandes**, M.F. Cabral, J. Rueff, C. Caneiras, J. Gaspar, M. Castro, J. Costa, N.G. Oliveira
   13$^{th}$ Annual Meeting of the Society for Free Radical Biology and Medicine, 2006, USA.

7. 15-membered macrocyclic compounds: thermodynamic stability studies for copper(II) and cytotoxicity evaluation in mammalian cells
   **A.S. Fernandes**, M.F. Cabral, C. Caneiras, N.G. Oliveira, M. Castro, J. Costa
   9th International Symposium on Metal Ions in Biology and Medicine, 2006, Portugal.

**Table of contents**

**List of Figures**

**List of Tables**

**Abbreviations**

| | |
|---|---|
| AP-1 | activator protein 1 |
| B3LYP | Becke 3-Parameter, Lee, Yang and Parr (hybrid functional) |
| CAT | catalase |
| CuDIPs | copper(II) 3',5'-diisopropylsalicylate |
| CuL1 | copper(II) complex of 1-oxa-4,7-diazacyclononane (Cu[9]ane$N_2O$) |
| CuL2 | copper(II) complex of 1-oxa-4,7-diazacyclononane-4,7-diacetic acid; Cu(*N*-ac$_2$[9]ane$N_2O$) |
| CuL3 | copper(II) complex of 1-oxa-4,7, 10, 13-tetraazacyclopentadecane; Cu([15]ane$N_4O$) |
| CuL4 | copper(II) complex of 1-oxa-4,7,10,13-tetraazacyclopentadecane-4,7,10,13-tetraacetic acid ; Cu(*N*-ac$_4$[15]ane$N_4O$) |
| CuL5 | copper(II) complex of 1,4-dioxa-7, 10, 13-triazacyclopentadecane; Cu([15]ane$N_3O_2$) |
| CuL6 | copper(II) complex of 7-methyl-3,7,11,17-tetraazabi-cyclo[11.3.l]heptadeca-1(17),13,15-triene; Cu(*N*-Mepy[14]ane$N_4$) |
| CuL7 | copper(II) complex of 3,7,11-tris(carboxymethyl)-3,7,11,17-tetraazabicyclo[11.3.l]heptadeca-1(17),13,15-triene; Cu(*N*-ac$_3$py[14]ane$N_4$) |
| CuL8 | copper(II) complex of 3,6,9,12,18-pentaaza-bicyclo[12.3.1]octadeca-1(18),14,16-triene; Cu(py[15]ane$N_5$) |
| CuL9 | copper(II) complex of 3,6,10,13,19-pentaaza-bicyclo[13.3.1]nonadeca-1(19),15,17-triene; Cu(py[16]ane$N_5$) |
| CuPs | copper(II) porphyrins |
| Cu(py[14]ane$N_4$) | copper(II) complex of 3,7,11,17-tetraazabicyclo[11.3.l]heptadeca-1(17),13,15-triene |
| Cu,Zn-SOD | copper, zinc-superoxide dismutase (SOD1) |
| CV | crystal violet |
| DHE | dihydroethidium |
| DMEM | Dulbecco's Modified Eagle's Medium |
| DMEM/F12 | DMEM/Nutrient Mixture F-12 Ham |
| DMF | dimethylformamide |

| | |
|---|---|
| DMSO | dimethylsulfoxide |
| Dox | doxorubicin |
| DTNB | 5,5'-dithiobis(2-nitrobenzoic acid) |
| $E_{1/2}$ | half wave potential |
| EC-SOD | extracellular superoxide dismutase (SOD3) |
| edta | ethylenediaminetetraacetic acid |
| EPR | electronic paramagnetic resonance |
| FePs | iron(III) porphyrins |
| FOLFOX | folinate, oxaliplatin, 5-fluorouracil regimen |
| γ-GCS | γ-glutamylcysteine synthetase |
| G-6-PDH | glucose-6-phosphate dehydrogenase |
| GPx | glutathione peroxidase |
| GR | glutathione reductase |
| GSH | reduced glutathione |
| GSHt | total glutathione content |
| GSSG | oxidised glutathione |
| GST | glutathione-S-transferase |
| 4-HNE | 4-hydroxynonenal |
| HIF-1α | hypoxia-inducible factor 1α |
| ICD | $NADP^+$-dependent isocitrate dehydrogenase |
| IL-1β | interleukin-1β |
| IL-6 | interleukin-6 |
| LPO | lipid peroxidation |
| mCB | monochlorobimane |
| MDA | malondialdehyde |
| MI | mitotic index |
| MnSOD | manganese-superoxide dismutase (SOD2) |
| MnPs | manganese (Mn) porphyrins |
| MnTDE-2-ImP | Mn(III) 5,10,15,20-tetrakis(*N*,*N'*-diethylimidazolium-2-yl)-porphyrin |
| MnTBAP | Mn(III) meso-tetrakis(4-carboxyphenyl)porphyrin |
| $MnTE\text{-}2\text{-}PyP^{5+}$ | Mn(III) 5,10,15,20-tetrakis(*N*-ethylpyridinium-2-yl)porphyrin |
| $MnTM\text{-}4\text{-}PyP^{5+}$ | Mn(III) 5,10,15,20-tetrakis(*N*-methylpyridinium-4-yl)porphyrin |

| | |
|---|---|
| MnTnHex-2-PyP$^{5+}$ | Mn(III) 5,10,15,20-tetrakis(*N*-n-hexylpyridinium-2-yl)porphyrin |
| MTT | thiazolyl blue tetrazolium bromide |
| NADH | nicotinamide adenine dinucleotide |
| NADPH | nicotinamide adenine dinucleotide phosphate |
| NBT | nitro blue tetrazolium |
| NF-kB | nuclear factor kB |
| NHE | normal hydrogen electrode |
| NMR | nuclear magnetic resonance |
| PARP | poly-ADP-ribose polymerase |
| PBS | phosphate buffered saline |
| PBN | α-phenyl-*tert*-butylnitrone |
| pCu | -log [$Cu^{2+}$] |
| PHGPx | phospholipid hydroperoxide glutathione peroxidase |
| PLED | dipyridoxyl ethylenediamine diacetate |
| RFU | relative fluorescence units |
| RNS | reactive nitrogen species |
| ROS | reactive oxygen species |
| RS | reactive species |
| salen | *N,N'*-bis-(salicylideneamino)ethane |
| SOD | superoxide dismutase |
| SODm | superoxide dismutase mimetics |
| TBHP | *tert*-butylhydroperoxide |
| TNB | 5-thio-2-nitrobenzoic acid |
| TNFα | tumor necrosis factor α |
| XO | xanthine oxidase |
| XXO | xanthine-xanthine oxidase system |

Charges are omitted throughout text for clarity

# Chapter 1

## GENERAL INTRODUCTION

### 1.1. Oxidative stress and reactive oxygen species

The term "oxidative stress" can be defined as an imbalance between oxidants and antioxidants in favor of the oxidants, potentially leading to damage [1]. Oxidants are formed as normal products of aerobic metabolism and their production is balanced by the antioxidant defenses [1]. Under pathophysiological conditions, due to an increased production of oxidants or to a failure of antioxidant defenses, oxidative damage may occur [2]. Oxidative damage seems to be implicated in several pathological processes including tissue injury, inflammatory disorders, cardiovascular diseases, pulmonary diseases, neurodegenerative diseases, and cancer [3, 4].

The collective term reactive species (RS) includes oxygen, nitrogen, chlorine, bromine and sulphur transient species with high chemical reactivity [4, 5]. These include free radicals, i.e., species containing one or more unpaired electrons, and non-radical derivatives [4]. Reactive oxygen species (ROS) encompass a variety of diverse chemical species including superoxide anion ($O_2^{\bullet-}$), hydroxyl radical ($HO^{\bullet}$), hydrogen peroxide ($H_2O_2$), singlet oxygen ($^1O_2$), alkoxyl radicals ($RO^{\bullet}$), and peroxyl radicals ($ROO^{\bullet}$) [4-6]. Some ROS, such as $O_2^{\bullet-}$ or $HO^{\bullet}$, are extremely unstable and reactive. In contrast, other ROS like $H_2O_2$ or $ROO^{\bullet}$ are relatively stable, with half-lives in the range of seconds. These species may diffuse away from their site of generation, transporting the radical or oxidant function to other target sites [1, 6]. Reactive nitrogen species (RNS), such as peroxynitrite ($ONOO^-$), are also relevant in numerous pathophysiological phenomena [7, 8]. Fig. 1.1 shows the generation pathways of ROS. Superoxide anion is formed in biological systems by the partial reduction of molecular oxygen. Reduction of $O_2^{\bullet-}$ with a second electron, as well as a two-electron reduction of $O_2$, generates $O_2^{2-}$, which leads to $H_2O_2$. The one-electron reduction of $H_2O_2$, that occurs in the presence of reduced transition metals like Cu(I) and Fe(II), originates $HO^{\bullet}$ [9, 10]. Other reactive species can be generated by the reaction of ROS with biological molecules (e.g. polyunsaturated lipids, thiols and nitric oxide (NO)) [3]. For example, the reaction between $O_2^{\bullet-}$ and NO originates $ONOO^-$, which is unstable at physiological pH and rapidly decomposes to form potent nitrating and oxidizing species [3, 4]. Other species that result from the reaction of RS with biomolecules are the radicals alkoxyl and peroxyl [11]. These can be generated by a variety of routes, including the reaction

of lipid peroxides with $HO_2^{\bullet}$, the breakdown of organic peroxides, and the reaction of RS with lipids or amino acid radicals [4, 11].

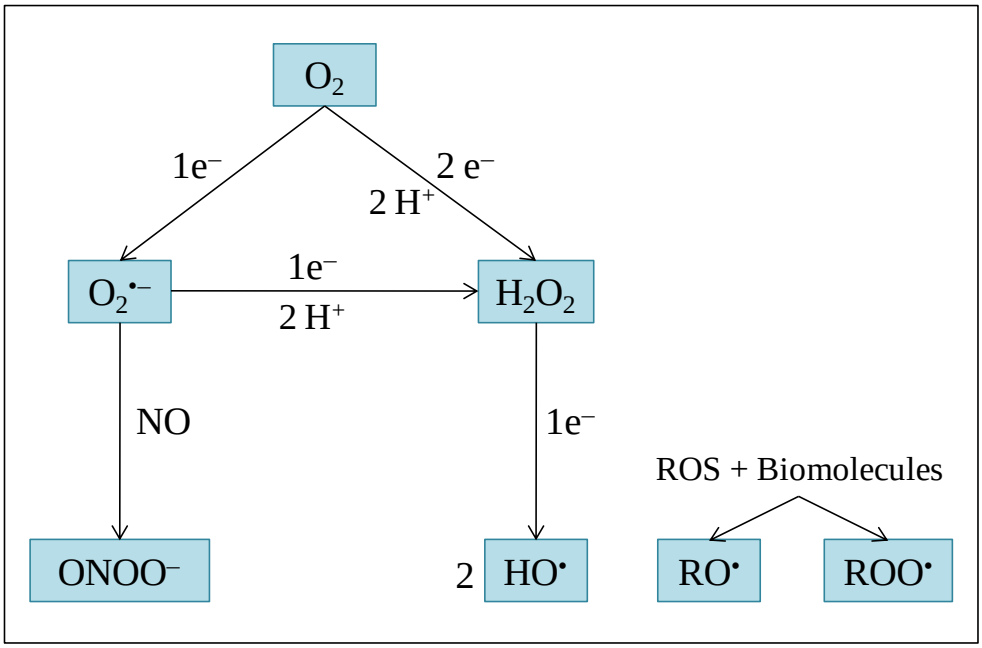


**Fig. 1.1** – Generation of the most relevant reactive oxygen species (adapted from [3]).

ROS can be generated as a result of normal intracellular metabolism. The majority of intracellular ROS production is derived from the mitochondria [6]. In fact, $O_2^{\bullet-}$ is formed from the uncoupling of the mitochondrial electron transport chain during oxidative phosphorylation [3, 10]. Also, the catalytic action of a variety of intracellular and extracellular oxidases like NADPH oxidase, xanthine oxidase or lipooxygenase, as well as the metabolism of arachidonic acid, gives rise to $O_2^{\bullet-}$ [4, 7]. Superoxide can also be produced by the phagocytic NADPH oxidase, during host defense responses, where $O_2^{\bullet-}$ is thought to act in cell-signaling and in the killing of foreign bacteria [3, 8, 10]. Other ROS are also generated in peroxisomes, as well as from a variety of cytosolic enzyme systems [6, 10]. Other process closely related with ROS formation is the lipid peroxidation (LPO), i.e., the oxidative deterioration of polynsaturated lipids (Fig. 1.2) [4]. LPO is initiated by addition of a RS (e.g. $HO^{\bullet}$, $HO_2^{\bullet}$, $RO^{\bullet}$, $ROO^{\bullet}$) to an unsaturated lipid or by hydrogen abstraction from a methylene group by a RS, forming a carbon radical. Carbon radicals often stabilize by molecular rearrangement generating conjugated dienes. Carbon radicals can also react with $O_2$, giving lipid peroxyl radicals

(LOO$^{\bullet}$). These radicals can abstract H$^{\bullet}$ from an adjacent lipid, propagating the process. The combination of LOO$^{\bullet}$ with H$^{\bullet}$ generates a lipid hydroperoxide (LOOH). The decomposition of LOOH in the presence of transition metal ions produces lipid alkoxyl radicals (LO$^{\bullet}$) that may also abstract H$^{\bullet}$ from unsaturated lipids, continuing the propagation of LPO. These phenomena may occur in biological membranes, leading to oxidative damage. In fact, the continued oxidation of fatty-acid side chains and their fragmentation to produce aldehydes and hydrocarbons may lead to loss of membrane integrity. In addition, products of lipid peroxidation (e.g. isoprostanes, malondialdehyde, 4-hydroxynonenal) may exert themselves deleterious effects [4], namely DNA damage and inhibition of proteins, leading to cytotoxicity, allergy, mutagenicity, and carcinogenicity phenomena [12].

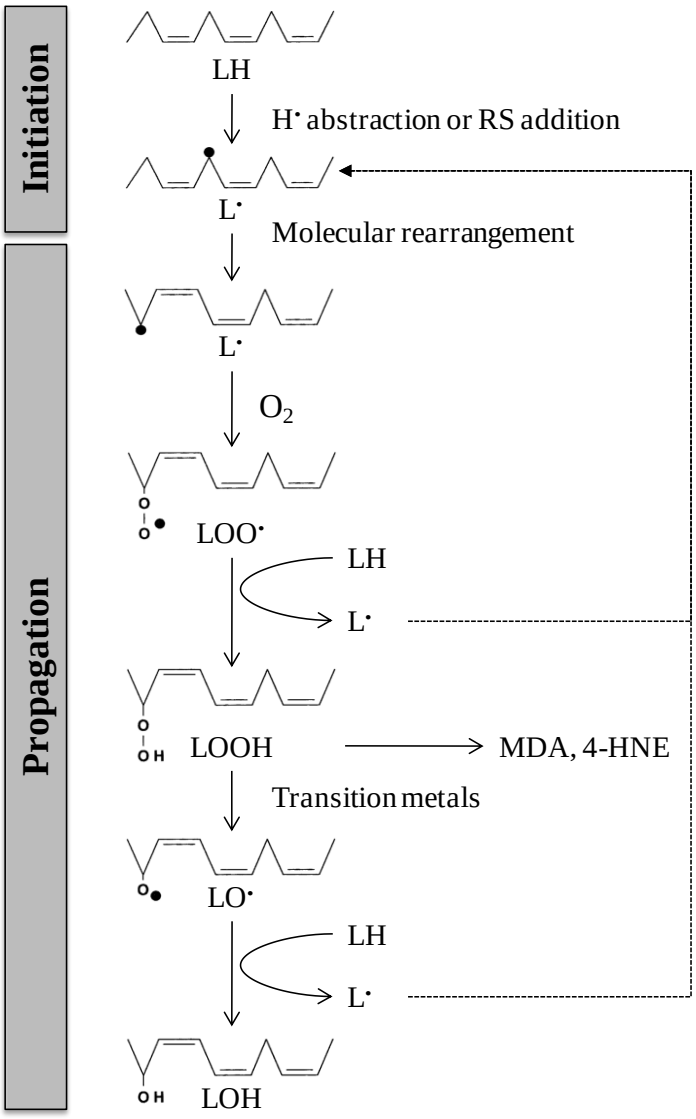


**Fig. 1.2** – Basic reaction sequence of lipid peroxidation (adapted from [4, 13, 14]). (LH, lipid; RS, reactive species; L$^{\bullet}$, carbon-centered radical; LOO$^{\bullet}$, lipid peroxyl radical; LOOH, lipid hydroperoxide; LO$^{\bullet}$, lipid alkoxyl radical; LOH, alcohol; MDA, malondialdehyde; 4-HNE, 4-hydroxynonenal).

Despite the endogeneous sources of ROS, a number of external agents can trigger ROS production [6]. Different types of radiation, like X-rays, ultraviolet, ultrasound, microwave, and ionizing radiation are known to generate ROS [1, 6]. Also, chemotherapeutic agents, hyperthermia, inflammatory cytokines and environmental toxins can shift cells into a state of oxidative stress [6].

Although high concentrations of ROS trigger oxidative damage, low concentrations of ROS are needed to regulate several key physiological processes [9, 10, 15]. These include cell differentiation, cell proliferation and apoptosis that are regulated by redox-sensitive signal transduction pathways [9, 10, 15].

### 1.1.1. Antioxidant defences

The production of ROS is counteracted by an intricate antioxidant defense system [6, 9]. An antioxidant has been defined as a substance that, when present at low concentrations compared with those of an oxidizable substrate, significantly delays or prevents oxidation of that substrate [2, 4, 11]. More recently, Halliwell and Gutteridge [4] altered this definition in order to account chaperones, repair systems and inhibitors of RS generation. An antioxidant is presently defined as any substance that delays, prevents or removes oxidative damage to a target molecule [4]. This concept includes non-enzymatic compounds, as well as antioxidant enzymes [1].

Non-enzymatic antioxidant defenses comprise a number of low molecular weight molecules with the ability to scavenge ROS [6, 10]. These include compounds synthesized *in vivo* (e.g. glutathione, bilirubin, pyruvate, melatonin, coenzyme Q, uric acid), as well as agents obtained from the diet (e.g. ascorbate, tocopherol, carotenoids, flavonoids) [4].

Eukaryotic cells possess an efficient antioxidant enzymatic network, as depicted in Fig. 1.3. The three major classes of antioxidant enzymes are the superoxide dismutases (SOD), catalases (CAT) and glutathione peroxidases (GPx) [1].

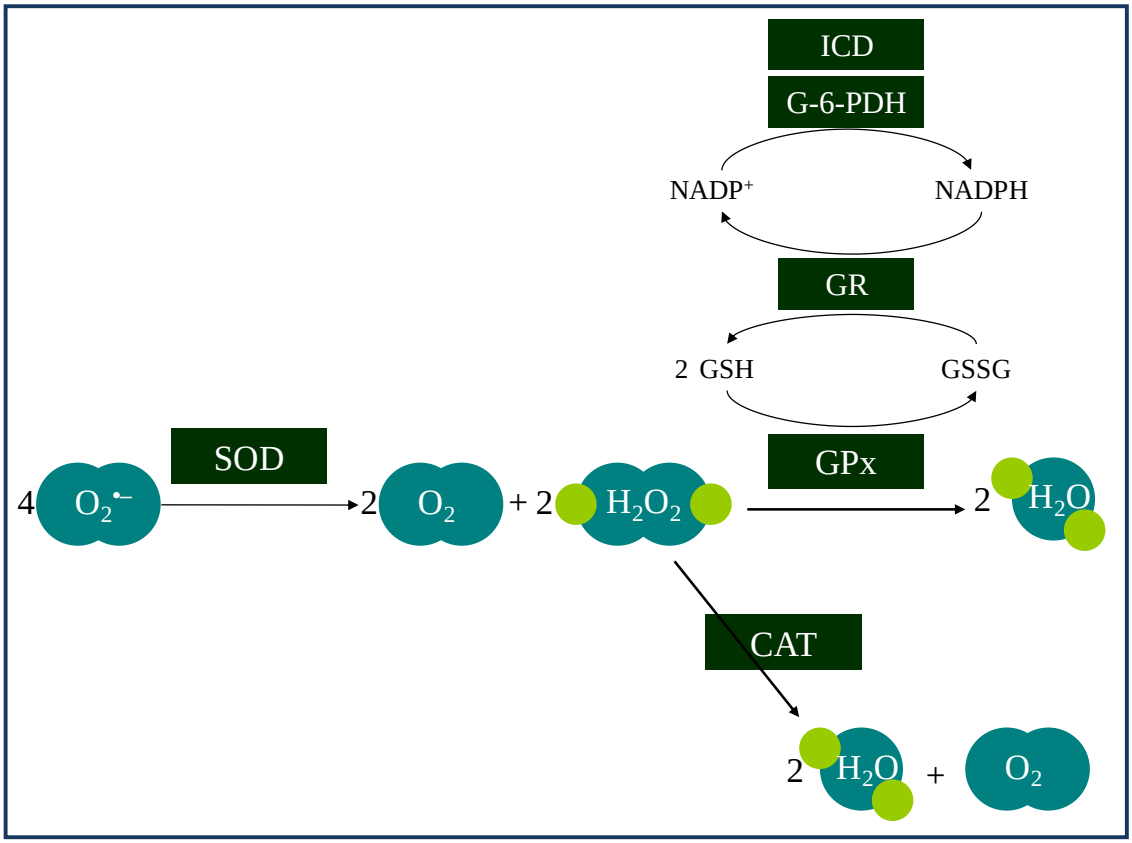


**Fig. 1.3** – Enzymatic antioxidant defenses: role of superoxide dismutases (SOD), catalases (CAT), glutathione peroxidases (GPx), glutathione reductase (GR), glucose-6-phosphate dehydrogenase (G-6-PDH), and $NADP^+$-dependent isocitrate dehydrogenase (ICD) on ROS detoxification (adapted from [9, 15]).

**Superoxide dismutase (SOD)**

Superoxide dismutases, which enzymatic activity was discovered in 1969 by McCord and Fridovich, are metalloproteins with oxido-reductase capacity that catalyze the dismutation of $O_2^{\bullet-}$ [16]. A dismutation reaction is defined as a reaction in which two like-molecules react to produce two different products (i.e. A + A → B + C) [3]. In the case of SOD, oxygen and $H_2O_2$ are formed from two $O_2^{\bullet-}$ [3], as shown in the following equations:

$$O_2^{\bullet-} + M^{(n+1)+} \rightarrow O_2 + M^{n+} \qquad \text{(Eq 1)}$$

$$\underline{O_2^{\bullet-} + M^{n+} + 2H^+ \rightarrow H_2O_2 + M^{(n+1)+}} \qquad \text{(Eq 2)}$$

Net reaction: $2O_2^{\bullet-} \rightarrow O_2 + H_2O_2$

The oxidized form of the metalloenzyme SOD ($M^{(n+1)+}$) reacts with one $O_2^{\bullet-}$ to form $O_2$ and generate the reduced form of the enzyme ($M^{n+}$) (Eq 1). In the second step of the dismutation reaction, the reduced enzyme reacts with another $O_2^{\bullet-}$ and two protons to form $H_2O_2$, regenerating the oxidized form of the enzyme (Eq 2).

Three different isoforms of SOD have been characterized in mammals. The SOD enzymes have a distinct genomic structure and are well compartmentalized [8]. Table I.1 summarizes the differences between the three SOD isoforms.

**Table I.1** – Types of SOD enzymes in mammals [4, 5, 8].

| | **SOD1** | **SOD2** | **SOD3 (EC-SOD)** |
|---|---|---|---|
| Active center | Cu(II)/(I) and Zn(II) | Mn(III)/(II) | Cu(II)/(I) and Zn(II) |
| Protein Structure | Homodimer | Homotetramer | Tetrameric glycoprotein |
| Genetic locus | 21q22.1 | 6q25.3 | 4p15.3-p15.1 |
| Location | Cytosol, nuclear compartments and mitochondrial inter-membrane space | Mitochondria matrix | Extracellular compartments (plasma, lymph, synovial fluid) |

The involvement of the three SOD isoforms in several pathological conditions has been unraveled by modulating the expression of the enzymes using knockout and transgenic models [8]. Down-regulation of SOD1 has been associated with neuronal death, reduced fertility and increased susceptibility to paraquat toxicity [5, 8]. On the other hand, the overexpression of this enzyme in transgenic mice was shown to protect the cerebral tissue in pathological conditions such as ischemia or Parkinson's disease [8]. Loss or reduction of the SOD2 activity has been associated with neurodegeneration, heart failure, and dilated cardiomyopathy [5, 8, 12]. The importance of SOD2 is also highlighted by the fact that, in contrast to SOD1 and SOD3, the SOD2 knock-out mice do not survive past 3 weeks of age [5, 12]. Furthermore, SOD2 gene has several polymorphisms which result in a reduction of the enzyme activity and were shown to be

associated with an increased risk of sporadic motor neuron disease, nonfamilial idiopathic cardiomyopathy, breast cancer and reduction of the tumour-suppressive effect of SOD2 [8, 17]. Studies with SOD3 knockout mice have shown that the loss of this enzyme activity is related to an impaired spatial learning and an increased sensitivity to hyperoxia exposure [8]

Further classes of SOD have been identified, namely nickel-containing SODs in *Streptomyces sp.* and some cyanobacteria, and iron-containing SODs in bacteria, algae, trypanosomes and higher plants [4, 5].

**Catalase (CAT)**

CAT enzymes are present in the peroxisomes of most aerobes and catalyze the direct decomposition of $H_2O_2$ to ground-state $O_2$ [4]. In animals, CAT is present in all organs and it is most concentrated in liver, kidney and erythrocytes [4, 18]. Human CAT is a tetrameric haemin-enzyme consisting of four identical subunits of 60 kDa, each containing Fe(III)-haem at its active site [4, 5, 18]. Its gene is located in chromosome 11, band p13 [18].

CAT enzymes catalyze the dismutation of $H_2O_2$. In fact, $H_2O_2$ oxidizes the heme iron of the resting enzyme to form an oxyferryl group with a π-cationic porphyrin radical, termed Compound I (Eq 3). This step is followed by oxidation of a second molecule of $H_2O_2$ by Compound I (Eq 4) [19]. The catalatic rate of mammalian CAT is among the highest of known enzymatic rates, and it is simply proportional to $H_2O_2$ concentration over a wide range of concentrations [19].

$$\text{CAT (Por-Fe}^{III}\text{)} + H_2O_2 \rightarrow \text{Compound I (Por}^{\bullet+}\text{-Fe}^{IV}\text{=O)} + H_2O \qquad \text{(Eq 3)}$$

$$\underline{\text{Compound I (Por}^{\bullet+}\text{-Fe}^{IV}\text{=O)} + H_2O_2 \rightarrow \text{CAT (Por-Fe}^{III}\text{)} + H_2O + O_2} \qquad \text{(Eq 4)}$$

Net reaction: $2\ H_2O_2 \rightarrow 2\ H_2O + O_2$

**Glutathione peroxidases (GPx)**

Peroxidases remove $H_2O_2$ by using it to oxidize another substrate [4]. GPx are selenium-containing peroxidases that degrade a variety of peroxides, namely $H_2O_2$ (Eq 5) and ROOH (Eq 6), by coupling their reduction with the oxidation of reduced glutathione (GSH) [4, 5].

$$2\ H_2O_2 + 2\ GSH \rightarrow GSSG + 2\ H_2O \qquad \text{(Eq 5)}$$

$$ROOH + 2\ GSH \rightarrow GSSG + H_2O + ROH \qquad \text{(Eq 6)}$$

GPx enzymes are widely distributed in animal tissues [4]. Four isoenzymes have been identified in humans, being the level of each isoform dependent of the tissue type [4, 5]. The classical GPx (GPx1) is cytosolic. GPx2 is an isoform present in the gastro-intestinal tract. In plasma and other extracellular fluids, a different isoenzyme (GPx3) is found. The fourth type is the phospholipid hydroperoxide glutathione peroxidase (PHGPx or GPx4), which has the ability to act upon peroxidized fatty acid residues within membranes and lipoproteins [4]. GPx4 is a monomer, while GPx1, GPx2 and GPx3 are tetramers. Each protein unit contains a selenium atom in the active site, in the form of selenocysteine. The catalytic activity of GPx is schematized in Fig. 1.4. During GPx catalysis, the selenol form of the enzyme is oxidized to selenenic acid by peroxides. This form reacts with reduced glutathione (GSH) to give $H_2O$ and a selenosulphide adduct. A second GSH molecule then regenerates the active form of the enzyme by attacking the selenosulphide to form oxidized glutathione (GSSG) [4, 20].

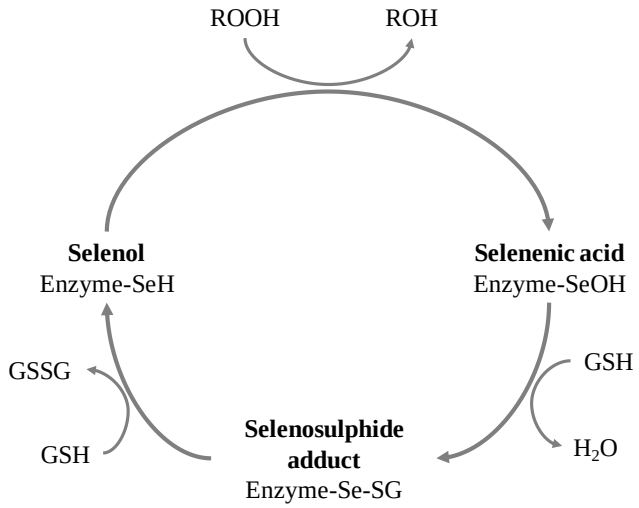


**Fig. 1.4** – Catalytic cycle of glutathione peroxidase (adapted from [20]).

The catalytic activity of GPx involves the oxidation of GSH in GSSG. However, in physiological conditions, the cellular ratio GSH/GSSG is high, because GSSG is reduced back to GSH by glutathione reductase (GR) [1, 4]. The catalytic activity of this enzyme requires NADPH, according to the following reaction (Eq 7):

$$GSSG + NADPH + H^+ \rightarrow 2\ GSH + NADP^+ \qquad \text{(Eq 7)}$$

Cellular NADPH can be provided by different sources, including Glucose-6-phosphate dehydrogenase (G-6-PDH) and $NADP^+$-dependent isocitrate dehydrogenase (ICD) (Fig. 1.3) [4].

In addition to being a cofactor for GPx enzymes, GSH plays other important antioxidant roles. This ubiquitous thiol-containing tripeptide can directly scavenge RS, such as $HO^\bullet$ and $^1O_2$ [10, 21]. Moreover, it is used by glutathione S-transferases (GSTs) to conjugate and eliminate reactive compounds, including products formed *in vivo* during oxidative stress [1, 4, 10, 21, 22]. Glutathione is also able to regenerate important antioxidants (e.g. Vitamins C and E) back to their active forms, being this capacity linked with the redox state of the glutathione disulphide-glutathione couple (GSSG/2GSH) [10]. This redox couple is a major contributor to the redox state of the cellular milieu. In a non-stressed cell, glutathione is present in the cytosol at a concentration between 1 and 10 mM, being ~99% in the form of GSH and ~1% as GSSG [4, 21].

### 1.1.2. Consequences of oxidative stress

A situation of oxidative stress, due to diminished antioxidant defenses or to an increase in the production of RS, may induce different cellular responses. These responses depend on the cell type and the severity of oxidative stress. As summarized in Fig. 1.5 mild oxidative stress may induce cell proliferation, while intense oxidation will result in cell injury and can even trigger cell death [4].

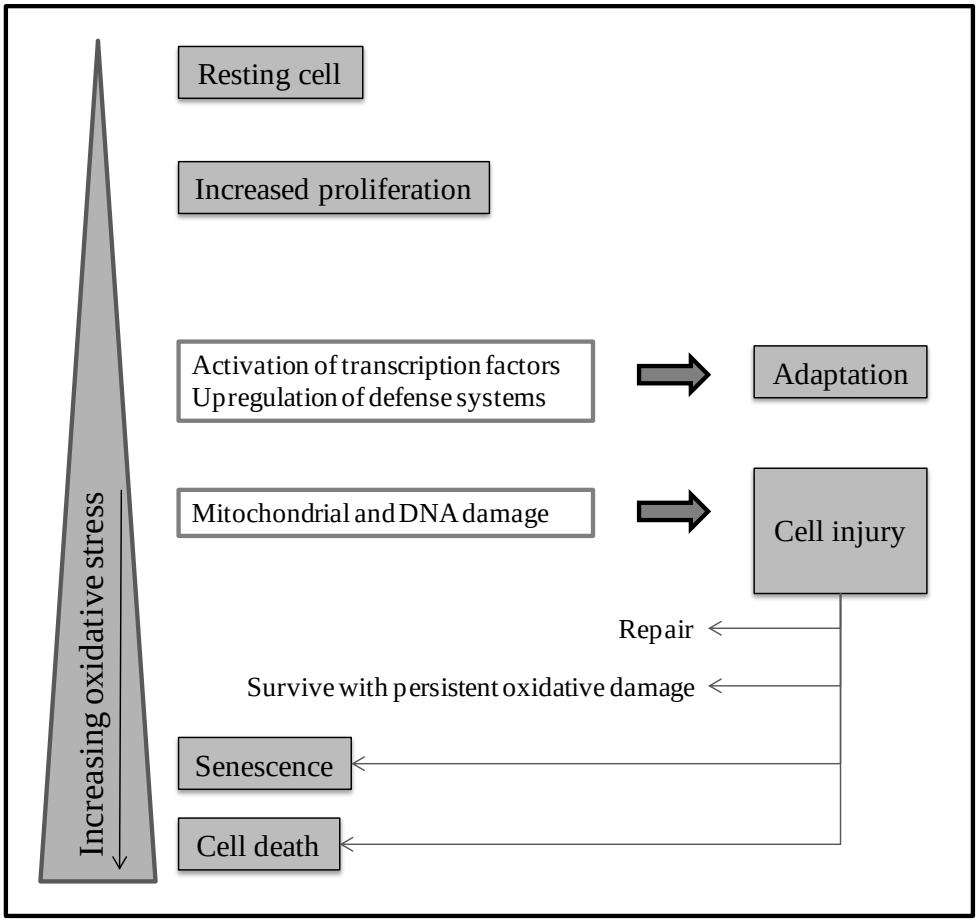


**Fig. 1.5** – Cellular responses to oxidative stress. Many cells respond to mild oxidative stress by proliferating. As oxidative stress increases, cells may up-regulate their defense systems as an adaptive response. Greater oxidative stress will lead to damage in biomolecules such as DNA, proteins, lipids, or carbohydrates, resulting in oxidative cell injury. Cells may recover from this damage by repairing it or displacing the damaged molecules, or they can survive with persistent lesions. In case of intense oxidative stress, cells may become senescent, i.e., they survive but are no longer able to divide. Under highly oxidizing conditions, mechanisms of cell death (apoptosis and necrosis) may be activated [4].

**Pro-inflammatory action of superoxide**

Under physiological circumstances, the levels of $O_2^{\bullet-}$ are kept under tight control by endogenous SOD [7]. However, in acute and chronic inflammation, the production of $O_2^{\bullet-}$ is increased at a rate that may overwhelm the capacity of the endogenous SOD to remove it. This imbalance results in superoxide-mediated damage [7, 8]. Some important pro-inflammatory roles for $O_2^{\bullet-}$ have been described [5, 7, 8] (Fig. 1.6), namely:

- endothelial cell damage and increased microvascular permeability;
- formation of chemotactic factors;
- recruitment of neutrophils at sites of inflammation;
- auto-catalytic destruction of neurotransmitters and hormones;
- lipid peroxidation and oxidation;
- DNA single-strand damage and activation of poly-ADP-ribose polymerase (PARP);
- formation of peroxynitrite, a potent cytotoxic RS that can nitrate and deactivate SOD and that causes the inactivation of nitric oxide;
- reduction of Fe(III) to Fe(II) with its consequent release from storage sites, so that it can react with $H_2O_2$ producing $HO^{\bullet}$ radicals.

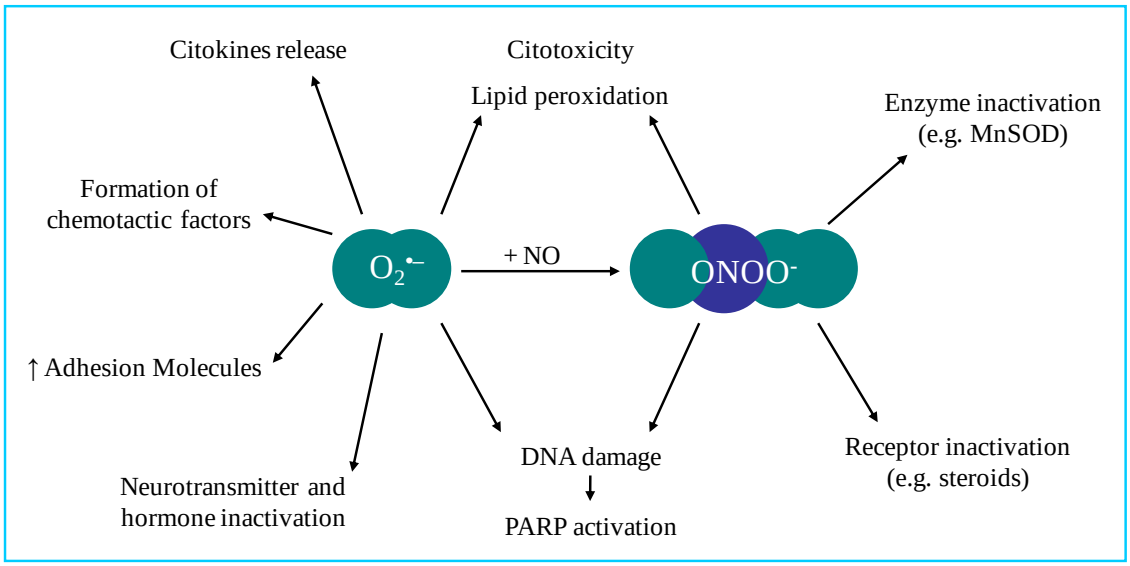


**Fig. 1.6** – Different roles of $O_2^{\bullet-}$ in inflammation. Excessive production of $O_2^{\bullet-}$ can lead to inflammation through various pathways, including the depletion of beneficial NO and the generation of deleterious $ONOO^-$ (adapted from [7, 8]).

These phenomena lead to tissue injury and inflammation that are involved in many diseases. Table I.2 presents some pathological conditions in which the involvement of superoxide anion has been suggested.

**Table I.2** – Clinical conditions in which the involvement of superoxide anion has been suggested [7, 8, 23].

| Category | Examples |
|---|---|
| Inflammatory conditions | Pain, Crohn's disease, osteoarthritis, dermatitis, psoriasis |
| Cardiovascular diseases | Ischemia-reperfusion injury, shock, atherosclerosis, stroke |
| Neurodegenerative diseases | Parkinson's, Alzheimer, amiotrophic lateral sclerosis |
| Pulmonary diseases | Asthma, hyperoxic lung damage, chronic obstructive pulmonary disease |
| Oncology | Side effects of chemotherapy and radiotherapy |
| Reproductive system | Erectile dysfunction, infertility |

Additionally to the phenomena described above, $O_2^{\bullet-}$ also seems to be involved in the processes of cell transformation, metastasis and angiogenesis [16].

The exposure to a number of xenobiotics may also result in the release and/or generation of $O_2^{\bullet-}$, being their toxic effects related with oxidative stress. This $O_2^{\bullet-}$ generation from xenobiotics can occur directly or upon metabolization, redox reactions, redox cycling processes, via lipid peroxidation or by stimulation of endogenous production of $O_2^{\bullet-}$. Examples of xenobiotics whose effects seem to be somehow related with $O_2^{\bullet-}$ are the pesticides paraquat and pentachlorophenol, and the transition metal vanadium, pointing out a role for $O_2^{\bullet-}$ in occupational toxicology. There are also several drugs (e.g. gentamicin, anthracyclines and rifamycin) whose action and toxic effects are, at least partially, related to $O_2^{\bullet-}$ generation [4, 24].

The removal of $O_2^{\bullet-}$ provides thus a unique strategy to manipulate numerous pathological processes, being a very promising approach to the treatment of a variety of diseases and intoxications in which $O_2^{\bullet-}$ plays a deleterious role.

## 1.2. Superoxide dismutase mimetics

Some therapeutic approaches have emerged based on the fact that the removal of $O_2^{\bullet-}$ modulates the course of numerous pathological processes. Efforts have been made towards a clinical use of SOD. A different strategy, that has shown very promising results, relies on the development of synthetic compounds with the capacity to mimic the native enzyme - SOD mimetics (SODm).

Protective and beneficial roles of SOD have been demonstrated in a broad range of diseases, both in preclinical and in clinical studies [8, 16]. Preclinical studies have revealed a protective role of SOD in animal models of a variety of pathological conditions, including: ischemia-reperfusion injury, transplant-induced reperfusion injury, inflammation, cancer, AIDS and pulmonary disorders [7]. Moreover, the overexpression of SOD in animal models has provided protection against the deleterious effects of a wide range of oxidative stress paradigms, such as stroke or Parkinson's disease [3, 7].

In terms of clinical data, a Cu,Zn-SOD prepared from bovine tissues – Orgotein, used to be applied as a human therapy in inflammatory conditions, namely in rheumatoid arthritis, osteoarthritis, and against the side effects associated with chemotherapy and radiotherapy [7]. Despite the encouraging anti-inflammatory properties demonstrated, Orgotein was responsible for immunological problems and was withdrawn from the market [7]. Besides this problem of antigenicity, the use of native SOD as a therapeutic agent presents high-manufacturing costs and limitations related with the large size of these proteins that limit their cell permeability and circulating half-life [3]. Moreover, SOD presents a bell-shaped dose-response curve, making difficult the precise restoration of optimal balance between $O_2^{\bullet-}$ and SOD [16]. Various attempts at modifying the SOD enzymes have been performed in order to improve their properties. These include the delivery of SOD by liposomes, the development of SOD conjugates, and the genetic engineering of the human proteins [4, 5, 16].

SOD mimetics constitute a different and promising strategy to remove of $O_2^{\bullet-}$, overcoming the limitations of the clinical use of native SOD. A SODm can be defined as a small synthetic molecule that achieve the destruction of $O_2^{\bullet-}$ at a rate of tens of

millions of times per second per molecule, mechanistically similar to endogenous SOD [7]. Taking into account that the ultimate goal is pharmaceutical use, these small molecules could have a number of advantages over the native enzyme. They are more likely to access inter- and intracellular spaces, are devoid of immunogenicity, exhibit longer half-lives, might be capable of oral administration, and they are easier to produce in large amounts and with lower costs than the enzymes [25, 26].

The very first studies on SODm begun in the late 1970s and early 1980s. Since then, a growing number of low molecular-weight catalytic antioxidants with the capacity to mimic SOD has been developed [3, 7, 27-30]. Nowadays, this is still an emergent field as can be confirmed by the increasing number of publications on this subject, and also by the expanding list of possible therapeutic applications of these compounds. In fact, SODm have shown very promising results in *in vitro* and *in vivo* models of a variety of pathological phenomena (e.g. inflammation, neurodegenerative diseases, cardiovascular diseases, pulmonary diseases and cancer), as well as in toxicological conditions (e.g. exposure to paraquat and to beryllium). This topic will be described in section 1.2.3.

### 1.2.1. Considerations for drug design

SODm should exhibit high rates of reaction with $O_2^{\bullet-}$ [3]. For a relevant SOD activity *in vivo*, the catalytic activity of SODm should be comparable or even superior to that of the native enzyme [7]. Most of the catalytic antioxidants are designed with redox-active metal centers that catalyze the dismutation reaction by a mechanism similar to that of the active-site metals of SOD [3, 4]. Only a few metals, namely Cu, Mn, Fe, and perhaps Ni, have the ability to form complexes with this activity [25]. To therapeutically use this property, these metals must be enclosed in a stable ligand. The number and type of donor atoms of the ligand, as well as the proper shape of the complex formed, must be taken into account in the rational design of novel SODm, in order to achieve antioxidants with fast catalytic rates [7]. Also the ligand charges can have a major effect in terms of catalytic rate, since the appropriate placement of positive charges may provide electrostatic guidance for the approach of $O_2^{\bullet-}$ to the active site of the SODm [28, 31]. The design of SODm with high catalytic rates leads to compounds

that are efficacious at very low concentrations, allowing therapeutic regimens with low inherent side effect probability [25].

In order to react as a true catalyst, rather than as a stoichiometric superoxide scavenger, it is required that a SODm presents a reversible redox behaviour. The SODm has to undergo a reduction in the presence of $O_2^{\bullet-}$ and its reduced form should be reoxidized by $O_2^{\bullet-}$ [32]. This capacity to allow both half-reactions of the catalytic cycle (Eq 8 and 9) depends on the half wave potential ($E_{1/2}$) of the metal site [28], being possible when this value is between -0.3 and +0.9 V [33].

$$O_2^{\bullet-} \rightarrow O_2 + e^- \qquad E_{1/2} = -320 \text{ mV} \qquad \text{(Eq 8)}$$

$$O_2^{\bullet-} + e^- + 2H^+ \rightarrow H_2O_2 \qquad E_{1/2} = +900 \text{ mV} \qquad \text{(Eq 9)}$$

All the natural SOD enzymes, regardless of the type of metal, exhibit redox potentials close to +300 mV *vs* NHE, which is the halfway between the redox potentials of the two half reactions of the catalytic cycle [26, 28]. Thus, a metal-centered redox potential of ~300 mV provides equal thermodynamically facilitation for both processes, driving energy to both half reactions and avoiding one or the other from becoming rate-limiting [26]. The determination of the redox potential of a SODm is therefore a very important parameter to be evaluated when developing novel catalytic antioxidants. Fig. 1.7 illustrates this point and shows the location in terms of $E_{1/2}$ of some of the SODm developed so far.

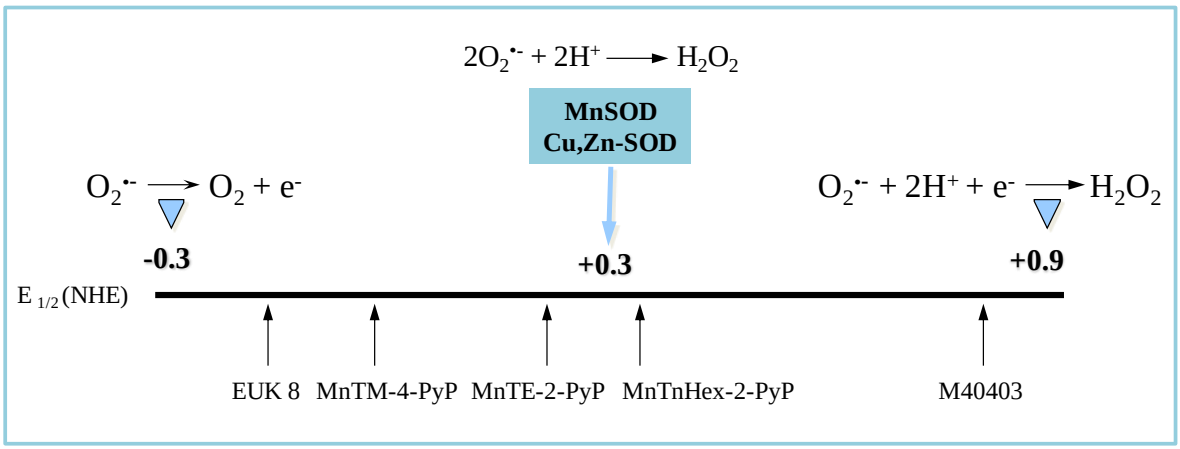


**Fig. 1.7** - Redox diagram for $O_2^{\bullet-}$ oxidation and reduction and the placement of some SODm on it (adapted from [33]).

Since many SODm are metal complexes, it is crucial that they present high stability to be used as pharmaceuticals [25]. The metal must be bound tightly to the ligand, to avoid ligand exchange and loss of activity [26]. Moreover, the release of a potentially harmful metal ion from the complex in an inappropriate biological compartment must be avoided [25]. When addressing a pharmaceutical application, several aspects of stability should be considered. Not only the inherent chemical, thermodynamic and kinetic stabilities of a complex are important [7, 25], but also the characteristics of the biological milieus and the pharmacokinetics of the SODm should be considered [7, 25, 26].

One important aspect of the stability issue is the thermodynamic stability of a complex, which can be evaluated by the determination of its stability constant [25]. Complexes with high values of stability constants are required to avoid dissociation. Other important parameter is the kinetic stability or dissociation rate of the complex. Ideally, the kinetics of excretion after an *in vivo* administration should be faster than the kinetics of complex dissociation [25]. Macrocycles, i.e. polydentate ligands whose structure consists of a ring with a minimum of nine atoms and containing at least three donor atoms [34], usually provide enhanced kinetic stability as compared to non-cyclic ligands [7].

In terms of biological stability, it is crucial that the complex is stably formed at physiological pH values. This includes not only pH 7.4, but also more acidic conditions, depending on the application of the SODm. Since metal complexes are susceptible to proton-assisted dissociation, this can constitute a problem in the acid pH of the stomach, in case of an oral administration. Also, if the target of a complex is an ischemic tissue, the complex must be stable at the lowered pH value (~5) of oxygen-deprived tissues [25]. The development of a stable SODm should also consider the biological redox environment. Most complexes are susceptible to oxidative ligand degradation. This may be a problem if a complex gets to the liver, due to the strong oxidizing environment of this organ [25]. Additionally, many complexes dissociate via reduction of the metal. In the reducing environment of most cells, the reduction of the metal center can lead to the decomposition of the complex [25]. Furthermore, when studying the stability of a complex it is also important to take into account the presence of endogenous chelators

(e.g. albumin, glutathione) in the biological milieus that can compete for the metal [7, 26].

Another significant aspect of drug design is the optimization of the bioavailability. Bioavailability greatly affects the *in vivo* efficacy and safety of a SODm and is dependent upon its size, charge, shape (conformational flexibility and overall geometry), and lipophilicity [28, 35]. When designing a novel SODm, chemical modifications on its structure to modify lipophilicity should be performed according to the target organ and final goal of the compound. For example, highly lipophilic drugs, with the ability to cross the blood/brain barrier, would be desired to treat neurodegenerative diseases [25, 35]. On the other hand, an SODm to be used in reperfusion injury following a myocardial infarct should be more hydrophilic, so that it can stay longer in circulation (water phase) [25]. The lipophilicity of a SODm may be assessed using thin-layer chromatography or by the determination of the partition coefficient between *n*-octanol and water [28].

The size and charge of a SODm can be exploited to target crucial cellular compartments [3]. Since mitochondria are the major source of $O_2^{\bullet -}$, many efforts have been made to obtain mitochondrially targeted catalytic antioxidants [28]. One successful approach to obtain mitochondria-targeted compounds is the attachment of the lipophilic cation triphenylphosphonium to antioxidants [36]. Because of its positive charge, this strategy also allows an accumulation of several-hundredfold within mitochondria driven by the membrane potential, enhancing the protection of mitochondria from oxidative damage. This approach has been applied to obtain mitochondria-targeted versions of SODm, namely with M40403 and tempol [36]. Other strategies that have been used to target antioxidants to mitochondria include the attachment of a cationic N-arylpyridyl group or of specific oligopeptides [28, 37].

Other characteristics should also be addressed in the development of novel SODm. The non-peptidic nature of these small molecules is important to avoid immunogenic reactions and degradation by proteases [7]. It is also important that a SODm compound could not be deactivated by peroxynitrite [7]. Finally, the purity of a SODm should be established very carefully, since even small-trace impurities might modify the SOD-like activity, affecting the therapeutic and/or mechanistic evaluations of the compound [28].

### 1.2.2. Classes of SODm

Most of the catalytic antioxidants contain a redox-active metal on their active center. The metal-containing SODm more extensively studied are manganese(III) metalloporphyrins (a), manganese(III) salen complexes (b) and manganese(II) cyclic polyamines (c) [3, 28]. Also, copper(II) (d) and iron(III) (e) complexes have been developed. A different class of SODm is constituted by nitroxides (f), a group of compounds that do not have a metal center in their structure. Many other compounds, with different chemical structures, have also been reported to possess SOD-like activity (g). These classes of SODm are briefly described below.

#### a) Manganese(III) porphyrins

This class of SODm is constituted by manganese(III) complexes in which the metal ion in enclosed in a porphyrin ligand. Porphyrins are naturally occurring macrocyclic compounds, which structure consists of a 16-atoms ring containing four nitrogen atoms, obtained by linking four tetrapyrrolic subunits with four methine bridges. The cavity of these macrocycle can properly accommodate a number of metal ions, forming metalloporphyrins [38]. Nature has developed natural metalloporphyrins as major prosthetic groups embedded in a variety of biomolecules (e.g. hemoglobin, myoglobin, nitric oxide synthase, cytochrome oxidase, cyt P450 systems, cycloxygenase) [28]. Synthetic metalloporphyrins appeared as a natural choice for developing SODm because these agents: (i) have chemical accessibility, (ii) are not antigenic, (iii) have a porphyrin core structure that can be chemically modified; (iv) are extremely stable; and (v) possess low molecular weight and can penetrate the cellular and subcellular membranes [28]. Metalloporphyrins were therefore the first compounds considered as SODm. Two scientists deeply influenced the design of metalloporphyrins as SODm, Irwin Fridovich, known for its outstanding work in free radical biology and medicine, and Peter Hambright, a pioneer in the water-soluble porphyrins' field [28]. The most stable and effective SODm developed so far are manganese-containing synthetic *meso*-substituted porphyrins [28].

Manganese porphyrins (MnPs) have the ability to scavenge a wide range of ROS, namely $O_2^{\bullet -}$, $ONOO^-$ and peroxyl radicals [39]. The SOD-like activity of the MnPs involves the alternate reduction and oxidation of the Mn center, which results in changes in valence between Mn(III) and Mn(II), much like native SODs [27]. The ability of MnPs to scavenge $ONOO^-$ is related to the formation of an oxo–Mn(IV) complex that is reduced to Mn(III) by endogenous antioxidants [40]. The mechanism of lipid peroxidation inhibition by MnPs is thought to be analogous to that mentioned for $ONOO^-$ scavenging [3, 39]. MnPs also have the ability to degrade $H_2O_2$ due to their extensive conjugated ring system that undergoes reversible one-electron oxidations. However, this CAT-like activity is negligible, being less than 1% of that of native enzymes [3]. The mitigation of oxidative stress injury by MnPs seems to involve not only the direct scavenging of ROS/RNS, but also the modulation of redox-active transcription factors, such as HIF-1α, NF-kB, and AP-1 [41-45].

Porphyrin ligands allow for a considerable range of redox potentials and lipophilicities, which are important features in the development of SODm for pharmaceutical purposes [25, 35]. Examples of some representative compounds of this class are depicted in Fig. 1.8.

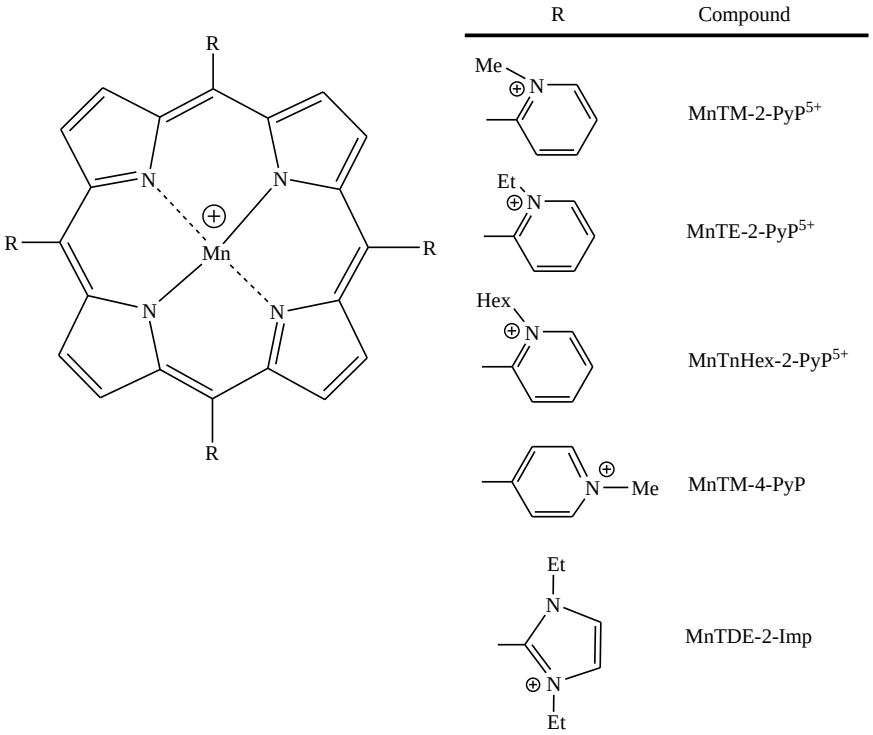


**Fig. 1.8** – Chemical structures of some representative MnPs.

This class of SODm is currently being developed by Aeolus Pharmaceuticals, which is a subsidiary of Incara Pharmaceuticals. The MnP AEOL 10150 (MnTDE-2-ImP) (Fig. 1.8) is currently undergoing clinical trials. Two phase I clinical trials to evaluate the safety, tolerability and pharmacokinetics of this compound administered by subcutaneous injection to patients with amyotrophic lateral sclerosis were successfully completed and no serious adverse effects were reported. A new clinical trial with AEOL 10150 is being prepared to evaluate its safety and efficacy in radiation protection [46].

**b) Manganese(III) salen complexes**

Other relevant Mn-containing SODm are the Mn(III)-salens complexes (salen = *N,N'*-bis-(salicylideneamino)ethane) [47, 48]. Fig. 1.9 shows four relevant SODm of this class.

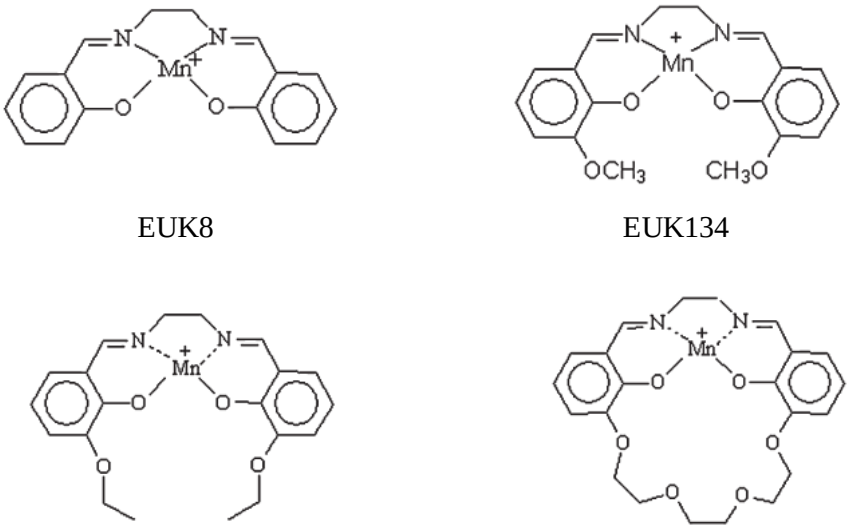


**Fig. 1.9** – Chemical structures of four representative salen-manganese complexes.

These compounds were previously developed by the Eukarion, Inc. company, being usually named as EUKs [3, 25]. Two compounds of the Eukarion portfolio achieved later stages of development: a topical formulation of EUK189 was studied in phase I clinical trials for radiotherapy-induced dermatitis, and EUK134 is currently used as an active cosmetic ingredient. Eukarion was then merged with Proteome Systems

Ltd. This company recently announced that it will cease the research in therapeutics and will focus its strengths on diagnostic products and changed its name to Tyrian Diagnostics [49].

The Mn moiety of these complexes is coordinated by four axial ligands that can be either N or O atoms [3, 4, 47]. The tetracoordination of Mn allows several possible valence states, which are thought to be important in the scavenging of a wide variety of ROS and, thus, contribute to the non-selective nature of these antioxidants [3]. In fact, Mn(III)-salens have been reported to have two key antioxidant properties – the scavenging of $O_2^{\bullet-}$and $H_2O_2$ [3, 25]. Moreover, their capacity to react with $ONOO^-$ and lipid peroxides has also been suggested [3, 4].

Mechanistic details on the SOD-like of these complexes activity have not been reported [3, 25, 48]. However, the Mn(III)-salens undergo quasi-reversible reductions in cyclic voltammetry experiments, what establishes that reduction of Mn(III) to Mn(II) is a thermodynamically viable step in the SOD activity of these complexes [25, 48].

Mn(III)-salens have been reported to have lower catalytic activity when compared to other classes of SODm. It is therefore possible that the protective effects observed in biological studies (Tables I.3 and I.4) are due to a combination of antioxidant reactions, rather than a true catalytic SOD activity [25]. This class of SODm presents other drawbacks, namely very low water solubility and limited stability [25, 48, 50].

### c) Mn(II) cyclic polyamines

A third class of SODm includes the Mn(II)-pentaazamacrocyclic complexes [48]. In these compounds, the Mn(II) is held by five coordination points and is only available for one-electron transfers [3, 4]. Thus, these complexes can transfer one electron to and from $O_2^{\bullet-}$ catalyzing its dismutation, but they are not reactive towards $H_2O_2$ or $ONOO^-$ [4]. Such specificity is desirable for mechanistic studies, but it would be disadvantageous for therapeutic purposes [28]. However, although these complexes are specific for $O_2^{\bullet-}$ in test tube reactions, this selectivity may not occur in more complex biological systems [3, 4]. During the dismutation of $O_2^{\bullet-}$, the Mn(II) at the

active center of the macrocyclic complex undergoes alternate oxidation and reduction, which results in an interchanging valence state between Mn(II) and Mn(III) [3, 28].

These compounds present reasonable thermodynamic stability, but excellent kinetic stability [25]. The chemical stability of Mn(II)pentaazacyclopentadecane complexes can be improved by increasing the number of substituents on the carbons of the inner ring of the macrocycle, while substituents on the nitrogens destroy activity [25]. Structure-activity studies revealed that a trans-cyclohexane substitution improves stability (thermodynamic and kinetic) and activity [25], and allowed the development of optimised compounds. M40403 and M40401 (Fig. 1.10) are pentaazacyclopentadecane analogues containing bis(cyclohexylpyridine) functionalities, that are very kinetically and oxidatively stable [7].

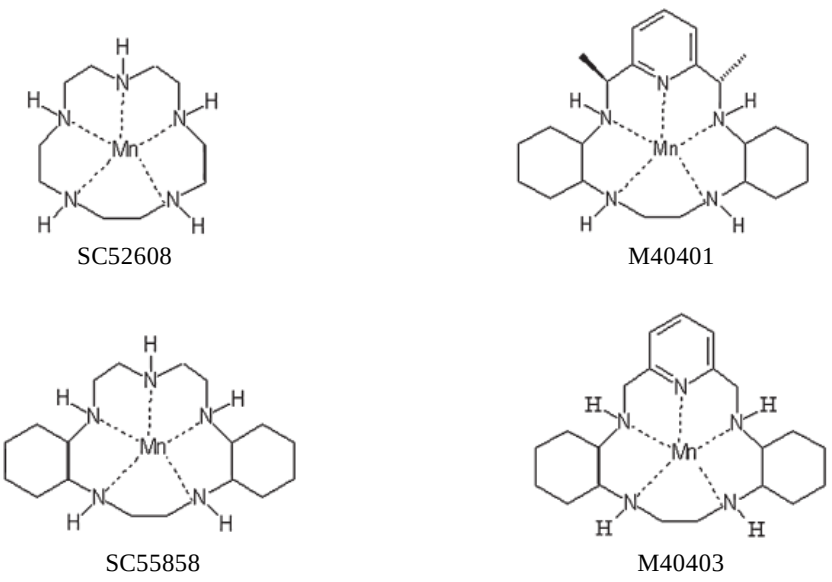


**Fig. 1.10** – Chemical structure of four representative Mn(II) cyclic polyamines.

Mn(II) cyclic polyamines have been developed at MetaPhore Pharmaceuticals and then at ActivBiotics. The most studied SODm of this class is M40403 (Fig. 1.10), which was introduced into human clinical testing in 2001. This complex has successfully completed a Phase I safety clinical trial in healthy human subjects [48]. Also, different phase II clinical trials have demonstrated the efficacy and safety of M40403, co-administered with opiods, in post-operative pain (following dental surgery

or bunionectomy) and in cancer pain. Two phase II clinical trials are now in preparation, to evaluate the effects of this SODm in oral mucositis and post-operative ileus. By removing $O_2^{\bullet -}$, M40403 was proposed to exert protective actions at three different pathways: the inhibition of $ONOO^-$ formation, sparing NO; the inhibition of neutrophil infiltration at the site of inflammation; and the inhibition of pro-inflammatory cytokine release (e.g. TNFα, IL-1β and IL-6) [48].

### d) Copper(II) complexes

Many copper(II)-based SODm have been proposed, either as binuclear or mononuclear complexes, with different classes of ligands, including derivatives of imidazoles, amines, pyridines, anti-inflammatory drugs (salicylates, indomethacin), amino acids, sulfonamides, peptides, imines, cyclodextrin, curcumin, triazines, quinoline and others [4, 51, 52]. Copper(II) complexes have been studied in different models of oxidative stress-related pathologies, as will be shown in section 1.2.3. Among these complexes, copper(II) 3',5'-diisopropylsalicylate (CuDIPs) is widely studied and is used as a cosmetic ingredient to protect skin from UV light-induced damage, boosting the Sun Protection Factor in sunscreens.

Although many Cu(II) complexes are efficient SODm *in vitro*, they tend to lose their activity *in vivo*, especially in the case of acyclic complexes. Many of the Cu(II) chelates described in the literature probably dissociate to release copper ions *in vivo* [4]. This can raise toxicity concerns due to the possible production of $HO^{\bullet}$ radical via Fenton chemistry [28]. Moreover, since many proteins and other biological chelators have high affinity for Cu(II) (e.g. albumin, copper chaperones, glutathione and metallothioneins) [53], the SODm complex can be inactivated in the biological milieu [51]. High stability constants are thus required to avoid the dissociation of the complex *in vivo*. This could be achieved by using macrocyclic ligands [25, 54]. The macrocyclic nature of the ligand seems important for the SOD mimetic activity of the corresponding complexes as well as for their stability in the presence of proteins, even if the metal ion does not lie inside the cavity [54]. Several macrocyclic copper complexes have been reported to scavenge superoxide anion [54-59]. Based on the structure of Cu,Zn-SOD active site, imidazolate-bridged binuclear Cu(II) complexes have been prepared and characterized

as SODm. Also in this type of complexes, the use of macrocyclic ligands has shown advantages, namely in terms of stability in a larger pH range [51].

Some studies on Cu(II) porphyrins (CuPs) as potential SODm have also been reported. Although some CuPs do not possess catalytic SOD activity (e.g. CuTM-4-PyP), other derivatives, namely $CuBr_8$TM-4-PyP, have significant SOD-like activity along with a very high stability. The occurrence of Fenton chemistry on Cu(II) site within porphyrins has not been explored [28].

In the development of Cu(II) complexes with SOD-like activity, it is necessary to find a balance between a sufficient stability for the complex to survive in *in vivo* conditions, and a certain flexibility that allows the change of metal coordination during the catalytic process [51]. Although many copper(II) complexes have been studied, most of them are not thermodynamically stable or highly active at the range of physiological pH [60]. For this reason, the identification of novel complexes with high stability and activity, together with low toxicity, is still a challenging issue in bioinorganic chemistry.

**e) Iron(III) complexes**

Iron(III) complexes would be attractive SODm since they exhibit high kinetic and thermodynamic stability. However, iron ions are prone to react with $H_2O_2$ via Fenton reaction, generating the highly toxic $HO^{\bullet}$ radical [25]. This reaction can occur both with iron complexes and with free aquo iron ions that can be released from the complex during redox cycle [25, 28]. Since $H_2O_2$ is one of the products of the $O_2^{\bullet-}$ dismutation, the possible occurrence of Fenton reaction may limit the application of iron complexes as SODm [25, 28].

A number of iron(III) complexes with non-macrocyclic polydentate ligands (e.g. aminopolycarboxylates and tripodal ligands) have been reported to possess SOD activity. However, it is not clear whether these complexes have true catalytic activity. Moreover, some of these complexes were shown to damage DNA due to $HO^{\bullet}$ generation [25]. Iron(III) complexes with pentaazacyclopentadecane derivatives have also been studied. However, their catalytic activities are considerable lower than those

of the Mn(II) analogues. Furthermore, their ability to produce $HO^{\bullet}$ radical makes these complexes considerably toxic [25]. Also some Fe(III) porphyrins (FePs) (e.g. FeTBAP and FeTMPyP) were shown to dismutate $O_2^{\bullet-}$ [4, 25, 28]. Along with the SOD-like activity, FePs can also react with $ONOO^-$ [4, 28]. Although some reports on the protective effects of FePs have been published, these compounds promote the Fenton reaction being their therapeutic potential, at least as catalytic antioxidants, limited by their inherent toxicity [25, 28, 61].

### f) Nitroxides

A number of compounds initially developed as free radical spin traps have been shown to have antioxidant properties, namely the capacity of reacting with $O_2^{\bullet-}$ [4, 62]. If a spin trap intercepts a biologically damaging radical, then it may protect against oxidative injury [4]. Nitroxides react with free radicals and form more stable free radical products. However, the rate of reaction with $O_2^{\bullet-}$ of most nitroxides is low, and thus large amounts (often millimolar levels) of these compounds are required for an effective activity [62]. Furthermore, many nitroxides are inefficient SODm at physiological pH [28]. During the $O_2^{\bullet-}$ dismutation, nitroxides ($RNO^{\bullet}$) cycle between the oxidized oxoammonium cation ($RNO^+$), and the reduced form hydroxylamine (RNOH). The oxoammonium cations have also the ability to react rapidly with $ONOO^-$ [28]. In the absence of a reducing agent, $RNO^+$ can oxidize various biomolecules including DNA. Under reducing conditions, the antioxidant activity of hydroxylamine occurs presumably through hydrogen atom donation and may account for the *in vivo* protective effects of nitroxides [28]. Also, many nitroxides can be metabolized to release NO and can inhibit enzymes that are endogenous sources of ROS [62].

These compounds are well tolerated in animals and can achieve high tissue levels [62]. Some examples of SODm of this class are oxano, 3-nitratomethyl-PROXYL and Tempol (Fig. 1.11) [4]. Also, the nitrone α-phenyl-*tert*-butylnitrone (PBN, Fig. 1.11), which reacts with radicals to give a nitroxide, has shown good results in oxidative stress models. However, its exact mechanism of action remains unclear [4].

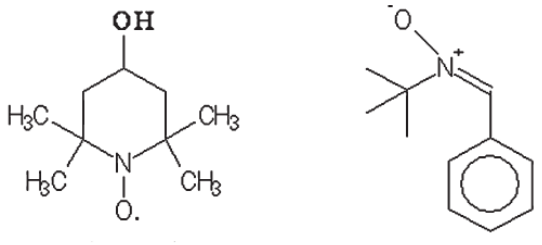


Tempol PBN

**Fig. 1.11** – Chemical structures of Tempol and PBN.

Tempol is the most studied compound of this class and has shown protective effects in a number of oxidative damage models (Table I.4). Moreover, Tempol is being studied in clinical trials to prevent radiation-induced alopecia. A phase I trial has demonstrated that the topical application of Tempol to the scalp before whole brain radiation is safe and well tolerated. A phase II study using a gel formulation of Tempol has been initiated [63].

### g) Other compounds with SOD-like activity

A new class of SODm has been developed by the company PledPharma AB and contains the manganese(II) complexes of dipyridoxyl ethylenediamine diacetate derivatives (PLED-derivatives). Among these compounds, mangafodipir (PP-095), which is already clinically approved as a magnetic resonance imaging contrast agent, has completed a phase II clinical trial in 2010. This study was conducted in patients operated for colon cancer and has shown that the pre-treatment with mangafodipir lowers the frequency and severity of adverse effects of FOLFOX (folinate, oxaliplatin, 5-fluorouracil) chemotherapy regimen. In addition, a phase II clinical study was started in 2009 using the PLED-derivative PP-099, to study whether this SODm reduces myocardial infarct size in patients undergoing primary percutaneous coronary intervention [64].

A number of porphyrin-related compounds, such as phthalocyanines, porphyrazines, biliverdins, corroles and texaphyrins, have also been explored as SOD mimics. Metal corroles (Mn, Fe and Ga) have been reported to exhibit high SOD-like

activity. In the case of Mn corroles, the Mn(IV)/Mn(III) redox couple is responsible for the $O_2^{\bullet-}$ dismutation. These complexes have also the ability to scavenge $ONOO^-$ and $H_2O_2$, which may account for the suppression of oxidative stress [28].

Cerium(IV) oxide ($CeO_2$) nanoparticles have also been investigated as SODm. The SOD activity of these nanoparticles was shown to depend on the size of the nanoparticles, as well as on the Ce (IV)/Ce(III) ratio in these materials [28]. Osmium tetraoxide ($OsO_4$), which is used in the treatment of arthritic joints, was also shown to exhibit a relevant SOD-like activity. The dismutation cycle is dependent on the Os(VIII)/Os(VII) redox couple [28].

SOD-like catalytic activity was also reported for some water-soluble fullerenes. In addition, some compounds of this class are able to directly react with hydroxyl, alkoxyl, alkylperoxyl and benzyl radicals. However the mechanism is not fully understood, the highly conjugated double bond system seems to be responsible for the antioxidant actions of these compounds [28]. Finally, some natural antioxidants of the polyphenol type were shown to possess SOD-like activity, namely honokiol, curcumin and apigenin [28].

### 1.2.3. Therapeutic opportunities of SODm

SODm have been shown to protect against oxidative damage in a wide range of cell and animal model systems. Tables I.3 and 1.4 summarize some of the studies reported in the literature.

**Table I.3** – Examples of protective effects reported using SODm in cell-based models.

| Model system | Cell type | SODm found to be protective |
|---|---|---|
| Hydrogen peroxide | Fibroblasts | MnTBAP [65] |
| | Endothelial | MnTM-4-PyP [66] |
| Oxygen and/or glucose deprivation | Neuronal | MnTBAP [67], MnTE-2-PyP [67, 68], MnTDE-2-ImP [68] |
| Paraquat | Epithelial | $MnBr_8TBAP$ [69] |
| | Neuronal | MnTDM [70], EUK134 [71], EUK189 [71] |
| Staurosporin | Neuronal | EUK134 [72], EUK189 [50], EUK207 [50] |
| 6-Hydroxydopamine | Neuronal | EUK134 [72], MnTBAP [73] |
| Hyperoxia | Epithelial | EUK134 [74] |
| UVB radiation | Keratinocytes | EUK134 [75] |
| Diesel exhaust particles | Epithelial | EUK8 [76] |
| Gentamicin | Cochlear cultures | M40403 [77] |
| HIV infection | Astrocytes | M40401 [78] |
| Berylium | Human peripheral blood cells | MnTBAP [79] |
| Hypoxanthine/xanthine oxidase, menadione, | Pancreatic cells | MnTM-4-PyP [80] |
| Endotoxin | Macrophages | MnTPPS [81], FeTMPS [81], FeTM-4-PyP [82] |

Adapted from [3, 26].

**Table I.4** – Examples of protective effects reported using SODm in animal models.

| Model system | Species | SODm found to be protective |
|---|---|---|
| **Lung** | | |
| Cigarette smoke injury | Rat | MnTDE-2-ImP [83] |
| Antigen-induced asthma | Mouse | MnTE-2-PyP [84] |
| Bronchopulmonary dysplasia | Baboon | MnTE-2-PyP [85] |
| Paraquat pneumotoxicity | Mouse | MnTBAP [86] |
| **Cardiovascular** | | |
| Heart ischemia–reperfusion | Rat | M40403 [87], EUK8 [88] |
| Hemorrhagic shock | Rat | EUK8, EUK134 [89] |
| Nitrate tolerance | Rat | MnTBAP [90] |
| Cardiac transplants | Rat | MnTM-4-PyP [91] |
| Ageing-associated cardiovascular dysfunction | Rat | Cu(II)-aspirinate [92] |
| Interleukin-2-induced hypotension | Mouse | M40403 [93] |
| **Central nervous system** | | |
| Spinal cord injury | Rat | MnTBAP [94] |
| Ischemia–reperfusion | Rat | MnTE-2-PyP [95] |
| | Mouse | MnTDE-2-ImP [68] |
| | Gerbil | M40401 [96] |
| Paraquat-induced neurotoxicity | Mouse | EUK189 [71] |
| Hyperalgesia | Rat | M40403 [97] |
| 6-Hydroxydopamine-induced parkinsonism | Mouse | Tempol [98] |
| Age-induced cognitive impairment | Mouse | EUK189, EUK207 [99] |
| Meningitis-induced hearing loss | Rat | MnTBAP [100] |
| **Liver** | | |
| Acetaminophen injury | Mouse | MnTBAP [101] |
| Ischemia–reperfusion | Rat | MnTDE-2-ImP [102] |
| **Gastrointestinal** | | |
| Acetic acid-induced colitis | Rat | MnTEGP [103] |
| Cerulein-induced pancreatitis | Mouse | M40401 [104] |
| **Renal** | | |
| Gentamicin injury | Rat | M40403 [24] |
| Endotoxin | Mouse | MnTE-2-PyP [105] |
| Ischemia–reperfusion | Rat | EUK134 [106], Tempol [107], MnTnHex-2-PyP [108] |

**Table I.4** *(cont.)*

| | | |
|---|---|---|
| **Other** | | |
| Peridontitis | Rat | M40403 [109] |
| Preeclampsia | Mouse | Tempol [110] |
| Collagen-induced arthritis | Rat | M40403 [111] |
| Cataracts | Rabbit | Tempol [112] |
| Diabetes-induced erectile dysfunction | Rat | Tempol [113] |
| Alloxan-induced diabetes | Mouse | Cu(II) complexes with 6-(benzylamino)purine derivatives [114] |

Adapted from [3, 4, 26].

Since $O_2^{\bullet-}$ is involved in many pathological phenomena (Table I.2), and due to the ability of catalytic antioxidants to scavenge the excess ROS restoring the redox balance of the tissues, the therapeutic possibilities for these compounds are broad. In fact, as shown in Table 1.4, pre-clinical studies suggest the usefulness of these antioxidants in a variety of diseases, in multiple organs and systems.

In addition to the aforementioned oxidative-stress related diseases, a promising role for SODm in cancer therapy has also been suggested. Many adverse effects of chemotherapy and radiotherapy are related to oxidative stress, namely the doxorubicin-induced cardiotoxicity [22, 115, 116], bleomycin-induced lung fibrosis [116, 117], radiation-induced lung injury (pneumonitis and fibrosis) [118]. SODm may therefore be promising antioxidants for the protection of non-tumoral tissues from chemotherapy and radiotherapy adverse effects. Some studies have been performed towards this application of SODm as exemplified in Table I.5. In addition, as mentioned in the above section, a few SODm are currently being tested in clinical trials to evaluate their role against the side effects of radiotherapy (AEOL 10150, EUK189, and Tempol) and chemotherapy (mangafodipir).

**Table I.5** – Examples of protective effects shown by SODm against adverse effects of chemotherapy and radiotherapy.

| **Anticancer agent** | **Adverse effect** | **Cell type or Animal species** | **SODm found to be protective** |
|---|---|---|---|
| Doxorubicin | Cardiotoxicity | Cardiomyocytes | MnTBAP [119] |
| Bleomycin | Lung fibrosis | Mouse | MnTBAP [117] |
| Cisplatin | Kidney epithelial cell apoptosis | LLC-PK kidney epithelial cells | $Cu(II)_2(3,5\text{-}DTBS)_4(Eth)_4$ [120] |
| Ionizing Radiation | Lung injury | Rat | EUK189 [118]<br>MnTE-2-PyP [121],<br>MnTnHex-2-PyP [121] |
| | Oral mucositis | Hamster | M40403 [122] |
| | Hair loss | Guinea pig | Tempol [123] |
| | Salivary hypofunction | Mouse | Tempol [124] |
| | Death and oxidative damage | Mouse; U937 premonocytic cells | MnTM-2-PyP [125, 126] |
| | | Rat | Cu(II) and Mn(IV) complexes with 2-methylaminopyridine [127] |

The potentialities of SODm in cancer therapy are not limited to the mitigation of chemo- and radiotherapy side effects. SODm have also been suggested to inhibit malignant transformation processes [17, 43]. Moreover, SODm can exert themselves antitumor effects or can potentiate established anticancer treatments, as explained below.

ROS are known to exert different effects in cell proliferation, either promoting or reducing it, according to their nature and to their intracellular level [128]. Tumor cells are usually under higher oxidative stress than normal cells [128] and use to present low MnSOD, Cu,Zn-SOD and CAT activities [15, 17]. Nicco *et al* [129] have proposed the following model describing the relationship between the level of $H_2O_2$ and the rate of cell growth (Fig. 1.12).

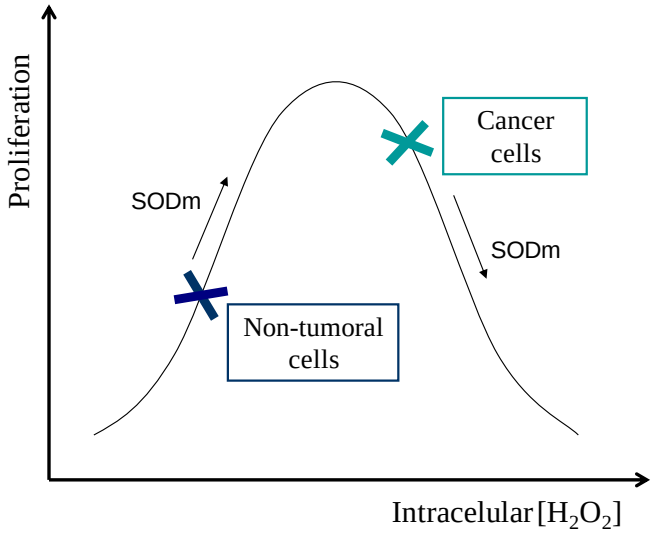


**Fig. 1.12 -** Schematic representation of the relationship between intracellular $H_2O_2$ levels and cell proliferation (adapted from [129]).

Changes in $O_2^{\bullet-}/H_2O_2$ balance alter the cellular redox state, which in turn affects signal transduction pathways modulating cell proliferation [17]. In non-tumoral cells, the basal level of $H_2O_2$ is low and its increase is associated with cell proliferation. On the other hand, the intracellular level of $H_2O_2$ in tumor cells is often close to the threshold of toxicity and a further increase in $H_2O_2$ concentration can trigger apoptotic pathways [129]. Compounds with SOD-like activity, while dismutating $O_2^{\bullet-}$, increase the $H_2O_2$ concentration and can thus reduce tumor growth or potentiate anticancer agents [128-130]. Moreover, if the complex reacts with the generated $H_2O_2$ via Fenton reaction originating the highly toxic $HO^{\bullet}$ radical, this can be a further advantage in promoting cancer cells' death [61, 128]. This may constitute an important approach to promote selective cell death between cancer and normal cells, since cancer cells usually possess lower antioxidant defences, being thus unable to efficiently detoxify $H_2O_2$ [17].

SODm can be useful in cancer treatment either alone or in combination with established antitumor treatments. Many anticancer strategies are known to produce ROS (e.g. doxorubicin, bleomycin, oxaliplatin, cisplatin, ionizing radiation) [15, 129]. The manipulation of antioxidants systems, and specifically the increase of SOD activity in cancer cells by the addition of SODm, may be an approach to potentiate these agents [15, 17, 129]. Some studies (Table I.6) have been performed in order to explore this therapeutic possibility of SODm.

**Table I.6** – Examples of studies focusing on the potential of SODm as anticancer agents.

| SODm | Model | Results observed |
|---|---|---|
| Tempol [131] | HL60 leukemia cells | Tempol exhibited an antiproliferative effect |
| Tempol [132] | Colon carcinoma cells | Tempol exhibited an antiproliferative effect and potentiated doxorubicin |
| 2-methylami-nopyridine complexes of Cu(II), Fe(III) and Mn(IV) [133] | Mouse implanted with Ehrlich carcinoma cells | The complexes decreased cell viability and tumor volume |
| MnTBAP, MnDPDP, CuDIPS [128] | CT26 colon carcinoma cells;<br>Hepa 1-6 hepatoma cells;<br>Mouse bearing CT26 and Hepa 1-6 tumors | SODm decreased cell proliferation and tumor volume;<br>SODm potentiated the effects of oxaliplatin |
| Mangafodipir, MnTBAP, CuDIPS [130] | CT26 colon carcinoma cells;<br>Mouse bearing CT26 tumors | SODm potentiated the cytotoxicity of oxaliplatin, paclitaxel and 5-fluorouracil;<br>Mangafodipir and CuDIPs abrogated tumor growth;<br>Mangafodipir enhanced the antitumoral effects of paclitaxel |
| MnTE-2-PyP [134] | Mice bearing 4T1 mammary carcinoma | MnTE-2-PyP augmented the effects of radiation in terms of tumor growth delay and devascularisation |
| MnTDE-2-ImP [135] | Mouse with prostate tumor | MnTDE-2-ImP increased radiation effectiveness |

SODm may thus be useful in chemotherapy, either reducing carcinogenesis, protecting non-tumoral tissues from the oxidative damage induced by anticancer agents, or potentiating their toxic effects in tumoral cells. This potentiation capacity can be a useful approach to overcome drug resistance, and some studies have already pointed out a beneficial role of SODm in the sensitization of chemotherapy-resistant tumor cells [131, 132].

## 1.3 References


[1] Sies, H. Oxidative stress: oxidants and antioxidants. *Exp Physiol* **82:**291-295; 1997.

[2] Halliwell, B. Biochemistry of oxidative stress. *Biochem Soc Trans* **35:**1147-1150; 2007.

[3] Day, B. J. Catalytic antioxidants: a radical approach to new therapeutics. *Drug Discov Today* **9:**557-566; 2004.

[4] Halliwell, B.; Gutterdige, J. M. C. *Free Radicals in Biology and Medicine.* New York: Oxford University Press; 2007.

[5] Mates, J. M. Effects of antioxidant enzymes in the molecular control of reactive oxygen species toxicology. *Toxicology* **153:**83-104; 2000.

[6] Finkel, T.; Holbrook, N. J. Oxidants, oxidative stress and the biology of ageing. *Nature* **408:**239-247; 2000.

[7] Salvemini, D.; Muscoli, C.; Riley, D. P.; Cuzzocrea, S. Superoxide dismutase mimetics. *Pulm Pharmacol Ther* **15:**439-447; 2002.

[8] Muscoli, C.; Cuzzocrea, S.; Riley, D. P.; Zweier, J. L.; Thiemermann, C.; Wang, Z. Q.; Salvemini, D. On the selectivity of superoxide dismutase mimetics and its importance in pharmacological studies. *Br J Pharmacol* **140:**445-460; 2003.

[9] Droge, W. Free radicals in the physiological control of cell function. *Physiol Rev* **82:**47-95; 2002.

[10] Valko, M.; Leibfritz, D.; Moncol, J.; Cronin, M. T.; Mazur, M.; Telser, J. Free radicals and antioxidants in normal physiological functions and human disease. *Int J Biochem Cell Biol* **39:**44-84; 2007.

[11] Halliwell, B.; Whiteman, M. Measuring reactive species and oxidative damage in vivo and in cell culture: how should you do it and what do the results mean? *Br J Pharmacol* **142:**231-255; 2004.

[12] Mates, J. M.; Perez-Gomez, C.; Nunez de Castro, I. Antioxidant enzymes and human diseases. *Clin Biochem* **32:**595-603; 1999.

[13] Young, I. S.; McEneny, J. Lipoprotein oxidation and atherosclerosis. *Biochem Soc Trans* **29:**358-362; 2001.

[14] Cadenas, E. Mitochondrial Oxidative / Nitrosative Stress and Cell Function. Spetses, Greece: SFRR-E Free Radical Summer School 2008.

[15] Oberley, L. W. Therapeutic Manipulation of the Intracellular Redox State. *American Association for Cancer Research Education Book***:**255-258; 2006.

[16] McCord, J. M.; Edeas, M. A. SOD, oxidative stress and human pathologies: a brief history and a future vision. *Biomed Pharmacother* **59:**139-142; 2005.

[17] Oberley, L. W. Mechanism of the tumor suppressive effect of MnSOD overexpression. *Biomed Pharmacother* **59:**143-148; 2005.

[18] Quan, F.; Korneluk, R. G.; Tropak, M. B.; Gravel, R. A. Isolation and characterization of the human catalase gene. *Nucleic Acids Res* **14:**5321-5335; 1986.

[19] Kirkman, H. N.; Gaetani, G. F. Mammalian catalase: a venerable enzyme with new mysteries. *Trends Biochem Sci* **32:**44-50; 2007.

[20] Mugesh, G.; Singh, H. B. Synthetic organoselenium compounds as antioxidants: glutathione peroxidase activity. *Chem Soc Rev* **29:**347-357; 2000.

[21] Pastore, A.; Federici, G.; Bertini, E.; Piemonte, F. Analysis of glutathione: implication in redox and detoxification. *Clin Chim Acta* **333:**19-39; 2003.

[22] Ramos, D. L.; Oliveira, N. G.; Pingarilho, M.; Gil, O. M.; Fernandes, A. S.; Rueff, J.; Gaspar, J. F. Modulation of doxorubicin genotoxicity in human lymphocytes by GSTs polymorphisms: possible role of *GSTp1* Ile105Val polymorphism. **in preparation**; 2010.

[23] Agarwal, A.; Nandipati, K. C.; Sharma, R. K.; Zippe, C. D.; Raina, R. Role of oxidative stress in the pathophysiological mechanism of erectile dysfunction. *J Androl* **27:**335-347; 2006.

[24] Cuzzocrea, S.; Mazzon, E.; Dugo, L.; Serraino, I.; Di Paola, R.; Britti, D.; De Sarro, A.; Pierpaoli, S.; Caputi, A.; Masini, E.; Salvemini, D. A role for superoxide in gentamicin-mediated nephropathy in rats. *Eur J Pharmacol* **450:**67-76; 2002.

[25] Riley, D. P. Functional mimics of superoxide dismutase enzymes as therapeutic agents. *Chem Rev* **99:**2573-2588; 1999.

[26] Crapo, J. D.; Day, B. J.; Fridovich, I. Development of Manganic Porphyrin Mimetics of Superoxide Dismutase Activity. *Madame Curie Bioscience Database: Ischemia-Reperfusion*: Landes Bioscience.

[27] Batinic-Haberle, I.; Benov, L.; Spasojevic, I.; Fridovich, I. The ortho effect makes manganese(III) meso-tetrakis(N-methylpyridinium-2-yl)porphyrin a powerful and potentially useful superoxide dismutase mimic. *J Biol Chem* **273:**24521-24528; 1998.

[28] Batinic-Haberle, I.; Rebouças, J. S.; Spasojević, I. Superoxide dismutase mimics: chemistry, pharmacology and therapeutic potential. *Antiox Redox Signal* **13:**877-918; 2010.

[29] Doctrow, S. R.; Huffman, K.; Marcus, C. B.; Tocco, G.; Malfroy, E.; Adinolfi, C. A.; Kruk, H.; Baker, K.; Lazarowych, N.; Mascarenhas, J.; Malfroy, B. Salen-manganese complexes as catalytic scavengers of hydrogen peroxide and cytoprotective agents: structure-activity relationship studies. *J Med Chem* **45:**4549-4558; 2002.

[30] Goldstein, S.; Samuni, A.; Merenyi, G. Reactions of nitric oxide, peroxynitrite, and carbonate radicals with nitroxides and their corresponding oxoammonium cations. *Chem Res Toxicol* **17:**250-257; 2004.

[31] Reboucas, J. S.; Spasojevic, I.; Tjahjono, D. H.; Richaud, A.; Mendez, F.; Benov, L.; Batinic-Haberle, I. Redox modulation of oxidative stress by Mn porphyrin-based therapeutics: the effect of charge distribution. *Dalton Trans***:**1233-1242; 2008.

[32] Schepetkin, I.; Potapov, A.; Khlebnikov, A.; Korotkova, E.; Lukina, A.; Malovichko, G.; Kirpotina, L.; Quinn, M. T. Decomposition of reactive oxygen species by copper(II) bis(1-pyrazolyl)methane complexes. *J Biol Inorg Chem* **11:**499-513; 2006.

[33] Crapo, J. Redox, kinetic, and biological necessities to create an effective metalloenzyme-mimetic in the oxidative stress arena. Sunrise Free Radical School - SFRBM; 2006.

[34] Lindoy, L. F. *The Chemistry of Macrocyclic Ligand Complexes.* Cambridge: Cambridge University Press; 1989.

[35] Lahaye, D.; Muthukumaran, K.; Hung, C. H.; Gryko, D.; Reboucas, J. S.; Spasojevic, I.; Batinic-Haberle, I.; Lindsey, J. S. Design and synthesis of manganese porphyrins with tailored lipophilicity: investigation of redox properties and superoxide dismutase activity. *Bioorg Med Chem* **15:**7066-7086; 2007.

[36] Murphy, M. P.; Smith, R. A. Targeting antioxidants to mitochondria by conjugation to lipophilic cations. *Annu Rev Pharmacol Toxicol* **47:**629-656; 2007.

[37] Asayama, S.; Kawamura, E.; Nagaoka, S.; Kawakami, H. Design of manganese porphyrin modified with mitochondrial signal peptide for a new antioxidant. *Mol Pharm* **3:**468-470; 2006.

[38] Goldoni, A. Porphyrins: fascinating molecules with biological significance. *Elettra Highlights: Atomic, Molecular and Supramolecular Studies***:**64-65; 2002.

[39] Patel, M.; Day, B. J. Metalloporphyrin class of therapeutic catalytic antioxidants. *Trends Pharmacol Sci* **20:**359-364; 1999.

[40] Ferrer-Sueta, G.; Vitturi, D.; Batinic-Haberle, I.; Fridovich, I.; Goldstein, S.; Czapski, G.; Radi, R. Reactions of manganese porphyrins with peroxynitrite and carbonate radical anion. *J Biol Chem* **278:**27432-27438; 2003.

[41] Moeller, B. J.; Cao, Y.; Li, C. Y.; Dewhirst, M. W. Radiation activates HIF-1 to regulate vascular radiosensitivity in tumors: role of reoxygenation, free radicals, and stress granules. *Cancer Cell* **5:**429-441; 2004.

[42] Rabbani, Z. N.; Spasojevic, I.; Zhang, X.; Moeller, B. J.; Haberle, S.; Vasquez-Vivar, J.; Dewhirst, M. W.; Vujaskovic, Z.; Batinic-Haberle, I. Antiangiogenic action of redox-modulating Mn(III) meso-tetrakis(N-ethylpyridinium-2-yl)porphyrin, MnTE-2-PyP(5+), via suppression of oxidative stress in a mouse model of breast tumor. *Free Radic Biol Med* **47:**992-1004; 2009.

[43] Zhao, Y.; Chaiswing, L.; Oberley, T. D.; Batinic-Haberle, I.; St Clair, W.; Epstein, C. J.; St Clair, D. A mechanism-based antioxidant approach for the reduction of skin carcinogenesis. *Cancer Res* **65:**1401-1405; 2005.

[44] Sheng, H.; Yang, W.; Fukuda, S.; Tse, H. M.; Paschen, W.; Johnson, K.; Batinic-Haberle, I.; Crapo, J. D.; Pearlstein, R. D.; Piganelli, J.; Warner, D. S. Long-term neuroprotection from a potent redox-modulating metalloporphyrin in the rat. *Free Radic Biol Med* **47:**917-923; 2009.

[45] Tse, H. M.; Milton, M. J.; Piganelli, J. D. Mechanistic analysis of the immunomodulatory effects of a catalytic antioxidant on antigen-presenting cells: implication for their use in targeting oxidation-reduction reactions in innate immunity. *Free Radic Biol Med* **36:**233-247; 2004.

[46] AEOL 10150 development *Aeolus Pharmaceuticals (http://www.aeoluspharma.com/AEOL10150dev.php);* 2007 (accessed February 2010).

[47] Baudry, M.; Etienne, S.; Bruce, A.; Palucki, M.; Jacobsen, E.; Malfroy, B. Salen-manganese complexes are superoxide dismutase-mimics. *Biochem Biophys Res Commun* **192:**964-968; 1993.

[48] Salvemini, D.; Riley, D. P.; Cuzzocrea, S. SOD mimetics are coming of age. *Nat Rev Drug Discov* **1:**367-374; 2002.

[49] Proteome systems focus on diagnostics strengthen and exits therapeutics business. *Tyrian Diagnostics (http://www.tyriandiagnostics.com/);* 2008 (accessed February 2010).

[50] Rosenthal, R. A.; Huffman, K. D.; Fisette, L. W.; Damphousse, C. A.; Callaway, W. B.; Malfroy, B.; Doctrow, S. R. Orally available Mn porphyrins with superoxide dismutase and catalase activities. *J Biol Inorg Chem* **14:**979-991; 2009.

[51] Arslantas, A. Development of Functional Models for a SOD. *Met Based Drugs* **9:**9-18; 2002.

[52] Palivan, C. G.; Balasubramanian, V.; Goodman, B. A. Global structure-activity analysis in drug development illustrated for active Cu/Zn superoxide dismutase mimics. *Eur J Inorg Chem***:**4634-4639; 2009.

[53] Bertinato, J.; L'Abbe, M. R. Maintaining copper homeostasis: regulation of copper-trafficking proteins in response to copper deficiency or overload. *J Nutr Biochem* **15:**316-322; 2004.

[54] Bienvenue, E.; Choua, S.; Lobo-Recio, M.-A.; Marzin, C.; Pacheco, P.; Seta, P.; Tarrago, G. Structure and superoxide dismutase activity of Ru(II), Cu(II), and Mn(II) macrocyclic complexes. *J Inorg Biochem* **57:**157-168; 1995.

[55] Kimura, E.; Sakonaka, A.; Nakamoto, M. Superoxide dismutase activity of macrocyclic polyamine complexes. *Biochim Biophys Acta* **678:**172-179; 1981.

[56] Kimura, E.; Yatsunami, A.; Watanabe, A.; Machida, R.; Koike, T.; Fujioka, H.; Kuramoto, Y.; Sumomogi, M.; Kunimitsu, K.; Yamashita, A. Further studies on superoxide dismutase activities of macrocyclic polyamine complexes of copper(II). *Biochim Biophys Acta* **745:**37-43; 1983.

[57] Durackova, Z.; Labuda, J. Superoxide dismutase mimetic activity of macrocyclic Cu(II)-tetraanhydroaminobenzaldehyde (TAAB) complex. *J Inorg Biochem* **58:**297-303; 1995.

[58] Autzen, S.; Korth, H.-G.; Boese, R.; de Groot, H.; Sustmann, R. Studies of pyridinyl-containing 14-membered macrocyclic copper(II) complexes. *Eur J Inorg Chem***:**1401-1410; 2003.

[59] Yaping, T.; Yunzhong, F.; Qinhui, L.; Mengchang, S.; Qin, L.; Wenmei, S. The inhibitory effects of 21 mimics of superoxide dismutase on luminol-mediated chemiluminescence emitted from PMA-stimulated polymorphonuclear leukocyte. *Free Radic Biol Med* **13:**533-541; 1992.

[60] Li, Q. X.; Luo, Q. H.; Li, Y. Z.; Shen, M. C. A study on the mimics of Cu-Zn superoxide dismutase with high activity and stability: two copper(II) complexes of 1,4,7-triazacyclononane with benzimidazole groups. *Dalton Trans***:**2329-2335; 2004.

[61] Ohse, T.; Nagaoka, S.; Arakawa, Y.; Kawakami, H.; Nakamura, K. Cell death by reactive oxygen species generated from water-soluble cationic metalloporphyrins as superoxide dismutase mimics. *J Inorg Biochem* **85:**201-208; 2001.

[62] Day, B. J. Antioxidants as potential therapeutics for lung fibrosis. *Antioxid Redox Signal* **10:**355-370; 2008.

[63] Metz, J. M.; Smith, D.; Mick, R.; Lustig, R.; Mitchell, J.; Cherakuri, M.; Glatstein, E.; Hahn, S. M. A phase I study of topical Tempol for the prevention of alopecia induced by whole brain radiotherapy. *Clin Cancer Res* **10:**6411-6417; 2004.

[64] *PledPharma AB (http://www.pledpharma.se);* 2010 (accessed July 2010).

[65] Milano, J.; Day, B. J. A catalytic antioxidant metalloporphyrin blocks hydrogen peroxide-induced mitochondrial DNA damage. *Nucleic Acids Res* **28:**968-973; 2000.

[66] Day, B. J.; Fridovich, I.; Crapo, J. D. Manganic porphyrins possess catalase activity and protect endothelial cells against hydrogen peroxide-mediated injury. *Arch Biochem Biophys* **347:**256-262; 1997.

[67] Li, Q. Y.; Pedersen, C.; Day, B. J.; Patel, M. Dependence of excitotoxic neurodegeneration on mitochondrial aconitase inactivation. *J Neurochem* **78:**746-755; 2001.

[68] Sheng, H.; Enghild, J. J.; Bowler, R.; Patel, M.; Batinic-Haberle, I.; Calvi, C. L.; Day, B. J.; Pearlstein, R. D.; Crapo, J. D.; Warner, D. S. Effects of metalloporphyrin catalytic antioxidants in experimental brain ischemia. *Free Radic Biol Med* **33:**947-961; 2002.

[69] Kachadourian, R.; Flaherty, M. M.; Crumbliss, A. L.; Patel, M.; Day, B. J. Synthesis and in vitro antioxidant properties of manganese(III) beta-octabromo-meso-tetrakis(4-carboxyphenyl)porphyrin. *J Inorg Biochem* **95:**240-248; 2003.

[70] Chen, P.; Li, A.; Zhang, M.; He, M.; Chen, Z.; Wu, X.; Zhao, C.; Wang, S.; Liang, L. Protective effects of a new metalloporphyrin on paraquat-induced oxidative stress and apoptosis in N27 cells. *Acta Biochim Biophys Sin (Shanghai)* **40:**125-132; 2008.

[71] Peng, J.; Stevenson, F. F.; Doctrow, S. R.; Andersen, J. K. Superoxide dismutase/catalase mimetics are neuroprotective against selective paraquat-mediated dopaminergic neuron death in the substantial nigra: implications for Parkinson disease. *J Biol Chem* **280:**29194-29198; 2005.

[72] Pong, K.; Doctrow, S. R.; Huffman, K.; Adinolfi, C. A.; Baudry, M. Attenuation of staurosporine-induced apoptosis, oxidative stress, and mitochondrial dysfunction by synthetic superoxide dismutase and catalase mimetics, in cultured cortical neurons. *Exp Neurol* **171:**84-97; 2001.

[73] Choi, W. S.; Yoon, S. Y.; Oh, T. H.; Choi, E. J.; O'Malley, K. L.; Oh, Y. J. Two distinct mechanisms are involved in 6-hydroxydopamine- and MPP+-induced dopaminergic neuronal cell death: role of caspases, ROS, and JNK. *J Neurosci Res* **57:**86-94; 1999.

[74] Buccellato, L. J.; Tso, M.; Akinci, O. I.; Chandel, N. S.; Budinger, G. R. Reactive oxygen species are required for hyperoxia-induced Bax activation and cell death in alveolar epithelial cells. *J Biol Chem* **279:**6753-6760; 2004.

[75] Decraene, D.; Smaers, K.; Gan, D.; Mammone, T.; Matsui, M.; Maes, D.; Declercq, L.; Garmyn, M. A synthetic superoxide dismutase/catalase mimetic (EUK-134) inhibits membrane-damage-induced activation of mitogen-activated protein kinase pathways and reduces p53 accumulation in ultraviolet B-exposed primary human keratinocytes. *J Invest Dermatol* **122:**484-491; 2004.

[76] Matsuo, M.; Shimada, T.; Uenishi, R.; Sasaki, N.; Sagai, M. Diesel exhaust particle-induced cell death of cultured normal human bronchial epithelial cells. *Biol Pharm Bull* **26:**438-447; 2003.

[77] McFadden, S. L.; Ding, D.; Salvemini, D.; Salvi, R. J. M40403, a superoxide dismutase mimetic, protects cochlear hair cells from gentamicin, but not cisplatin toxicity. *Toxicol Appl Pharmacol* **186:**46-54; 2003.

[78] Mollace, V.; Salvemini, D.; Riley, D. P.; Muscoli, C.; Iannone, M.; Granato, T.; Masuelli, L.; Modesti, A.; Rotiroti, D.; Nistico, R.; Bertoli, A.; Perno, C. F.; Aquaro, S. The contribution of oxidative stress in apoptosis of human-cultured astroglial cells induced by supernatants of HIV-1-infected macrophages. *J Leukoc Biol* **71:**65-72; 2002.

[79] Dobis, D. R.; Sawyer, R. T.; Gillespie, M. M.; Huang, J.; Newman, L. S.; Maier, L. A.; Day, B. J. Modulation of lymphocyte proliferation by antioxidants in chronic beryllium disease. *Am J Respir Crit Care Med* **177:**1002-1011; 2008.

[80] Moriscot, C.; Candel, S.; Sauret, V.; Kerr-Conte, J.; Richard, M. J.; Favrot, M. C.; Benhamou, P. Y. MnTMPyP, a metalloporphyrin-based superoxide dismutase/catalase mimetic, protects INS-1 cells and human pancreatic islets from an in vitro oxidative challenge. *Diabetes Metab* **33:**44-53; 2007.

[81] Misko, T. P.; Highkin, M. K.; Veenhuizen, A. W.; Manning, P. T.; Stern, M. K.; Currie, M. G.; Salvemini, D. Characterization of the cytoprotective action of peroxynitrite decomposition catalysts. *J Biol Chem* **273:**15646-15653; 1998.

[82] Kang, J. L.; Lee, H. S.; Pack, I. S.; Leonard, S.; Castranova, V. Iron tetrakis (n-methyl-4'-pyridyl) porphyrinato (FeTMPyP) is a potent scavenging antioxidant and an inhibitor of stimulant-induced NF-kappaB activation of raw 264.7 macrophages. *J Toxicol Environ Health A* **64:**291-310; 2001.

[83] Smith, K. R.; Uyeminami, D. L.; Kodavanti, U. P.; Crapo, J. D.; Chang, L. Y.; Pinkerton, K. E. Inhibition of tobacco smoke-induced lung inflammation by a catalytic antioxidant. *Free Radic Biol Med* **33:**1106-1114; 2002.

[84] Chang, L. Y.; Crapo, J. D. Inhibition of airway inflammation and hyperreactivity by an antioxidant mimetic. *Free Radic Biol Med* **33:**379-386; 2002.

[85] Chang, L. Y.; Subramaniam, M.; Yoder, B. A.; Day, B. J.; Ellison, M. C.; Sunday, M. E.; Crapo, J. D. A catalytic antioxidant attenuates alveolar structural remodeling in bronchopulmonary dysplasia. *Am J Respir Crit Care Med* **167:**57-64; 2003.

[86] Day, B. J.; Crapo, J. D. A metalloporphyrin superoxide dismutase mimetic protects against paraquat-induced lung injury in vivo. *Toxicol Appl Pharmacol* **140:**94-100; 1996.

[87] Masini, E.; Cuzzocrea, S.; Mazzon, E.; Marzocca, C.; Mannaioni, P. F.; Salvemini, D. Protective effects of M40403, a selective superoxide dismutase mimetic, in myocardial ischaemia and reperfusion injury in vivo. *Br J Pharmacol* **136:**905-917; 2002.

[88] Xu, Y.; Armstrong, S. J.; Arenas, I. A.; Pehowich, D. J.; Davidge, S. T. Cardioprotection by chronic estrogen or superoxide dismutase mimetic treatment in the aged female rat. *Am J Physiol Heart Circ Physiol* **287:**H165-171; 2004.

[89] Izumi, M.; McDonald, M. C.; Sharpe, M. A.; Chatterjee, P. K.; Thiemermann, C. Superoxide dismutase mimetics with catalase activity reduce the organ injury in hemorrhagic shock. *Shock* **18:**230-235; 2002.

[90] Frame, M. D.; Fox, R. J.; Kim, D.; Mohan, A.; Berk, B. C.; Yan, C. Diminished arteriolar responses in nitrate tolerance involve ROS and angiotensin II. *Am J Physiol Heart Circ Physiol* **282:**H2377-2385; 2002.

[91] Nilakantan, V.; Zhou, X.; Hilton, G.; Shi, Y.; Baker, J. E.; Khanna, A. K.; Pieper, G. M. Antagonizing reactive oxygen by treatment with a manganese (III) metalloporphyrin-based superoxide dismutase mimetic in cardiac transplants. *J Thorac Cardiovasc Surg* **131:**898-906; 2006.

[92] Radovits, T.; Gero, D.; Lin, L. N.; Loganathan, S.; Hoppe-Tichy, T.; Szabo, C.; Karck, M.; Sakurai, H.; Szabo, G. Improvement of aging-associated cardiovascular dysfunction by the orally administered copper(II)-aspirinate complex. *Rejuvenation Res* **11:**945-956; 2008.

[93] Samlowski, W. E.; Petersen, R.; Cuzzocrea, S.; Macarthur, H.; Burton, D.; McGregor, J. R.; Salvemini, D. A nonpeptidyl mimic of superoxide dismutase, M40403, inhibits dose-limiting hypotension associated with interleukin-2 and increases its antitumor effects. *Nat Med* **9:**750-755; 2003.

[94] Leski, M. L.; Bao, F.; Wu, L.; Qian, H.; Sun, D.; Liu, D. Protein and DNA oxidation in spinal injury: neurofilaments--an oxidation target. *Free Radic Biol Med* **30:**613-624; 2001.

[95] Mackensen, G. B.; Patel, M.; Sheng, H.; Calvi, C. L.; Batinic-Haberle, I.; Day, B. J.; Liang, L. P.; Fridovich, I.; Crapo, J. D.; Pearlstein, R. D.; Warner, D. S. Neuroprotection from delayed postischemic administration of a metalloporphyrin catalytic antioxidant. *J Neurosci* **21:**4582-4592; 2001.

[96] Mollace, V.; Iannone, M.; Muscoli, C.; Palma, E.; Granato, T.; Modesti, A.; Nistico, R.; Rotiroti, D.; Salvemini, D. The protective effect of M40401, a superoxide dismutase mimetic, on post-ischemic brain damage in Mongolian gerbils. *BMC Pharmacol* **3:**8; 2003.

[97] Wang, Z. Q.; Porreca, F.; Cuzzocrea, S.; Galen, K.; Lightfoot, R.; Masini, E.; Muscoli, C.; Mollace, V.; Ndengele, M.; Ischiropoulos, H.; Salvemini, D. A newly identified role for superoxide in inflammatory pain. *J Pharmacol Exp Ther* **309:**869-878; 2004.

[98] Liang, Q.; Smith, A. D.; Pan, S.; Tyurin, V. A.; Kagan, V. E.; Hastings, T. G.; Schor, N. F. Neuroprotective effects of TEMPOL in central and peripheral nervous system models of Parkinson's disease. *Biochem Pharmacol* **70:**1371-1381; 2005.

[99] Liu, R.; Liu, I. Y.; Bi, X.; Thompson, R. F.; Doctrow, S. R.; Malfroy, B.; Baudry, M. Reversal of age-related learning deficits and brain oxidative stress in mice with superoxide dismutase/catalase mimetics. *Proc Natl Acad Sci U S A* **100:**8526-8531; 2003.

[100] Klein, M.; Koedel, U.; Pfister, H. W.; Kastenbauer, S. Meningitis-associated hearing loss: protection by adjunctive antioxidant therapy. *Ann Neurol* **54:**451-458; 2003.

[101] Ferret, P. J.; Hammoud, R.; Tulliez, M.; Tran, A.; Trebeden, H.; Jaffray, P.; Malassagne, B.; Calmus, Y.; Weill, B.; Batteux, F. Detoxification of reactive oxygen species by a nonpeptidyl mimic of superoxide dismutase cures acetaminophen-induced acute liver failure in the mouse. *Hepatology* **33:**1173-1180; 2001.

[102] Hines, I. N.; Hoffman, J. M.; Scheerens, H.; Day, B. J.; Harada, H.; Pavlick, K. P.; Bharwani, S.; Wolf, R.; Gao, B.; Flores, S.; McCord, J. M.; Grisham, M. B. Regulation of postischemic liver injury following different durations of ischemia. *Am J Physiol Gastrointest Liver Physiol* **284:**G536-545; 2003.

[103] Choudhary, S.; Keshavarzian, A.; Yong, S.; Wade, M.; Bocckino, S.; Day, B. J.; Banan, A. Novel antioxidants zolimid and AEOL11201 ameliorate colitis in rats. *Dig Dis Sci* **46:**2222-2230; 2001.

[104] Cuzzocrea, S.; Genovese, T.; Mazzon, E.; Di Paola, R.; Muia, C.; Britti, D.; Salvemini, D. Reduction in the development of cerulein-induced acute pancreatitis by treatment with M40401, a new selective superoxide dismutase mimetic. *Shock* **22:**254-261; 2004.

[105] Wang, W.; Jittikanont, S.; Falk, S. A.; Li, P.; Feng, L.; Gengaro, P. E.; Poole, B. D.; Bowler, R. P.; Day, B. J.; Crapo, J. D.; Schrier, R. W. Interaction among nitric oxide, reactive oxygen species, and antioxidants during endotoxemia-related acute renal failure. *Am J Physiol Renal Physiol* **284:**F532-537; 2003.

[106] Chatterjee, P. K.; Patel, N. S.; Kvale, E. O.; Brown, P. A.; Stewart, K. N.; Mota-Filipe, H.; Sharpe, M. A.; Di Paola, R.; Cuzzocrea, S.; Thiemermann, C. EUK-134 reduces renal dysfunction and injury caused by oxidative and nitrosative stress of the kidney. *Am J Nephrol* **24:**165-177; 2004.

[107] Fujii, T.; Takaoka, M.; Ohkita, M.; Matsumura, Y. Tempol protects against ischemic acute renal failure by inhibiting renal noradrenaline overflow and endothelin-1 overproduction. *Biol Pharm Bull* **28:**641-645; 2005.

[108] Saba, H.; Batinic-Haberle, I.; Munusamy, S.; Mitchell, T.; Lichti, C.; Megyesi, J.; MacMillan-Crow, L. A. Manganese porphyrin reduces renal injury and mitochondrial damage during ischemia/reperfusion. *Free Radic Biol Med* **42:**1571-1578; 2007.

[109] Di Paola, R.; Mazzon, E.; Rotondo, F.; Dattola, F.; Britti, D.; De Majo, M.; Genovese, T.; Cuzzocrea, S. Reduced development of experimental periodontitis by treatment with M40403, a superoxide dismutase mimetic. *Eur J Pharmacol* **516:**151-157; 2005.

[110] Hoffmann, D. S.; Weydert, C. J.; Lazartigues, E.; Kutschke, W. J.; Kienzle, M. F.; Leach, J. E.; Sharma, J. A.; Sharma, R. V.; Davisson, R. L. Chronic tempol prevents hypertension, proteinuria, and poor feto-placental outcomes in BPH/5 mouse model of preeclampsia. *Hypertension* **51:**1058-1065; 2008.

[111] Salvemini, D.; Mazzon, E.; Dugo, L.; Serraino, I.; De Sarro, A.; Caputi, A. P.; Cuzzocrea, S. Amelioration of joint disease in a rat model of collagen-induced arthritis by M40403, a superoxide dismutase mimetic. *Arthritis Rheum* **44:**2909-2921; 2001.

[112] Sasaki, H.; Lin, L. R.; Yokoyama, T.; Sevilla, M. D.; Reddy, V. N.; Giblin, F. J. TEMPOL protects against lens DNA strand breaks and cataract in the x-rayed rabbit. *Invest Ophthalmol Vis Sci* **39:**544-552; 1998.

[113] Kawakami, T.; Urakami, S.; Hirata, H.; Tanaka, Y.; Nakajima, K.; Enokida, H.; Shiina, H.; Ogishima, T.; Tokizane, T.; Kawamoto, K.; Miura, K.; Ishii, N.; Dahiya, R. Superoxide dismutase analog (Tempol: 4-hydroxy-2, 2, 6, 6-tetramethylpiperidine 1-oxyl) treatment restores erectile function in diabetes-induced impotence. *Int J Impot Res* **21:**348-355; 2009.

[114] Starha, P.; Travnicek, Z.; Herchel, R.; Popa, I.; Suchy, P.; Vanco, J. Dinuclear copper(II) complexes containing 6-(benzylamino)purines as bridging ligands: synthesis, characterization, and in vitro and in vivo antioxidant activities. *J Inorg Biochem* **103:**432-440; 2009.

[115] Singal, P. K.; Li, T.; Kumar, D.; Danelisen, I.; Iliskovic, N. Adriamycin-induced heart failure: mechanism and modulation. *Mol Cell Biochem* **207:**77-86; 2000.

[116] Kaiserova, H.; den Hartog, G. J.; Simunek, T.; Schroterova, L.; Kvasnickova, E.; Bast, A. Iron is not involved in oxidative stress-mediated cytotoxicity of doxorubicin and bleomycin. *Br J Pharmacol* **149:**920-930; 2006.

[117] Oury, T. D.; Thakker, K.; Menache, M.; Chang, L. Y.; Crapo, J. D.; Day, B. J. Attenuation of bleomycin-induced pulmonary fibrosis by a catalytic antioxidant metalloporphyrin. *Am J Respir Cell Mol Biol* **25:**164-169; 2001.

[118] Langan, A. R.; Khan, M. A.; Yeung, I. W.; Van Dyk, J.; Hill, R. P. Partial volume rat lung irradiation: the protective/mitigating effects of Eukarion-189, a superoxide dismutase-catalase mimetic. *Radiother Oncol* **79:**231-238; 2006.

[119] Konorev, E. A.; Kennedy, M. C.; Kalyanaraman, B. Cell-permeable superoxide dismutase and glutathione peroxidase mimetics afford superior protection against doxorubicin-induced cardiotoxicity: the role of reactive oxygen and nitrogen intermediates. *Arch Biochem Biophys* **368:**421-428; 1999.

[120] Wangila, G. W.; Nagothu, K. K.; Steward, R., 3rd; Bhatt, R.; Iyere, P. A.; Willingham, W. M.; Sorenson, J. R.; Shah, S. V.; Portilla, D. Prevention of cisplatin-induced kidney epithelial cell apoptosis with a Cu superoxide dismutase-mimetic [copper2II(3,5-ditertiarybutylsalicylate)4(ethanol)4]. *Toxicol In Vitro* **20:**1300-1312; 2006.

[121] Gauter-Fleckenstein, B.; Fleckenstein, K.; Owzar, K.; Jiang, C.; Batinic-Haberle, I.; Vujaskovic, Z. Comparison of two Mn porphyrin-based mimics of superoxide dismutase in pulmonary radioprotection. *Free Radic Biol Med* **44:**982-989; 2008.

[122] Murphy, C. K.; Fey, E. G.; Watkins, B. A.; Wong, V.; Rothstein, D.; Sonis, S. T. Efficacy of superoxide dismutase mimetic M40403 in attenuating radiation-induced oral mucositis in hamsters. *Clin Cancer Res* **14:**4292-4297; 2008.

[123] Cuscela, D.; Coffin, D.; Lupton, G. P.; Cook, J. A.; Krishna, M. C.; Bonner, R. F.; Mitchell, J. B. Protection from radiation-induced alopecia with topical application of nitroxides: fractionated studies. *Cancer J Sci Am* **2:**273-278; 1996.

[124] Cotrim, A. P.; Sowers, A. L.; Lodde, B. M.; Vitolo, J. M.; Kingman, A.; Russo, A.; Mitchell, J. B.; Baum, B. J. Kinetics of tempol for prevention of xerostomia following head and neck irradiation in a mouse model. *Clin Cancer Res* **11:**7564-7568; 2005.

[125] Lee, J. H.; Lee, Y. M.; Park, J. W. Regulation of ionizing radiation-induced apoptosis by a manganese porphyrin complex. *Biochem Biophys Res Commun* **334:**298-305; 2005.

[126] Lee, J. H.; Park, J. W. A manganese porphyrin complex is a novel radiation protector. *Free Radic Biol Med* **37:**272-283; 2004.

[127] Abou-Seif, M. A.; El-Naggar, M. M.; El-Far, M.; Ramadan, M.; Salah, N. Amelioration of radiation-induced oxidative stress and biochemical alteration by SOD model compounds in pre-treated gamma-irradiated rats. *Clin Chim Acta* **337:**23-33; 2003.

[128] Laurent, A.; Nicco, C.; Chereau, C.; Goulvestre, C.; Alexandre, J.; Alves, A.; Levy, E.; Goldwasser, F.; Panis, Y.; Soubrane, O.; Weill, B.; Batteux, F. Controlling tumor growth by modulating endogenous production of reactive oxygen species. *Cancer Res* **65:**948-956; 2005.

[129] Nicco, C.; Laurent, A.; Chereau, C.; Weill, B.; Batteux, F. Differential modulation of normal and tumor cell proliferation by reactive oxygen species. *Biomed Pharmacother* **59:**169-174; 2005.

[130] Alexandre, J.; Nicco, C.; Chereau, C.; Laurent, A.; Weill, B.; Goldwasser, F.; Batteux, F. Improvement of the therapeutic index of anticancer drugs by the superoxide dismutase mimic mangafodipir. *J Natl Cancer Inst* **98:**236-244; 2006.

[131] Gariboldi, M. B.; Rimoldi, V.; Supino, R.; Favini, E.; Monti, E. The nitroxide tempol induces oxidative stress, p21(WAF1/CIP1), and cell death in HL60 cells. *Free Radic Biol Med* **29:**633-641; 2000.

[132] Ravizza, R.; Gariboldi, M. B.; Passarelli, L.; Monti, E. Role of the p53/p21 system in the response of human colon carcinoma cells to Doxorubicin. *BMC Cancer* **4:**92; 2004.

[133] El-Naggar, M. M.; El-Waseef, A. M.; El-Halafawy, K. M.; El-Sayed, I. H. Antitumor activities of vanadium(IV), manganese(IV), iron(III), cobalt(II) and copper(II) complexes of 2-methylaminopyridine. *Cancer Lett* **133:**71-76; 1998.

[134] Moeller, B. J.; Batinic-Haberle, I.; Spasojevic, I.; Rabbani, Z. N.; Anscher, M. S.; Vujaskovic, Z.; Dewhirst, M. W. A manganese porphyrin superoxide dismutase mimetic enhances tumor radioresponsiveness. *Int J Radiat Oncol Biol Phys* **63:**545-552; 2005.

[135] Gridley, D. S.; Makinde, A. Y.; Luo, X.; Rizvi, A.; Crapo, J. D.; Dewhirst, M. W.; Moeller, B. J.; Pearlstein, R. D.; Slater, J. M. Radiation and a metalloporphyrin radioprotectant in a mouse prostate tumor model. *Anticancer Res* **27:**3101-3109; 2007.

# Chapter 2

# AIM

The global aim of this thesis is to contribute to the development of the SODm field, especially in two promising classes of macrocyclic compounds: a) manganese(III) porphyrins and b) macrocyclic copper(II) complexes.

## a) Manganese(III) porphyrins

MnPs have already shown remarkable protective effects in models of oxidative stress. However, a thorough knowledge on their effects at the cellular level is still lacking. Therefore, this thesis aims to contribute to fill this gap, shedding light on the role and potentialities of MnPs as catalytic antioxidants. In this context, the *para*-substituted porphyrin MnTM-4-PyP (Chapter 3) and two *ortho* analogues (Chapter 4) were studied.

### *Para-substituted porphyrin MnTM-4-PyP (Chapter 3)*

In chapter 3, the goal was to evaluate the cellular effects of the well established SODm MnTM-4-PyP (commercially available), in V79 Chinese hamster cells, a well-characterized lung fibroblast cell line widely used for cytotoxicity and cytogenetic studies, using the following approaches:

- The assessment of the antioxidant role of MnTM-4-PyP towards the toxicity of three oxidative stress inducers: the xanthine/xanthine oxidase (XXO) system, which is an extracellular $O_2^{\bullet-}$ generator; t*ert*-butylhydroperoxide (TBHP), a short chain analogue of lipid hydroperoxides; and Doxorubicin (Dox), an anticancer drug that undergoes a redox-cycling process generating $O_2^{\bullet-}$.
- The characterization of the effects of this MnP *per se*, as well as its role on the protection against the three mentioned oxidants, in terms of cell viability, cell division and intracellular levels of $O_2^{\bullet-}$.

With the data obtained within Chapter 3 we aimed not only to provide a better comprehension of the cellular effects of this MnP, but also to establish oxidative stress

validated models, to be used as tools for the study of the novel compounds developed within the scope of this thesis (Chapters 5 and 6).

***Ortho-substituted MnPs: MnTE-2-PyP and MnTnHex-2-PyP (Chapter 4)***

The establishment of a collaboration between the CBT-iMed.UL and the Radiation Oncology Department of Duke University, allowed the study of two optimized *ortho*-substituted MnPs, MnTE-2-PyP and MnTnHex-2-PyP. In Chapter 4 the goal was to characterize the effects of these MnPs in different perspectives that include:

- The evaluation of these MnPs against the TBHP-induced cell injury, assessing endpoints of cell viability and intracellular $O_2^{\bullet -}$ generation.
- The study of the effects of these MnPs on the glutathione status, since this is crucial to understand the cellular redox balance and so far there are no studies committed to this point.

**b) Macrocyclic copper(II) complexes**

The second key aim of this thesis is to develop novel macrocyclic copper(II) complexes with SODm activity. As mentioned in Chapter 1, most of the Cu(II) compounds developed so far are not thermodynamically stable or highly active in physiological conditions, and the use of macrocyclic ligands has been pointed out as an approach to overcome these limitations. In this regard, nine macrocyclic copper(II) complexes were synthesized and characterized in terms of thermodynamic and structural properties, biochemical activity and biological effects.

***Novel macrocyclic copper(II) complexes with SODm activity (Chapters 5 and 6)***

In this context, the aim of the present thesis was to study two different types of macrocyclic copper(II) complexes. For the first series complexes (Chapter 5), the

cyclization of the ligands was carried out by the Richman and Atkins' method. A second series of compounds (Chapter 6) comprised four pyridine-containing macrocyclic copper(II) complexes, and the correspondent ligands were synthesized using a templated method for the cyclization reaction. With the obtained complexes, the following goals were pursued:

- To characterize the complexes in terms of thermodynamic stability, structural features and electrochemical properties.
- To evaluate the capacity of the copper(II) complexes to scavenge $O_2^{\bullet -}$ *in vitro*.
- To evaluate the cytotoxicity of the copper(II) complexes in V79 cells.
- To select the complexes that presented better chemical and biochemical properties and study their potential antioxidant role in the cellular models validated in Chapter 3 (XXO and TBHP).
- To assess the potential role in chemotherapy of the most promising macrocyclic copper(II) complexes, by evaluating their cytotoxicity profile, as well as their ability to modulate the cytotoxicity of the anticancer drugs oxaliplatin and Dox, in tumoral (MCF7) and non-tumoral (MCF10A) human mammary cell lines.

# Chapter 3

## Oxidative injury in V79 Chinese hamster cells: protective role of the superoxide dismutase mimetic MnTM-4-PyP

This Chapter was adapted from:

Oxidative injury in V79 Chinese hamster cells: protective role of the superoxide dismutase mimetic MnTM-4-PyP. A.S. Fernandes, J. Serejo, J. Gaspar, M.F. Cabral, A.F. Bettencourt, J. Rueff, M. Castro, J. Costa, N.G. Oliveira. Cell Biology and Toxicology (2010) 26, 91–101.

**Abstract**

This Chapter focused on three different models of oxidative stress: the extracellular superoxide anion generator XXO; TBHP, an analogue of lipid hydroperoxides; and the anticancer drug Dox. Superoxide and peroxyl radicals, among other ROS could be effectively scavenged by MnTM-4-PyP, a polyfunctional catalytic antioxidant. In this work, the role of MnTM-4-PyP on the protection against the cytotoxicity induced by the three aforementioned oxidants was addressed. The effect of MnTM-4-PyP (0.1-100 μM) was evaluated in V79 cells, using the MTT reduction and the crystal violet (CV) assays, as well as the mitotic index (MI). Also, the generation of intracellular ROS was studied by the fluorescence probe dihydroethidium (DHE). MnTM-4-PyP has shown significant protective effects against the cytotoxicity of XXO and TBHP, markedly increasing the cell viability and reducing the intracellular level of ROS. However, no considerable protection occurred against Dox. The three oxidants caused a MI reduction that was not altered by MnTM-4-PyP. In summary, MnTM-4-PyP appears to be a promising agent for the protection against oxidative injury. However, it has shown differential responses, reinforcing the need to study different experimental models for the adequate evaluation of its potentialities as a catalytic antioxidant.

### 3.1. Introduction

The overproduction of ROS is associated with inflammation and tissue injury, being related to a large number of pathophysiological and toxicological conditions [1]. There are several available models of oxidative stress inducers varying in the species involved and in the site of formation of those species. According to the oxidative pathways involved in each model, they could be useful to understand different pathological conditions.

The XXO system is an efficient extracellular superoxide anion generator that was found to be cytotoxic in different mammalian cells [2, 3]. The overload of superoxide anion in the extracellular space is implicated in vascular diseases [4], thus justifying the study of the extracellular generation of this species. In the XXO system, xanthine (X) is oxidized to uric acid by xanthine oxidase (XO), in aerobic conditions, with concomitant production of $O_2^{\bullet -}$ [5] (Fig. 3.1). Furthermore, while acting upon xanthine, XO can produce hydrogen peroxide and cause lipid peroxidation [6].

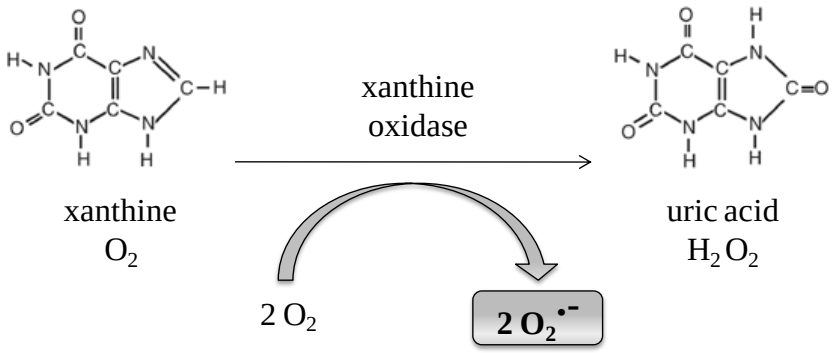


**Fig. 3.1** – Generation of $O_2^{\bullet -}$ by the xanthine – xanthine oxidase system.

TBHP (Fig. 3.2) is a short chain analogue of lipid hydroperoxides that mimics the toxic effect of peroxidized fatty acids, being thus commonly used as a model of lipid peroxidation [7-9]. TBHP penetrates cell membranes easily [10] and generates peroxyl radicals in the cytosol [9].The mechanisms of cytotoxicity of this oxidant comprise not only the generation of ROS, but also changes in mitochondrial permeability [9], oxidative DNA damage, and the depletion of the reduced form of glutathione [7].

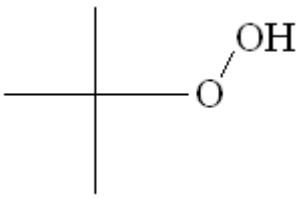


**Fig. 3.2** – Chemical structure of *tert*-butylhydroperoxide.

The anthracycline anticancer drug Dox is a quinone that undergoes a one-electron-reduction within the cell, originating a semi-quinone free radical. This bioreductive activation may be catalyzed by different oxidoreductases, namely the NADPH cytochrome P450 reductases of the endoplasmic reticulum and nuclear envelope, the mitochondrial NADH dehydrogenase and the cytosolic xanthine oxidase [1, 11, 12]. The generated semi-quinone radical donates its unpaired electron to oxygen, forming superoxide radicals. By reducing oxygen to $O_2^{\bullet -}$, the Dox molecule is regenerated [11] (Fig. 3.3). Along with this redox-cycling process, ROS can be generated as a response to delayed perturbation of cell metabolism and function resulting from the treatment with Dox [13]. The production of hydroxyl radical and peroxynitrite by Dox, as well as the occurrence of lipid peroxidation, has also been reported [11, 14, 15]. Besides the ROS generation, Dox can hinder DNA synthesis by intercalation into the DNA or inhibition of topoisomerase II activity [11, 16]. These mechanisms seem to play a major role in the antitumor capacity of Dox. However, despite being widely used in a variety of solid tumors and hematological malignancies, the clinical use of this drug is limited by the occurrence of cardiotoxic effects, which are thought to be mainly due to an increase in oxidative stress [11, 15].

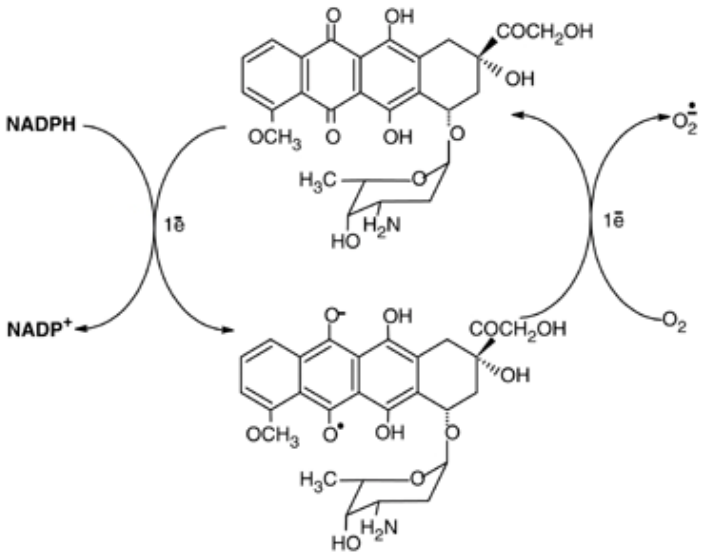


**Fig. 3.3** – Doxorubicin redox-cycling (adapted from [17]). Dox undergoes a one-electron reduction within the cell, originating a semi-quinone free radical. This radical donates its unpaired electron to oxygen, forming $O_2^{\bullet -}$ and regenerating the Dox molecule [11].

The involvement of ROS in several oxidative stress disorders has justified the study of low molecular weight SODm. Among these agents, MnPs have shown promising results due to their ability to scavenge a wide range of ROS, namely $O_2^{\bullet -}$, $ONOO^-$ and $ROO^\bullet$ radicals [18]. As described in Chapter 1 (section 1.2.2.), the SOD-like activity of the MnPs depends on changes in valence of the Mn center between Mn(III) and Mn(II) [18, 19]. The activity of MnPs over $ONOO^-$, as well as their capacity to inhibit lipid peroxidation, is related to the formation of an oxo–Mn(IV) complex that is reduced to Mn(III) by endogenous antioxidants [18-20].

The manganese(III)tetrakis-(1-methyl-4-pyridyl) porphyrin (MnTM-4-PyP) (Fig. 3.4) possesses important characteristics for a catalytic antioxidant: cell-permeability, water solubility, reversible redox behaviour with an appropriate reduction potential, high catalytic rate constant for $O_2^{\bullet -}$ dismutation [21] and the ability to inhibit lipid peroxidation [18, 19]. In addition, MnTM-4-PyP has shown promising results in different experimental models, such as cerebral ischemia [22], cardiac transplants [23], and neurodegeneration [24]. Despite these relevant data, only few cell-based studies have been reported and there is still the need to explore the behavior of MnTM-4-PyP in different models of oxidative stress.

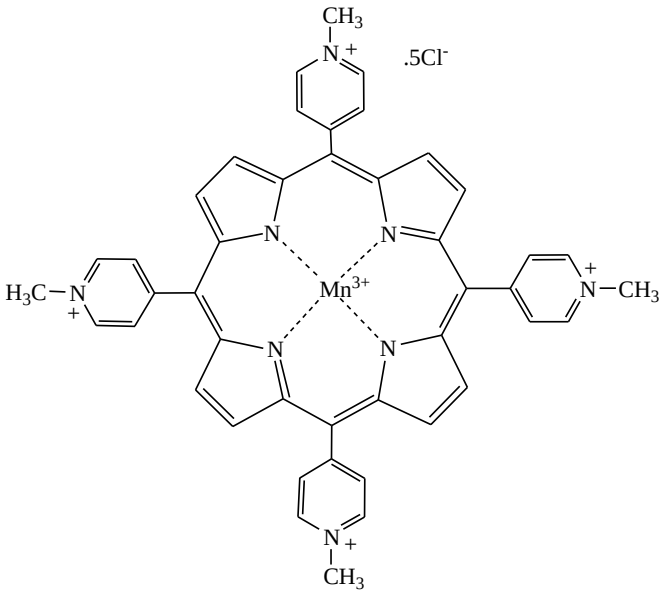


**Fig. 3.4 -** Chemical structure of the Mn(III) porphyrin MnTM-4-PyP.

In this context, the aim of this Chapter was to address the role of MnTM-4-PyP on the protection against the cytotoxicity induced by the aforementioned oxidants XXO, TBHP and Dox, in V79 cells. Complementary cytotoxicity endpoints, the MTT reduction and the CV assays, as well as the MI analysis as a measure of cell division, were studied. Moreover, the ROS generation induced by these oxidants and the effect of MnTM-4-PyP were assessed with the fluorescence probe DHE.

## 3.2. Materials and Methods

### *3.2.1. Chemicals*

Phosphate buffered saline (PBS; 0.01 M phosphate buffer, 0.138 M NaCl, 0.0027 M KCl, pH 7.4), Ham's F-10 medium, newborn calf serum, penicillin-streptomycin solution, trypsin, thiazolyl blue tetrazolium bromide (MTT), CV, Giemsa dye, xanthine, XO, TBHP, and Dox were obtained from Sigma-Aldrich. MnTM-4-PyP was purchased from Calbiochem (purity ≥ 95% by TLC). Colchicine was acquired from Fluka. Dimethylsulfoxide (DMSO) was obtained from Duchefa Biochimie. Ethanol, methanol and acetic acid were obtained from Merck. DHE was purchased from Molecular Probes. A 10 mM stock solution of DHE was prepared in DMSO, aliquotized and stored under $N_2$, at −18 ºC.

### *3.2.2. V79 Cells culture*

Wild-type V79 Chinese Hamster Cells (MZ), kindly provided by Prof. H.R. Glatt (Germany), were routinely maintained in 175 $cm^2$ culture flasks (Sarstedt) using Ham's F-10 medium, supplemented with 10% newborn calf serum and 1% antibiotic solution (penicillin-streptomycin) as the cell culture medium. The cells were kept at 37°C, under an atmosphere containing 5% $CO_2$.

### *3.2.3. Cytotoxicity assays*

For the cytotoxicity evaluation, two assays were performed. Due to the limitations inherent to each method and since the assessment of an effect on cellular viability may depend on the assay chosen, it is usually recommended the use of mechanistically different endpoints for a correct evaluation of xenobiotic cytotoxicity [25]. Therefore, the MTT assay, which is a measure of mitochondrial function [26], was primarily used. The CV method, which is a colorimetric determination of adherent cells [25, 27], was used as a confirmatory assay.

*3.2.3.1. MTT Reduction assay*

In this method, MTT (yellow salt) is converted by the mitochondrial enzymes of viable cells into a purple formazan (Fig. 3.5) which can be measured at 595 nm. The absorbance is proportional to the number of viable cells [28].

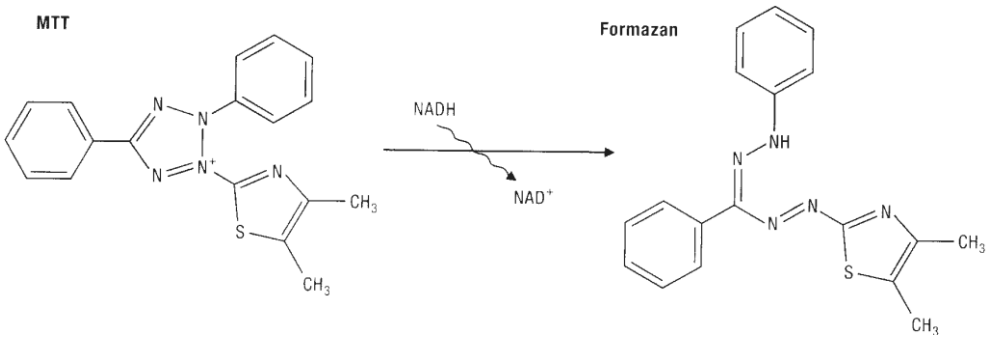


**Fig. 3.5** – MTT reduction in live cells by mitochondrial reductase results in the formation of a formazan derivative.

Approximately $6 \times 10^3$ cells were cultured in 200 μL of culture medium per well in 96-well plates and incubated for 24 hours at 37 °C under a 5% $CO_2$ atmosphere. The cells were then treated for a further 24 h period with each of the oxidants: X (240 μM)/XO (20 U/L), TBHP (100 μM) or Dox (2.5 μM) in the presence or absence of MnTM-4-PyP (0.1-100 μM). The concentrations of the oxidants were chosen so that a near equitoxic effect was achieved, with a decrease of ~50% in cell viability. Further concentrations were studied for TBHP (25, 50 and 200 μM) and Dox (5, 10 and 20 μM). The cytotoxicity induced by MnTM-4-PyP *per se* was also evaluated in the same experimental conditions. After the treatments, the cells were washed with culture medium and MTT (0.5 mg/mL in culture medium) was added to each well [29]. The cells were grown for a further period of 2.5 h and then carefully washed with PBS. DMSO (200 μL) was added to each well to solubilize the formazan crystals and absorbance was read at 595 nm. Two to eight independent experiments were performed and eight replicate cultures were used for each concentration in each independent experiment.

*3.2.3.2. Crystal Violet assay*

Approximately $3.5 \times 10^3$ cells were cultured in 200 μL of culture medium per well in 96-well plates and incubated at 37°C under a 5% $CO_2$ atmosphere. As in the MTT assay, the cells were grown for 24 h and then exposed to the oxidants described above with or without MnTM-4-PyP for a 24 h period. After the incubation, the cells were washed with PBS to remove non-adherent cells. The adherent cells were fixed with 96% ethanol for 10 min and then stained with 0.1% crystal violet in 10% ethanol for 5 min at room temperature. After staining, the extracellular dye was removed by rinsing thoroughly the cell monolayers with tap water. The remaining cell-attached dye was dissolved in 200 μL of 96% ethanol with 1% acetic acid, and the absorbance was measured at 595 nm. Two to four independent experiments were performed, each one comprising eight replicate cultures.

*3.2.4. Evaluation of the Mitotic Index*

Approximately $4 \times 10^5$ cells were cultured in 25 $cm^2$ culture flasks for 24 h. Afterwards, cells were exposed for 15 h to MnTM-4-PyP (2.5 and 100 μM), and/or to the oxidants: X (240 μM)/XO (40 U/L), TBHP (50 μM) or Dox (50 nM). These concentrations of the oxidants led to an evident MI reduction, yet to measurable values, thus allowing the detection of the possible effects of MnTM-4-PyP. A 15 h incubation period was chosen since it corresponds roughly to the duration of one cell cycle of V79 cells. After the exposure to the aforementioned agents, the culture medium was replaced by fresh medium and colchicine (0.7 μg/ml) was added. Cells were incubated for a further period of 2.5 h, and harvested by trypsinization. After a 3 min hypotonic treatment with 75 mM KCl at 37 ºC, the cells were fixed with methanol/acetic acid (3:1), and slides were prepared and stained with Giemsa (4% (v/v) in 0.01 M phosphate buffer, pH 6.8) for 10 min. Two to four independent experiments were performed for each sample. For each individual experiment, at least 1000 cells were scored using a 400× magnification on a light microscope, and the fraction of cells in mitosis - mitotic index, was determined.

*3.2.5. DHE fluorimetric assay*

DHE is a cell permeable probe that reacts with $O_2^{\bullet -}$ to form the fluorescent product 2-hydroxyethidium (Fig. 3.6) [30]. Although its reaction with other ROS may interfere with the fluorescence peak, the oxidation of DHE is mostly superoxide dependent [31, 32]. Therefore, the fluorescence intensity reflects approximately the intracellular levels of $O_2^{\bullet -}$.

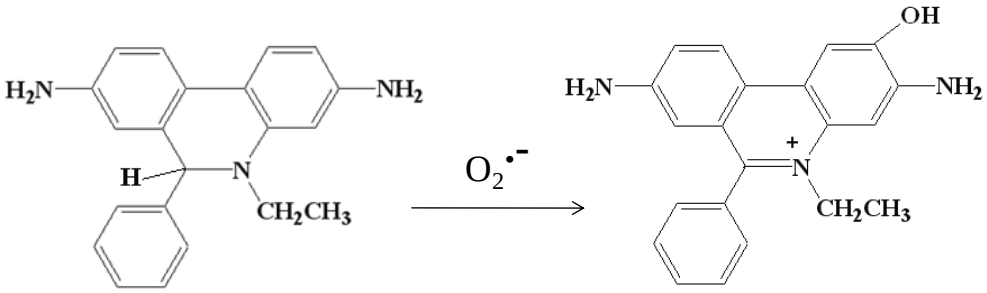


Dihydroethium (DHE) 2-Hydroxyethidium (2-OH-E$^+$)

**Fig. 3.6** – Reaction of dihydroethidium with $O_2^{\bullet -}$, originating the fluorescent product 2-hydroxyethidium.

In this assay, approximately $2 \times 10^4$ cells/well were cultured for 24 hours in 96-well plates (black-wall/clear-bottom - Costar 3603). Afterwards, the cells were exposed for 3 h to the oxidant systems in the presence or absence of MnTM-4-PyP and to DHE at a final concentration of 10 μM. The concentrations of the oxidants were: X (240 μM)/XO (100 and 200 U/L), TBHP (1 and 2 mM) and Dox (2.5, 5 and 10 μM). These concentrations of the oxidants allowed a marked increase in the fluorescence intensity. A 3 h incubation period was chosen due to the instability of ROS and also to avoid a pronounced cell death. Otherwise, changes in fluorescence intensity could result from differences in the number of cells and not necessarily in the level of ROS. After the treatments, the cells were carefully washed with PBS. 200 μL of PBS were then added to each well and the fluorescence was determined in a Zenyth 3100 microplate reader, using $\lambda_{excitation}$ = 485 nm and $\lambda_{emission}$ = 595 nm. The results were expressed as percentages of non-treated control cells, after subtracting the background fluorescence. Two to six

independent experiments were performed, each comprising six replicate cultures for each experimental point.

### *3.2.6. Statistical analysis*

The Kolmogorov-Smirnov test was used to assess the normality of continuous variables. For the variables with a normal distribution the homogeneity of the variances was evaluated using the Levene test, and the differences in mean values of the results observed in cultures with different treatments were evaluated by the Student's t-test. For non normal variables the Mann-Whitney test was used. All analyses were performed with the SPSS statistical package (version 15, SPSS Inc. Chicago IL).

### 3.3. Results and Discussion

The association of oxidative stress with several pathologies supports the development of polyfunctional antioxidants, such as MnTM-4-PyP. Despite the extensive research with this SODm, cell-based studies focused on oxidant models that exert their toxicity through distinct mechanisms are still required. In this context, this Chapter is focused on three oxidant systems: XXO, an extracellular $O_2^{\bullet-}$ generator; TBHP that generates $ROO^{\bullet}$ radicals in the cytosol; and Dox, which generates $O_2^{\bullet-}$ intracellularly.

#### *3.3.1. Effects of MnTM-4-PyP*

To properly study the XXO, TBHP and Dox oxidant models in the presence of MnTM-4-PyP, the effects induced by this compound *per se* were firstly evaluated in V79 cells. In the MTT reduction assay (Fig. 3.7A – white bars), after a 24 h-incubation period with MnTM-4-PyP, no cytotoxic effects were observed at lower concentrations (1, 10 and 50 μM). However, a decrease of ~12% in the MTT reduction was noticed at 100 μM ($P < 0.05$).

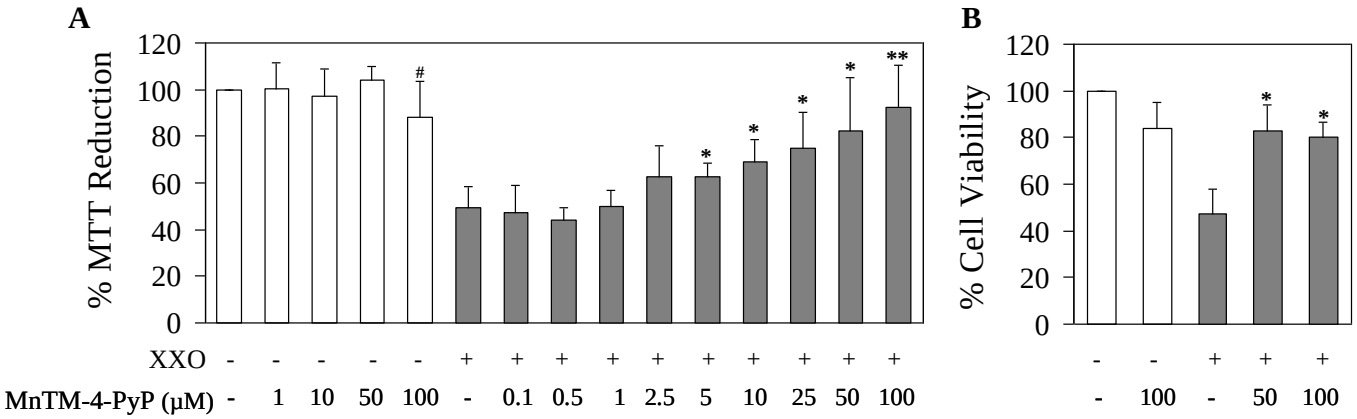


**Fig. 3.7 -** Effect of MnTM-4-PyP on the cytotoxicity induced by xanthine (240 μM) plus xanthine oxidase (20 U/L) in V79 cells - grey bars. Cells were incubated with increasing concentrations of MnTM-4-PyP in the presence of XXO for 24 h, and then submitted to the MTT (A) or to the CV (B) assays. (*$P < 0.05$ and **$P < 0.01$, when compared with XXO-treated cells without MnTM-4-PyP). The white bars present the cytotoxicity of MnTM-4-PyP *per se*. ($^{\#}$ $P < 0.05$ when compared with control cells).

The toxicity of MnTM-4-PyP (100 μM, 24 h) was confirmed by the CV method (Fig. 3.7B – white bars), where a ~16% decrease in cell viability was found. These results are in accordance to those reported by Kim *et al* [33], who have also observed a decrease in cell proliferation with MnTM-4-PyP.

The MI was evaluated as a measure of cell division and proliferation. This endpoint gives information on the possible cell cycle arrest induced by a given agent in colchicine-treated viable cells. The results are presented in Table III.1. Control cells presented a MI value of 9.0%, which was reduced to 7.8% by MnTM-4-PyP (2.5 and 100 μM).

**Table III.1** – Mitotic indices presented by V79 cells treated with the oxidants under study, in the absence or presence of MnTM-4-PyP.

| Treatment | [MnTM-4-PyP] (μM) | Mitotic Index[a] |
|---|---|---|
| Negative control | 0 | 9.0 ± 1.0 |
| MnTM-4-PyP | 2.5 | 7.8 ± 2.5 |
| | 100 | 7.8 ± 2.7 |
| Xanthine (240 μM) + XO (40 U/L) | 0 | 2.9 ± 0.1 ### |
| | 100 | 3.4 ± 1.1 |
| TBHP (50 μM) | 0 | 4.1 ± 0.5 ## |
| | 2.5 | 3.7 ± 0.3 |
| Dox (50 nM) | 0 | 5.5 ± 0.4 ## |
| | 100 | 5.2 ± 0.4 |

[a] These results are mean values ± SD from two to four independent experiments. Cells were exposed to the compounds for 15 h before colchicine treatment. At least 1000 cells were scored for each sample in each independent experiment ($^{\#\#}P < 0.01$ and $^{\#\#\#}P \leq 0.001$, when compared with non-treated control cells).

The exposure of V79 cells to MnTM-4-PyP (100 μM) for a 3 h-period resulted in a decrease of the levels of intracellular ROS ($P < 0.05$), as depicted in Fig. 3.8 (white bars). Decreases in the hydroxyethidium fluorescence were also observed by other authors using different mammalian cell lines exposed to MnTM-4-PyP [32] or other MnPs [34]. Although the DHE assay was performed using a shorter incubation period than the cell viability and MI assays, the abrogation of basal ROS herein observed may contribute to explain the decrease in those parameters, since ROS can act as signalling molecules in cell proliferation [1]. However, other mechanisms may be involved since it has been reported that MnPs could interfere with biological structures like DNA [35, 36] or lipid membranes [37].

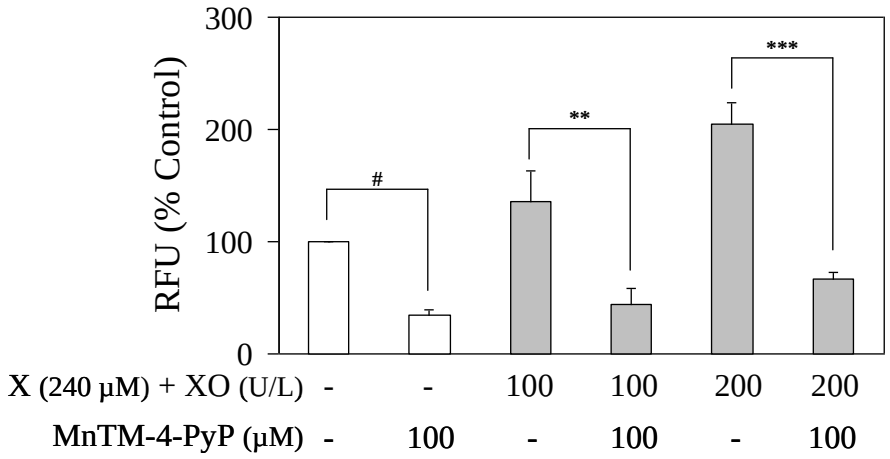


**Fig. 3.8** - Effect of MnTM-4-PyP on the intracellular superoxide anion levels, in the absence (white bars) or presence (grey bars) of xanthine (240 μM) plus xanthine oxidase (100 or 200 U/L), as evaluated by the oxidation of DHE. Values (mean ± SD) represent relative fluorescence units (RFU) and are expressed as percentages of the control cells. ($^{\#}P < 0.05$ when compared with non-treated control cells; $^{**}P < 0.01$ and $^{***}P < 0.001$ when compared with XXO-treated cells without MnTM-4-PyP).

*3.3.2. Effects of MnTM-4-PyP in XXO-treated cells*

XXO has been extensively used to study the antioxidant profile of a given compound [2, 3]. However, scarce information is available concerning the role of SODm, and especially MnTM-4-PyP on the modulation of the toxicity induced by this system. When V79 cells were exposed for 24 h to X (240 μM)/XO (20 U/L), a significant decrease in cell

viability was observed ($P < 0.05$), both in the MTT and in the CV assays (Fig. 3.7 – grey bars). The addition of MnTM-4-PyP to XXO exposed cells led to a pronounced protective effect. As shown in the MTT results (Fig. 3.7A – grey bars), the protection was dose-dependent and for concentrations of 5 μM and higher the effect of MnTM-4-PyP against the XXO-induced toxicity was statistically significant ($P < 0.05$). A maximum protection was achieved with 100 μM of MnTM-4-PyP, which allowed the cell survival to increase from ~50% to ~90% ($P < 0.01$). In the CV assay, a significant effect ($P < 0.05$) was also observed for concentrations of 50 μM and 100 μM of MnTM-4-PyP, as depicted in Fig. 3.7B – grey bars. Thus, the 100 μM concentration of MnTM-4-PyP was selected for the DHE and MI assays. These protective effects can be explained by the SOD-like activity of MnTM-4-PyP. Since XXO is an extracellular generator of superoxide, the dismutation of this radical by MnTM-4-PyP in the extracellular medium is likely to contribute to the protection observed. It is also important to mention that a control experiment was performed in order to exclude the possibility of a direct inhibition of XO by MnTM-4-PyP (data not shown). While xanthine is oxidized by XO, concomitantly to the production of $O_2^{\bullet-}$, uric acid is produced (Fig. 3.1) and its production can be monitored at 293 nm [5, 38]. As it was also previously shown by Faulkner *et al* [21] using different experimental conditions, MnTM-4-PyP did not decrease the production of uric acid by XXO, confirming that the generation $O_2^{\bullet-}$ by XXO was not inhibited. Therefore, the effects observed in the biological assays are effectively due to the disproportionation of the superoxide anion and not a consequence of an inhibition of the $O_2^{\bullet-}$ generation.

In the DHE assay, V79 cells were incubated for 3 h with xanthine (240 μM) plus XO (100 and 200 U/L). Despite the fact that XXO produces superoxide in the extracellular medium, our results indicate that also the intracellular level of ROS is increased after an exposure to this oxidant system (Fig. 3.8 – grey bars). This is in accordance with other authors that using different mammalian cell lines also found increases in the intracellular ROS in XXO-treated cells [39, 40]. Some authors pointed out that the XXO system can produce $H_2O_2$ along with superoxide [6]. Since the DHE probe is considered to be quite insensitive to $H_2O_2$ [31] superoxide appears to be the major species involved in the DHE fluorescence in cells treated with XXO. The exposure of XXO-treated cells to MnTM-4-PyP (100 μM) led to a decrease in the fluorescence intensity to values lower than those presented by the non-treated control cells (Fig. 3.8); this reduction can be explained by the dismutation of superoxide by MnTM-4-PyP.

The exposure of V79 cells to X (240 μM)/XO (40 U/L) resulted in a pronounced reduction of the MI value, from 9.0% to 2.9% ($P \leq 0.001$) (Table III.1). In fact, many oxidative agents are known to impair cell division, dramatically reducing the MI and other proliferation indices [41, 42]. The concomitant incubation with MnTM-4-PyP only led to a slight and non-significant increase of the MI, to a value of 3.4 %, indicating a negligible effect of MnTM-4-PyP at the cell division level.

### *3.3.3. Effects of MnTM-4-PyP in TBHP-treated cells*

Despite the extensive use of TBHP as an oxidant model, few studies to assess the effect of MnPs towards this agent are available. Figs. 3.9 and 3.10 show the effect of MnTM-4-PyP against the cytotoxicity induced by TBHP.

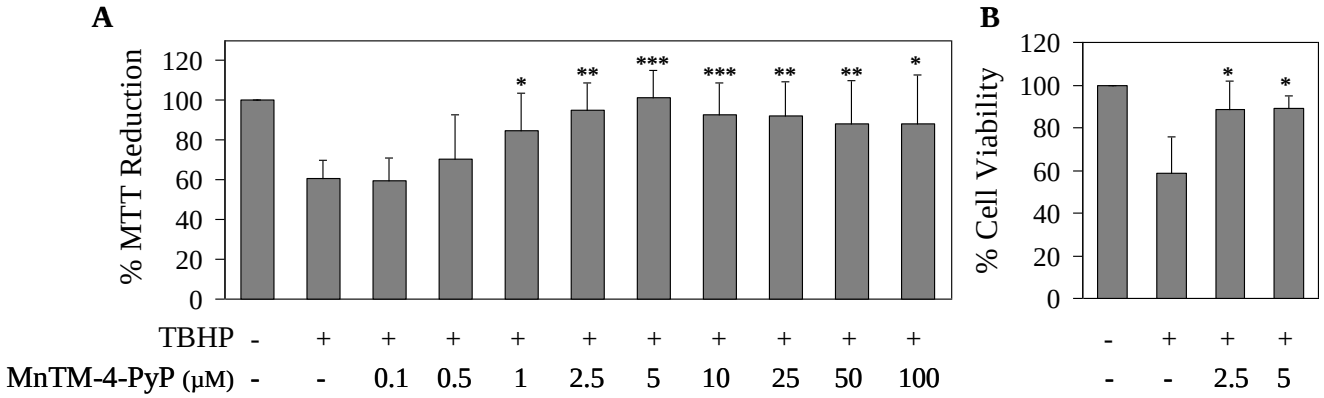


**Fig. 3.9 -** Effect of MnTM-4-PyP on the cytotoxicity induced by TBHP (100 μM) in V79 cells. Cells were incubated with increasing concentrations of MnTM-4-PyP in the presence of TBHP for 24 h, and then submitted to the MTT (A) or to the CV (B) assays.
(* $P \leq 0.05$, ** $P \leq 0.01$ and *** $P \leq 0.001$, when compared with TBHP-treated cells without MnTM-4-PyP).

The exposure of V79 cells to TBHP (100 μM) resulted in a considerable decrease in the MTT reduction ($P < 0.001$), as well as in the CV staining ($P < 0.05$). When the effect of MnTM-4-PyP against TBHP-induced cytotoxicity was studied using the MTT assay, a marked protective effect was observed (Fig. 3.9A). This protection was significant for all

concentrations of MnTM-4-PyP ≥ 1 μM. MnTM-4-PyP (2.5 and 5 μM) has also shown a significant protection ($P \leq 0.05$) using the CV assay (Fig. 3.9B).

To further characterize this profile of protection, studies were performed with a range of TBHP concentrations (25 - 200 μM), using the MTT assay. The results are depicted in Fig. 3.10 and confirm that low concentrations of MnTM-4-PyP (2.5, 5 and 10 μM) can be effective in the reduction of TBHP-induced cytotoxicity. Concentrations of MnTM-4-PyP of 2.5 and 5 μM were therefore chosen for the MI evaluation and the DHE assay.

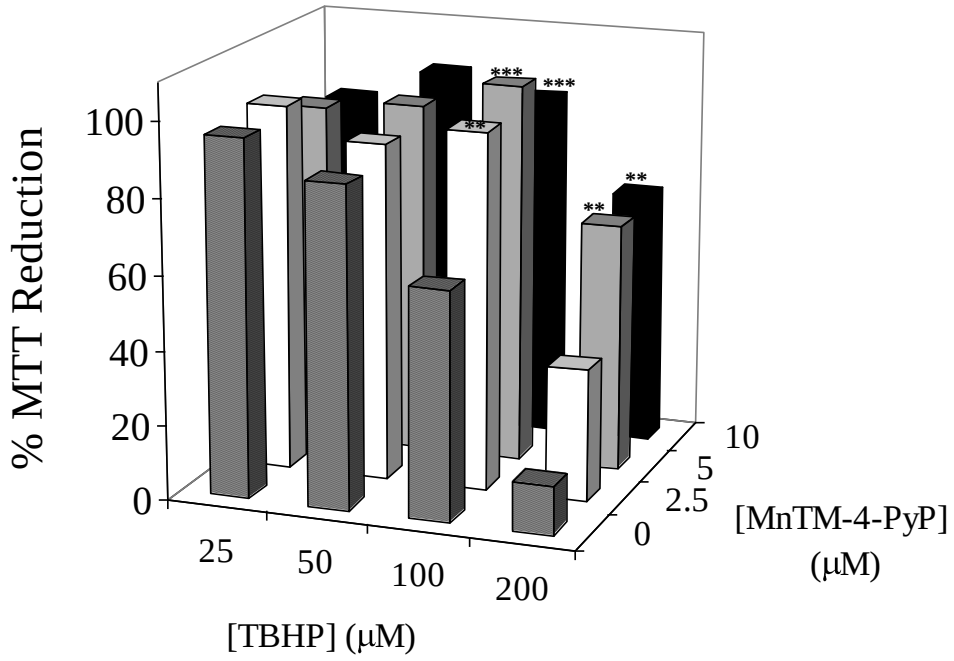


**Fig. 3.10 -** Effect of MnTM-4-PyP on the cytotoxicity induced by TBHP in V79 cells, as evaluated by the MTT assay. Cells were incubated with increasing concentrations of MnTM-4-PyP (2.5-10 μM) in the presence of different concentrations of TBHP (25-200 μM) for 24 h. (**$P$ < 0.01 and ***$P$ < 0.001, when compared with cells treated with the same concentration of TBHP in the absence of MnTM-4-PyP).

As shown by the DHE assay, the exposure to TBHP (1.0 and 2.0 mM, 3 h) led to a significant increase in the intracellular level of $O_2^{\bullet-}$ in V79 cells (Fig. 3.11). An increase in the fluorescence intensity was also observed by Scanlon and Reynolds [43] after exposing DHE-loaded neurons to TBHP. Additionally, the production of $O_2^{\bullet-}$ by TBHP was previously reported by Awe *et al* [10]. In the present experiments, MnTM-4-PyP (5.0 μM) completely abolished the effect of TBHP ($P < 0.05$, Fig. 3.11), suggesting that the scavenging of ROS, including superoxide anion may be involved in the protection afforded by this SODm. In addition, MnTM-4-PyP has previously shown the capacity to inhibit lipid peroxidation [44]. The ability of MnTM-4-PyP to decompose peroxyl radicals may therefore be a relevant mechanism for the abrogation of the TBHP toxicity.

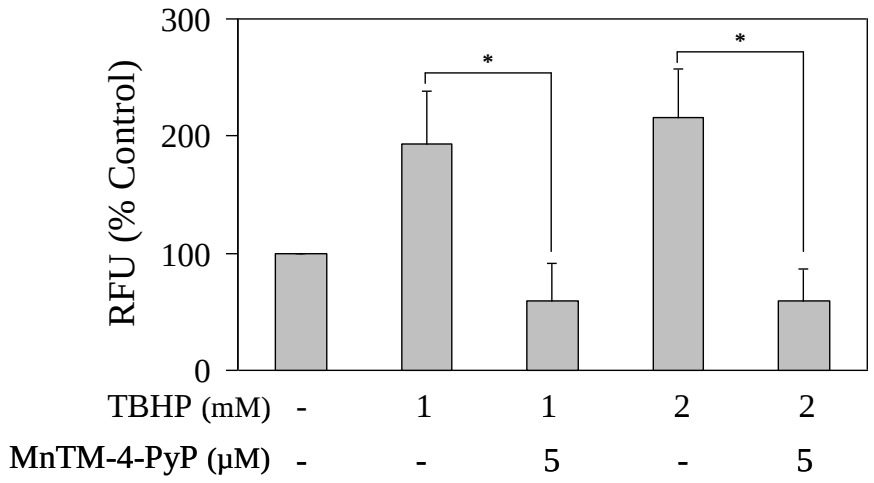


**Fig. 3.11** - Effect of MnTM-4-PyP on the intracellular superoxide anion levels in cells treated with TBHP (1.0 or 2.0 mM), as evaluated by the oxidation of DHE. Values (mean ± SD) represent relative fluorescence units (RFU) and are expressed as percentages of the control cells. (*$P < 0.05$ when compared with TBHP-treated cells without MnTM-4-PyP).

The exposure of V79 cells to TBHP (50 μM) led to a reduction of the MI value from 9.0% to 4.1% ($P < 0.01$). The concomitant incubation with MnTM-4-PyP did not change considerably the MI value (Table III.1). This absence of effect by MnTM-4-PyP that was also above mentioned for the XXO system may be a consequence of DNA repair. When oxidative DNA damage occurs, cell cycle arrest is essential to allow time to deal with the inflicted damage, thus preventing the propagation of potentially deleterious errors [45].

*3.3.4. Effects of MnTM-4-PyP in Dox-treated cells*

As aforementioned, Dox can injure cells through different mechanisms, including the generation of ROS. The incubation of V79 cells with Dox (2.5 μM) for 24 h resulted in a significant inhibition of the MTT reduction ($P < 0.01$). The treatment with MnTM-4-PyP (1 - 100 μM), did not alter the % MTT reduction presented by Dox, as shown in Fig. 3.12A.

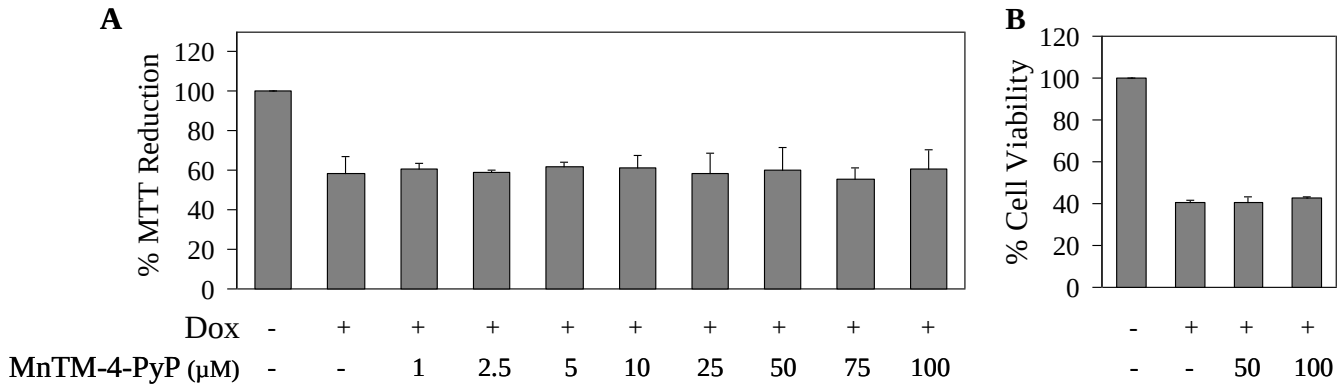


**Fig. 3.12 -** Effect of MnTM-4-PyP on the cytotoxicity induced by Dox in V79 cells. Cells were incubated with increasing concentrations of MnTM-4-PyP in the presence of Dox (2.5 μM) for 24 h, and then submitted to the MTT assay (A). The panel B represents the results obtained with the CV assay for the exposure of V79 cells to MnTM-4-PyP and Dox (5 μM).

To confirm these data, studies were performed using a range of Dox concentrations up to 20 μM. Only slight but non-significant protective effects were observed (Fig. 3.13). The CV staining (Fig. 3.12B) was performed for Dox (5 μM) in the presence of MnTM-4-PyP (50 and 100 μM) and no changes in cell viability were observed. Also, the cell division impairment induced by Dox (50 nM), expressed as a decrease in the MI value from 9.0% to 5.5% ($P < 0.01$), was not considerably changed by MnTM-4-PyP (Table III.1).

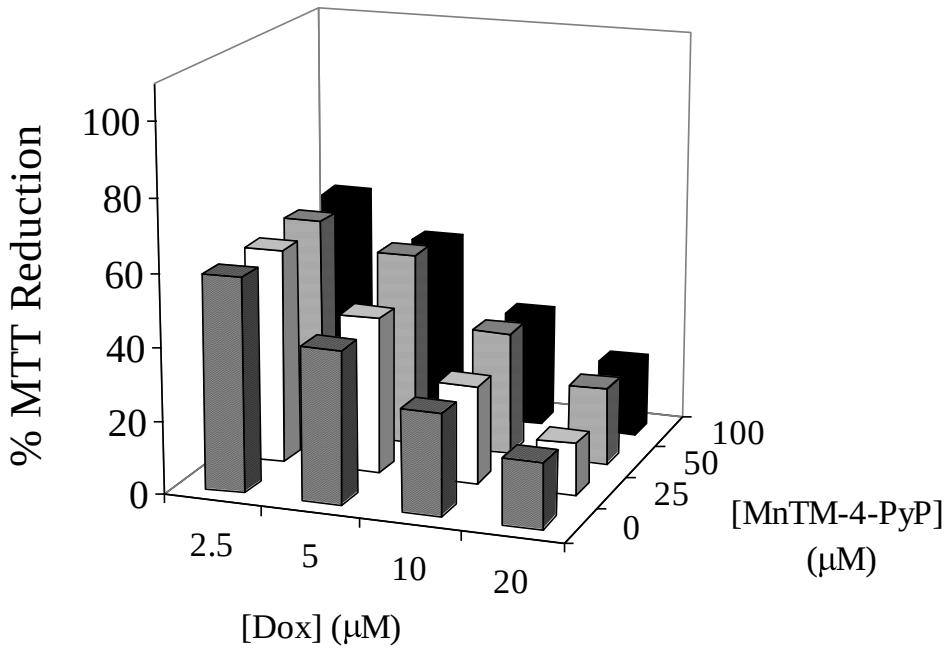


**Fig. 3.13 -** Effect of MnTM-4-PyP on the cytotoxicity induced by Dox in V79 cells, as evaluated by the MTT assay. Cells were incubated with increasing concentrations of MnTM-4-PyP (25-100 μM) in the presence of different concentrations of Dox (2.5-20 μM) for 24 h.

In the DHE assay, the intracellular production of ROS was observed in cells exposed to Dox (2.5, 5 and 10 μM) for 3 h (Fig. 3.14). The concomitant incubation with MnTM-4-PyP (100 μM) resulted in a significant decrease of fluorescence for 2.5 μM of Dox. The fluorescence intensity of cells treated with 5 μM of Dox has also decreased in the presence of MnTM-4-PyP (non significant), although no effect was observed for the 10 μM concentration. At this concentration, we can not rule out that the generation of $O_2^{\bullet -}$ can somehow overwhelm the activity of MnTM-4-PyP. Further studies using more potent *ortho*-subsituted MnPs, namely MnTM-2-PyP, MnTE-2-PyP or MnTnHex-2-PyP [36, 46] could give some additional insight on this matter. *Ortho*-substituted porphyrins also possess different stericity than the *para*- analogues. Being bulkier, they interact differently with biological molecules, what may give additional mechanistic insights particularly in relation to Dox.

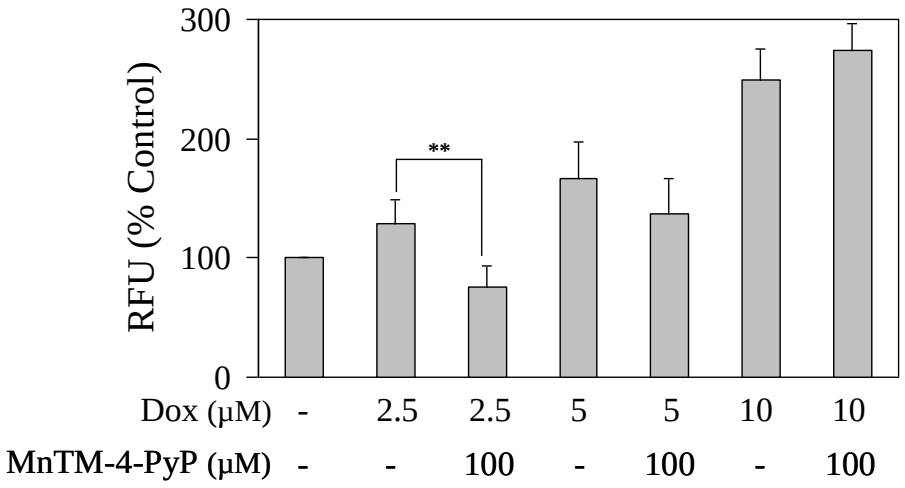


**Fig. 3.14 -** Effect of MnTM-4-PyP on the superoxide anion levels in cells treated with Dox (2.5, 5 or 10 μM), as evaluated by the oxidation of DHE. Values (mean ± SD) represent relative fluorescence units (RFU) and are expressed as percentages of the control cells. (**$P < 0.01$ when compared with Dox-treated cells without MnTM-4-PyP).

The results presented here suggest the complexity of mechanisms of action presented by Dox. It is usually mentioned that while Dox-induced cardiotoxicity seems to be mediated by free radicals formation, the antitumor activity of this drug is mainly due to non-radical dependant mechanisms [1, 11, 15]. Cell type specificities may therefore be involved in this lack of protection. Konorev *et al* [47] have reported protective results using a different manganese porphyrin – MnTBAP, in Dox-treated cardiomyocytes. It has been reported that cardiomyocytes are particularly vulnerable to the oxidative stress induced by Dox because of their relatively modest antioxidant defenses [1, 11, 15]. This fact may justify the diverse responses to oxidative stress and antioxidants between cardiomyocytes and other cell types. To clarify the potential role of MnTM-4-PyP against Dox-toxicity in mammalian cells, similar studies using cardiomyocytes should also be considered.

### *3.3.5. Conclusion*

In this Chapter, MnTM-4-PyP presented differential responses, depending on the oxidant system. Clear protective effects were observed against the cytotoxicity of XXO and

TBHP, whereas no considerable protection was found for Dox. These results emphasize the importance of the mechanisms of toxicity inherent to each oxidant model on the responses of MnTM-4-PyP, and reinforce the need to study different models and experimental conditions for the adequate evaluation of the potentialities of a catalytic antioxidant. Moreover, the data obtained within this Chapter allowed the validation of two models of oxidative stress injury, XXO and TBHP, in which the well established SODm MnTM-4-PyP was a protective antioxidant. These models are useful tools to study novel SODm compounds and were applied to study the potential antioxidant effects of macrocyclic copper(II) complexes synthesized and developed within the scope of the present thesis (Chapters 5 and 6).

### 3.4 - References


[1] Halliwell, B.; Gutterdige, J. M. C. *Free Radicals in Biology and Medicine.* New York: Oxford University Press; 2007.

[2] Li, Y.; Cao, Z.; Zhu, H. Upregulation of endogenous antioxidants and phase 2 enzymes by the red wine polyphenol, resveratrol in cultured aortic smooth muscle cells leads to cytoprotection against oxidative and electrophilic stress. *Pharmacol Res* **53:**6-15; 2006.

[3] Rah, D. K.; Han, D. W.; Baek, H. S.; Hyon, S. H.; Park, J. C. Prevention of reactive oxygen species-induced oxidative stress in human microvascular endothelial cells by green tea polyphenol. *Toxicol Lett* **155:**269-275; 2005.

[4] Fattman, C. L.; Schaefer, L. M.; Oury, T. D. Extracellular superoxide dismutase in biology and medicine. *Free Radic Biol Med* **35:**236-256; 2003.

[5] Bienvenue, E.; Choua, S.; Lobo-Recio, M.-A.; Marzin, C.; Pacheco, P.; Seta, P.; Tarrago, G. Structure and superoxide dismutase activity of Ru(II), Cu(II), and Mn(II) macrocyclic complexes. *J Inorg Biochem* **57:**157-168; 1995.

[6] Kellogg, E. W., 3rd; Fridovich, I. Superoxide, hydrogen peroxide, and singlet oxygen in lipid peroxidation by a xanthine oxidase system. *J Biol Chem* **250:**8812-8817; 1975.

[7] Lazze, M. C.; Pizzala, R.; Savio, M.; Stivala, L. A.; Prosperi, E.; Bianchi, L. Anthocyanins protect against DNA damage induced by tert-butyl-hydroperoxide in rat smooth muscle and hepatoma cells. *Mutat Res* **535:**103-115; 2003.

[8] Park, J. E.; Yang, J. H.; Yoon, S. J.; Lee, J. H.; Yang, E. S.; Park, J. W. Lipid peroxidation-mediated cytotoxicity and DNA damage in U937 cells. *Biochimie* **84:**1199-1205; 2002.

[9] Piret, J. P.; Arnould, T.; Fuks, B.; Chatelain, P.; Remacle, J.; Michiels, C. Mitochondria permeability transition-dependent tert-butyl hydroperoxide-induced apoptosis in hepatoma HepG2 cells. *Biochem Pharmacol* **67:**611-620; 2004.

[10] Awe, S. O.; Adeagbo, A. S. Analysis of tert-butyl hydroperoxide induced constrictions of perfused vascular beds in vitro. *Life Sci* **71:**1255-1266; 2002.

[11] Keizer, H. G.; Pinedo, H. M.; Schuurhuis, G. J.; Joenje, H. Doxorubicin (adriamycin): a critical review of free radical-dependent mechanisms of cytotoxicity. *Pharmacol Ther* **47:**219-231; 1990.

[12] Berthiaume, J. M.; Wallace, K. B. Adriamycin-induced oxidative mitochondrial cardiotoxicity. *Cell Biol Toxicol* **23:**15-25; 2007.

[13] Minotti, G.; Menna, P.; Salvatorelli, E.; Cairo, G.; Gianni, L. Anthracyclines: molecular advances and pharmacologic developments in antitumor activity and cardiotoxicity. *Pharmacol Rev* **56:**185-229; 2004.

[14] Denicola, A.; Radi, R. Peroxynitrite and drug-dependent toxicity. *Toxicology* **208:**273-288; 2005.

[15] Takemura, G.; Fujiwara, H. Doxorubicin-induced cardiomyopathy from the cardiotoxic mechanisms to management. *Prog Cardiovasc Dis* **49:**330-352; 2007.

[16] Kiyomiya, K.; Matsuo, S.; Kurebe, M. Differences in intracellular sites of action of Adriamycin in neoplastic and normal differentiated cells. *Cancer Chemother Pharmacol* **47:**51-56; 2001.

[17] Kostrzewa-Nowak, D.; Paine, M. J.; Wolf, C. R.; Tarasiuk, J. The role of bioreductive activation of doxorubicin in cytotoxic activity against leukaemia HL60-sensitive cell line and its multidrug-resistant sublines. *Br J Cancer* **93:**89-97; 2005.

[18] Patel, M.; Day, B. J. Metalloporphyrin class of therapeutic catalytic antioxidants. *Trends Pharmacol Sci* **20:**359-364; 1999.

[19] Day, B. J. Catalytic antioxidants: a radical approach to new therapeutics. *Drug Discov Today* **9:**557-566; 2004.

[20] Ferrer-Sueta, G.; Vitturi, D.; Batinic-Haberle, I.; Fridovich, I.; Goldstein, S.; Czapski, G.; Radi, R. Reactions of manganese porphyrins with peroxynitrite and carbonate radical anion. *J Biol Chem* **278:**27432-27438; 2003.

[21] Faulkner, K. M.; Liochev, S. I.; Fridovich, I. Stable Mn(III) porphyrins mimic superoxide dismutase in vitro and substitute for it in vivo. *J Biol Chem* **269:**23471-23476; 1994.

[22] Sharma, S. S.; Gupta, S. Neuroprotective effect of MnTMPyP, a superoxide dismutase/catalase mimetic in global cerebral ischemia is mediated through reduction of oxidative stress and DNA fragmentation. *Eur J Pharmacol* **561:**72-79; 2007.

[23] Nilakantan, V.; Zhou, X.; Hilton, G.; Shi, Y.; Baker, J. E.; Khanna, A. K.; Pieper, G. M. Antagonizing reactive oxygen by treatment with a manganese (III) metalloporphyrin-based superoxide dismutase mimetic in cardiac transplants. *J Thorac Cardiovasc Surg* **131:**898-906; 2006.

[24] Wang, T.; Liu, B.; Qin, L.; Wilson, B.; Hong, J. S. Protective effect of the SOD/catalase mimetic MnTMPyP on inflammation-mediated dopaminergic neurodegeneration in mesencephalic neuronal-glial cultures. *J Neuroimmunol* **147:**68-72; 2004.

[25] Chiba, K.; Kawakami, K.; Tohyama, K. Simultaneous evaluation of cell viability by Neutral Red, MTT and Crystal violet staining assays of the same cells. *Toxicol In Vitro* **12:**251-258; 1998.

[26] Carmichael, J.; DeGraff, W. G.; Gazdar, A. F.; Minna, J. D.; Mitchell, J. B. Evaluation of a tetrazolium-based semiautomated colorimetric assay: assessment of chemosensitivity testing. *Cancer Res* **47:**936-942; 1987.

[27] Mickuviene, I.; Kirveliene, V.; Juodka, B. Experimental survey of non-clonogenic viability assays for adherent cells in vitro. *Toxicol In Vitro* **18:**639-648; 2004.

[28] Mitchell, J. B. Potential applicability of nonclonogenic measurements to clinical oncology. *Radiat Res* **114:**401-414; 1988.

[29] Alves, I.; Oliveira, N. G.; Laires, A.; Rodrigues, A. S.; Rueff, J. Induction of micronuclei and chromosomal aberrations by the mycotoxin patulin in mammalian cells: role of ascorbic acid as a modulator of patulin clastogenicity. *Mutagenesis* **15:**229-234; 2000.

[30] Zhao, H.; Joseph, J.; Fales, H. M.; Sokoloski, E. A.; Levine, R. L.; Vasquez-Vivar, J.; Kalyanaraman, B. Detection and characterization of the product of hydroethidine and intracellular superoxide by HPLC and limitations of fluorescence. *Proc Natl Acad Sci U S A* **102:**5727-5732; 2005.

[31] Tarpey, M. M.; Wink, D. A.; Grisham, M. B. Methods for detection of reactive metabolites of oxygen and nitrogen: in vitro and in vivo considerations. *Am J Physiol Regul Integr Comp Physiol* **286:**R431-444; 2004.

[32] Peshavariya, H. M.; Dusting, G. J.; Selemidis, S. Analysis of dihydroethidium fluorescence for the detection of intracellular and extracellular superoxide produced by NADPH oxidase. *Free Radic Res* **41:**699-712; 2007.

[33] Kim, B. Y.; Han, M. J.; Chung, A. S. Effects of reactive oxygen species on proliferation of Chinese hamster lung fibroblast (V79) cells. *Free Radic Biol Med* **30:**686-698; 2001.

[34] Rose, P.; Whiteman, M.; Huang, S. H.; Halliwell, B.; Ong, C. N. beta-Phenylethyl isothiocyanate-mediated apoptosis in hepatoma HepG2 cells. *Cell Mol Life Sci* **60:**1489-1503; 2003.

[35] Ferrer-Sueta, G.; Batinic-Haberle, I.; Spasojevic, I.; Fridovich, I.; Radi, R. Catalytic scavenging of peroxynitrite by isomeric Mn(III) N-methylpyridylporphyrins in the presence of reductants. *Chem Res Toxicol* **12:**442-449; 1999.

[36] Batinic-Haberle, I.; Benov, L.; Spasojevic, I.; Fridovich, I. The ortho effect makes manganese(III) meso-tetrakis(N-methylpyridinium-2-yl)porphyrin a powerful and potentially useful superoxide dismutase mimic. *J Biol Chem* **273:**24521-24528; 1998.

[37] Gauter-Fleckenstein, B.; Fleckenstein, K.; Owzar, K.; Jiang, C.; Batinic-Haberle, I.; Vujaskovic, Z. Comparison of two Mn porphyrin-based mimics of superoxide dismutase in pulmonary radioprotection. *Free Radic Biol Med* **44:**982-989; 2008.

[38] Dillon, C. T.; Hambley, T. W.; Kennedy, B. J.; Lay, P. A.; Zhou, Q.; Davies, N. M.; Biffin, J. R.; Regtop, H. L. Gastrointestinal toxicity, antiinflammatory activity, and superoxide dismutase activity of copper and zinc complexes of the antiinflammatory drug indomethacin. *Chem Res Toxicol* **16:**28-37; 2003.

[39] Mody, N.; Parhami, F.; Sarafian, T. A.; Demer, L. L. Oxidative stress modulates osteoblastic differentiation of vascular and bone cells. *Free Radic Biol Med* **31:**509-519; 2001.

[40] Bai, X. C.; Lu, D.; Liu, A. L.; Zhang, Z. M.; Li, X. M.; Zou, Z. P.; Zeng, W. S.; Cheng, B. L.; Luo, S. Q. Reactive oxygen species stimulates receptor activator of NF-kappaB ligand expression in osteoblast. *J Biol Chem* **280:**17497-17506; 2005.

[41] Dumont, P.; Burton, M.; Chen, Q. M.; Gonos, E. S.; Frippiat, C.; Mazarati, J. B.; Eliaers, F.; Remacle, J.; Toussaint, O. Induction of replicative senescence biomarkers by sublethal oxidative stresses in normal human fibroblast. *Free Radic Biol Med* **28:**361-373; 2000.

[42] Santoro, A.; Lioi, M. B.; Monfregola, J.; Salzano, S.; Barbieri, R.; Ursini, M. V. L-Carnitine protects mammalian cells from chromosome aberrations but not from inhibition of cell proliferation induced by hydrogen peroxide. *Mutat Res* **587:**16-25; 2005.

[43] Scanlon, J. M.; Reynolds, I. J. Effects of oxidants and glutamate receptor activation on mitochondrial membrane potential in rat forebrain neurons. *J Neurochem* **71:**2392-2400; 1998.

[44] Day, B. J.; Batinic-Haberle, I.; Crapo, J. D. Metalloporphyrins are potent inhibitors of lipid peroxidation. *Free Radic Biol Med* **26:**730-736; 1999.

[45] Harrington, E. A.; Bruce, J. L.; Harlow, E.; Dyson, N. pRB plays an essential role in cell cycle arrest induced by DNA damage. *Proc Natl Acad Sci U S A* **95:**11945-11950; 1998.

[46] Lahaye, D.; Muthukumaran, K.; Hung, C. H.; Gryko, D.; Reboucas, J. S.; Spasojevic, I.; Batinic-Haberle, I.; Lindsey, J. S. Design and synthesis of manganese porphyrins with tailored lipophilicity: investigation of redox properties and superoxide dismutase activity. *Bioorg Med Chem* **15:**7066-7086; 2007.

[47] Konorev, E. A.; Kennedy, M. C.; Kalyanaraman, B. Cell-permeable superoxide dismutase and glutathione peroxidase mimetics afford superior protection against doxorubicin-induced cardiotoxicity: the role of reactive oxygen and nitrogen intermediates. *Arch Biochem Biophys* **368:**421-428; 1999.

# Chapter 4

## Protective role of *ortho*-substituted Mn(III) *N*-alkylpyridylporphyrins against the oxidative injury induced by *tert*-butylhydroperoxide

This Chapter was adapted from:

Protective role of *ortho*-substituted Mn(III) *N*-alkylpyridylporphyrins against the oxidative injury induced by *tert*-butylhydroperoxide. A.S. Fernandes, J. Gaspar, M.F. Cabral, J. Rueff, M. Castro, I. Batinic-Haberle, J. Costa, N.G. Oliveira. Free Radical Research (2010) 44, 430-440.

**Abstract**

This Chapter addresses the role of two *ortho*-substituted Mn(III) *N*-alkylpyridylporphyrins, alkyl being ethyl in MnTE-2-PyP$^{5+}$ and n-hexyl in MnTnHex-2-PyP$^{5+}$, on the protection against the oxidant TBHP. Their protective role was studied in V79 cells using endpoints of cell viability (MTT and CV assays), intracellular $O_2^{\bullet-}$ generation (DHE assay) and glutathione status (DTNB and monochlorobimane assays). MnPs *per se* did not show cytotoxicity in V79 cells (up to 25 μM, 24 h). The exposure to TBHP resulted in a significant decrease in cell viability and in an increase in the intracellular $O_2^{\bullet-}$ levels. Also, TBHP depleted total and reduced glutathione and increased GSSG. The two MnPs counteracted remarkably the effects of TBHP. Even at low concentrations, both MnPs were protective in terms of cell viability and abrogated the intracellular $O_2^{\bullet-}$ increase in a significant way. Also, they augmented markedly the total and reduced glutathione contents in TBHP-treated cells, highlighting the multiple mechanisms of protection of these SODm, which at least partially may be ascribed to their electron-donating ability.

## 4.1. Introduction

Manganese porphyrins (MnPs) are among the most effective functional catalytic antioxidants [1, 2] and have been showing remarkable effects in different models of oxidative stress [3]. As stated in Chapter 1 (section 1.2.2), these compounds have the ability to scavenge a wide range of ROS, namely $O_2^{\bullet-}$, $ONOO^-$ and $ROO^\bullet$ radicals due to their several *in vivo* easily accessible oxidation states (+2, +3, +4, +5) [3]. Furthermore, the mitigation of oxidative damage by MnPs seems to involve the modulation of cellular redox-based metabolic pathways (e.g. HIF-1α, NF-kB, and AP-1 transcription factors) [4-8].

In Chapter 3 the ability of the Mn(III) *para* methylpyridylporphyrin MnTM-4-PyP, to cope with the cytotoxicity induced by XXO, TBHP and Dox was studied, and the possibility of evaluating *ortho*-substituted analogues was raised. *Ortho*-substituted porphyrins have been developed based on structure-activity relationship [1, 9, 10] and possess among the highest catalytic rate constants for $O_2^{\bullet-}$ dismutation, due to a combined effect of inductive, resonance, steric and electrostatic factors [9]. When the positive charge is moved from *para* onto *ortho* position of the pyridyl groups, i.e. closer to the porphyrin ring, the redox potential at the manganese site shifts to around +300 mV *vs* NHE. This is the midway potential between the oxidation and reduction of $O_2^{\bullet-}$ which allows equal facilitation for both steps of dismutation process, and thus the optimal $k_{cat}$ on thermodynamic basis. Another factor that contributes to the antioxidant potency of the *ortho* isomers is the presence of positive charges close to the porphyrin ring that guide negatively charged $O_2^{\bullet-}$ to the metal center [1, 11, 12]. It has been further demonstrated that $k_{cat}$ for the $O_2^{\bullet-}$ dismutation parallels the rate constant for $ONOO^-$ reduction. Same thermodynamic as well as electrostatic facilitation for the approach of negatively charged $ONOO^-$ to the Mn site is assured [13]. Finally, and as stated above, the same mechanism of action with $ROO^\bullet$ as with $ONOO^-$ is presumably operative. When compared to *para* analogues, the *ortho* isomers are further bulkier and thus do not interact significantly with nucleic acids, and are in turn expected to be less toxic [9]. This Chapter studies two *ortho*-substituted MnPs, MnTE-2-PyP and MnTnHex-2-PyP (Fig. 4.1). These MnPs are nearly identical in terms of $O_2^{\bullet-}$ dismuting and $ONOO^-$ reducing abilities [1, 13]. However, MnTnHex-2-PyP is 13 500-fold more lipophilic than MnTE-2-PyP, and thus more prone to enter the cell [14, 15].

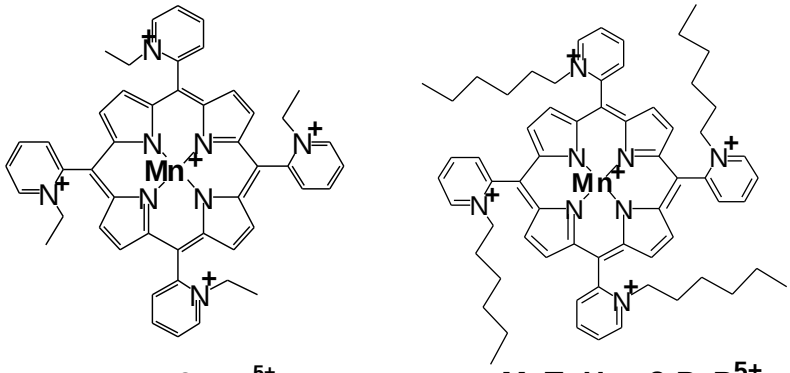


**Fig. 4.1 -** Chemical structures of the Mn(III) porphyrins MnTE-2-PyP and MnTnHex-2-PyP.

*Ortho*-substituted MnPs have already shown remarkable protective effects in *in vitro* and *in vivo* models of oxidative stress injuries [2, 6, 7]. However, a thorough knowledge on the effects at the cellular level is still missing. In Chapter 3, MnTM-4-PyP showed to be a potent antioxidant against the toxic effects of TBHP in V79 cells. In the present Chapter, the protection afforded by MnTE-2-PyP and MnTnHex-2-PyP against the same oxidative stress inducer is evaluated. This work also aims to explore if enhanced lipophilicity of the hexyl analogue makes it a more potent compound in this model. Recently 6 MnPs, 3 Mn salens and 2 Mn cyclic polyamines in radioprotection of ataxia telangiectasia cells were compared, among them MnTE-2-PyP and MnTnHex-2-PyP [16]. While MnTnHex-2-PyP was efficacious, the equally potent antioxidant, but hydrophilic MnTE-2-PyP was not. The study indicated the critical role of compound bioavailability and suggested that the accumulation of the hexyl analogue within mitochondria may be in the origin of its efficacy.

As mentioned in Chapter 3, TBHP is a short chain analogue of lipid hydroperoxides that has been often used as a model to investigate the mechanism of cell injury initiated by acute oxidative stress in a variety of cells [17-22]. Because of the higher stability and presence of the hydrophobic butyl moiety which allows easier membrane penetration, TBHP provides a convenient alternative to the natural oxidants hydrogen peroxide and lipid hydroperoxide [22]. TBHP penetrates cell membranes [22, 23] and can generate free radical intermediates, namely alkoxyl and peroxyl radicals [20, 24] and superoxide anion

[23]. Cell injury can consequently occur by different phenomena, including changes in mitochondrial permeability [24], oxidative DNA damage, lipid peroxidation [25] and apoptosis [21]. Moreover, inside the cell, TBHP can be reduced to *t*-butanol by GPx [22], promoting the depletion of intracellular GSH as reported in hepatocytes and other cell types [20, 22, 25-29]. Glutathione is the main nonenzymatic antioxidant defense within the cell; the GSH/GSSG ratio reflects the cellular redox state [17, 30]. Since thiol homeostasis determines critical aspects of cell function and response [19], an imbalance at this level will further contribute to cell injury.

The present Chapter aims to evaluate and compare the role of optimized MnPs MnTE-2-PyP and MnTnHe2-PyP against TBHP-induced cell injury, using a multilevel approach. In order to achieve these goals two complementary cell viability assays (MTT and CV) were used. ROS generation was assessed using the fluorescence probe DHE. The total glutathione (GSHt) and the oxidized glutathione (GSSG) contents were measured by the 5,5'-dithiobis(2-nitrobenzoic acid) (DTNB) assay. Also, the reduced glutathione, expressed as a percentage of the GSH content relatively to non treated control cells was assessed using the monochlorobimane (mCB) assay.

## 4.2. Materials and Methods

### *4.2.1. Chemicals*

PBS, Ham's F-10 medium, newborn calf serum, penicillin-streptomycin solution, trypsin, MTT, CV, TBHP, 5-sulfosalicylic acid, glutathione reductase from baker's yeast, GSH, DTNB, nicotinamide adenine dinucleotide phosphate (NADPH), and glutathione-S-transferase (GST) from equine liver were obtained from Sigma-Aldrich. A stock solution of GST (10 U/mL) was prepared in PBS with 10% glycerol, aliquotized and stored at −18 ºC. DMSO and ethanol were purchased from Merck. GSSG and mCB were obtained from Fluka. A stock solution of mCB (10 mM) was prepared in ethanol, aliquotized and stored at −18 ºC. DHE was purchased from Molecular Probes. MnTE-2-PyP and MnTnHex-2-PyP were synthesized at Duke University as previously described [31].

### *4.2.2. MTT Reduction assay*

Cytotoxicity assays were carried out in V79 cells, cultured as described in Chapter 3 (3.2.2). The MTT reduction assay was performed according to the protocol described in Chapter 3 (3.2.3.1). V79 cells were treated for 24 h with TBHP (100 – 300 µM) in the presence or absence of MnPs (0.1-25 µM). The cytotoxicity induced by the MnPs *per se* was evaluated under the same experimental conditions. After the treatments, the assay was carried out as described in the previous Chapter. Three to six independent experiments were performed and eight replicate cultures were used for each concentration in each independent experiment.

### *4.2.3. Crystal Violet assay*

The CV assay was performed as described in Chapter 3 (3.2.3.2). Cells were exposed for a 24 h period to TBHP (100 µM) with or without the MnPs (1-25 µM). Three to seven independent experiments were performed, each one comprising eight replicate cultures.

*4.2.4. DHE fluorimetric assay*

The DHE assay was performed as described in Chapter 3 (3.2.5), being V79 cells exposed for three hours to TBHP (100 µM) in the presence or absence of the MnPs (5 µM). Five independent experiments were performed, each comprising six replicate cultures for each experimental point.

*4.2.5. DTNB assay*

The DTNB assay [32-34] was used to quantify the GSHt and GSSG contents. This method is simple and convenient, and is based on the reaction of DTNB with GSH, generating a product spectrophotometrically detectable at 412 nm (Fig. 4.2) [34].

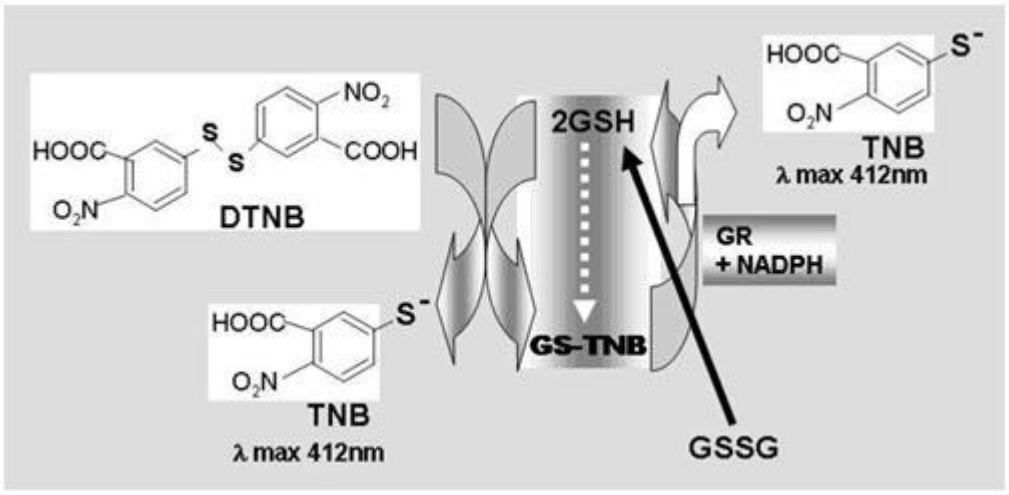


**Fig. 4.2 –** Fundamentals of the DTNB assay (from [34]). GSH reacts with DTNB [5,5'-dithiobis(2-nitrobenzoic acid)] to form TNB (5-thio-2-nitrobenzoic acid) and the adduct GS-TNB. GS-TNB, as well as GSSG, is then reduced to GSH by glutathione reductase (GR) in the presence of NADPH. The TNB formed can be measured at 412 nm [34].

V79 cells were cultured in Petri dishes (~$3.0 \times 10^4$ cells/mL of culture medium) and incubated for 24 h at 37°C, under a 5% $CO_2$ atmosphere. The culture medium was then replaced by fresh medium and cells were treated for a further 24 h period with TBHP (100 µM) in the presence or absence of the MnPs (5 µM). After this incubation, cells were

carefully washed, scrapped with ice-cold PBS and centrifuged for 10 min at 200 x *g*. The obtained pellet was suspended in PBS and submitted to two freeze-thaw cycles (-80 ºC / room temperature). An aliquot of this lysate was saved for the analysis of protein content by the Bradford assay and for the mCB assay. Sulfosalicylic acid was added to the remaining volume of lysate at a final concentration of 3%, and this suspension was centrifuged for 10 min, at 12 000 x *g*, 4 ºC. The obtained supernatant was divided for the quantification of the GSHt and GSSG. GSH and GSSG standard solutions were prepared in 3% sulfosalicylic acid. For the GSSG quantification, both samples and GSSG standards were treated with 2-vinylpyridine (2.5%) to derivatize GSH. The pH was adjusted to ~6 with triethanolamine and the samples were incubated for 1 h, at 4 ºC before the assay.

In a 96-well microplate, the GSHt and GSSG samples and standards were mixed with a freshly made solution containing glutathione reductase and DTNB, in phosphate buffer 0.1 M (pH 7.0, containing 1 mM edta). The reaction was started by the addition of NADPH. The final concentrations in the reaction mixture were 0.125 U/mL of glutathione reductase, 0.028 mg/mL of DTNB and 43 µM of NADPH. The kinetics of the absorbance increase at 405 nm was recorded at 4 min intervals over a 20 min period. The glutathione concentration in the samples was calculated by comparing the slopes of the sample with those of the correspondent standard curve, and the result was expressed in nmol/mg protein. At least nine independent experiments were performed for the GSHt content and four were performed for the GSSG determination. Each independent experiment comprised the analysis of all samples and standards in duplicate.

*4.2.6. mCB assay*

The mCB assay was adapted from Kamencic *et al* [35]. mCB is a probe that reacts with GSH generating an adduct (Fig. 4.3) that can be detected by fluorimetry [35, 36].

In a black 96-well microplate, PBS was added to 20 µL of the cell lysate (section 4.2.5), 1 U/mL GST, and 100 µM mCB at a final volume of 100 µL. The reaction microplate incubated 30 min in the dark, at 37 ºC, 100 rpm. The mCB–glutathione adduct was then measured in a Zenyth 3100 multimode detection microplate reader, using $\lambda_{excitation}$ = 405 nm and $\lambda_{emission}$ = 465 nm. The results were expressed as %GSH of non-treated

control cells, after subtracting the background fluorescence and normalizing to the protein content. At least five independent experiments were performed, each comprising two duplicate measurements.

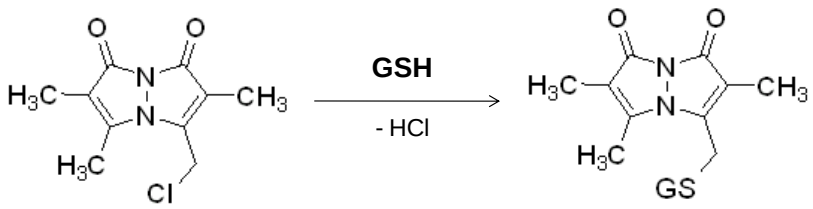


**Fig. 4.3 –** Fundamentals of the mCB assay. The reaction of the non-fluorescent monochlorobimane (mCB) with reduced glutathione generates the highly fluorescent mCB-glutathione conjugate.

*4.2.7. Stability of MnPs*

The stability of MnPs under the experimental conditions described in the previous assays was evaluated by UV/Vis spectroscopy, using the supernatants of the cell cultures incubated for 24 h with MnPs (5 µM) and/or TBHP (100 µM). The supernatant of non-treated control cultures was used as reference to adjust the baseline. Two independent assays were performed. Both for MnTE-2-PyP and for MnTnHex-2-PyP, the UV/Vis spectra of the supernatant of cultures treated with each MnP alone were identical to those of cultures treated with "MnP+TBHP". Therefore, under these experimental conditions, MnPs remain stable and no oxidative degradation occurs.

*4.2.8. Statistical analysis*

The statistical analysis of the data was processed as described in Chapter 3 (section 3.2.6).

## 4.3. Results and Discussion

The most active SODm described so far are among the *ortho*-substituted MnPs [1, 2, 37]. However, a thorough knowledge on the effects of these compounds at the cellular level is still lacking. In this context, this Chapter studies the effects of two *ortho*-substituted MnPs, MnTE-2-PyP and MnTnHex-2-PyP, against the cytotoxic effects induced by TBHP in V79 cells. Albeit TBHP is commonly used as an oxidant model, few studies to assess the effect of catalytic antioxidants towards this agent are available.

### *4.3.1. Cytotoxicity profile of MnTE-2-PyP and MnTnHex-2-PyP*

The effects induced by MnTE-2-PyP and MnTnHex-2-PyP *per se* were firstly evaluated in V79 cells, at concentrations up to 25 μM. After a 24 h-incubation period, no cytotoxicity was observed for MnPs, either using the MTT (Fig. 4.4) or the CV assay (data not shown). Interestingly, with *Escherichia coli* toxicity of MnTnHex-2-PyP was observed already at ≥ 3 μM levels [15, 37].

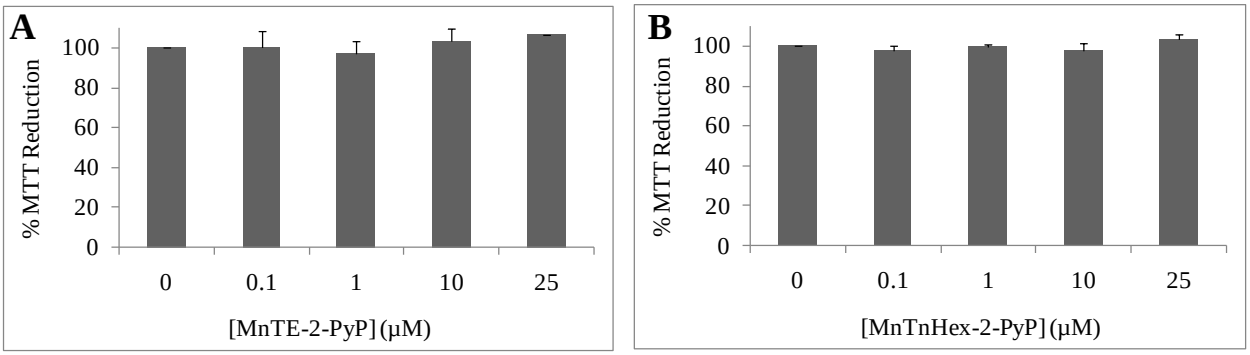


**Fig. 4.4 -** Cytotoxicity evaluation of MnTE-2-PyP (A) and MnTnHex-2-PyP (B). V79 cells were treated with the MnPs for 24 h and then submitted to the MTT assay.

### *4.3.2. Effects of MnTE-2-PyP and MnTnHex-2-PyP against TBHP-induced cytotoxicity*

Figs. 4.5 and 4.6 show the effect of MnTE-2-PyP against the cytotoxicity induced by TBHP. The exposure of V79 cells to TBHP (100 μM) resulted in a considerable decrease in the MTT reduction ($P < 0.01$), as well as in the CV staining ($P < 0.001$). The simultaneous treatment with MnTE-2-PyP led to a significant increase in the MTT

reduction when compared with TBHP-treated cells, even for the 0.1 μM concentration (Fig. 4.5A). At 5 μM, MnTE-2-PyP was highly protective, reverting the decrease in MTT reduction induced by TBHP ($P < 0.05$). The CV assay confirmed the significant protective effects of MnTE-2-PyP (1, 5 and 25 μM) against the TBHP-induced cytotoxicity (Fig. 4.5B).

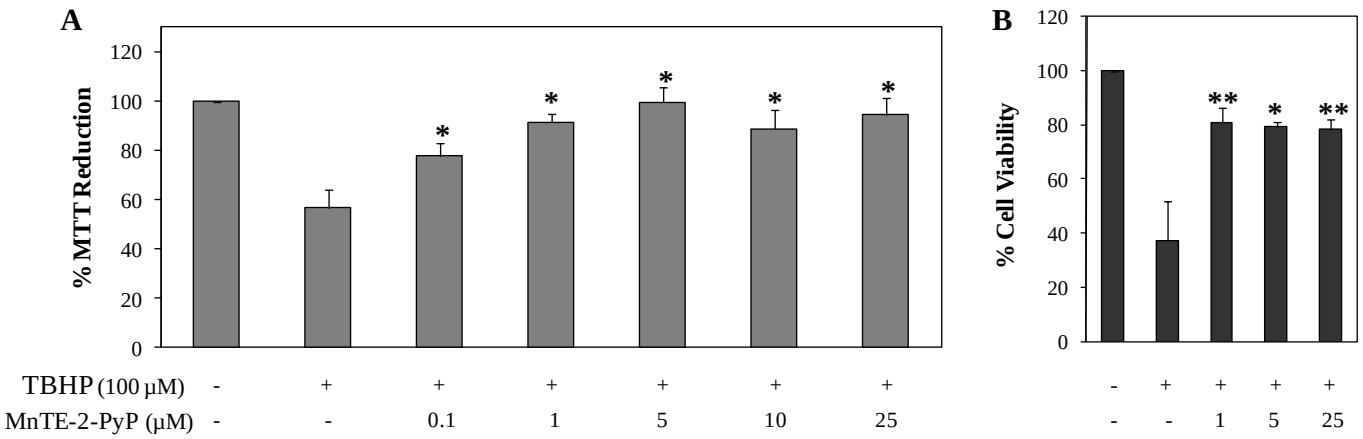


**Fig. 4.5 -** Effect of MnTE-2-PyP on the cytotoxicity induced by TBHP (100 μM) in V79 cells. Cells were incubated with increasing concentrations of MnTE-2-PyP in the presence of TBHP for 24 h, and then submitted to the MTT (A) or to the CV staining (B) assays. (*$P \leq 0.05$ and **$P \leq 0.01$, when compared with TBHP-treated cells in the absence of MnTE-2-PyP).

To assess the effect of MnTE-2-PyP in more severe conditions, experiments using higher concentrations of TBHP were performed. As depicted in Fig. 4.6, cultures treated for 24 h with 200 and 300 μM of TBHP showed a drastic cell death. The co-incubation with MnTE-2-PyP (1, 5 and 25 μM) showed significant protective effects ($P < 0.05$).

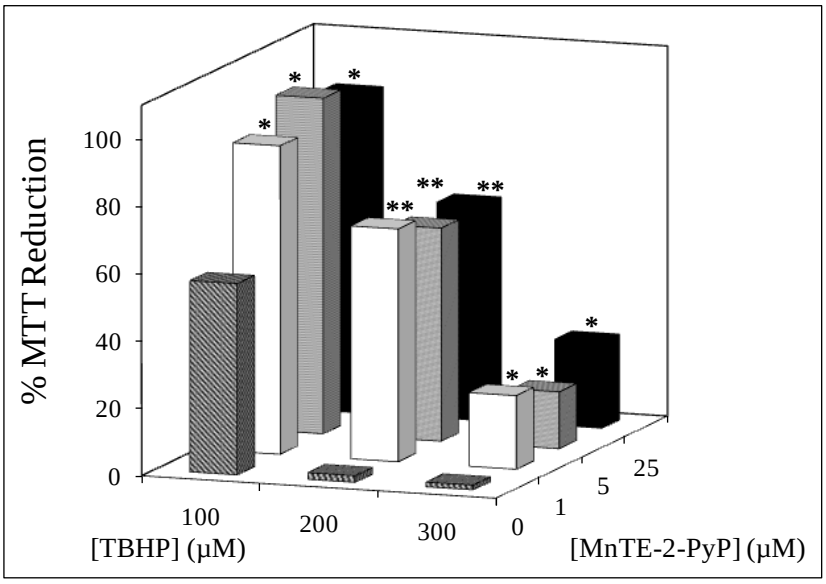


**Fig. 4.6 -** Effect of MnTE-2-PyP on the cytotoxicity induced by TBHP in V79 cells, as evaluated by the MTT assay. Cells were incubated with increasing concentrations of MnTE-2-PyP (1-25 μM) in the presence of different concentrations of TBHP (100-300 μM) for 24 h. (**P* ≤ 0.05 and ***P* < 0.01, when compared with cells treated with the same concentration of TBHP in the absence of MnTE-2-PyP).

The effect of MnTnHex-2-PyP against the TBHP-induced cytotoxicity is shown in Figs. 4.7 and 4.8. In the MTT assay (Fig. 4.7A) this MnP also exerted a considerable protective effect, which was statistically significant ($P < 0.05$) for concentrations ≥ 1 μM. Like MnTE-2-PyP, 5 μM of MnTnHex-2-PyP was the lowest concentration that exhibited a maximum reversal of cell viability. Both MnPs have shown remarkable protective effects against the cytotoxicity induced by TBHP. The protection afforded by MnPs was lower in the CV assay than observed with the MTT assay, what may be attributed to the aforementioned mechanistic differences of the methods and also to the experimental protocols.

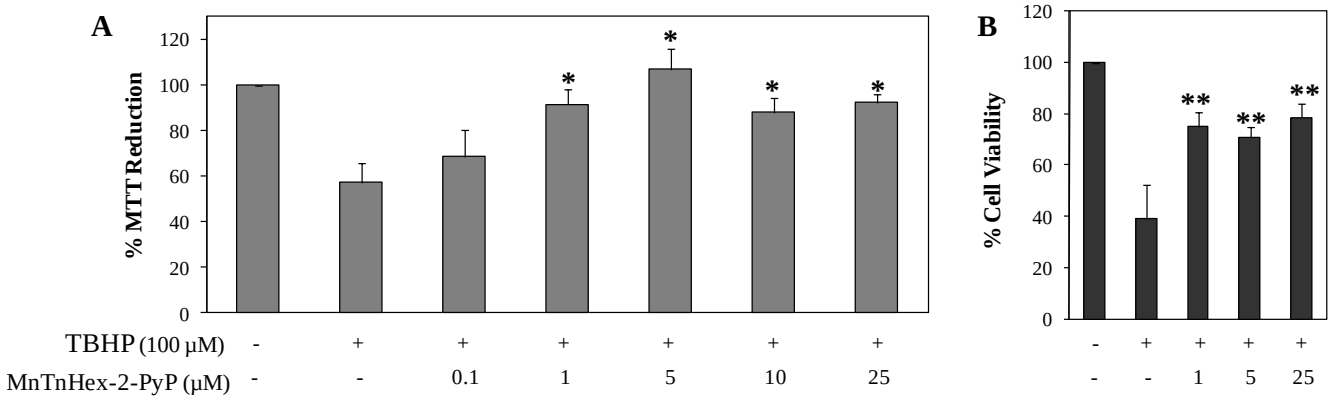


**Fig. 4.7 -** Effect of MnTnHex-2-PyP on the cytotoxicity induced by TBHP (100 μM) in V79 cells. Cells were incubated with increasing concentrations of MnTnHex-2-PyP in the presence of TBHP for 24 h, and then submitted to the MTT (A) or to the CV staining (B) assays. (**P* ≤ 0.05 and ***P* ≤ 0.01, when compared with TBHP-treated cells in the absence of MnTnHex-2-PyP).

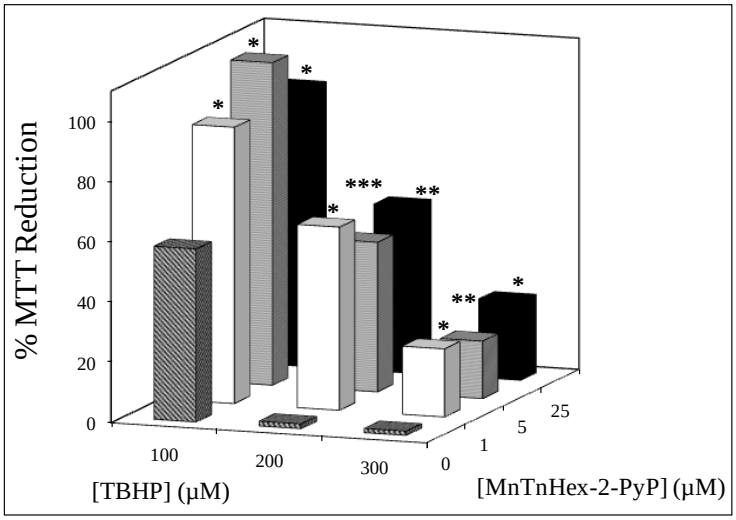


**Fig. 4.8 -** Effect of MnTnHex-2-PyP on the cytotoxicity induced by TBHP in V79 cells, as evaluated by the MTT assay. Cells were incubated with increasing concentrations of MnTnHex-2-PyP (1-25 μM) in the presence of different concentrations of TBHP (100-300 μM) for 24 h. (**P* ≤ 0.05, ***P* < 0.01 and ****P* < 0.001, when compared with cells treated with the same concentration of TBHP in the absence of MnTnHex-2-PyP).

In Chapter 3, the performance of MnTM-4-PyP, a *para*-substituted MnP, was evaluated in the same oxidative stress model. In the present work, both MnTE-2-PyP and MnTnHex-2-PyP were more effective than the *para*- analogue, showing better protectiveness at lower concentrations. This higher performance may be attributed to the greater antioxidant potency, since the *ortho* analogues have higher catalytic rate constant for $O_2^{\bullet-}$ dismutation and $ONOO^-$ reduction, and presumably higher rate constant for the reaction with peroxyl radicals than *para* isomers as well [38, 39]. The reaction with peroxyl radical involves formation of $O=Mn^{IV}P$, which is also involved in the reaction with $ONOO^-$; the reactivity is related to the electron-deficiency of MnP that is similar with all *ortho* substituted alkylpyridylporphyrins; therefore the ability of MnPs to remove both $ONOO^-$ and peroxyl radical is likely similar also.

The two MnPs have shown comparable cytoprotection profiles with both CV (Fig. 4.5B and 4.7B) and MTT assays (Fig. 4.5A, 4.6, 4.7A and 4.8). However, with MnTE-2-PyP the significant protective effects were seen at lower concentrations (0.1 μM). Furthermore, MnTE-2-PyP led to slightly higher cell viabilities in the CV assay, as well as in cultures treated with 200 μM of TBHP. It has been reported that MnTE-2-PyP and MnTnHex-2-PyP possess identical antioxidant potency with respect to $O_2^{\bullet-}$, $ONOO^-$ and $CO_3^{\bullet-}$ [13, 31]. Since MnTnHex-2-PyP is more prone to enter the cell due to its 4 orders of magnitude higher lipophilicity [14, 15] one could expect this MnP to be more efficient than the ethyl analogue at lower concentrations. However, our results showed a slightly higher potency for MnTE-2-PyP. It has been reported that V79 cells have endocytic activity [40]. In view of this, it is possible that despite the higher lipophilicity of MnTnHex-2-PyP, both MnPs have been uptaken by V79 cells in a similar way. It is also possible that the protective effects occurred in extracellular millieu, plasma membrane and cytosolic space, rather than in mitochondria. As stated in Introduction (section 4.1), were the effects expected on mitochondrial level we would anticipate enhanced protectiveness of MnTnHex-2-PyP.

*4.3.3. Effects of MnTE-2-PyP and MnTnHex-2-PyP against TBHP-induced ROS generation*

The data on the intracellular generation of superoxide anion, as evaluated by the DHE assay, are depicted in Fig. 4.9. The exposure of V79 cells to TBHP (100 µM) led to a significant increase in the fluorescence intensity ($P < 0.01$), indicating the intracellular production of $O_2^{\bullet-}$ by TBHP. The intracellular ROS production has been previously reported as an early event in TBHP-induced cytotoxicity [41], what justifies the observed increase in a 3 h incubation period. When cells were exposed to TBHP and MnTE-2-PyP or MnTnHex-2-PyP (5 µM), the fluorescence intensities returned to values lower than those presented by control cells ($P < 0.01$).

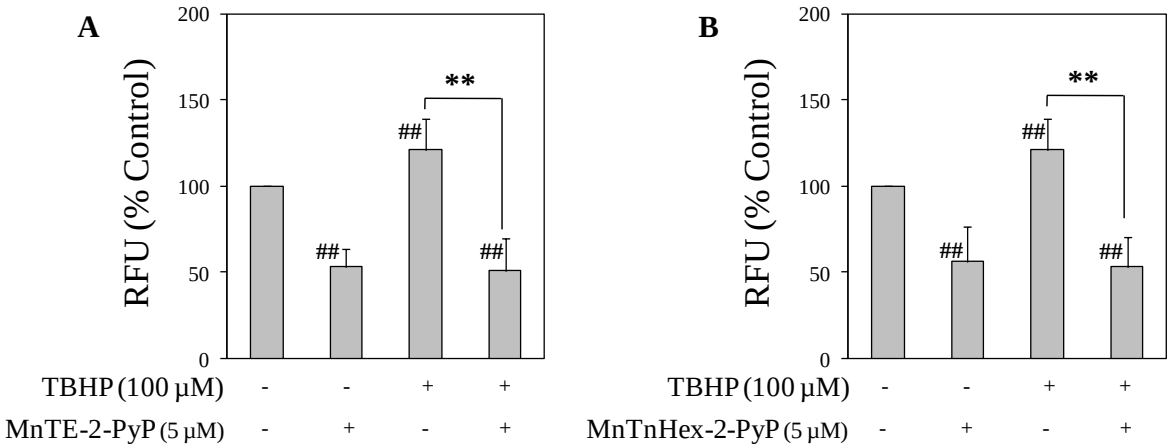


**Fig. 4.9 -** Effect of MnTE-2-PyP (A) and MnTnHex-2-PyP (B) on the DHE oxidation in V79 cells treated with TBHP (100 µM). Values (mean ± SD) represent relative fluorescence units (RFU), which approximately reflect the levels of superoxide anion, expressed as percentages of the control cells. ($^{\#\#}P < 0.01$, when compared with non-treated control cells; $^{**}P < 0.01$, when compared with cells treated with TBHP in the absence of MnP).

The effect of the MnPs on the $O_2^{\bullet-}$ levels of cells treated with higher concentrations of TBHP (1.0 and 2.0 mM) was also tested. Even in this case, the presence of MnPs decreased significantly the fluorescence intensities to values lower than controls (data not shown). These results suggest that the scavenging of superoxide anion should be involved in the protection of the MnPs observed in the cytotoxicity assays. Along with the SOD-like

activity, the ability of MnPs to decompose peroxyl radicals should also be a relevant mechanism for the abrogation of TBHP effects. The two MnPs showed a similar efficiency in reducing the intracellular ROS. It is also important to mention that cells treated only with the MnPs, either MnTE-2-PyP or MnTnHex-2-PyP, exhibited a considerable reduction in the hydroxyethidium fluorescence ($P < 0.01$) which could be ascribed to the abrogation of some level of oxidative stress that cells experience while growing in the medium or of the basal cellular ROS content.

### *4.3.4. Effects of MnTE-2-PyP and MnTnHex-2-PyP on the changes in glutathione status induced by TBHP*

Glutathione is the main nonenzymatic antioxidant defense within the cell and its content, as well as the GSH/GSSG ratio, reflects the cellular redox state [22, 30, 42]. Under normal conditions, reduced GSH is largely predominant over GSSG, while with oxidative stress the percentage of GSSG can increase considerably [43]. To evaluate the glutathione status of cells submitted to different treatments, we have used two complementary approaches. The classical DTNB assay was used to determine the total glutathione content and the GSSG concentration, and the fluorimetric mCB assay to assess the reduced form of glutathione. The results of the DTNB assay are shown in Table IV.1.

V79 cells, upon treatment with 100 μM TBHP, exhibited a marked depletion in the total glutathione content, that decreased from 7.69 to 2.50 nmol/mg prot ($P < 0.001$). When cells were concomitantly exposed to TBHP and MnTE-2-PyP or MnTnHex-2-PyP, the GSHt increased to 16.54 and 19.71 nmol/mg prot, respectively. These increases were statistically significant ($P < 0.001$), when compared to the GSHt content of cells exposed only to TBHP. These cells also exhibited GSHt levels significantly above those of non-treated control cells ($P < 0.001$). The MnPs *per se* did not considerably change the GSHt content of V79 cells. Similar results were found for the *para* analogue MnTM-4-PyP. While this MnP *per se* did not alter significantly the GSHt levels, V79 cells co-treated with MnTM-4-PyP and TBHP presented a GSHt content of 19.22 ± 4.05 nmol/mg prot, a value that is significantly above control cells ($P \leq 0.001$) and TBHP-treated cells ($P < 0.01$) (data not shown).

In control cells, as well as in cells treated only with MnTE-2-PyP or MnTnHex-2-PyP (5 μM), the levels of GSSG were low, having a small contribution for the total glutathione content. When V79 cells were treated with 100 μM TBHP, the GSSG level increased significantly ($P < 0.01$), accounting considerably for the GSHt observed in this case (Table IV.1). Cells co-treated with TBHP and MnTE-2-PyP or MnTnHex-2-PyP, although had very high GSHt contents, did not show remarkable GSSG concentrations.

**Table IV.1 -** Effect of MnTE-2-PyP and MnTnHex-2-PyP on the changes in glutathione status induced by TBHP in V79 cells, as evaluated by the DTNB assay.

| | Total GSH[a] (nmol/mg prot) | GSSG[b] (nmol/mg prot) |
|---|---|---|
| Non-treated control cells | 7.69 ± 3.07 | 0.20 ± 0.10 |
| MnTE-2-PyP 5 μM | 8.20 ± 2.20 | 0.22 ± 0.19 |
| MnTnHex-2-PyP 5 μM | 7.34 ± 3.77 | 0.18 ± 0.11 |
| TBHP 100 μM | 2.50 ± 2.90 $^{\#\#\#}$ | 1.07 ± 0.30 $^{\#\#}$ |
| TBHP 100 μM + MnTE-2-PyP 5 μM | 16.54 ± 4.92 $^{\#\#\#, ***}$ | 0.46 ± 0.11 $^{\#, *}$ |
| TBHP 100 μM + MnTnHex-2-PyP 5 μM | 19.71 ± 5.53 $^{\#\#\#, ***}$ | 1.58 ± 0.36 $^{\#}$ |

[a] Values represent mean ± SD of at least nine independent experiments
[b] Values represent mean ± SD of four independent experiments
$^{\#}P < 0.05$, $^{\#\#}P < 0.01$ and $^{\#\#\#}P < 0.001$, when compared with non-treated control cells
$^{*}P < 0.05$ and $^{***}P < 0.001$, when compared with cells treated with TBHP alone

The data obtained using the mCB assay, which detects the reduced form of glutathione (GSH) are depicted in Fig. 4.10. These results are expressed as a percentage of the GSH content of non treated control cells, that presented an average fluorescence value of 3.1 x $10^4$ RFU/μg prot. The treatment of V79 cells with the MnPs (5 μM) did not alter the GSH content. Cells treated with 100 μM TBHP showed a dramatic GSH depletion, having only ~22% of the GSH of control cells ($P < 0.001$). When cells were incubated simultaneously with TBHP and MnTE-2-PyP or MnTnHex-2-PyP, their GSH level increased markedly, not only restoring the depletion induced by TBHP ($P < 0.01$), but also reaching GSH values ~1.5 fold higher than those of control cells ($P < 0.001$).

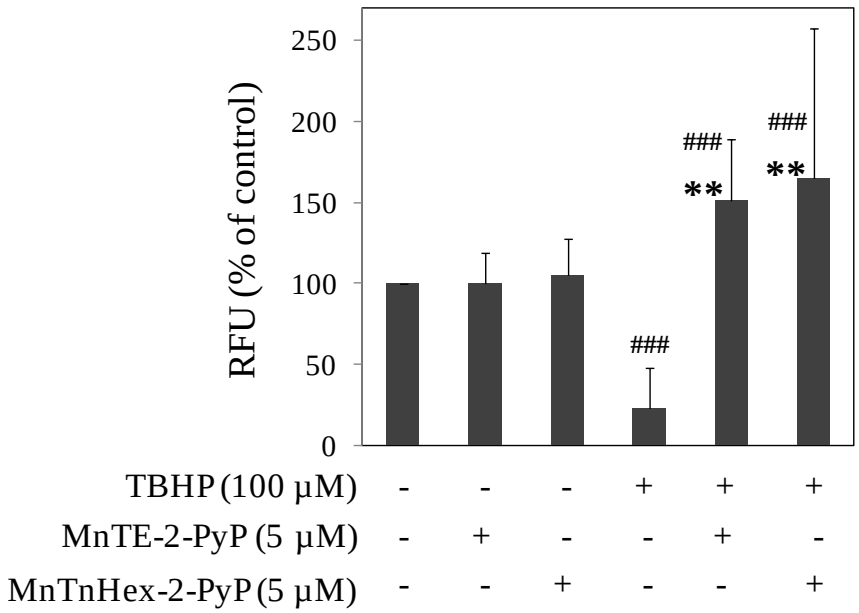


**Fig. 4.10 -** Effect of MnTE-2-PyP and MnTnHex-2-PyP (5 µM) on the GSH depletion induced by TBHP (100 µM) in V79 cells, as evaluated by the mCB assay. Values (mean ± SD) represent relative fluorescence units (RFU) expressed as percentages of the control cells, after normalizing to the protein content of the lysate. Control cells exhibited an average fluorescence value of 3.1 x $10^4$ RFU/µg prot. ($^{###}P < 0.001$, when compared with non-treated control cells; $^{**}P < 0.01$, when compared with cells treated with TBHP in the absence of MnP).

Glutathione can reduce different hydroperoxides and radicals, and it has been reported to be depleted after an exposure to TBHP [19, 20, 26, 28]. In addition, TBHP was previously shown to increase the GSSG level [17, 44-46]. Our results concur with these previous reports either in terms of GSH depletion or GSSG increase.

The intracellular level of GSH is regulated by the γ-glutamylcysteine synthetase (γ-GCS) activity and by the availability of the precursor cysteine [47]. γ-GCS activity is rate limiting in the synthesis of GSH and this enzyme is subject to feedback regulation by the concentrations of glutathione [43]. Previous studies have shown that organic peroxides, and specifically TBHP, can stimulate the *de novo* biosynthesis of GSH [45, 47], by up-regulating the expression of γ-GCS mRNA [44] and by increasing the activity of this enzyme [47]. In fact, Ochi [47] reported an increase in γ-GCS activity in V79 cells after a 1 h-exposure to 100 µM TBHP. It is therefore expectable that TBHP is stimulating this

enzyme under the used experimental conditions. However, due to the ROS and lipid peroxides that TBHP generates and also due to the glutathione peroxidase activity with this peroxide, the GSH formed is extensively consumed, oxidized to GSSG and extruded from cells [48-50], resulting in the depletion of GSHt and GSH and in the increase of GSSG. Conversely, in the presence of MnPs, an effective increase in the GSHt and GSH contents was observed. Along with the possible increase in γ-GCS-related activity, MnPs themselves seem to scavenge ROS, including lipid peroxides that are produced by TBHP insult, reducing the consumption of GSH. Our results provided herein add to other evidences that MnPs, due to their multiple possible oxidation states (+2, +3, +4, +5), are both potent ROS/RNS scavengers, and powerful modulators of cellular redox-based metabolic pathways [5-7, 51]. In addition, a MnP was previously shown to counteract the oxidative inactivation of isocitrate dehydrogenase [52] increasing the cellular supply of NADPH, which levels are known to be suppressed in TBHP-treated cells [53, 54]. This may be also contributing to the increase in the GSH contents observed in cells treated with TBHP and MnPs.

### *4.3.5. Conclusion*

This Chapter shows that *ortho*-substituted MnPs are extremely potent antioxidants, with the ability to cope with the cellular damage induced by TBHP, even at low micromolar concentrations. Their clear protective effect in V79 cells was observed in terms of cytotoxicity and intracellular superoxide level. Also, for the first time, the results presented here reveal that these MnPs have an important role in enhancing reducing environment, which in turn favors reduced glutathione, thus assuring normal cellular redox status.

## 4.4 References


[1] Reboucas, J. S.; DeFreitas-Silva, G.; Spasojevic, I.; Idemori, Y. M.; Benov, L.; Batinic-Haberle, I. Impact of electrostatics in redox modulation of oxidative stress by Mn porphyrins: protection of SOD-deficient Escherichia coli via alternative mechanism where Mn porphyrin acts as a Mn carrier. *Free Radic Biol Med* **45:**201-210; 2008.

[2] Batinic-Haberle, I.; Rebouças, J. S.; Spasojević, I. Superoxide dismutase mimics: chemistry, pharmacology and therapeutic potential. *Antiox Redox Signal* **in press**; 2010.

[3] Patel, M.; Day, B. J. Metalloporphyrin class of therapeutic catalytic antioxidants. *Trends Pharmacol Sci* **20:**359-364; 1999.

[4] Moeller, B. J.; Batinic-Haberle, I.; Spasojevic, I.; Rabbani, Z. N.; Anscher, M. S.; Vujaskovic, Z.; Dewhirst, M. W. A manganese porphyrin superoxide dismutase mimetic enhances tumor radioresponsiveness. *Int J Radiat Oncol Biol Phys* **63:**545-552; 2005.

[5] Zhao, Y.; Chaiswing, L.; Oberley, T. D.; Batinic-Haberle, I.; St Clair, W.; Epstein, C. J.; St Clair, D. A mechanism-based antioxidant approach for the reduction of skin carcinogenesis. *Cancer Res* **65:**1401-1405; 2005.

[6] Rabbani, Z. N.; Spasojevic, I.; Zhang, X.; Moeller, B. J.; Haberle, S.; Vasquez-Vivar, J.; Dewhirst, M. W.; Vujaskovic, Z.; Batinic-Haberle, I. Antiangiogenic action of redox-modulating Mn(III) meso-tetrakis(N-ethylpyridinium-2-yl)porphyrin, MnTE-2-PyP(5+), via suppression of oxidative stress in a mouse model of breast tumor. *Free Radic Biol Med* **47:**992-1004; 2009.

[7] Sheng, H.; Yang, W.; Fukuda, S.; Tse, H. M.; Paschen, W.; Johnson, K.; Batinic-Haberle, I.; Crapo, J. D.; Pearlstein, R. D.; Piganelli, J.; Warner, D. S. Long-term neuroprotection from a potent redox-modulating metalloporphyrin in the rat. *Free Radic Biol Med* **47:**917-923; 2009.

[8] Tse, H. M.; Milton, M. J.; Piganelli, J. D. Mechanistic analysis of the immunomodulatory effects of a catalytic antioxidant on antigen-presenting cells: implication for their use in targeting oxidation-reduction reactions in innate immunity. *Free Radic Biol Med* **36:**233-247; 2004.

[9] Batinic-Haberle, I.; Benov, L.; Spasojevic, I.; Fridovich, I. The ortho effect makes manganese(III) meso-tetrakis(N-methylpyridinium-2-yl)porphyrin a powerful and potentially useful superoxide dismutase mimic. *J Biol Chem* **273:**24521-24528; 1998.

[10] Batinic-Haberle, I.; Spasojevic, I.; Hambright, P.; Benov, L.; A.L.Crumbliss; Fridovich, I. Relationship among redox potentials, proton dissociation constants of pyrrolic nitrogens, and in vitro and in vivo superoxide dismutating activities of manganese(III) and iron(III) water-soluble porphyrins. *Inorg Chem* **38:**4011-4022; 1999.

[11] Reboucas, J. S.; Spasojevic, I.; Tjahjono, D. H.; Richaud, A.; Mendez, F.; Benov, L.; Batinic-Haberle, I. Redox modulation of oxidative stress by Mn porphyrin-based therapeutics: the effect of charge distribution. *Dalton Trans***:**1233-1242; 2008.

[12] Spasojevic, I.; Batinic-Haberle, I.; Reboucas, J. S.; Idemori, Y. M.; Fridovich, I. Electrostatic contribution in the catalysis of O2*- dismutation by superoxide dismutase mimics. MnIIITE-2-PyP5+ versus MnIIIBr8T-2-PyP+. *J Biol Chem* **278:**6831-6837; 2003.

[13] Ferrer-Sueta, G.; Vitturi, D.; Batinic-Haberle, I.; Fridovich, I.; Goldstein, S.; Czapski, G.; Radi, R. Reactions of manganese porphyrins with peroxynitrite and carbonate radical anion. *J Biol Chem* **278:**27432-27438; 2003.

[14] Kos, I.; Reboucas, J. S.; DeFreitas-Silva, G.; Salvemini, D.; Vujaskovic, Z.; Dewhirst, M. W.; Spasojevic, I.; Batinic-Haberle, I. Lipophilicity of potent porphyrin-based antioxidants: comparison of ortho and meta isomers of Mn(III) N-alkylpyridylporphyrins. *Free Radic Biol Med* **47:**72-78; 2009.

[15] Okado-Matsumoto, A.; Batinic-Haberle, I.; Fridovich, I. Complementation of SOD-deficient Escherichia coli by manganese porphyrin mimics of superoxide dismutase activity. *Free Radic Biol Med* **37:**401-410; 2004.

[16] Pollard, J. M.; Reboucas, J. S.; Durazo, A.; Kos, I.; Fike, F.; Panni, M.; Gralla, E. B.; Valentine, J. S.; Batinic-Haberle, I.; Gatti, R. A. Radioprotective effects of manganese-containing superoxide dismutase mimics on ataxia-telangiectasia cells. *Free Radic Biol Med* **47:**250-260; 2009.

[17] Nardini, M.; Pisu, P.; Gentili, V.; Natella, F.; Di Felice, M.; Piccolella, E.; Scaccini, C. Effect of caffeic acid on tert-butyl hydroperoxide-induced oxidative stress in U937. *Free Radic Biol Med* **25:**1098-1105; 1998.

[18] Lee, K. J.; Choi, C. Y.; Chung, Y. C.; Kim, Y. S.; Ryu, S. Y.; Roh, S. H.; Jeong, H. G. Protective effect of saponins derived from roots of Platycodon grandiflorum on tert-butyl hydroperoxide-induced oxidative hepatotoxicity. *Toxicol Lett* **147:**271-282; 2004.

[19] Macone, A.; Matarese, R. M.; Gentili, V.; Antonucci, A.; Dupre, S.; Nardini, M. Effect of aminoethylcysteine ketimine decarboxylated dimer, a natural sulfur compound present in human plasma, on tert-butyl hydroperoxide-induced oxidative stress in human monocytic U937 cells. *Free Radic Res* **38:**705-714; 2004.

[20] Alia, M.; Ramos, S.; Mateos, R.; Bravo, L.; Goya, L. Response of the antioxidant defense system to tert-butyl hydroperoxide and hydrogen peroxide in a human hepatoma cell line (HepG2). *J Biochem Mol Toxicol* **19:**119-128; 2005.

[21] Kanupriya; Prasad, D.; Sai Ram, M.; Sawhney, R. C.; Ilavazhagan, G.; Banerjee, P. K. Mechanism of tert-butylhydroperoxide induced cytotoxicity in U-937 macrophages by alteration of mitochondrial function and generation of ROS. *Toxicol In Vitro* **21:**846-854; 2007.

[22] Voloboueva, L. A.; Liu, J.; Suh, J. H.; Ames, B. N.; Miller, S. S. (R)-alpha-lipoic acid protects retinal pigment epithelial cells from oxidative damage. *Invest Ophthalmol Vis Sci* **46:**4302-4310; 2005.

[23] Awe, S. O.; Adeagbo, A. S. Analysis of tert-butyl hydroperoxide induced constrictions of perfused vascular beds in vitro. *Life Sci* **71:**1255-1266; 2002.

[24] Piret, J. P.; Arnould, T.; Fuks, B.; Chatelain, P.; Remacle, J.; Michiels, C. Mitochondria permeability transition-dependent tert-butyl hydroperoxide-induced apoptosis in hepatoma HepG2 cells. *Biochem Pharmacol* **67:**611-620; 2004.

[25] Sohn, J. H.; Han, K. L.; Lee, S. H.; Hwang, J. K. Protective effects of panduratin A against oxidative damage of tert-butylhydroperoxide in human HepG2 cells. *Biol Pharm Bull* **28:**1083-1086; 2005.

[26] Park, J. E.; Yang, J. H.; Yoon, S. J.; Lee, J. H.; Yang, E. S.; Park, J. W. Lipid peroxidation-mediated cytotoxicity and DNA damage in U937 cells. *Biochimie* **84:**1199-1205; 2002.

[27] Chu, C. Y.; Tseng, T. H.; Hwang, J. M.; Chou, F. P.; Wang, C. J. Protective effects of capillarisin on tert-butylhydroperoxide-induced oxidative damage in rat primary hepatocytes. *Arch Toxicol* **73:**263-268; 1999.

[28] Hwang, J. M.; Wang, C. J.; Chou, F. P.; Tseng, T. H.; Hsieh, Y. S.; Lin, W. L.; Chu, C. Y. Inhibitory effect of berberine on tert-butyl hydroperoxide-induced oxidative damage in rat liver. *Arch Toxicol* **76:**664-670; 2002.

[29] Martin, C.; Martinez, R.; Navarro, R.; Ruiz-Sanz, J. I.; Lacort, M.; Ruiz-Larrea, M. B. tert-Butyl hydroperoxide-induced lipid signaling in hepatocytes: involvement of glutathione and free radicals. *Biochem Pharmacol* **62:**705-712; 2001.

[30] Schafer, F. Q.; Buettner, G. R. Redox environment of the cell as viewed through the redox state of the glutathione disulfide/glutathione couple. *Free Radic Biol Med* **30:**1191-1212; 2001.

[31] Batinic-Haberle, I.; Spasojevic, I.; Stevens, R. D.; Hambright, P.; Fridovich, I. Manganese(III) *meso*-tetrakis(*ortho*-*N*-alkylpyridyl)porphyrins. Synthesis, characterization and catalysis of $O_2^{\cdot-}$ dismutation. *J Chem Soc, Dalton Trans***:**2689-2696; 2002.

[32] Anderson, M. E. Determination of glutathione and glutathione disulfide in biological samples. *Methods Enzymol* **113:**548-555; 1985.

[33] Tietze, F. Enzymic method for quantitative determination of nanogram amounts of total and oxidized glutathione: applications to mammalian blood and other tissues. *Anal Biochem* **27:**502-522; 1969.

[34] Rahman, I.; Kode, A.; Biswas, S. K. Assay for quantitative determination of glutathione and glutathione disulfide levels using enzymatic recycling method. *Nat Protoc* **1:**3159-3165; 2006.

[35] Kamencic, H.; Lyon, A.; Paterson, P. G.; Juurlink, B. H. Monochlorobimane fluorometric method to measure tissue glutathione. *Anal Biochem* **286:**35-37; 2000.

[36] Oliveira, N. G.; Pingarilho, M.; Martins, C.; Fernandes, A. S.; Vaz, S.; Martins, V.; Rueff, J.; Gaspar, J. F. Cytotoxicity and chromosomal aberrations induced by acrylamide in V79 cells: role of glutathione modulators. *Mutat Res* **676:**87-92; 2009.

[37] Kos, I.; Benov, L.; Spasojevic, I.; Reboucas, J. S.; Batinic-Haberle, I. High lipophilicity of meta Mn(III) N-alkylpyridylporphyrin-based superoxide dismutase mimics compensates for their lower antioxidant potency and makes them as effective as ortho analogues in protecting superoxide dismutase-deficient Escherichia coli. *J Med Chem* **52:**7868-7872; 2009.

[38] Day, B. J.; Batinic-Haberle, I.; Crapo, J. D. Metalloporphyrins are potent inhibitors of lipid peroxidation. *Free Radic Biol Med* **26:**730-736; 1999.

[39] Bloodsworth, A.; O'Donnell, V. B.; Batinic-Haberle, I.; Chumley, P. H.; Hurt, J. B.; Day, B. J.; Crow, J. P.; Freeman, B. A. Manganese-porphyrin reactions with lipids and lipoproteins. *Free Radic Biol Med* **28:**1017-1029; 2000.

[40] Muller, L.; Kikuchi, Y.; Probst, G.; Schechtman, L.; Shimada, H.; Sofuni, T.; Tweats, D. ICH-harmonised guidances on genotoxicity testing of pharmaceuticals: evolution, reasoning and impact. *Mutat Res* **436:**195-225; 1999.

[41] Pias, E. K.; Ekshyyan, O. Y.; Rhoads, C. A.; Fuseler, J.; Harrison, L.; Aw, T. Y. Differential effects of superoxide dismutase isoform expression on hydroperoxide-induced apoptosis in PC-12 cells. *J Biol Chem* **278:**13294-13301; 2003.

[42] Biswas, S. K.; Rahman, I. Environmental toxicity, redox signaling and lung inflammation: the role of glutathione. *Mol Aspects Med* **30:**60-76; 2009.

[43] Pastore, A.; Federici, G.; Bertini, E.; Piemonte, F. Analysis of glutathione: implication in redox and detoxification. *Clin Chim Acta* **333:**19-39; 2003.

[44] Kaur, P.; Kaur, G.; Bansal, M. P. Upregulation of AP1 by tertiary butyl hydroperoxide induced oxidative stress and subsequent effect on spermatogenesis in mice testis. *Mol Cell Biochem* **308:**177-181; 2008.

[45] Ochi, T. Mechanism for the changes in levels of glutathione upon exposure of cultured mammalian cells to tertiary-butylhydroperoxide and diamide. *Arch Toxicol* **67:**401-410; 1993.

[46] Tormos, C.; Javier Chaves, F.; Garcia, M. J.; Garrido, F.; Jover, R.; O'Connor, J. E.; Iradi, A.; Oltra, A.; Oliva, M. R.; Saez, G. T. Role of glutathione in the induction of apoptosis and c-fos and c-jun mRNAs by oxidative stress in tumor cells. *Cancer Lett* **208:**103-113; 2004.

[47] Ochi, T. Menadione causes increases in the level of glutathione and in the activity of gamma-glutamylcysteine synthetase in cultured Chinese hamster V79 cells. *Toxicology* **112:**45-55; 1996.

[48] Eklow, L.; Moldeus, P.; Orrenius, S. Oxidation of glutathione during hydroperoxide metabolism. A study using isolated hepatocytes and the glutathione reductase inhibitor 1,3-bis(2-chloroethyl)-1-nitrosourea. *Eur J Biochem* **138:**459-463; 1984.

[49] Hayes, J. D.; McLellan, L. I. Glutathione and glutathione-dependent enzymes represent a co-ordinately regulated defence against oxidative stress. *Free Radic Res* **31:**273-300; 1999.

[50] Ozaki, M.; Aoki, S.; Masuda, Y. K(+)-linked release of oxidized glutathione induced by tert-butyl hydroperoxide in perfused rat liver is independent of lipid peroxidation and cell death. *Jpn J Pharmacol* **65:**183-191; 1994.

[51] Moeller, B. J.; Cao, Y.; Li, C. Y.; Dewhirst, M. W. Radiation activates HIF-1 to regulate vascular radiosensitivity in tumors: role of reoxygenation, free radicals, and stress granules. *Cancer Cell* **5:**429-441; 2004.

[52] Batinic-Haberle, I.; Benov, L. T. An SOD mimic protects NADP+-dependent isocitrate dehydrogenase against oxidative inactivation. *Free Radic Res* **42:**618-624; 2008.

[53] Liu, H.; Kehrer, J. P. The reduction of glutathione disulfide produced by t-butyl hydroperoxide in respiring mitochondria. *Free Radic Biol Med* **20:**433-442; 1996.

[54] Petcu, L. G.; Plaut, G. W. NADP-specific isocitrate dehydrogenase in regulation of urea synthesis in rat hepatocytes. *Biochem J* **190:**581-592; 1980.

# Chapter 5

## Development of macrocyclic copper(II) complexes: synthesis, superoxide scavenging activity, structural studies and biological evaluation

The work described in this Chapter was partially published in:

Macrocyclic copper(II) complexes: superoxide scavenging activity, structural studies and cytotoxicity evaluation. A.S. Fernandes, J. Gaspar, M.F. Cabral, C. Caneiras, R. Guedes, J. Rueff, M. Castro, J. Costa, N.G. Oliveira. Journal of Inorganic Biochemistry (2007) 101, 849-858.

Some data presented in this Chapter was adapted from:

Macrocyclic copper(II) complexes as superoxide scavengers: Insights from a DFT study. J.M. Matxain, D.J.V.A. dos Santos, A.S. Fernandes, M.F. Cabral, J. Costa, M. Castro, N.G. Oliveira, R.C. Guedes, *to be submitted*.

**Abstract**

In this Chapter, five macrocyclic copper(II) complexes (CuL1-CuL5) were synthesized and evaluated *in vitro* for their ability to scavenge the $O_2^{\bullet-}$ generated by the XXO system, using the NBT and the DHE assays. $IC_{50}$ values in the low micromolar range were found in four out of five macrocyclic complexes studied, demonstrating their effective ability to scavenge $O_2^{\bullet-}$. Spectroscopic and electrochemical studies were performed in order to correlate the structural features of the complexes with their $O_2^{\bullet-}$ scavenger activity. The complexes did not show considerable toxicity in V79 cells (up to 100 µM, 24 h, MTT assay). From the aforementioned studies, the complexes CuL3 and CuL4, that exhibited high stability and effective $O_2^{\bullet-}$ scavenging activity, were selected to be evaluated in the oxidative stress models validated in Chapter 3 (XXO and TBHP). The ability of the complexes to counteract these oxidants was studied using endpoints of cell viability (MTT and CV assays) and intracellular ROS generation (DHE assay). CuL3 was slightly protective against TBHP, but it exerted a pro-oxidant effect in XXO-treated cells. For CuL4, no considerable effects were observed. The ability of CuL3 and CuL4 to generate $HO^{\bullet}$ radical via Fenton reaction was studied by the DNA stand break analysis. These complexes can react with $H_2O_2$ leading to $HO^{\bullet}$, being this reaction reverted in the presence of catalase. The cytotoxicity profile of CuL3 and CuL4 was also studied in human breast carcinoma cells (MCF7) and the compounds did not show toxic effects (up to 100 µM, 24 h, MTT assay). Their ability to potentiate the anticancer drug Dox was studied in MCF7 cells, using the MTT assay, but no significant effects were observed. Although CuL4 exhibited promising chemical and biochemical properties *in vitro*, this complex did not present relevant effects in the cell-based experiments performed in this Chapter. For CuL3, a modest effect was observed in TBHP-treated cells. Further studies should be performed for a better comprehension of the biological potentialities of these complexes.

## 5.1. Introduction

Copper is an essential element involved in several biological functions, acting as a catalytic component of many metalloenzymes, including SOD. Therefore, copper(II) complexes can enclose a SOD mimetic activity hindering increased levels of ROS. Biological effects of the SODm are related to their structures. High thermodynamic stability constants are required to avoid the dissociation of the complex *in vivo*, what could be achieved by using macrocyclic ligands [1]. The macrocyclic nature of the ligand is important for the SOD-like activity of the corresponding complexes as well as for their stability in the presence of biological chelators, even if the metal ion does not lie inside the cavity [2]. Several macrocyclic copper(II) complexes have been reported to scavenge superoxide anion [2-7].

Previous studies have demonstrated that chemical modifications in the ring size, donor atoms and substituents on the macrocycles, may have profound effects both on the stability and the SOD-like activities of the respective complexes [3, 4]. A copper(II) complex which possesses SODm activity should have a flexible arrangement of the ligands around the copper(II) ion in order to allow an easy reduction to copper(I). In addition, a copper(II) SODm complex should enclose a certain stability, avoiding thus dissociation in the acid region and should possess an accessible site in order to easily bind the $O_2^{\bullet-}$ radical and, hence to give a quick reduction to copper(I). Finally, an equatorial field of medium strength is required because strong ones do not favour the attack of $O_2^{\bullet-}$ to the accessible apical sites [8].

Although many copper(II) complexes have been studied, most of them are not thermodynamically stable or highly active at the range of physiological pH [9]. For this reason, novel complexes with high stability and activity, together with low toxicity, are still needed. Another important feature is the solubility of the compounds. Some of the SODm that have been developed, despite of their effective catalytic activity, are not water soluble. It is estimated that ~ 40% of the compounds that enter the development phase fail to reach the market, mainly due to poor biopharmaceutical properties, in which low aqueous solubility is included [10]. Hence, the water solubility presented by the complexes under study is definitely an important favorable characteristic.

In this Chapter, five low molecular weight copper(II) macrocyclic complexes are described, focusing on their possible application as superoxide scavenging agents. The ability of those copper(II) complexes to scavenge $O_2^{\bullet-}$ was evaluated and spectroscopic studies were performed in order to correlate the structural features of the complexes with their scavenging

activity. In addition, the cytotoxicity of these complexes was assessed in V79 cells. From these studies, the most promising compounds were selected and additional cell based assays were performed in order to further characterize the potential of these complexes as SODm therapeutic agents. In Chapter 3, two oxidative stress models, XXO and TBHP, were validated with the well established SODm MnTM-4-PyP. Therefore, in the present Chapter, V79 cells were treated with these oxidative stress inducers and the capacity of the complexes to abrogate the inflicted damage was evaluated.

As explained in Chapter 1, SODm, while dismutating $O_2^{\bullet-}$, may increase the intracellular $H_2O_2$ concentration. Hence, SODm can have an anticancer activity, either reducing tumor growth or potentiating established anticancer agents [11-13], such as Dox. This anthracycline is commonly used in breast cancer chemotherapy and exerts its cytotoxic effect by different mechanisms, including the interference in DNA synthesis and ROS generation [14-16]. As described in Chapter 3, Dox undergoes redox cycling reactions within the cell, leading to the generation of $O_2^{\bullet-}$ [14]. If a copper(II) complex with SOD-like activity is present, it can disproportionate $O_2^{\bullet-}$ into $H_2O_2$. If this complex reacts with $H_2O_2$ to form $HO^{\bullet}$, this can be a further advantage in promoting cancer cells' death [17], as schematized in Fig. 5.1.

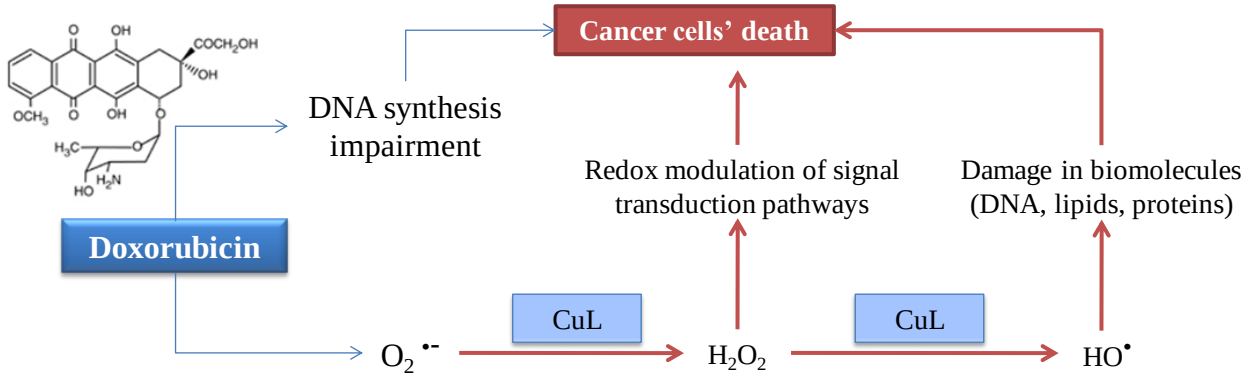


**Fig. 5.1** – Potential activity of Cu(II) complexes (CuL) with SOD-like activity as boosters of Doxorubicin anticancer properties.

In view of this, the potential application in cancer therapy of the most promising complexes was addressed in this Chapter. Their capacity to generate $HO^{\bullet}$ was evaluated *in vitro* and the toxicity of the complexes was studied in breast carcinoma cells (MCF7). Furthermore, the ability of the complexes to potentiate the toxic effects of Dox was evaluated.

## 5.2. Materials and Methods

### *5.2.1 Chemicals*

PBS, caffeic acid, xanthine, xanthine oxidase, nitroblue tetrazolium chloride monohydrate (NBT), MTT, CV, trypsin, Ham's F-10 medium, 30% hydrogen peroxide (w/w), newborn calf serum, penicillin-streptomycin solution, Dulbecco's Modified Eagle's Medium (DMEM), foetal bovine serum, insulin solution from bovine pancreas, TBHP, Dox, catalase from bovine liver, and Cu,Zn-SOD from human erythrocytes were obtained from Sigma-Aldrich. Cu,Zn-SOD was reconstituted in PBS and the concentration of the resultant solution (7.9 μM) was calculated taking into account a molecular weight for the enzyme of 32,500 [18]. DMSO was obtained from Merck. Chelex 100 resin was acquired to Biorad. Copper(II) nitrate-trihydrate, disodium ethylenediaminetetracetate ($Na_2H_2$edta) and DHE were purchased from Fluka. Pst1 enzyme was obtained from Fermentas.

### *5.2.2. Synthetic procedures*

#### *5.2.2.1. Synthesis of the macrocycles*

The macrocyclic ligands used for the preparation of the copper(II) complexes studied in the present work are shown in Scheme 3.1 and were synthesized as previously described [19-21].

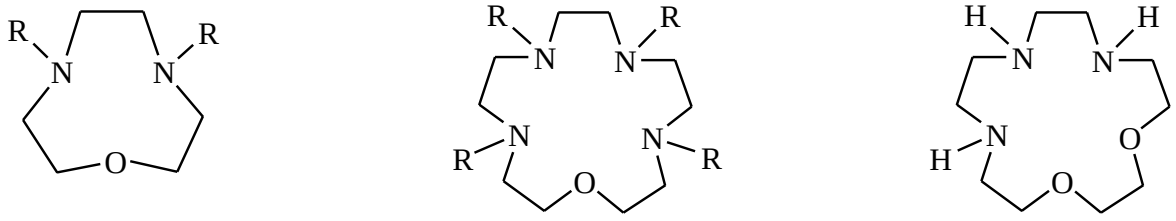


**L1 -** R = H

**L2 -** R = $CO_2H$

**L3 -** R = H

**L4 -** R = $CO_2H$

**L5**

**Scheme 3.1** (Charges are omitted for simplicity)

All the compounds were obtained in good yield and were characterized by $^{1}H$ and $^{13}C$ NMR spectroscopy on a Bruker Avance 400 spectrometer. The references used for the NMR measurements were 3-(trimethylsilyl)propionic acid-$d_4$ sodium salt for $^{1}H$ NMR and 1,4-dioxan for $^{13}C$ NMR.

As represented in Fig. 5.2, L1 was synthesized by Richman and Atkins' procedure [22], involving the condensation of the disodium salt of 1,4,*N*,*N'*-bis(*p*-toluenesulfonyl)-1,4-diaminoethane with 1-*O*,5-*O*-di(*p*-toluenesulfonyl)-3-oxapentane-1,5-diol, at 110 ºC in dry dimethylformamide (DMF). The protective groups of the ditosylated cyclic amine were removed by a reductive cleavage with a mixture of glacial acetic acid, 48% hydrobromic acid and phenol during 28 h under reflux [19]. $^{1}H$ NMR ($D_2O$): $\delta$ (ppm) 3.06 (t, 4 H), 3.34 (s, 4 H), 3.75 (t, 4 H).

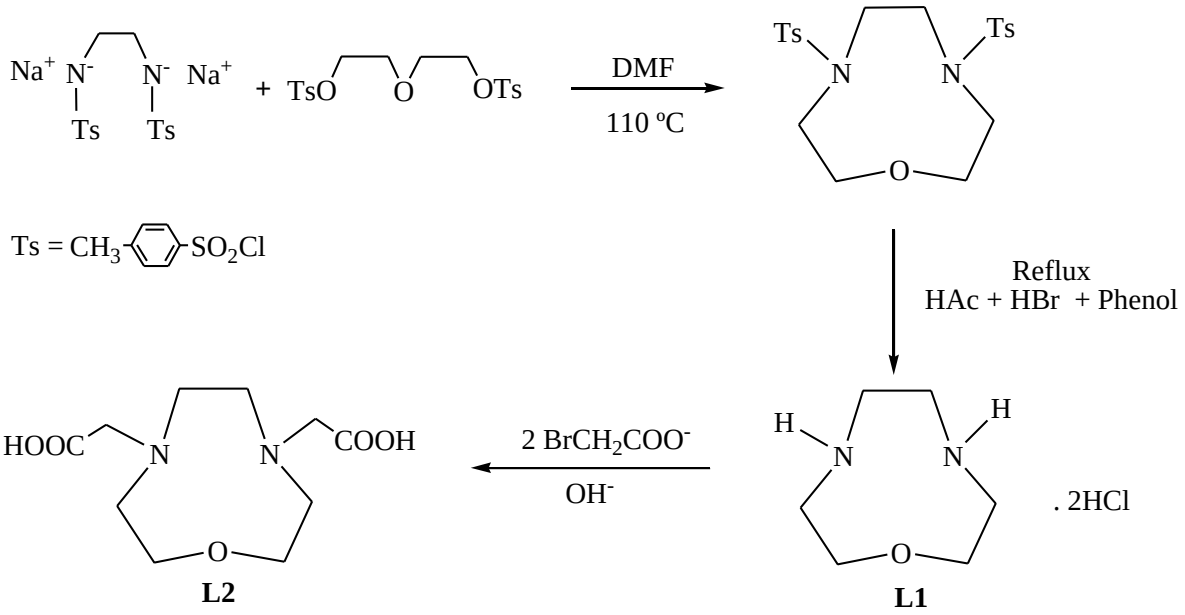


**Fig. 5.2** – Schematic representation of the synthesis of the ligands L1 and L2.

L2 was synthesized by condensation of the parent amine L1, with potassium bromoacetate in an aqueous basic solution [19] (Fig. 5.2). $^{1}H$ NMR ($D_2O$): $\delta$ (ppm) 3.19 (t, 4 H), 3.25 (s, 4 H), 3.68 (s, 4 H), 3.80 (t, 4 H). $^{13}C$ NMR ($D_2O$): $\delta$ 52.16, 54.70, 57.27, 66.21, 171.53.

L3 was also prepared according to the Richman and Atkins' method [22], involving the condensation of the disodium salt of 3,6,*N*,*N'*-tetra(*p*-toluenesulfonyl)-3,6-diazaoctane-1,8-diamine with 1-*O*,5-*O*-di(*p*-toluenesulfonyl)-3-oxapentane-1,5-diol, in dry DMF for 6 h. In a second step, the protective groups were removed by a reductive cleavage [20, 23], as described above (Fig. 5.3). $^{1}$H NMR ($D_2O$): $\delta$ (ppm) 3.21 (s, 4 H), 3.29 (m, 8 H), 3.37 (t, 4 H), 3.73 (t, 4 H). $^{13}$C NMR ($D_2O$): $\delta$ 42.73, 43.19, 43.87, 46.50, 65.67.

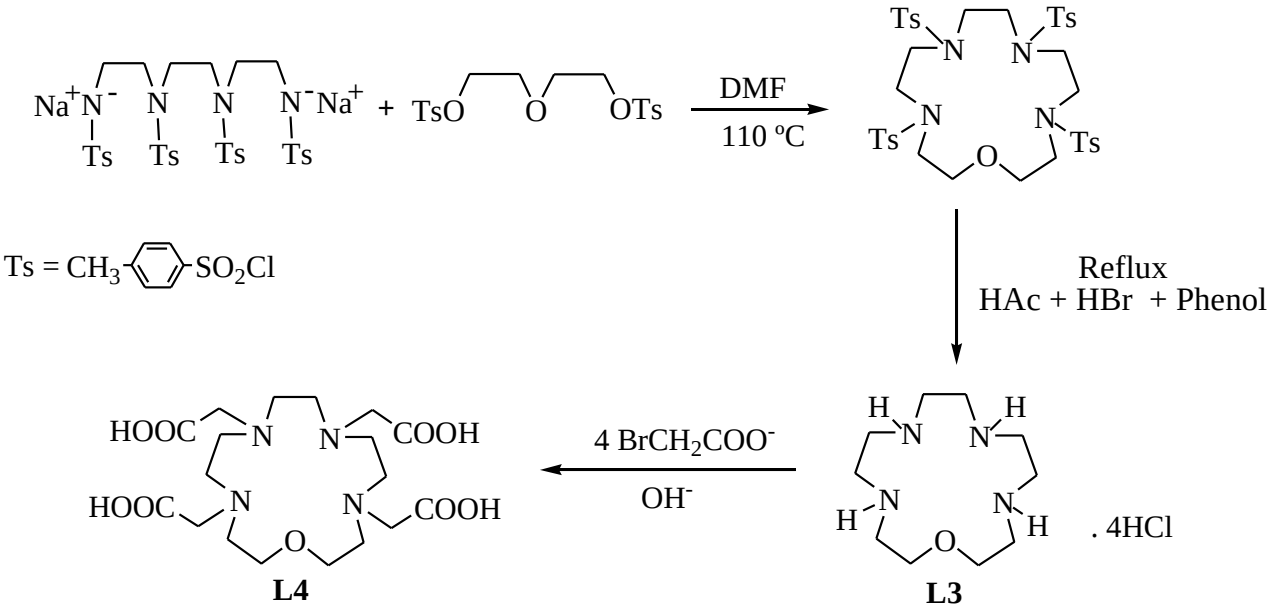


**Fig. 5.3** – Schematic representation of the synthesis of the ligands L3 and L4.

L4 was synthesized by condensation of the parent amine L3 with potassium bromoacetate in an aqueous alkaline solution [21] (Fig. 5.3). $^{1}$H NMR ($D_2O$): $\delta$ (ppm) 3.42 (s, 4 H), 3.55 (t, 4 H), 3.64 (t, 4 H), 3.77 (t, 4 H), 3.85 (s, 4 H), 4.09 (s, 4 H), 4.15 (t, 4 H). $^{13}$C NMR ($D_2O$): $\delta$ 50.00, 51.72, 53.23, 54.67 (d), 55.02, 64.89, 168.59, 171.79.

L5 was prepared by the same method of L3, using 1-*O*,8-*O*-di(*p*-toluenesulfonyl)-3,6-dioxaoctane-1,8-diol and the disodium salt of 3,*N*,*N'*-tri(*p*-toluenesulfonyl)-3-azapentane-1,5-diamine [20] (Fig. 5.4). $^{1}$H NMR ($D_2O$): $\delta$ (ppm) 3.52 (t, 4 H), 3.69 (m, 8 H), 3.82 (s, 4 H), 3.94 (t, 4 H).$^{13}$C NMR ($D_2O$): $\delta$ 42.73, 43.04, 45.90, 65.30, 69.86.

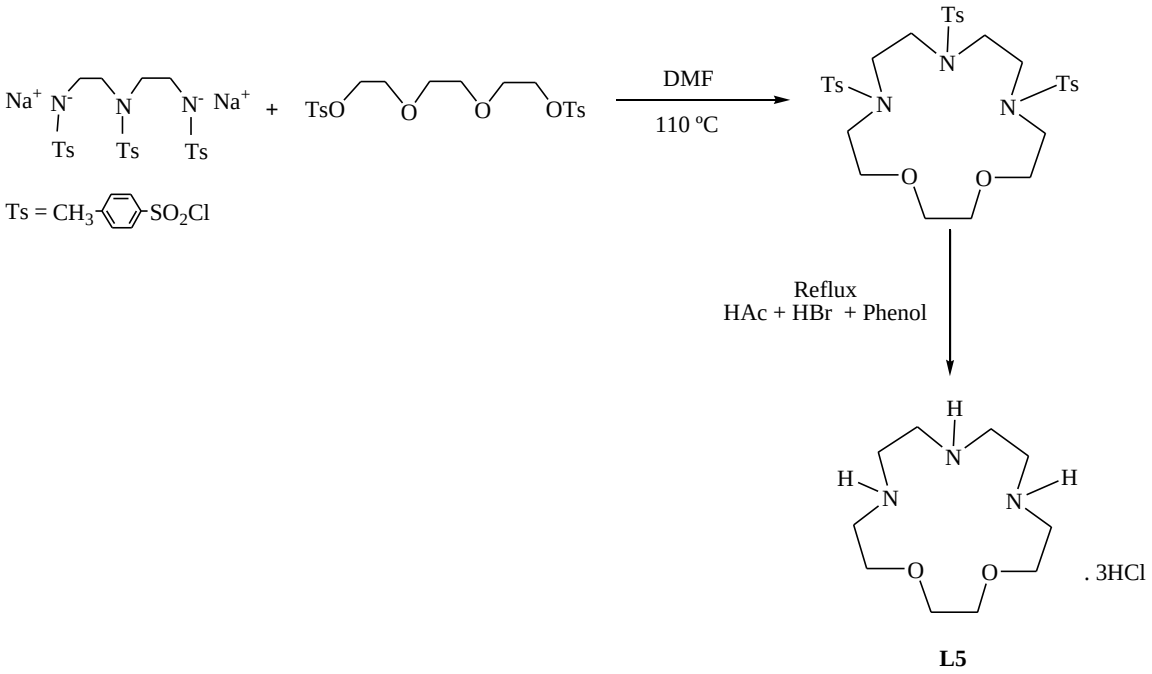


**Fig. 5.4** – Schematic representation of the synthesis of the ligand L5.

Aqueous macrocycles solutions were prepared at ~2.5 × $10^{-3}$ M, and their concentrations were determined by potentiometric titrations.

*5.2.2.2. Synthesis of the macrocyclic copper(II) complexes*

Copper(II) complexes were prepared by adding an aqueous solution of the nitrate salt (4.0 μmol) previously standardized by titration with $Na_2H_2$edta [24] to an aqueous solution of the ligands (4.2 μmol). After stirring at room temperature, KOH solution was added until pH 7.4. The solvent was removed under reduced pressure and the residue was taken up in 2 mL of PBS. At micromolar concentrations, water molecules can act as competing ligands for copper(II), modifying the species distributions towards less coordinated species. To avoid this problem, when copper(II) complexes were prepared, a small excess of ligand was used in order to increase the complexation of the copper(II) ions [25].

The values of the stability constants of Cu(II) with the ligands were previously determined from potentiometric titrations, performed at 25.0 ± 0.1°C and 0.10 M ionic strength [19-21]. The constants values were calculated by fitting the potentiometric data obtained using the SUPERQUAD [26] or HYPERQUAD programs [27].

Species distribution curves were calculated for the aqueous solutions containing Cu(II) and each ligand (L1-L5) at a molar ratio of 1:1, using the Hyss program [28]. The species concentrations in solution were determined at physiological pH. Simulations of the species distribution in the presence of 0.01 M phosphate buffer were also performed. For these calculations, the stability constants for copper(II)-hydrogenophosphate [29] as well as the protonation constants for phosphoric acid [30] were considered, in order to calculate the percentage of each species present at pH 7.4.

Theoretical calculations on the copper(II) complexes were performed within density functional theory [31], by Matxain et al [32]. Structure optimizations were carried out in gas phase, using the B3LYP hybrid functional [33] and the 6-31+G(d,p) [34] basis set for C, N, O and H, and the Stuttgart pseudopotentials [35] for Cu. Single point calculations using the 6-311++G(3df,3p) basis set for all atoms, and the integral equation formalism of the polarized continuum model (IEFPCM) of Tomasi and co-workers [36] were performed on the optimized gas-phase structures to estimate the effects of bulk solvation. All the calculations were performed with Gaussian03 software [37].

### *5.2.3. Superoxide scavenging activity*

The superoxide scavenging activity of the complexes was studied by using their ability to scavenge $O_2^{\bullet-}$, generated by the XXO system (Fig. 3.1), trough two different endpoints: the reduction of NBT and the oxidation of DHE. Copper(II) and Cu,Zn-SOD from human erythrocytes were used as controls.

#### *5.2.3.1 NBT assay*

The NBT assay is a simple and convenient method widely used for superoxide quantification and in SODm research [38]. In this assay, while $O_2^{\bullet-}$ is generated, NBT is reduced, developing a blue formazan colour which is associated with an increase in the absorbance at 560 nm [39]. When a scavenger compound is added, it competes with the NBT for the oxidation of the generated superoxide anions. Therefore, there is a decrease in the rate of the NBT reduction, which leads to lower absorbance increases. The more effective the compound, the lower the concentration which inhibits the NBT reduction in 50% ($IC_{50}$) [2].

The conditions of the NBT assay were adapted from Kovala-Demertzi *et al*. [39]. The reaction system (final volume = 1 mL) contained 0.2 mM of xanthine, 0.6 mM of NBT in phosphate buffer 0.1 M, pH 7.8. Each complex (CuL1-CuL5) was added to the reaction mixture in different concentrations up to 40 μM. The reaction was started by the addition of XO (6 mU/mL), an activity which allowed to yield the absorbance change between 0.030 and 0.040 per minute, at 560 nm, 25 °C. The extent of NBT reduction was followed spectrophotometrically, by measuring the increase of the absorbance at 560 nm on a Hitachi U-2001 spectrophotometer, for 3 min. Each experiment was performed in duplicate and each concentration generated a time dependent curve. From its linear domain, the slope (Abs/min) was calculated. The percentage of inhibition for each concentration was calculated as follows: [100- (slope/slope control)*100]. The $IC_{50}$ of each compound was defined as the concentration which inhibited 50% of the NBT reduction by $O_2^{\bullet-}$ produced in the XXO system.

*5.2.3.2 DHE assay*

As referred in Chapter 3, DHE is a probe that undergoes oxidation by $O_2^{\bullet-}$ giving the fluorescent product 2-hydroxyethidium (Fig. 3.6). This probe can be applied either to cell-based experiments or to "test tube" assays. In the present section, DHE was used to detect the amount of $O_2^{\bullet-}$ present in a "test tube" system, allowing the determination of the superoxide scavenging activity of the complexes. This assay was performed in 96-well microplates. Each well (200 μL) contained 0.2 mM of xanthine and phosphate buffer 0.1 M, pH 7.8. The tested compounds (CuL1-CuL4), diluted in phosphate buffer pH 7.8, were added to the reaction mixture (10 μL). Different concentrations up to 80 μM were tested for each complex. In what concerns CuL5, since it revealed no activity using the NBT assay (see Results and Discussion section), only the highest concentration (80 μM) was tested. DHE aliquots (10 mM, DMSO) were diluted 1:100 in phosphate buffer pH 7.8. DHE was added to each well at a final concentration of 10 μM. The reaction was started by the addition of XO (5 mU/mL). The reaction was performed at 25 °C, and the extent of DHE oxidation was followed by measuring the increase of the fluorescence on a Zenyth 3100 microplate reader, for 60 min, using $\lambda_{excitation}$ = 485 nm and $\lambda_{emission}$ = 595 nm. Each experimental point was performed using eight replicates. Two independent experiments were performed for each concentration of the different complexes. Each concentration generated a time course curve. From its linear domain, the slope was calculated. The percentage of inhibition for each concentration was determined as described above (5.2.3.1). The $IC_{50}$ of each

compound was defined as the concentration which inhibited 50% of the DHE oxidation by the $O_2^{\bullet-}$ produced in the XXO system.

*5.2.3.3. Xanthine oxidase inhibition assay*

The possibility of an inhibition of the $O_2^{\bullet-}$ generating system XXO by the copper(II) complexes under study was also evaluated. This was performed by following at 293 nm, during 5 min, the uric acid produced after xanthine was oxidized by XO in aerobic conditions concomitantly to the production of $O_2^{\bullet-}$ (Fig. 3.1). The assay was performed for each complex (80 μM) at the same experimental conditions described above (5.2.3.1.), with the exception of the NBT solution, which was replaced for equal volume of phosphate buffer [40]. Caffeic acid (50 μM), a recognized XO inhibitor, was used as positive control. Each experiment was performed in duplicate.

*5.2.4. Structural studies*

*5.2.4.1 Spectroscopic studies*

Spectroscopic studies are useful tools that give information on the copper environment in a complex, shedding light on its potential SOD-like activity [41]. EPR spectroscopy measures the absorption of microwave radiation by an unpaired electron when it is placed in a strong magnetic field [42]. The hyperfine coupling constants from EPR spectroscopy, along with the d–d transitions from electronic spectra, are parameters that characterize the first coordination sphere around the metal [41].

The electronic spectra of the complexes were performed using a UNICAM model UV-4 spectrophotometer. The complexes were prepared in aqueous solutions at $1.20 \times 10^{-3}$ M (1:1 ratio) in 0.1 M in $KNO_3$. For CuL2, CuL3, CuL4 and CuL5 the solutions' pH was 7.38, 7.41, 7.37, and 7.38, respectively.

EPR spectroscopy measurements of the copper(II) complexes were recorded with a Bruker EMX 300 spectrometer equipped with a continuous-flow cryostat for liquid nitrogen, operating at X-band. The complexes were prepared at $1.25 \times 10^{-3}$ M (1:1 ratio) in water (1.0 M

in $NaClO_4$). The spectra of CuL2, CuL3, CuL4 and CuL5 were recorded at the pH values of 7.39, 7.35, 7.40 and 7.40, respectively.

*5.2.4.2. Electrochemistry*

Cyclic voltammetry is an electroanalytical technique widely used to study redox processes. It enables the search of redox couples and offers a rapid location of the redox potentials of the electroactive species. This technique was therefore used to characterize the electrochemical behavior of the complexes.

A BAS CV-50W Voltammetric Analyzer connected to a BAS/Windows data acquisition software was used for the electrochemical measurements. Cyclic voltammetry experiments were performed in a glass cell MF-1082 from BAS in a C-2 cell enclosed in a Faraday cage, at room temperature under nitrogen atmosphere. The reference electrode was Ag/AgCl (MF-2079 from BAS) and its potential was −44 mV relative to a saturated calomel electrode. The auxiliary electrode was a 7.5 cm platinum wire (MW-1032 from BAS) with a gold-plated connector. The working electrode was a glassy carbon (MF-2012 from BAS). Between each cyclic voltammetry scan the working electrode was electrocleaned by multicycle scanning in the supporting electrolyte solution, polished on diamond 1 μm and on alumina 0.3 μm, according to standard procedures. The aqueous solutions of the complexes were prepared at $1.20 \times 10^{-3}$ M (1:1 ratio) in 0.1 M $KNO_3$ (supporting electrolyte). The voltammograms of CuL2, CuL3, CuL4 and CuL5 were performed at the pH values of 7.39, 7.35, 7.40 and 7.40, respectively. Cyclic voltammograms were recorded in the region from +1.0 to -1.0 V *versus* Ag/AgCl, varying the scan rate from 10 to 100 mV $s^{-1}$. The half wave potentials $E_{1/2}$ were calculated approximately from $(E_{pa} + E_{pc})/2$.

*5.2.5. Evaluation of the cytotoxicity profile of the macrocyclic copper(II) complexes in V79 cells*

Cytotoxicity assays were performed in V79 cells, cultured as described in Chapter 3 (3.2.2). The protocol used for the MTT assay is described in Chapter 3 (3.2.3.1). Cells were exposed to different concentrations of the macrocyclic copper(II) complexes (1, 10, 50 and 100 μM) dissolved in PBS, during a 24 h period. Hydrogen peroxide (10 mM) was used as

positive control. Two independent experiments were performed and four replicate cultures were used for each complex concentration in each independent experiment.

### *5.2.6. Evaluation of the potential protective effect of CuL3 and CuL4 against the oxidative injury induced by XXO and by* TBHP

From the results of the previous assays, CuL3 and CuL4 were selected to be further studied in cell-based experiments. The potential antioxidant activity of these copper(II) complexes was studied in V79 cells, using XXO and TBHP as oxidative stress inducers.

#### *5.2.6.1 MTT Reduction assay*

The MTT assay was performed as described in Chapter 3 (3.2.3.1). At *t*=24 h, the cells were treated for a further 24 h-period with each of the oxidants, X (240 µM)/XO (20 U/L) or TBHP (100 µM), in the absence or presence of each complex (5, 25, 50, and 100 µM). Two to four independent experiments were performed as described above and eight replicate cultures were used for each complex concentration in each independent experiment.

#### *5.2.6.2 Crystal Violet assay*

Since CuL3 has shown some protection against the TBHP-induced cytotoxicity in the MTT assay, a second cell viability method – the CV staining, was carried out as a confirmatory assay. As in the MTT assay, the cells were grown for 24 h and then exposed to TBHP (100 µM) with or without CuL3 (5, 25, 50 and 100 µM) for a 24 h period. The CV assay was carried out as described in Chapter 3 (3.2.3.2). Five independent experiments were performed, each one comprising eight replicate cultures.

*5.2.6.3. DHE fluorimetric assay*

To assess whether the protective effect against TBHP observed for CuL3 was related to the superoxide scavenging activity of this complex, the DHE assay was used. This cell permeable probe was used to detect the intracellular levels of $O_2^{\bullet -}$ as described in Chapter 3 (3.2.5). V79 cells were exposed for 3 h to TBHP (100 µM) and/or CuL3 (100 µM) and to DHE (10 µM). Five independent experiments were performed, each comprising six replicate cultures for each experimental point.

*5.2.7. DNA strand break analysis*

The generation of $HO^{\bullet}$ radical by the copper(II) complexes CuL3 and CuL4 was evaluated by the DNA strand break analysis. The underlying principle of this method is schematized in Fig. 5.5.

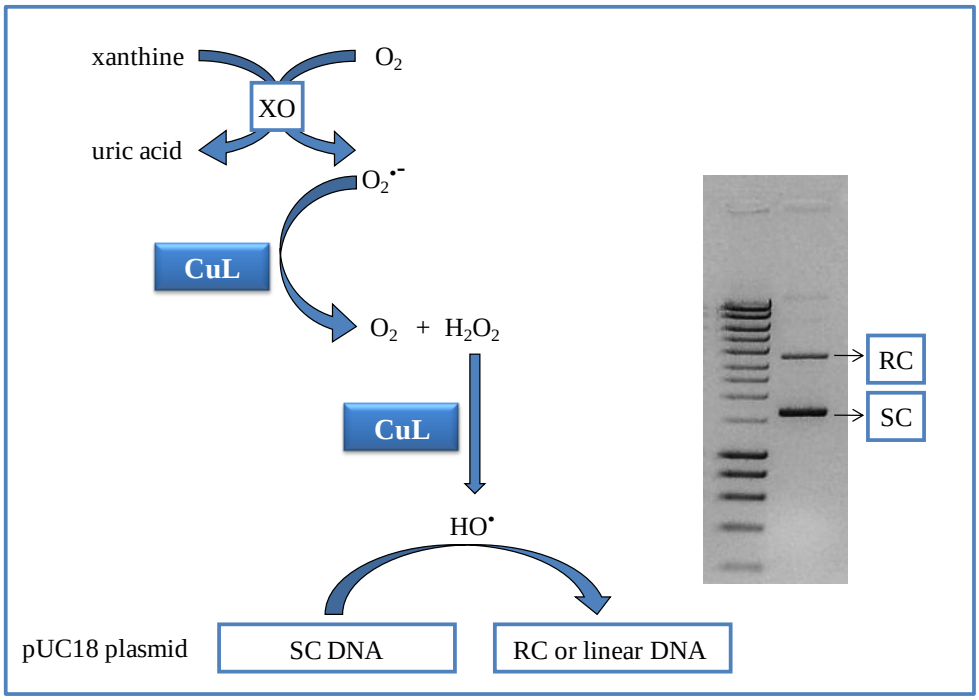


**Fig. 5.5** – Fundamentals of the DNA strand break analysis. The disproportionation of $O_2^{\bullet -}$ by the copper(II) complexes originates $H_2O_2$. If the complex undergoes Fenton chemistry, $HO^{\bullet}$ radical is generated in the system. This radical attacks the phosphodiester backbone of supercoiled plasmid DNA producing relaxed circular DNA [43]. This relaxed circular molecule migrates more slowly than the supercoiled form during gel electrophoresis (XO, xanthine oxidase; SC, supercoiled; RC, relaxed circular).

*Escherichia coli* strain DH5α containing plasmid pUC 18 was kindly provided by Dr. Michel Kranendonk. Plasmid pUC 18 DNA was amplified in the host strain and extracted using a Qiagen plasmid kit. To confirm that the extracted DNA corresponded to pUC 18, a restriction assay was performed. The enzyme used was Pst1, since pUC18 DNA has one recognition site for this enzyme. The protocol for digestion was carried out according to the manufacturer's instructions. As expected, the agarose gel revealed a single band that corresponded to the size of pUC 18 DNA (2686 base pairs). It is also important to mention that a gel electrophoresis of the extracted DNA has shown that ~100% of the DNA was in the supercoiled form, thus assuring its quality.

Plasmid DNA was incubated with the reaction mixtures, in 5 mM sodium phosphate buffer pH 7.4 pre-treated with chelex 100 resin. Superoxide anion was generated from 5 U/L of XO plus 200 μM xanthine. XXO plus copper(II) (6.7 μM) were used as a positive control for the generation of $HO^{\bullet}$ radical. The effects of catalase (221 U/mL) and SOD (0.04 μM) on the reversion of the plasmid cleavage were studied and heat-inactivated enzymes were used as controls. CuL3 and CuL4 were tested at 100 μM. After a 2 h incubation, in the dark, at 37ºC, loading buffer was added to the samples and they were analysed by electrophoresis at 150 V in 1% agarose gel in Tris-Borate-edta buffer. The gels were stained with ethidium bromide. The approximate fluorescence of the bands was estimated by densitometry, using the LabWorks software. The optical density of supercoiled DNA was corrected by a factor of 1.4 because, when stained with ethidium bromide, the relaxed circular form gives a fluorescence intensity 1.4-fold higher than the supercoiled form [44]. At least two independent experiments were performed, each including three gel lanes for sample.

### *5.2.8. Evaluation of the cytotoxicity profile of the macrocyclic copper(II) complexes CuL3 and CuL4 in MCF7 cells*

#### *5.2.8.1. MCF7 Cells culture*

MCF7 cells, a human breast carcinoma cell line, were purchased from DSMZ. MCF7 cells were cultured in DMEM supplemented with 10% foetal bovine serum, 1% antibiotic solution (penicillin-streptomycin) and 0.01 mg/mL insulin. Cells were kept at 37°C, under an atmosphere containing 5% $CO_2$.

*5.2.8.2 MTT Reduction assay*

The toxicity of CuL3 and CuL4 was evaluated in MCF7 cells, using the MTT assay. Briefly, ~6.5 × $10^3$ cells were cultured in 200 μL of culture medium per well in 96-well plates and incubated at 37°C under a 5% $CO_2$ atmosphere. The cells were grown for 48 h and then exposed to different concentrations of the macrocyclic copper(II) complexes (1, 10, 25, 50 and 100 μM) during a 24 h-period. The MTT assay was then performed as described in Chapter 3 (3.2.3.1). At least two independent experiments were performed and at least four 4 individual cultures were used for each complex concentration in each independent experiment.

*5.2.9. Evaluation of the possible role of the macrocyclic copper(II) complexes CuL3 and CuL4 on the potentiation of Dox cytotoxicity in MCF7 cells*

The studies on the modulation of the cytotoxicity of Dox were also carried out in MCF7 cells using the aforementioned MTT protocol. After growing for 48 h, cells were exposed to Dox (50, 100, 500, 1000 and 5000 nM) in the absence or presence of 100 μM CuL3 or CuL4, for 24 h. Two to five independent experiments were performed, each comprising at least 4 individual cultures.

*5.2.10. Statistical analysis*

The results obtained in points 5.2.6 and 5.2.9 were submitted to a statistical analysis as described in Chapter 3 (3.2.6).

## 5.3. Results and Discussion

Macrocycles and their metal complexes have been suggested as promising agents for the diagnosis and treatment of different diseases and toxicological conditions [45-47]. In addition, some macrocyclic complexes have been suggested as a potential class of SOD mimics, mainly because of their high thermodynamic stability [1, 2].

Most of the catalytic antioxidants have a redox-active metal center [1, 48], but only a few metal ions have the ability to catalyze the dismutation of $O_2^{\bullet-}$ to hydrogen peroxide and oxygen. It is well known that copper(II) aqueous ion is a very potent superoxide scavenger [1]. The low $IC_{50}$ values found using $Cu(NO_3)_2$ in this work are consistent with the values found for other Cu(II) salts [2] and show the efficacy of Cu(II) in the disproportionation of $O_2^{\bullet-}$.

Human serum albumin has a high-affinity site for copper(II) [49] precluding the use of free copper(II) as a therapeutic SOD mimetic. In fact, in blood plasma, albumin exists in very high concentration, binding to the non-ceruloplasmin copper fraction and acting thus as a copper transport protein [9, 49]. Therefore, if free Cu(II) ions were administered, they would be immediately complexed by serum albumin, losing their ability to dismutate the $O_2^{\bullet-}$ [2]. Within mammalian cells, the binding of Cu(II) by cellular components also occurs, and copper chaperones, glutathione and metallothioneins, among other proteins, may be involved [50]. Since the intracellular milieu has an extraordinary overcapacity for chelation of copper(II), free copper availability is extremely restricted, even when cells are exposed to an elevation of the medium's copper concentration [51]. In view of this, copper(II) must be enclosed in a stable ligand, which protects it from being chelated by serum and cellular components. Additionally, this ligand must allow copper(II) to switch its redox state and dismutate $O_2^{\bullet-}$. It has been described that if the ligand is a macrocycle, the metal complex may have higher biological stability [1, 2].

### *5.3.1. Chemical characterization and superoxide scavenging activity of the complexes*

The knowledge of the stability constants' values for the copper(II) complexes is a very important issue for the prediction of their behaviour *in vivo*. High stability constants are required to avoid dissociation of the complex in *in vivo* systems. The stability constants values of the macrocyclic copper(II) complexes under study were determined in previous works [19-21] and

are shown in Table V.1. All complexes, except CuL1, showed reasonably high values of stability constants (log $K_{ML}$ > 13). L3 and L4 have indeed shown the highest values (log $K_{ML}$ = ~20).

**Table V.1 –** Stepwise stability constants (log *K*) for the copper(II) complexes of L1-L5.

| **Equilibrium quotient** | **L1** [a] | **L2** [a] | **L3** [b] | **L4** [c] | **L5** [b] |
|---|---|---|---|---|---|
| [CuL]/[Cu][L] | 10.80 | 13.37 | 20.34 | 19.23 | 15.72 |
| [CuHL]/[CuL][H] | - | - | - | 4.38 | - |
| $[Cu_2L]/[Cu][CuL]$ | - | - | - | 4.56 | - |
| $[CuL_2]/[CuL][L]$ | 8.80 | - | - | - | - |
| [CuL]/[CuLOH][H] | - | - | 10.4 | (8.1) | 8.87 |

[a] $I$ = 0.10 M $KNO_3$; $T$ = 25.0 ºC [19]
[b] $I$ = 0.10 M $KNO_3$; $T$ = 25.0 ºC [20]
[c] $I$ = 0.10 M $N(CH_3)_4NO_3$ $T$ = 25.0 ºC [21]

To properly evaluate the SOD-like activity of a copper(II) complex, it is crucial to know its species distribution. The concentration of the different species in solution can be calculated by a simulation approach, based on the knowledge of the stability constants of the different complex species. A correct speciation will allow the identification the species formed in particular conditions, which may be responsible for the $O_2^{\bullet-}$ scavenger activity [52]. Speciation studies also provide information on the absence or presence of non-complexed copper(II). Since free Cu(II) ion is known to be an efficient catalyst of $O_2^{\bullet-}$, its presence would lead to the misinterpretation of the results of the SOD-like activity assays [8]. The species distribution diagrams and the pCu values were therefore obtained from the values of the stability constants of the macrocyclic copper(II) complexes, using the Hyss program [28]. The concentration used in these simulations was 10 μM of Cu(II) at a molar ratio 1:1 with L1-L5. This value was chosen because it is in the range of $IC_{50}$ values of the active superoxide scavenging complexes. The results obtained under these conditions and at physiological pH (7.4) are shown in Table V.2. In these simulations, no free copper(II) ions are likely to be found in solution for the copper(II) macrocyclic complexes, except in the case of L1 (~ 5.1% of aqueous copper(II) ion). This can be explained by the fact that under these conditions (molar ratio 1:1) the complexation of L1 with copper(II) is not fulfilled. EPR spectra confirmed the absence copper(II) impurities in the CuL2-CuL5 solutions.

**Table V.2 -** Species distribution and pCu values calculated for an aqueous solution containing Cu(II) (10 μM) and each ligand (10.5 μM) at a molar ratio of 1:1 (charges on metal ions and complexes were omitted for simplicity).

| **Ligand** | **Species** (% relative to the total amount of Cu(II)) | **pCu** |
|---|---|---|
| **L1*** | 79.8% CuL + 12.4% $CuL_2$ + 5.1% Cu + 2.6% CuOH + 0.1% $Cu(OH)_2$ | 6.29 |
| **L2**** | 100.0% CuL | 8.90 |
| **L3** | 99.9% CuL + 0.1% CuOH | 15.39 |
| **L4** | 0.1% CuHL + 83.3% CuL + 16.6% CuLOH | 13.44 |
| **L5** | 96.7% CuL + 3.3% CuLOH | 11.22 |

* 12.8% CuL + 41.2% $CuL_2$ + 27.2% $CuHPO_4$ + 17.6% $Cu(HPO_4)_2$ + 1.1% $Cu(HPO_4)_3$, in 0.01 M phosphate buffer, pH 7.4.
** 93.9% CuL + 3.6% $CuHPO_4$ + 2.3% $Cu(HPO_4)_2$ + 0.2% $Cu(HPO_4)_3$, in 0.01 M phosphate buffer, pH 7.4.

The copper(II) complexes were initially redissolved in PBS and this solution was used in both the biochemical and cytotoxicity assays. In order to give an even more accurate speciation in the used conditions, the possible competition between the phosphate species present in high levels in the buffer and the copper(II) complexes under study was considered. Having this in mind, the species concentrations at pH 7.4 were recalculated. Using this approach, no changes were found for the species in solution at pH 7.4 for CuL3, CuL4 and CuL5. In what concerns to CuL1 and, in a lesser extent to CuL2, the presence of high phosphate concentration derived in some differences in the species in solution, giving rise to the appearance of $CuHPO_4$, $Cu(HPO_4)_2$ and $Cu(HPO_4)_3$ at pH 7.4 (Table V.2 - footnote).

The superoxide scavenging effects of the macrocyclic copper(II) complexes determined by both the NBT and DHE methods, are depicted in Fig. 5.6. The correspondent $IC_{50}$ values determined for the complexes under study, as well as for Cu(II), are presented in Table V.3. A very good correlation between the NBT and DHE assays was found (r = 0.979). The $IC_{50}$ values obtained for the macrocyclic copper(II) complexes using the NBT assay, were consistently higher, approximately 3-fold, than those obtained with the DHE assay (Table V.3). The DHE fluorimetric method was previously reported as a more sensitive and specific assay for $O_2^{\bullet-}$ when compared to the NBT assay [53], what may somehow explain these results. However, other authors have pointed out that DHE could enhance the rate of superoxide dismutation [54].

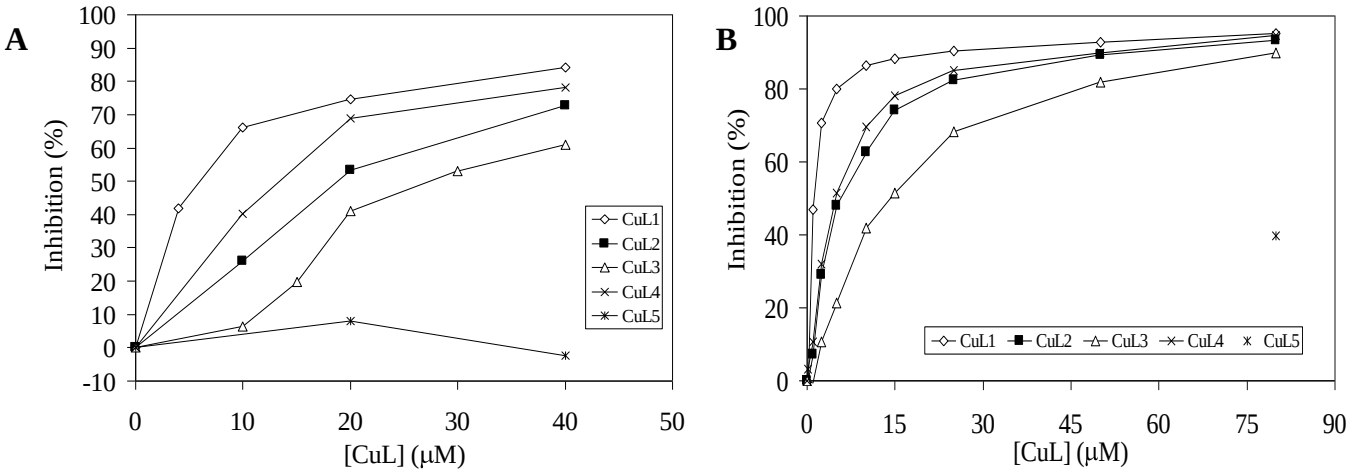


**Fig. 5.6 -** Effect of the macrocyclic copper(II) complexes CuL1- CuL5 on the inhibition of the NBT reduction **(A)** and DHE oxidation **(B)** by the XXO generated superoxide.

**Table V.3 -** Superoxide scavenging activity for the copper(II) compounds and native Cu,Zn-SOD.

| **Compound** | **$IC_{50}$ (μM)** | |
|---|---|---|
| | **NBT assay** | **DHE assay** |
| CuL1 | 6.86 | 1.07 |
| CuL2 | 18.84 | 5.03 |
| CuL3 | 30.82 | 11.78 |
| CuL4 | 13.94 | 4.66 |
| CuL5 | N.D. | N.D. |
| Cu(II) | 0.28 | 0.11 |
| Cu,Zn-SOD | 0.017 | 0.001 |

N.D., Not Determined

Since both NBT and DHE methods involve the activity of XO it is of utmost importance to ascertain that the results obtained are in fact due to a SOD-like activity and not a consequence of the inhibition of XO. The monitoring of the production of uric acid revealed that the active copper complexes (CuL1, CuL2, CuL3, and CuL4), at 80 μM, did not inhibit XO. Caffeic acid at the same experimental conditions inhibited 47.0% and 59.8% of uric acid production at 180 and 290 s, respectively. Some authors have also pointed out that Cu(II) ion could inhibit XO at mM

concentrations [55]. However, in our experimental conditions, using 80 μM of $Cu(NO_3)_2$, that inhibition did not occur.

For both assays and for all the complexes studied, the native human Cu,Zn-SOD was used as a positive control. As expected, a dose-dependent inhibition was found both for NBT reduction and DHE oxidation (data not shown). The $IC_{50}$ values for the enzyme were determined in the same experimental conditions used for the study of the complexes and revealed to be extremely low, in the nM range (Table V.3).

Four of the five macrocyclic copper(II) complexes studied (CuL1, CuL2, CuL3 and CuL4) have an effective ability to scavenge the $O_2^{\bullet-}$ with $IC_{50}$ in the low micromolar range (Fig. 5.6, Table V.3). The most active was CuL1 followed by CuL4, CuL2 and finally by CuL3. In what concerns to CuL5, no $IC_{50}$ value was calculated because no superoxide scavenging activity was found using the NBT assay (Fig. 5.6A). Using the DHE method an inhibition of < 40% was found at 80 μM, which may be considered as a low superoxide scavenging activity (Fig. 5.6B).

The superoxide scavenging activities of the complexes under study are in the same range of those reported for other metal complexes [56-58]. However, compounds with higher activity (e.g. some Mn salens and MnPs) have also been described [56, 59, 60], despite some of them are not readily water soluble. Nevertheless, focusing on the previously reported macrocyclic copper(II) complexes, which are more similar to the presented compounds, it is noticeable that the complexes under study are generally more active, having lower $IC_{50}$ values [3, 6].

In what concerns the four active macrocyclic copper(II) complexes and regardless the analytical method, we can observe that CuL1 is the most effective compound for $O_2^{\bullet-}$ scavenging (Fig. 5.6, Table V.3). However, as it was aforementioned in this discussion, at physiological pH and in the molar ratio used, the complexation of L1 with copper(II) is not complete (Table V.2), a consequence of the low stability constant of L1 for copper (log $K_{ML}$= 10.8). Thus, we can not rule out that the presence of free copper in the reaction system could contribute to the low $IC_{50}$ found for the complex of L1. Moreover, in the presence of phosphate buffer, the percent Cu(II) complexed with L1 markedly decreased with a concomitant increase of Cu(II) complexed with hydrogenophosphate (Table V.2 - footnote). For CuL2 this problem is not so relevant, although we should not disregard the presence of Cu(II) complexed with hydrogenophosphate, which may contribute in some extent to the dismutation of $O_2^{\bullet-}$ [52]. For the complexes CuL3, CuL4 and CuL5, this question is not applicable.

In an attempt to find out a structural-$O_2^{\bullet-}$ scavenging activity correlation for the complexes with higher thermodynamically stability (CuL2-CuL5), Visible and EPR spectroscopic studies, as well as theoretical calculations, were performed. In addition, the electrochemical behaviour of the complexes was studied by cyclic voltammetry.

The SOD-like activity is known to depend on structural features, namely on the conformation of the active site. Too stable square-planar geometries may not be favourable for the $O_2^{\bullet-}$ dismutation [3], while more distorted arrangements lead to higher SOD activity [61]. The EPR parameters provide data on the copper(II) environment in the complex, giving insights on its geometry. According to the ligand field theory [62-64], the $g_z$ value increases and the $A_z$ value decreases as the planar ligand field becomes weaker or as the axial ligand field becomes stronger and this occurs with the simultaneous red-shift of the *d-d* absorption bands in the electronic spectra. This sequence, in principle, parallels the degree of distortion from square-planar to square pyramidal, $C_{4v}$, and then to octahedral ($O_h$) or tetragonal ($D_{4h}$) geometries. The EPR parameters for copper(II) complexes are determined by the chemical composition and the physical constraints on the atoms nearest to the metal ion. On the basis of the Peisach and Blumberg approach [65], which accounts for the close relationship between $g_{||}$ and $A_{||}$ for equatorially coordinated S = ½ paramagnetic metal complexes some important properties of the copper(II) complexes may be determined. In this case, the actual composition of the equatorial atom donor set may be evaluated from the EPR data using the diagrams of $g_{||}$ and $A_{||}$ values compiled by the authors for a series of model compounds. The quotient $g_{||}/A_{||}$ is an empirical measure for the degree of tetrahedral distortion, being a relevant parameter to understand the SOD-like activity of the complexes [41]. This quotient ranges from ~ 105 to 135 cm for square-planar structures and increases markedly on the introduction of tetrahedral distortion [66]. Spectroscopic visible data and EPR parameters for Cu(II) complexes in water solution are collected in Table V.4. The EPR spectra of the copper(II) complexes are shown in Fig. 5.7.

**Table V.4 -** Spectroscopic X-band EPR data for the Cu(II) complexes of L2-L5 and Cu,Zn-SOD.

| Complex | Visible band $\lambda_{max}$/nm ($\varepsilon_{molar}$/ M cm$^{-1}$) | EPR parameters $A_i \times 10^{-4}$ cm$^{-1}$; $g_{\|\|}/A_{\|\|} \times$ cm | | | | | | |
|---|---|---|---|---|---|---|---|---|
| | | $g_z$ | $g_y$ | $g_z$ | $A_x$ | $A_y$ | $A_z$ | $g_{\|\|}/A_{\|\|}$* |
| CuL2 | 638 (100) | 2.041 | 2.053 | 2.225 | 18.1 | 22.9 | 190.7 | 117 |
| CuL3 | 580 (141) | 2.042 | 2.046 | 2.192 | 30.0 | 27.9 | 199.4 | 110 |
| CuL4-1 | | 2.036 | 2.104 | 2.295 | 4.5 | 30.2 | 158.6 | 145 |
| CuL4-2 | 674 (86) | 2.037 | 2.076 | 2.239 | 1.7 | 13.4 | 176.2 | 127 |
| CuL5 | 634 (111) | 2.044 | 2.049 | 2.228 | 26.6 | 27.7 | 183.4 | 122 |
| Cu,Zn-SOD [67] | 680 (150) | - | - | 2.271 | - | - | 140 | 162 |

* Considering $g_z$ as $g_{||}$ and $A_z$ as $A_{||}$.

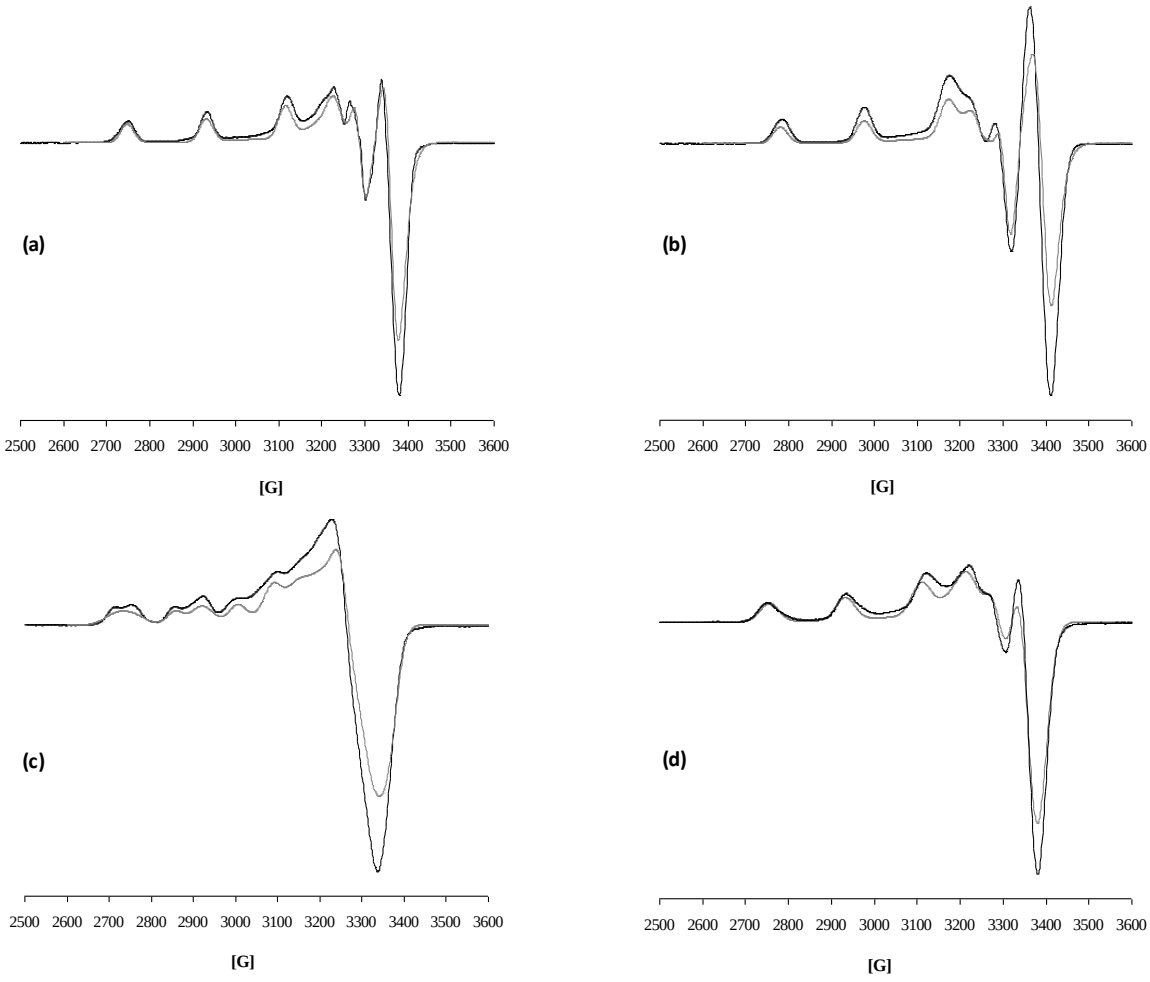


**Fig. 5.7 -** EPR X-band spectra of the Cu(II) complexes of L2-L5 in 1:1 ratio at the pH = 7.39 for CuL2 **(a)**, pH = 7.35 for CuL3 **(b)**, pH = 7.40 for CuL4 **(c)** and pH = 7.40 for CuL5 **(d)** in 1.0 M $NaClO_4$. The spectra were recorded at 116 K, microwave power of 2.0 mW and modulation amplitude of 1.0 mT. The frequency (ν) was of 9.41 GHz. The simulated spectra are below of the experimental ones (grey line).

The simulation of the spectra [68] indicates three different principal values of *g*, showing that the Cu(II) ion in these complexes is in a rhombically-distorted ligand field. All the complex species show parameters which are characteristic of rhombic symmetry with elongation of the axial bonds and a $d_{x^2-y^2}$ ground state. Elongated rhombic-octahedral, rhombic square-coplanar or distorted square pyramidal stereochemistries would be consistent with these data, but trigonal-bipyramidal or tetragonal geometries involving compression of axial bonds should be excluded [21, 69]. It is important to mention that the structures obtained by the theoretical calculations were consistent with those proposed based on the spectroscopic data [32].

The spectrum of CuL2 (Fig. 5.7a) exhibits the presence of one species. The $g_{||}$ value (considering $g_z$ as $g_{||}$) and $A_{||}$ value (considering $A_z$ as $A_{||}$) parameters are according with two nitrogen and two oxygen donor atoms coordinated to the metal center in the equatorial plane. These parameters, as well as the value of the maximum of the visible band (Table V.4) and the B3LYP optimized geometry (Fig. 5.8), suggest a square-pyramidal structure where the equatorial plane is determined by the two nitrogen and two oxygen atoms and one oxygen atom is in the apical position.

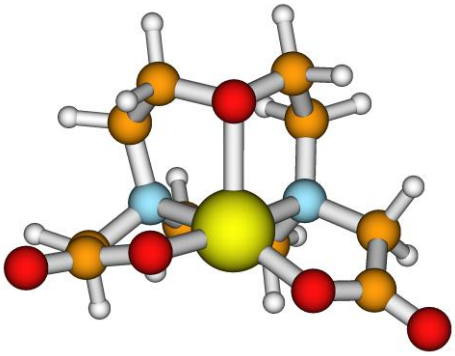

**Fig. 5.8 -** B3LYP Optimized geometry of CuL2 complex (yellow = copper(II), blue = N, red = O, orange = C, white = H).

The data obtained for CuL3 spectrum, together with the position of the d-d absorption band (Fig. 5.7b and Table V.4) point out to a square-pyramidal structure where the equatorial plane is determined by the four nitrogen atoms and one oxygen atom is in the apical position (Fig. 5.9). Although this complex has an effective $O_2^{\bullet-}$ scavenging activity, it presents higher $IC_{50}$ values. The reason for this behavior can be related to the strong equatorial ligand field which does not favour the attack of $O_2^{\bullet-}$ to the accessible apical sites.

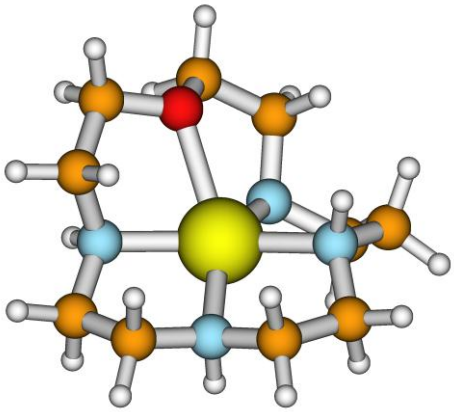

**Fig. 5.9 -** B3LYP Optimized geometry of CuL3 complex (yellow = copper(II), blue = N, red = O, orange = C, white = H).

The spectrum of CuL4 is shown in Fig. 5.7c and exhibits the presence of two species (CuL4-1 and CuL4-2). The EPR parameters and electronic spectrum determined in this work (Table V.4) are in agreement to those published before [21]. In CuL4-1, copper(II) is in a distorted octahedral environment having two nitrogen and two oxygen atoms coordinated directly to the metal ion. Two oxygen atoms accomplish the octahedral geometry. In terms of the factor $g_{||}/A_{||}$, CuL4-1 appears to have some tetrahedral distortion of the copper(II) arrangement, being the complex structurally most similar to Cu,Zn-SOD [67] (Table V.4). In what concerns to the CuL4-2 species the EPR parameters are completely different, having lower $g_{||}$ and higher $A_{||}$ values, indicating a stronger equatorial field. An octahedral distorted geometry is also proposed but having three nitrogen and one oxygen atoms in the equatorial plane and two oxygen atoms in axial positions (Fig. 5.10).

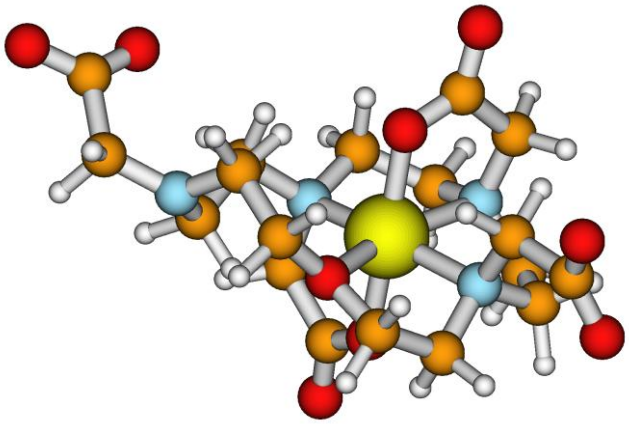

**Fig. 5.10 -** B3LYP Optimized geometry of CuL4 complex (yellow = copper(II), blue = N, red = O, orange = C, white = H).

Fig. 5.7d presents the spectrum of CuL5 and Table V.4 lists the spectral parameters obtained. The values of $g_{||}$ and $A_{||}$ are consistent with two nitrogen and two oxygen donor atoms coordinated to the metal center in the equatorial plane. These parameters and also the value of the maximum of the visible band (Table V.4) indicate penta- or hexacoordination environments for the Cu(II). Although no X-ray structure analysis of this copper(II) complex is available, the

literature reports an X-ray structure for a dimer of the same macrocycle with $Ni^{2+}$. The crystal structure of the compound consists of $[NiL5Cl]^{+}$ and $[NiL5(H_2O)]^{2+}$ complex cations. The coordination environment for each metal is octahedral, determined by three nitrogen and two oxygen atoms of the ligand and completed by secondary species from the medium ($Cl^-$ and water, respectively) [70]. It is important to mention that in this structure one nitrogen atom is in an axial position. Considering this X-ray structure, the data from the theoretical calculations and the results of the spectroscopic studies, we may propose that in the case of CuL5, the same octahedral environment seems probable. The absence of scavenging activity of CuL5 may be justified by the presence of an N atom of the macrocyclic backbone at the axial position (Fig. 5.11), that causes steric hindrance to the approach of the $O_2^{\bullet -}$.

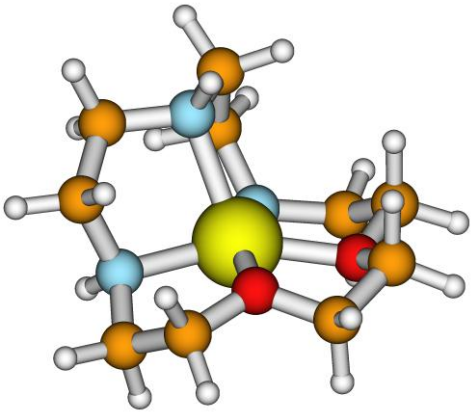

**Fig. 5.11** - B3LYP Optimized geometry of CuL5 complex (yellow = copper(II), blue = N, red = O, orange = C, white = H).

The redox behaviour of CuL2-CuL5 in aqueous solutions was studied by cyclic voltammetry. All of the complexes exhibited irreversible waves, except CuL3. This may suggest that the SOD-like activity exhibited by the complexes CuL2 and CuL4 is due to a stoichiometric scavenging activity. The copper(II) complex of L3 displays a single quasi-reversible one-electron ($i_{pa}/i_{pc}$ = 1.3; $E_{pa}$ = -0.528 V; $E_{pc}$ = -0.617 V; $\Delta E_p$ = 89 mV) reduction wave at -0.573 V *versus* Ag/AgCl, which is assigned to Cu(II)/Cu(I). This may suggest a catalytic behaviour. However, the value of $E_{1/2}$ for CuL3 is more negative than those reported for SOD mimetic compounds. Also, the value of $\Delta E_p$ is lower than those reported for SODm compounds (from 114 to 121 mV) [71], which might explain the mild activity exhibited by this complex on the biochemical assays.

*5.3.2. Cytotoxicity profile of the complexes*

While some of these compounds have shown to be effective scavengers of the $O_2^{\bullet-}$, they may also be toxic to mammalian cells. In fact, cytotoxicity is a common limitation for the pharmaceutical use of new compounds. Therefore, we measured the cytotoxic effects of macrocyclic copper(II) complexes using the MTT test in V79 cells. Cell survival was evaluated using a standard 24 h incubation with the copper(II) complexes. The concentrations evaluated were in the range of those tested in the superoxide scavenging assays. In general, the macrocyclic complexes showed only a slight cytotoxic effect of approximately 5 to 15% and no dose-response effects were observed. Interestingly, CuL5, the complex that did not show a superoxide scavenging activity, revealed the highest cytotoxicity (Fig. 5.12). Despite of the potential cytotoxicity of Cu(II), due to its ability to generate hydroxyl radical and to displace other metal co-factors from metalloenzymes [50], in our experiments Cu(II) ions did not exhibit notable cytotoxic effects, in the range of concentrations studied (Fig. 5.12).

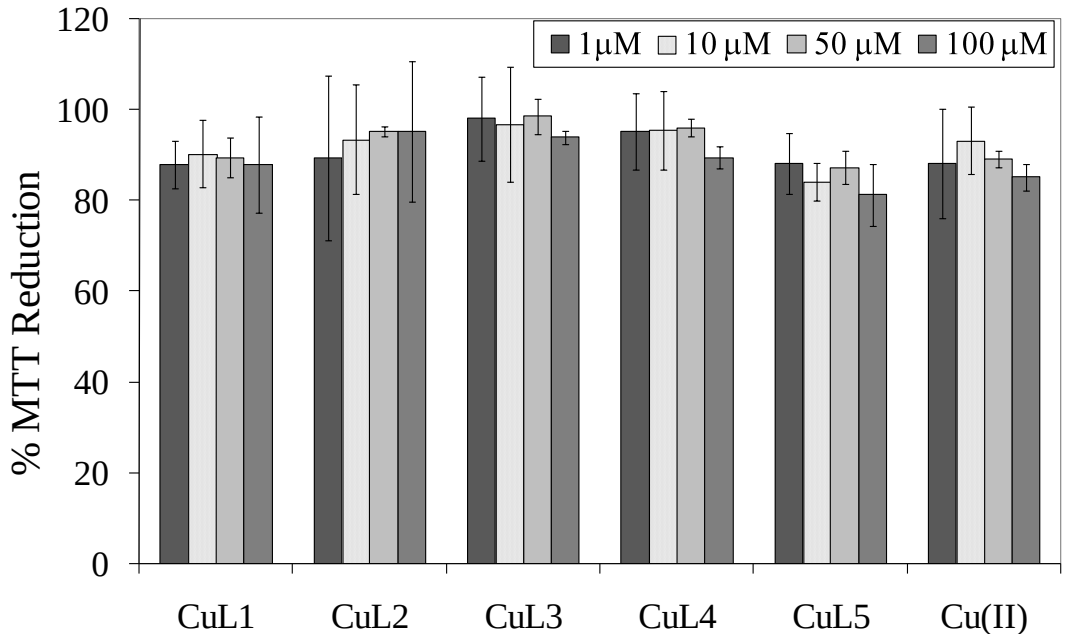


**Fig. 5.12 -** Cell viability of V79 cells treated with different concentrations of the macrocyclic copper(II) complexes CuL1-CuL5 and Cu(II), for 24 h. Values (mean ± SD) are percentages relative to non-treated control cells.

*5.3.3. Studies on CuL3 and CuL4 as potential antioxidants*

From the results above described, CuL3 and CuL4 gather a number of favourable characteristics and were therefore selected to be further evaluated. In fact, these complexes have high stability constant and pCu values, being less prone to undergo dissociation *in vivo*, an important requisite for a bioactive metal complex. Moreover, CuL3 and CuL4 have shown an effective $O_2^{\bullet-}$ scavenging activity and exhibited low cytotoxicity in the range of concentrations tested (up to 100 μM). The antioxidant effect of these complexes was therefore evaluated in the oxidative stress models established in Chapter 3 and validated for the recognized SODm MnTM-4-PyP. The first oxidant used was the XXO system, that generates $O_2^{\bullet-}$ extracellularly. The obtained results are presented in Fig. 5.13.

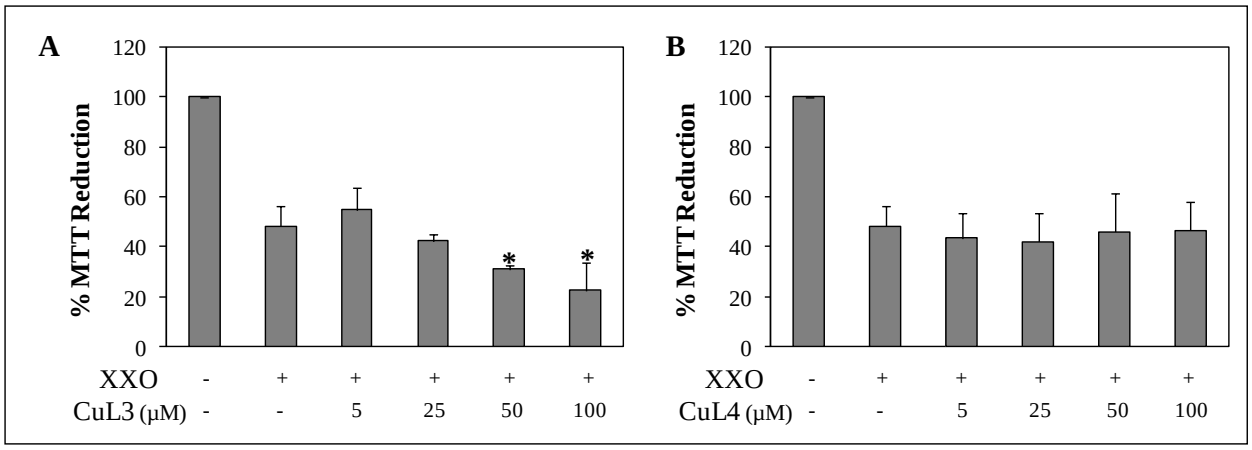


**Fig. 5.13 -** Effect of CuL3 and CuL4 on the cytotoxicity induced by xanthine (240 μM) plus xanthine oxidase (20 U/L) in V79 cells. Cells were incubated with increasing concentrations of the complexes in the presence of XXO for 24 h, and then submitted to the MTT assay (**P* < 0.05, when compared with cells treated with XXO alone).

As depicted in Fig. 5.13, when V79 cells were exposed for 24 h to X (240 μM)/XO (20 U/L), a significant decrease in cell survival was observed ($P < 0.05$). The addition of CuL3 did not afford protection to XXO-exposed cells. On the contrary, this complex exhibited a dose-dependent pro-oxidant effect (Fig. 5.13A). Concentrations of 50 and 100 μM of CuL3 have indeed significantly reduced the cellular viability ($P < 0.05$). A pro-oxidant action was also reported for other SODm compounds [72, 73]. Pérez *et al* [73] have in fact demonstrated that a SODm can exert different actions in cells, either scavenging or producing free radicals, depending upon the prevailing redox pathways. The pro-oxidant effect of CuL3 may also be

explained by the possible occurrence of Fenton chemistry. A loss of copper from the complex during the redox cycling could occur, whereby "free" Cu would give rise to highly oxidizing $HO^{\bullet}$ species. Fenton chemistry may be also operative at reduced copper still bound to the ligand [72]. In what concerns to CuL4, the addition of this complex (up to 100 μM), did not alter the % MTT reduction presented by XXO-treated cells (Fig. 5.13B).

TBHP, an analogue of lipid hydroperoxides, was used as a second model of oxidative stress to further evaluate the potential effects of CuL3 and CuL4. The exposure of V79 cells to TBHP (100 μM) resulted in a considerable decrease in cell viability ($P < 0.05$). The simultaneous exposure to CuL3 led to a mild increase in the MTT reduction (Fig. 5.14A), although this protective effect was not statistically significant. It is also important to mention that a high variability was observed in these experiments. To confirm this antioxidant activity of CuL3, a second cell viability method was used – the CV assay. The results are depicted in Fig. 5.14B. Using this assay, only a minor effect was observed (~5% increase in cell viability, *N.S.*), and only for the highest concentration of CuL3 (100 μM).

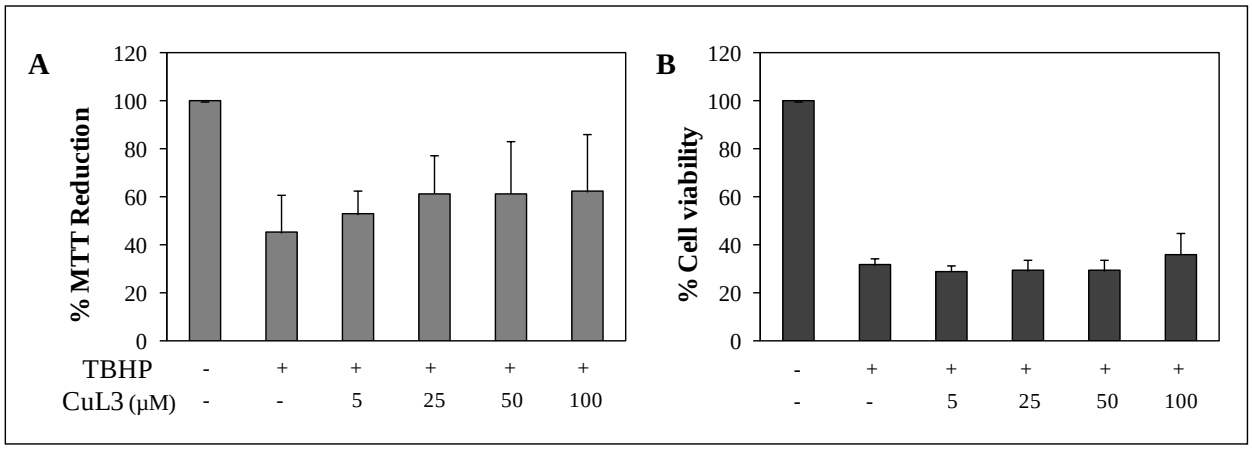


**Fig. 5.14 -** Effect of CuL3 on the cytotoxicity induced by TBHP (100 μM) in V79 cells. Cells were incubated with increasing concentrations of the complex in the presence of TBHP for 24 h, and then submitted to the MTT (A) or to the CV (B) assay.

To assess whether the protective effect of CuL3 is related to its $O_2^{\bullet-}$ scavenging activity, the intracellular production of this free radical was evaluated using the DHE assay. As depicted in Fig. 5.15, CuL3 (100 μM) *per se* did not alter the intracellular levels of $O_2^{\bullet-}$. On the contrary, cells exposed to 100 μM of TBHP exhibited a significant increase in $O_2^{\bullet-}$ production ($P < 0.01$). In cells co-treated with CuL3 and TBHP, the intracellular $O_2^{\bullet-}$ returned to levels close to those

presented by control cells (P<0.01 *versus* TBHP alone). These results indicate that the scavenging of $O_2^{\bullet-}$ by CuL3 is occurring in this oxidative stress model, being probably accounting for the slight increase in cell viability observed. Other mechanisms may also be involved in this effect. This protection of CuL3 in terms of intracellular $O_2^{\bullet-}$ levels also suggests that this complex is cell-permeable in V79 cells.

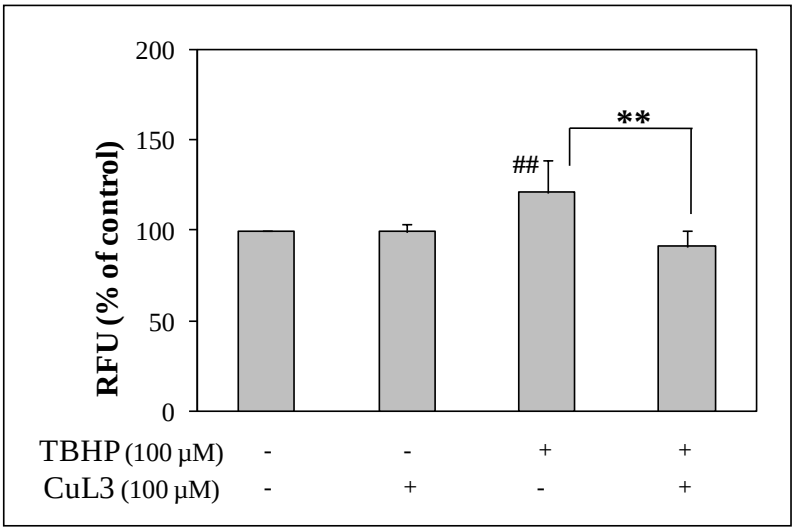


**Fig. 5.15 -** Effect of CuL3 on the DHE oxidation in V79 cells treated with TBHP (100 µM). Values (mean ± SD) represent relative fluorescence units (RFU), which approximately reflect the levels of $O_2^{\bullet-}$, expressed as percentages of the control cells ($^{\#\#}P < 0.01$, when compared with non-treated control cells; $^{**}P < 0.01$, when compared with cells treated with TBHP in the absence of CuL3).

The potential effect of CuL4 against TBHP-induced toxicity was also studied and the obtained results are depicted in Fig. 5.16. This complex, up to 100 µM, did not significantly alter the decrease in MTT reduction induced by TBHP. Although CuL4 has shown an efficient $O_2^{\bullet-}$ scavenging *in vitro*, with a low $IC_{50}$ value, this complex failed to protect cells exposed to the oxidative stress inducers XXO and TBHP. This absence of antioxidant activity of CuL4 in cell-based experiments may be assigned to a possible insufficient catalytic rate of the reaction between the complex and $O_2^{\bullet-}$. It is possible that $O_2^{\bullet-}$ reacts faster with a biological target than with CuL4. If that is so, the presence of CuL4 will not counteract the oxidative damage induced by this free radical.

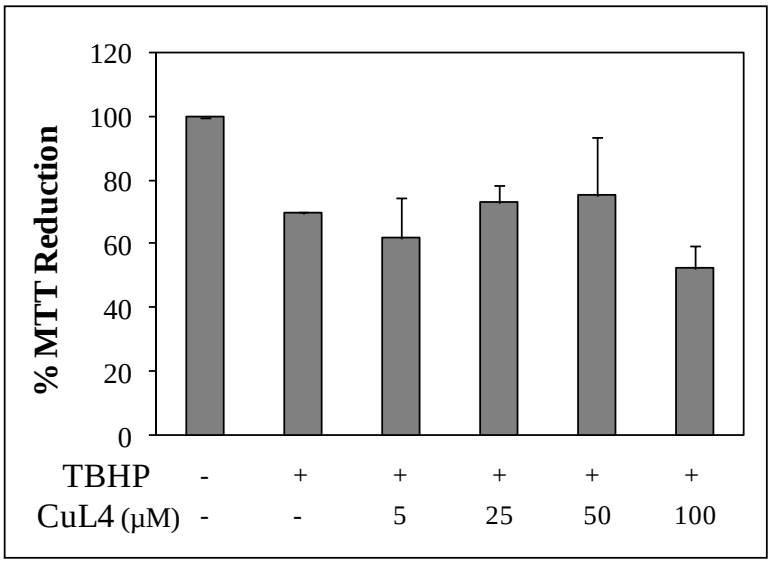


**Fig. 5.16 -** Effect of CuL4 on the cytotoxicity induced by TBHP (100 μM) in V79 cells. Cells were incubated with increasing concentrations of the complex in the presence of TBHP for 24 h, and then submitted to the MTT assay.

*5.3.4. $HO^{\bullet}$ radical generation by CuL3 and CuL4*

CuL3 and CuL4 were also evaluated for their capacity to generate $HO^{\bullet}$ radical. This information is useful to explain the eventual toxic and pro-oxidant effects of the complexes under some conditions, as well as to give some insight on the possibilities of these complexes as anticancer agents. In the DNA strand break analysis, the generation of $HO^{\bullet}$ radical leads to an attack in plasmid DNA, resulting in a decrease of the percentages of DNA in the supercoiled form. To validate the experimental system, a set of controls were analysed, as depicted in Fig. 5.17.

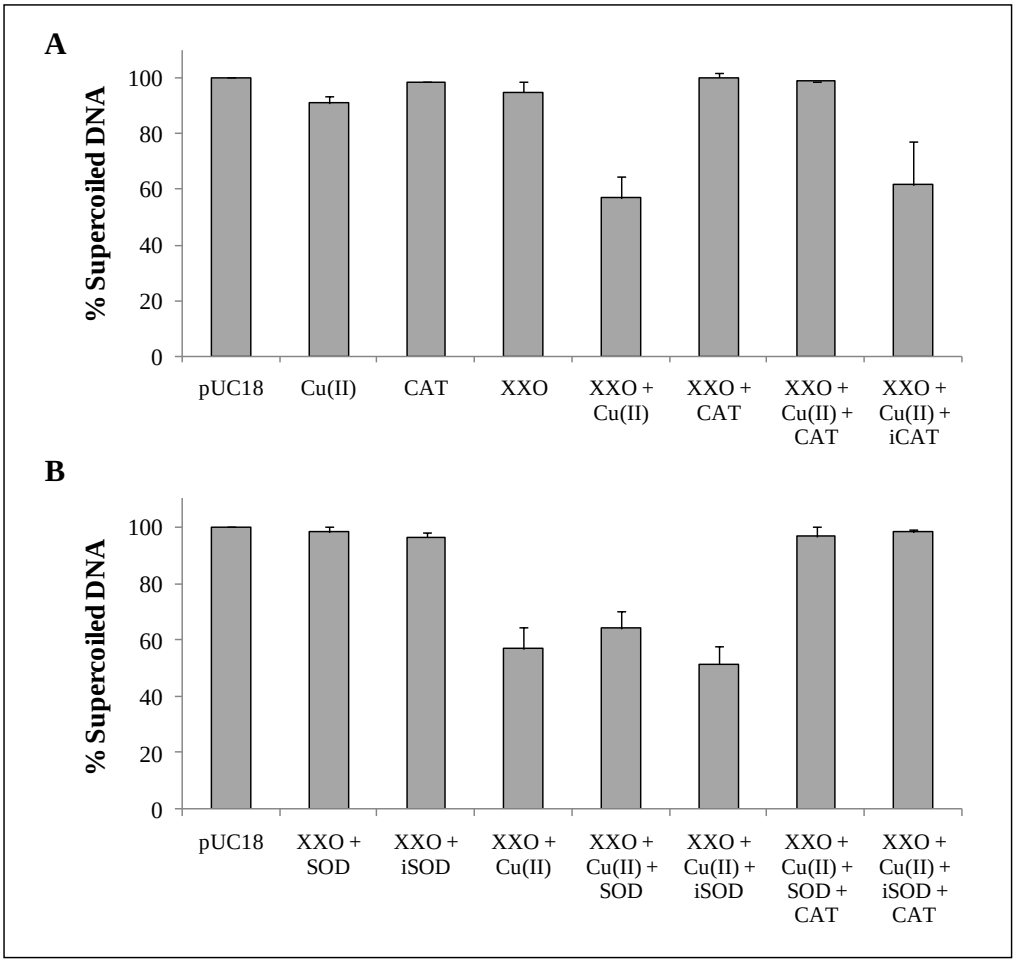


**Fig. 5.17 –** Validation of the DNA strand break analysis protocol. Results are expressed as percentages of DNA in the supercoiled form (CAT, catalase; XXO, xanthine-xanthine oxidase; iCAT, heat-inactivated catalase; SOD, superoxide dismutase; iSOD, heat-inactivated superoxide dismutase).

As shown in Fig. 5.17A, Cu(II), CAT and XXO, *per se*, did not decrease the % of supercoiled (SC) DNA. However, the incubation of pUC18 with XXO plus Cu(II) resulted in a considerable DNA breakage, indicating the generation of $HO^{\bullet}$. Since XXO can produce both $O_2^{\bullet-}$ and $H_2O_2$, $HO^{\bullet}$ radicals may be generated either by Haber-Weiss or Fenton reactions:

$Cu(II) + O_2^{\bullet-} \rightarrow Cu(I) + O_2$

$\underline{Cu(I) + H_2O_2 \rightarrow Cu(II) + HO^{\bullet} + HO^-}$ (Fenton reaction)

Net: $O_2^{\bullet-} + H_2O_2 \rightarrow O_2 + HO^{\bullet} + HO^-$ (Haber-Weiss reaction)

The reversion of this effect in the presence of CAT indicates that $H_2O_2$ is an intermediate in $HO^{\bullet}$ generation. The absence of effect of heat-inactivated CAT confirms that is the catalytic degradation of $H_2O_2$ that is avoiding the formation of $HO^{\bullet}$, and not an unspecific reaction such as $HO^{\bullet}$ trapping by the protein. The results obtained with SOD (Fig. 5.17B) support the major role of $H_2O_2$, but not of $O_2^{\bullet-}$, as an intermediate in $HO^{\bullet}$ generation and, therefore, in DNA cleavage. The results obtained with CuL3 and CuL4 are shown in Fig. 5.18.

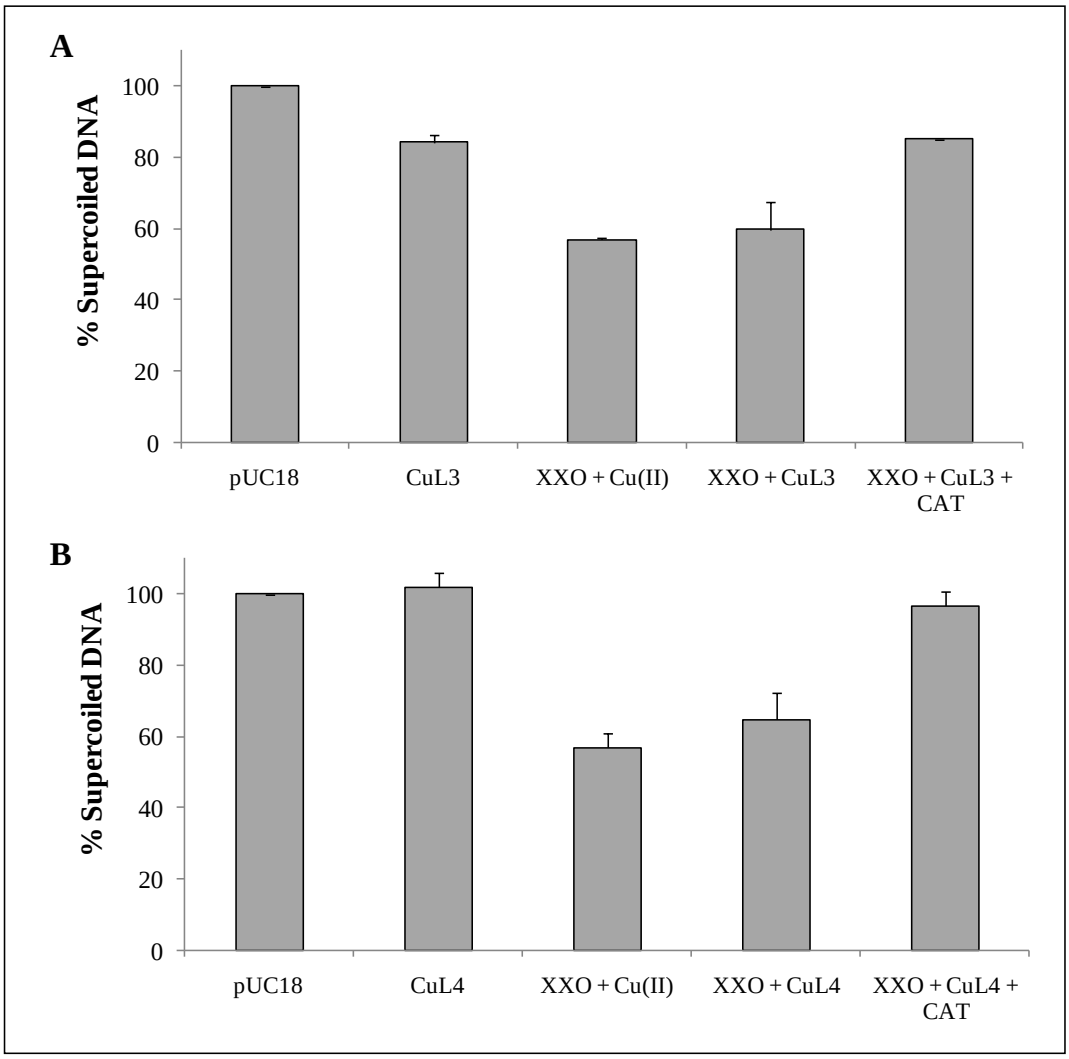


**Fig. 5.18 –** Evaluation of $HO^{\bullet}$ generation by CuL3 (A) and CuL4 (B), by the DNA strand break analysis. Results are expressed as % DNA in the supercoiled form (XXO, xanthine-xanthine oxidase; CAT, catalase).

As depicted in Fig. 5.18A, CuL3 *per se*, reduced the % SC DNA to values of ~84%. These results indicate that CuL3 can attack DNA exerting some kind of chemical nucleasic

activity. Other macrocyclic copper(II) complexes have previously shown the capacity to interact with DNA by intercalation, hydrogen bonding, van der Waals forces, hydrophobic interaction or coordination between the Cu(II) in the complex and the base nitrogen in DNA. Some macrocyclic copper(II) complexes have indeed been developed as artificial restriction enzymes [74]. Also, SODm of other classes, namely MnPs, have been previously reported to interact with nucleic acids [75] and to degrade those [76]. Although CuL3 has shown to have nucleasic activity *in vitro*, it may not attack DNA *in vivo*. CuL3 may not enter the nucleus. Furthermore, nuclear DNA is organized in a complex supramolecular structure, being less prone to be cleaved. The absence of considerable toxicity in cells treated with CuL3 suggests that DNA damage should not occur in cells at a considerable extent. When pUC18 was incubated with XXO and CuL3, a marked decrease in the % SC DNA was observed. This result indicates that CuL3 reacts with $H_2O_2$ by Fenton chemistry, and that this complex is devoid of catalasic activity. In the presence of CAT, the % SC DNA returned to ~85%, confirming the involvement of $H_2O_2$ in $HO^{\bullet}$ generation.

In what concerns to CuL4 (Fig. 5.18B), no nucleasic activity was found. Although it is structurally related with CuL3, it presents a more distorted structure, which may difficult the interaction with nucleic acids [75]. CuL4, as observed with CuL3, has the ability to generate $HO^{\bullet}$ in the presence of $O_2^{\bullet-}$ and possess no CAT-like activity. The reversion of the effect in the presence of CAT confirms again the participation of $H_2O_2$ in the formation of $HO^{\bullet}$. Also, the capacity of CAT to inhibit the $HO^{\bullet}$ generation suggests that this reaction may not occur in cells with an efficient enzymatic antioxidant system. However, when the enzymatic defenses are depleted or the ROS level is increased (e.g. in cancer cells), the detoxification capacities of CAT and GPx enzymes can be overwhelmed. In these cases, the production of $HO^{\bullet}$ by CuL3 and CuL4 may constitute a strategy to potentiate cell death.

### *5.3.5. Studies on CuL3 and CuL4 as potential anticancer agents*

Since CuL3 and CuL4 have both superoxide scavenging activity and the ability to generate $HO^{\bullet}$, their potential application in cancer therapy was studied. These studies were performed in MCF7 human breast carcinoma cells, since it was previously demonstrated that the overexpression of SOD in these cells suppressed their proliferation, being $H_2O_2$ the mediator of the effect [77]. The toxicity of CuL3 and CuL4 (up to 100 µM, 24 h) was evaluated using the

MTT assay. As presented in Fig. 5.19, these complexes were not cytotoxic in the range of concentrations tested.

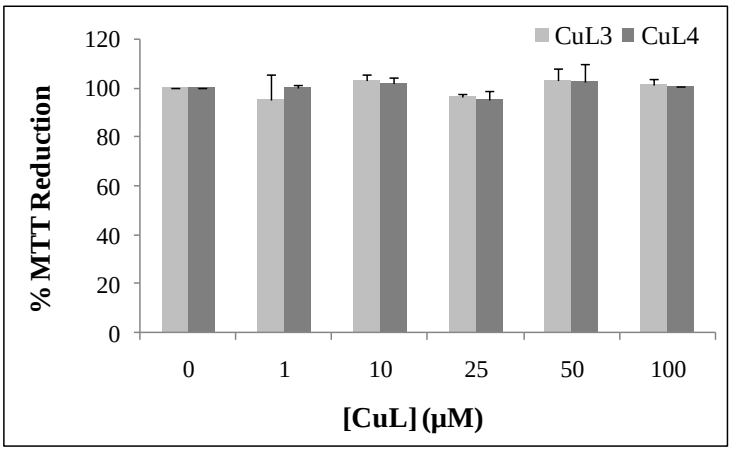


**Fig. 5.19 -** Cell viability of MCF7 cells treated with different concentrations of CuL3 and CuL4, for 24 h, as evaluated by the MTT assay. Values (mean ± SD) are percentages relative to non-treated control cells.

The ability of CuL3 and CuL4 to modulate the toxic effects of Dox was also studied. As shown in Fig. 5.20, Dox (50 nM -5 µM) reduced the viability of MCF7 cells in a dose-dependent way. The addition of CuL3 or CuL4 to Dox-treated cells did not significantly alter their viability.

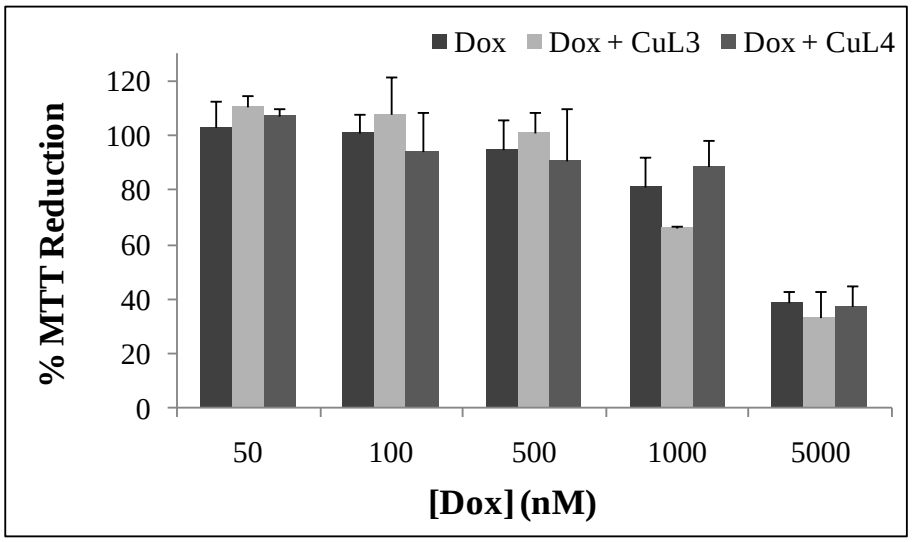


**Fig. 5.20 -** Effect of CuL3 and CuL4 on the cell viability of MCF7 cells treated with doxorubicin (Dox), as evaluated by the MTT assay. Cells were incubated with increasing concentrations of Dox in the absence (darker bars) or presence of 100 µM of each complex, for 24 h. Values (mean ± SD) are percentages relative to non-treated control cells (100%).

Different reasons can be proposed to explain the absence of toxicity of CuL3 and CuL4 in MCF7 cells, as well as the lack of potentiation of Dox effects. One possibility is that the uptake of these macrocyclic copper(II) complexes by MCF7 cells may not be sufficient to reach an effective intracellular concentration. It is also possible that the catalytic rate of the reaction of the complexes with $O_2^{\bullet-}$ may not be high enough to afford an extra SOD-like activity to the cell and, therefore, the $O_2^{\bullet-}/H_2O_2$ balance will not be altered. Other hypothesis is that, although the complexes may be dismutating $O_2^{\bullet-}$ into $H_2O_2$, the increase in $H_2O_2$ concentration is not sufficient to overwhelm the detoxification capacities of CAT and GPx enzymes. If cells can efficiently detoxify $H_2O_2$, no Fenton chemistry is likely to occur. Since Dox has different mechanisms of cytotoxity, including an important role at the DNA level [15, 16], it is also possible that an eventual increase in $H_2O_2$ and even in $HO^{\bullet}$, may not account considerably for the overall cytotoxicity of this drug.

### *5.3.6. Conclusion*

In this Chapter, five macrocyclic copper(II) complexes were synthesized and characterized. Four of them exhibited SOD-like activity and, among those, CuL3 and CuL4 were selected for biological studies due to their higher thermodynamic stability. However, CuL4 did not show biological activity in the cellular models studied. In what concerns to CuL3, differential effects were observed according to the model. This complex exhibited pro-oxidant effects in XXO-treated V79 cells and slight antioxidant properties against TBHP, while it was ineffective in the studies performed with MCF7 cells. These results illustrate the dual nature of SODm compounds that may exert either antioxidant or pro-oxidant actions in cells [73]. The redox modulation of cellular pathways is therefore a complex issue and different models must be studied in order to find out the potential of a SODm for therapeutic purposes.

## 5.4. References


[1] Riley, D. P. Functional mimics of superoxide dismutase enzymes as therapeutic agents. *Chem Rev* **99:**2573-2588; 1999.

[2] Bienvenue, E.; Choua, S.; Lobo-Recio, M.-A.; Marzin, C.; Pacheco, P.; Seta, P.; Tarrago, G. Structure and superoxide dismutase activity of Ru(II), Cu(II), and Mn(II) macrocyclic complexes. *J Inorg Biochem* **57:**157-168; 1995.

[3] Kimura, E.; Sakonaka, A.; Nakamoto, M. Superoxide dismutase activity of macrocyclic polyamine complexes. *Biochim Biophys Acta* **678:**172-179; 1981.

[4] Kimura, E.; Yatsunami, A.; Watanabe, A.; Machida, R.; Koike, T.; Fujioka, H.; Kuramoto, Y.; Sumomogi, M.; Kunimitsu, K.; Yamashita, A. Further studies on superoxide dismutase activities of macrocyclic polyamine complexes of copper(II). *Biochim Biophys Acta* **745:**37-43; 1983.

[5] Durackova, Z.; Labuda, J. Superoxide dismutase mimetic activity of macrocyclic Cu(II)-tetraanhydroaminobenzaldehyde (TAAB) complex. *J Inorg Biochem* **58:**297-303; 1995.

[6] Autzen, S.; Korth, H.-G.; Boese, R.; de Groot, H.; Sustmann, R. Studies of pyridinyl-containing 14-membered macrocyclic copper(II) complexes. *Eur J Inorg Chem***:**1401-1410; 2003.

[7] Yaping, T.; Yunzhong, F.; Qinhui, L.; Mengchang, S.; Qin, L.; Wenmei, S. The inhibitory effects of 21 mimics of superoxide dismutase on luminol-mediated chemiluminescence emitted from PMA-stimulated polymorphonuclear leukocyte. *Free Radic Biol Med* **13:**533-541; 1992.

[8] Pogni, R.; Baratto, M. C.; Busi, E.; Basosi, R. EPR and O2.- scavenger activity: Cu(II)-peptide complexes as superoxide dismutase models. *J Inorg Biochem* **73:**157-165; 1999.

[9] Li, Q. X.; Luo, Q. H.; Li, Y. Z.; Shen, M. C. A study on the mimics of Cu-Zn superoxide dismutase with high activity and stability: two copper(II) complexes of 1,4,7-triazacyclononane with benzimidazole groups. *Dalton Trans***:**2329-2335; 2004.

[10] Hidalgo, I. J. Assessing the absorption of new pharmaceuticals. *Curr Top Med Chem* **1:**385-401; 2001.

[11] Alexandre, J.; Nicco, C.; Chereau, C.; Laurent, A.; Weill, B.; Goldwasser, F.; Batteux, F. Improvement of the therapeutic index of anticancer drugs by the superoxide dismutase mimic mangafodipir. *J Natl Cancer Inst* **98:**236-244; 2006.

[12] Laurent, A.; Nicco, C.; Chereau, C.; Goulvestre, C.; Alexandre, J.; Alves, A.; Levy, E.; Goldwasser, F.; Panis, Y.; Soubrane, O.; Weill, B.; Batteux, F. Controlling tumor growth by modulating endogenous production of reactive oxygen species. *Cancer Res* **65:**948-956; 2005.

[13] Nicco, C.; Laurent, A.; Chereau, C.; Weill, B.; Batteux, F. Differential modulation of normal and tumor cell proliferation by reactive oxygen species. *Biomed Pharmacother* **59:**169-174; 2005.

[14] Keizer, H. G.; Pinedo, H. M.; Schuurhuis, G. J.; Joenje, H. Doxorubicin (adriamycin): a critical review of free radical-dependent mechanisms of cytotoxicity. *Pharmacol Ther* **47:**219-231; 1990.

[15] Kiyomiya, K.; Matsuo, S.; Kurebe, M. Differences in intracellular sites of action of Adriamycin in neoplastic and normal differentiated cells. *Cancer Chemother Pharmacol* **47:**51-56; 2001.

[16] Minotti, G.; Menna, P.; Salvatorelli, E.; Cairo, G.; Gianni, L. Anthracyclines: molecular advances and pharmacologic developments in antitumor activity and cardiotoxicity. *Pharmacol Rev* **56:**185-229; 2004.

[17] Ohse, T.; Nagaoka, S.; Arakawa, Y.; Kawakami, H.; Nakamura, K. Cell death by reactive oxygen species generated from water-soluble cationic metalloporphyrins as superoxide dismutase mimics. *J Inorg Biochem* **85:**201-208; 2001.

[18] Keele, B. B., Jr.; McCord, J. M.; Fridovich, I. Further characterization of bovine superoxide dismutase and its isolation from bovine heart. *J Biol Chem* **246:**2875-2880; 1971.

[19] Cabral, M. F.; Costa, J.; Delgado, R.; Silva, J. J. R. F. d.; Vilhena, M. F. Protonation and metal complexation studies on some oxa-diaza macrocyclic ligands. *Polyhedron* **9:**2847-2857; 1990.

[20] Cabral, M. F.; Delgado, R. Metal complexes of pentadentate macrocyclic ligands containing oxygen and nitrogen as donor atoms. *Helv Chim Acta* **77:**515-524; 1994.

[21] Cabral, M. F.; Delgado, R. 4,7,10,13-Tetrakis(carboxymethyl)-1-oxa-4,7,10,13-tetraazacyclopentadecane and properties of its metal complexes. *Polyhedron* **18:**3479-3489; 1999.

[22] Richman, J. E.; Atkins, T. J. Nitrogen analogs of crown ethers. *J Am Chem Soc* **96:**2268-2270; 1974.

[23] Snyder, H. R.; Heckert, R. E. A method for the rapid cleavage of sulfonamides. *J Am Chem Soc* **74:**2006-2009; 1952.

[24] Schwarzenbach, G.; Flaschka, H. A. *Complexometric titrations.* London: Methuen and Co; 1969.

[25] Delagrange, S.; Delgado, R.; Nepveu, F. Mn2+, Co2+, Cu2+ and Zn2+ complexes with two macrocyclic ligands bearing L-lactate-like functions: potentiometric studies and evaluation of superoxide-scavenging properties of the Mn2+ complex. *J Inorg Biochem* **81:**65-71; 2000.

[26] Gans, P.; Sabatini, A.; Vacca, A. SUPERQUAD: an improved general program for computation of formation constants from potentiometric data. *J Chem Soc, Dalton Trans***:**1195-1200; 1985.

[27] Gans, P.; Sabatini, A.; Vacca, A. Investigation of equilibria in solution. Determination of equilibrium constants with the HYPERQUAD suite of programs. *Talanta* **43:**1739-1753; 1996.

[28] Alderighi, L.; Gans, P.; Ienco, A.; Peters, D.; Sabatini, A.; Vacca, A. Hyperquad simulation and speciation (HySS): a utility program for the investigation of equilibria involving soluble and partially soluble species *Coord Chem Rev* **184:**311-318 1999.

[29] Pettit, L. D.; Powell, K. J. IUPAC Stability Constants Database. UK: Academic Software, Sourby Old Farm, Timble, Ottley, Yorks.; 2004.

[30] Smith, R. M.; Martell, A. E.; Motekaitis, R. J. Nist Critical stability constants of metal complexes database. Gaithersburg: U.S. Department of Commerce; 1998.

[31] Hohenberg, P.; Kohn, W. Inhomogeneous Electron Gas. *Phys Rev* **136:**B864-B871; 1964.

[32] Matxain, J. M.; Santos, D. J. V. A. d.; Fernandes, A. S.; Cabral, M. F.; Costa, J.; Castro, M.; Oliveira, N. G.; Guedes, R. C. Macrocyclic copper(II) complexes as superoxide scavengers: Insights from a DFT study. Portugal: 9º Encontro Nacional de Química-Física; 2009.

[33] Becke, A. D. Density-functional thermochemistry. III. The role of exact exchange. *J Chem Phys* **98:**5648-5652; 1993.

[34] Petersson, G. A.; Bennett, A.; Tensfeldt, T. G.; Al-Laham, M. A.; Shirley, W. A.; Mantzaris, J. A complete basis set model chemistry. I. The total energies of closed-shell atoms and hydrides of the first-row atoms. *J Chem Phys* **89:**2193-2218; 1988.

[35] Jr., T. H. D.; Hay, P. J. *Modern Theoretical Chemistry.* New York: Plenum; 1976.

[36] Miertuš, S.; Scrocco, E.; Tomasi, J. Electrostatic Interaction of a Solute with a Continuum. A Direct Utilization of ab initio Molecular Potentials for the Prevision of Solvent Effects. *Chem Phys* **55:**117-129; 1981.

[37] Frisch, M. J.; Trucks, G. W.; Schlegel, H. B.; Scuseria, G. E.; Rob, M. A.; Cheeseman, J. R.; Jr., J. A. M.; Vreven, T.; Kudin, K. N.; Burant, J. C.; Millam, J. M.; Iyengar, S. S.; Tomasi, J.; Barone, V.; Mennucci, B.; Cossi, M.; Scalmani, G.; Rega, N.; Petersson, G. A.; Nakatsuji, H.; Hada, M.; Ehara, M.; Toyota, K.; Fukuda, R.; Hasegawa, J.; Ishida, M.; Nakajima, T.; Honda, Y.; Kitao, O.; Nakai, H.; Klene, M.; Li, X.; Knox, J. E.; Hratchian, H. P.; Cross, J. B.; Bakken, V.; Adamo, C.; Jaramillo, J.; Gomperts, R.; Stratmann, R. E.; Yazyev, O.; Austin, A. J.; Cammi, R.; Pomelli, C.; Ochterski, J. W.; Ayala, P. Y.; Morokuma, K.; Voth, G. A.; Salvador, P.; Dannenberg, J. J.; Zakrzewski, V. G.; Dapprich, S.; Daniels, A. D.; Strain, M. C.; Farkas, O.; Malick, D. K.; Rabuck, A. D.; Raghavachari, K.; Foresman, J. B.; Ortiz, J. V.; Cui, Q.; Baboul, A. G.; Clifford, S.; Cioslowski, J.; Stefanov, B. B.; Liu, G.; Liashenko, A.; Piskorz, P.; Komaromi, I.; Martin, R. L.; Fox, D. J.; Keith, T.; Al-Laham, M. A.; Peng, C. Y.; Nanayakkara, A.; Challacombe, M.; Gill, P. M. W.; Johnson, B.; Chen, W.; Wong, M. W.; Gonzalez, C.; Pople, J. A. Gaussian 03. Wallingford, CT: Gaussian, Inc.; 2003.

[38] Zhou, J. Y.; Prognon, P. Raw material enzymatic activity determination: a specific case for validation and comparison of analytical methods--the example of superoxide dismutase (SOD). *J Pharm Biomed Anal* **40:**1143-1148; 2006.

[39] Kovala-Demertzi, D.; Galani, A.; Demertzis, M. A.; Skoulika, S.; Kotoglou, C. Binuclear copper(II) complexes of tolfenamic: synthesis, crystal structure, spectroscopy and superoxide dismutase activity. *J Inorg Biochem* **98:**358-364; 2004.

[40] Ciuffi, M.; Cellai, C.; Franchi-Micheli, S.; Zilletti, L.; Ginanneschi, M.; Chelli, M.; Papini, A. M.; Paoletti, F. An in vivo, ex vivo and in vitro comparative study of activity of copper oligopeptide complexes vs Cu(II) ions. *Pharmacol Res* **38:**279-287; 1998.

[41] Palivan, C. G.; Balasubramanian, V.; Goodman, B. A. Global structure-activity analysis in drug development illustrated for active Cu/Zn superoxide dismutase mimics. *Eur J Inorg Chem***:**4634-4639; 2009.

[42] Tissue, B. M. Electron Paramagnetic Resonance (EPR, ESR) Spectroscopy. *The Chemistry Hypermedia Project*: http://www.files.chem.vt.edu/chem-ed/spec/spin/epr.html; 2000 (accessed June 2010).

[43] Yu, J. W.; Yoon, S. S.; Yang, R. Iron chlorin e6 scavenges hydroxyl radical and protects human endothelial cells against hydrogen peroxide toxicity. *Biol Pharm Bull* **24:**1053-1059; 2001.

[44] Xavier, S.; Yamada, K.; Samuni, A. M.; Samuni, A.; DeGraff, W.; Krishna, M. C.; Mitchell, J. B. Differential protection by nitroxides and hydroxylamines to radiation-induced and metal ion-catalyzed oxidative damage. *Biochim Biophys Acta* **1573:**109-120; 2002.

[45] Liang, X.; Sadler, P. J. Cyclam complexes and their applications in medicine. *Chem Soc Rev* **33:**246-266; 2004.

[46] Marques, F.; Guerra, K. P.; Gano, L.; Costa, J.; Campello, M. P.; Lima, L. M.; Delgado, R.; Santos, I. 153Sm and 166Ho complexes with tetraaza macrocycles containing pyridine and methylcarboxylate or methylphosphonate pendant arms. *J Biol Inorg Chem* **9:**859-872; 2004.

[47] Marques, F.; Gano, L.; Paula Campello, M.; Lacerda, S.; Santos, I.; Lima, L. M.; Costa, J.; Antunes, P.; Delgado, R. 13- and 14-membered macrocyclic ligands containing methylcarboxylate or methylphosphonate pendant arms: chemical and biological evaluation of their (153)Sm and (166)Ho complexes as potential agents for therapy or bone pain palliation. *J Inorg Biochem* **100:**270-280; 2006.

[48] Day, B. J. Catalytic antioxidants: a radical approach to new therapeutics. *Drug Discov Today* **9:**557-566; 2004.

[49] Lovstad, R. A. A kinetic study on the distribution of Cu(II)-ions between albumin and transferrin. *Biometals* **17:**111-113; 2004.

[50] Bertinato, J.; L'Abbe, M. R. Maintaining copper homeostasis: regulation of copper-trafficking proteins in response to copper deficiency or overload. *J Nutr Biochem* **15:**316-322; 2004.

[51] Rae, T. D.; Schmidt, P. J.; Pufahl, R. A.; Culotta, V. C.; O'Halloran, T. V. Undetectable intracellular free copper: the requirement of a copper chaperone for superoxide dismutase. *Science* **284:**805-808; 1999.

[52] Costanzo, L. L.; De Guidi, G.; Giuffrida, S.; Rizzarelli, E.; Vecchio, G. Determination of superoxide dismutase-like activity of copper(II) complexes. Relevance of the speciation for the correct interpretation of in vitro O2- scavenger activity. *J Inorg Biochem* **50:**273-281; 1993.

[53] Munzel, T.; Afanas'ev, I. B.; Kleschyov, A. L.; Harrison, D. G. Detection of superoxide in vascular tissue. *Arterioscler Thromb Vasc Biol* **22:**1761-1768; 2002.

[54] Benov, L.; Sztejnberg, L.; Fridovich, I. Critical evaluation of the use of hydroethidine as a measure of superoxide anion radical. *Free Radic Biol Med* **25:**826-831; 1998.

[55] Dillon, C. T.; Hambley, T. W.; Kennedy, B. J.; Lay, P. A.; Zhou, Q.; Davies, N. M.; Biffin, J. R.; Regtop, H. L. Gastrointestinal toxicity, antiinflammatory activity, and superoxide dismutase activity of copper and zinc complexes of the antiinflammatory drug indomethacin. *Chem Res Toxicol* **16:**28-37; 2003.

[56] Baudry, M.; Etienne, S.; Bruce, A.; Palucki, M.; Jacobsen, E.; Malfroy, B. Salen-manganese complexes are superoxide dismutase-mimics. *Biochem Biophys Res Commun* **192:**964-968; 1993.

[57] Patel, R. N.; Singh, N.; Shukla, K. K.; Gundla, V. L.; Chauhan, U. K. Synthesis, structure and biomimetic properties of Cu(II)-Cu(II) and Cu(II)-Zn(II) binuclear complexes: possible models for the chemistry of Cu-Zn superoxide dismutase. *J Inorg Biochem* **99:**651-663; 2005.

[58] Giblin, G. M.; Box, P. C.; Campbell, I. B.; Hancock, A. P.; Roomans, S.; Mills, G. I.; Molloy, C.; Tranter, G. E.; Walker, A. L.; Doctrow, S. R.; Huffman, K.; Malfroy, B. 6,6'-Bis(2-hydroxyphenyl)-2,2'-bipyridine manganese(III) complexes: a novel series of superoxide dismutase and catalase mimetics. *Bioorg Med Chem Lett* **11:**1367-1370; 2001.

[59] Schepetkin, I.; Potapov, A.; Khlebnikov, A.; Korotkova, E.; Lukina, A.; Malovichko, G.; Kirpotina, L.; Quinn, M. T. Decomposition of reactive oxygen species by copper(II) bis(1-pyrazolyl)methane complexes. *J Biol Inorg Chem* **11:**499-513; 2006.

[60] Faulkner, K. M.; Liochev, S. I.; Fridovich, I. Stable Mn(III) porphyrins mimic superoxide dismutase in vitro and substitute for it in vivo. *J Biol Chem* **269:**23471-23476; 1994.

[61] Gonzalez-Alvarez, M.; Alzuet, G.; Borras, J.; del Castillo Agudo, L.; Garcia-Granda, S.; Montejo-Bernardo, J. M. Comparison of protective effects against reactive oxygen species of mononuclear and dinuclear Cu(II) complexes with N-substituted benzothiazolesulfonamides. *Inorg Chem* **44:**9424-9433; 2005.

[62] Yokoi, H.; Sai, M.; Isobe, T.; Ohsawa, S. ESR studies of the copper(II) complexes of amino acids. *Bull Chem Soc Jpn* **45:**2189-2195; 1972.

[63] Lau, P. W.; Lin, W. C. Electron spin resonance and electronic structure of some metalloporphyrins *J Inorg Nucl Chem* **37:**2389-2398; 1975.

[64] Costa, J.; Delgado, R. Metal complexes of macrocyclic ligands containing pyridine. *Inorg Chem* **32:**5257-5265; 1993.

[65] Peisach, J.; Blumberg, W. E. Structural implications derived from the analysis of electron paramagnetic resonance spectra of natural and artificial copper proteins. *Arch Biochem Biophys* **165:**691-708; 1974.

[66] Gonzalez-Alvarez, M.; Alzuet, G.; Borras, J.; Castillo Agudo, L.; Montejo-Bernardo, J. M.; Garcia-Granda, S. Development of novel copper(II) complexes of benzothiazole- N-sulfonamides as protective agents against superoxide anion. Crystal structures of [Cu( N-2-(4-methylbenzothiazole)benzenesulfonamidate)(2)(py)(2)] and [Cu( N-2-(6-nitrobenzothiazole)naphthalenesulfonamidate)(2)(py)(2)]. *J Biol Inorg Chem* **8:**112-120; 2003.

[67] Müller, J.; Schübl, D.; Maichle-Mössmer, C.; Strähle, J.; Weser, U. Structure-function correlation of Cu(II)-and Cu(I)-di-Schiff-base complexes during the catalysis of superoxide dismutation *J Inorg Biochem* **75:**63-69; 1999.

[68] Neese, F. Diploma thesis. Germany: University of Konstanz; 1993.

[69] Hathaway, B. J. Copper. *Coord Chem Rev* **52:**87-169; 1983.

[70] Bazzicalupi, C.; Bencini, A.; Berni, E.; Bianchi, A.; Giorgi, C.; Paoletti, P.; Valtancoli, B. Complexation of Ni(II) and Co(II) with 1,4-Dioxa-7,10,13-triazacyclopentadecane (L). Crystal Structure of [NiLCl][NiL(H2O)](ClO4)3 and Macrocycle-Induced Dioxygen Binding. *Ind Eng Chem Res* **39:**3484-3488 2000.

[71] Liu, C.-M.; Xiong, R.-G.; You, X.-Z.; Liu, Y.-J.; Cheung, K.-K. Crystal structure and some properties of a novel potent $Cu_2Zn_2SOD$ model schiff base copper(II) complex *$[Cu(bppn)](ClO_4)_2$*$_2 \cdot H_2O$ *Polyhedron* **15:**4565-4571; 1996.

[72] Batinic-Haberle, I.; Rebouças, J. S.; Spasojević, I. Superoxide dismutase mimics: chemistry, pharmacology and therapeutic potential. *Antiox Redox Signal* **13:**877-918; 2010.

[73] Perez, M. J.; Cederbaum, A. I. Antioxidant and pro-oxidant effects of a manganese porphyrin complex against CYP2E1-dependent toxicity. *Free Radic Biol Med* **33:**111-127; 2002.

[74] Liu, J.; Zhang, H.; Chen, C.; Deng, H.; Lu, T.; Ji, L. Interaction of macrocyclic copper(II) complexes with calf thymus DNA: effects of the side chains of the ligands on the DNA-binding behaviors. *Dalton Trans***:**114-119; 2003.

[75] Batinic-Haberle, I.; Benov, L.; Spasojevic, I.; Fridovich, I. The ortho effect makes manganese(III) meso-tetrakis(N-methylpyridinium-2-yl)porphyrin a powerful and potentially useful superoxide dismutase mimic. *J Biol Chem* **273:**24521-24528; 1998.

[76] Mourgues, S.; Kupan, A.; Pratviel, G.; Meunier, B. Use of short duplexes for the analysis of the sequence-dependent cleavage of DNA by a chemical nuclease, a manganese porphyrin. *Chembiochem* **6:**2326-2335; 2005.

[77] Weydert, C. J.; Waugh, T. A.; Ritchie, J. M.; Iyer, K. S.; Smith, J. L.; Li, L.; Spitz, D. R.; Oberley, L. W. Overexpression of manganese or copper-zinc superoxide dismutase inhibits breast cancer growth. *Free Radic Biol Med* **41:**226-237; 2006.

# Chapter 6

## Development of pyridine-containing macrocyclic copper(II) complexes with superoxide scavenging activity. Studies on CuL8 as a novel chemotherapy sensitizer for breast cancer

The work described in this Chapter was adapted from:

Two macrocyclic pentaaza compounds containing pyridine evaluated as novel chelating agents in copper(II) and nickel(II) overload. A.S. Fernandes, M.F. Cabral, J. Costa, M. Castro, R. Delgado, M.G.B. Drew, V. Félix. Journal of Inorganic Biochemistry (2010), *under final revision.*

and from:

Pyridine-containing macrocyclic copper(II) complexes with superoxide scavenging activity: CuPy[15]ane$N_5$ as a novel chemotherapy sensitizer for breast cancer. A.S. Fernandes, J. Costa, J. Gaspar, J. Rueff, M.F. Cabral, M. Castro, N.G. Oliveira, *to be submitted*.

**Abstract**

In this Chapter, four pyridine-containing aza-macrocyclic copper(II) complexes (CuL6-CuL9) were prepared, varying in their ring size (14 to 16 atoms) and/or in the substituents. Studies were performed on their thermodynamic stability (potentiometric titrations), structural features (Vis spectroscopy and EPR), electrochemical properties (cyclic voltammetry), and superoxide scavenging activity (NBT and DHE assays). Two out of four complexes (CuL6 and CuL8) were effective superoxide scavengers, with $IC_{50}$ values in the micromolar range. The cytotoxicity profile of the four complexes was studied by the MTT assay, in V79 cells, as well as in non-tumoral (MCF10A) and tumoral (MCF7) human mammary cells. All the complexes with the exception of CuL7 were devoid of considerable toxic effects. The potential antioxidant of CuL8, the most promising complex, was studied in V79 cells exposed to XXO and TBHP. However, no protective effects were found in these models. Using the DNA strand break analysis, CuL8 was shown to generate hydroxyl radical. Hence, this complex was studied as a redox modulator of Dox and oxaliplatin effects in tumoral (MCF7) and non-tumoral (MCF10A) human mammary cells, by the MTT assay. The obtained results showed that CuL8 can indeed enhance the therapeutic index of Dox, and specially of oxaliplatin, in mammary cells, by both protecting normal cells and increasing the antitumoral effect in breast carcinoma cells. CuL8 is thus a promising compound to be further studied as a chemotherapy sensitizer.

## 6.1. Introduction

Metal complexes with macrocyclic ligands have been designed as chemical models of metalloenzymes [1, 2]. Among those, macrocyclic copper(II) complexes have been developed as mimics of SOD [3-6]. Aza-macrocyclic ligands received considerable attention during the last decade due to their relationship to biomimetic and catalytic systems, because many coordination compounds with aza-macrocycles are electrocatalytically active in redox reactions [1]. To be used as a redox drug, macrocyclic complexes with high kinetic and thermodynamic stabilities towards metal release are required. In the previous Chapter, five macrocyclic copper(II) complexes were synthesised and studied as $O_2^{\bullet -}$ scavengers. In this Chapter, ligands containing a pyridine ring in the macrocyclic backbone were studied. The presence of coordination sites belonging to nitrogen heteroaromatic rings seems to be important for a SOD-like activity not affected by biological chelators [4]. In addition, it was also previously pointed out that the π-electrons in the pyridine ring may favourably respond to the Cu(II)-$O_2^{\bullet -}$ interaction [5, 7]. Another advantage of macrocycles incorporating a pyridine is the faster kinetics of complex formation [8].

The *N*-functionalization of aza-macrocycles may enhance their metal-ion selectivity and the stability of metal complexes depending on the coordination properties of the pendant arms [1]. The attachment of coordinating groups to the donor atoms of the macrocycle may change the geometry of the complex and its redox properties [9]. Non-coordinating *n*-alkyl pendant arms may also participate in various equilibria and may have practical applications on the modulation of the hydrophobic properties, metal selectivity and redox properties [1, 10, 11].

In this Chapter, four water soluble pyridine-containing macrocyclic copper(II) complexes were synthesized and studied. Besides the studies on the antioxidant properties of the complexes, the compounds were assessed towards a possible application as chemotherapy adjuvants.

As described in Chapter 1 (section 1.2.3), chemotherapy is a field in which the therapeutic redox modulation by SODm may have promising clinical applications. Most anticancer drugs exert their activity at least in part though the generation of ROS [12]. Also, many adverse effects of chemotherapy are related to oxidative stress [13-16].

SODm may therefore be promising antioxidants for the protection of non-tumoral tissues from chemotherapy adverse effects. As mentioned in Chapter 1, ROS can exert different effects in cell proliferation, either promoting or reducing it, according to their nature and to their intracellular level [12]. Tumor cells are usually under higher oxidative stress than normal cells [12] and are nearly always low in SOD and catalase activities [17]. While in non-tumoral cells, the basal level of $H_2O_2$ is low and its increase is associated with cell proliferation, the intracellular level of $H_2O_2$ in tumor cells is close to the threshold of toxicity. In this case, a further increase in $H_2O_2$ concentration will trigger cell death [18]. SODm compounds can increase the $H_2O_2$ concentration as a result of $O_2^{\bullet-}$ dismutation, and may thus reduce tumor growth or potentiate anticancer agents [12, 18, 19]. Furthermore, as mentioned in Chapters 1 and 5, if a SODm can react with $H_2O_2$ generating hydroxyl radical, it can have an additional advantage in promoting cancer cells' death. For this purpose, copper complexes are advantageous over manganese-containing SODm since they are prone to undergo Fenton chemistry. In view of this, one of the goals of this Chapter was to develop macrocyclic copper(II) complexes with SOD-like activity as chemotherapy adjuvants in breast cancer treatment. Breast cancer was chosen, since it has been reported that breast tumor tissue have higher levels of oxidative stress than normal breast tissue [20]. Furthermore, it was previously shown that MnSOD overexpression leads to a suppression in the proliferation of human breast carcinoma MCF-7 cells, being $H_2O_2$ the mediator of the effect [21]. Similar results were found for the overexpression of Cu,Zn-SOD [22].

Two well established anticancer drugs were studied: Dox and oxaliplatin. The anticancer drug Dox is commonly used in a variety of tumors, and is an essential component of breast cancer treatment [23, 24]. The mechanisms of Dox cytotoxicity were previously described in Chapters 3 and 5, and include the interference in DNA synthesis and the generation of ROS, namely $O_2^{\bullet-}$ [24-26]. As depicted in Fig. 5.1 (Chapter 5), if a copper(II) complex with SOD-like activity is present, it can disproportionate $O_2^{\bullet-}$ into $H_2O_2$. If this complex reacts with $H_2O_2$ to form $HO^{\bullet}$, this will further potentiate tumor cells' death [27]. On the other hand, non-tumoral cells would be spared due to their higher antioxidant capacity (Fig. 6.1).

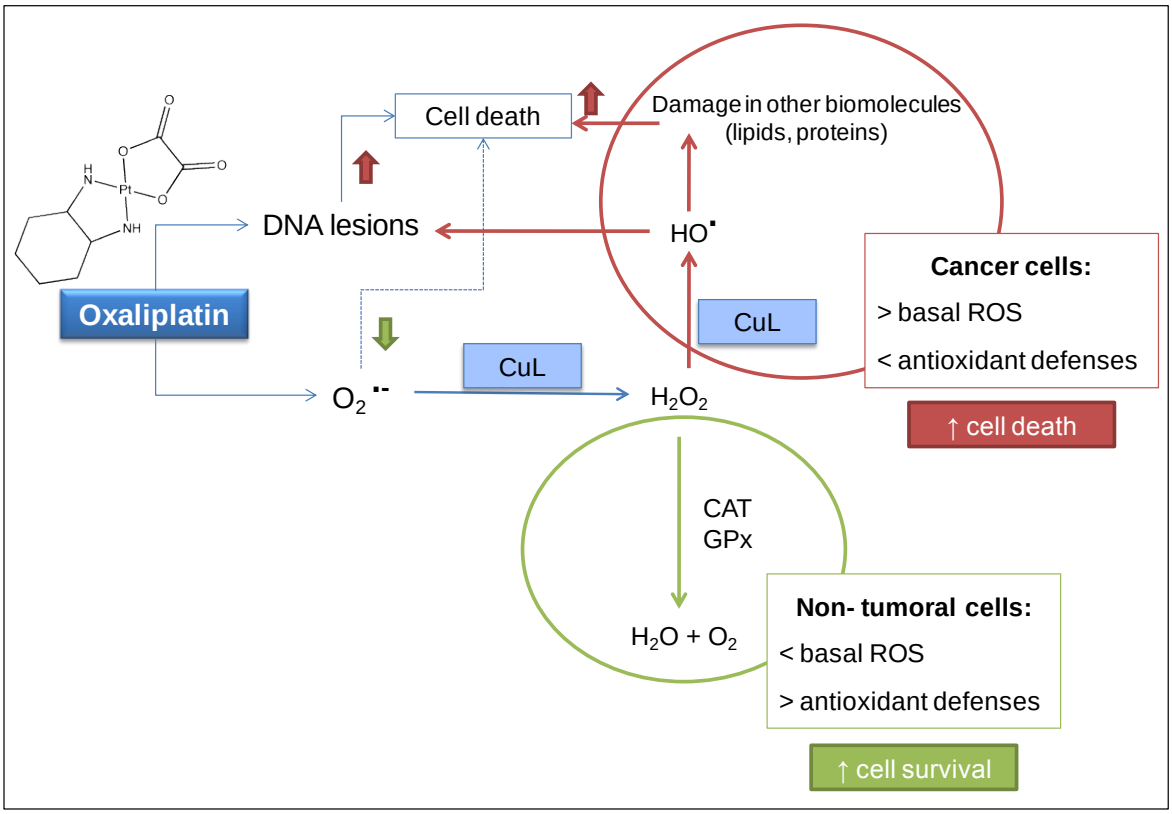


**Fig. 6.1** – Potential activity of Cu(II) complexes with SOD-like activity as redox modulators of oxaliplatin cytotoxicity. (CuL = copper(II) complex; ROS = reactive oxygen species; CAT = catalase; GPx = glutathione peroxidase)

Oxaliplatin (Fig. 6.1) is a platinum-based chemotherapy drug that forms mainly intra-strand links between two adjacent guanine residues or a guanine and an adenine, disrupting DNA replication [28]. Oxaliplatin is commonly used in combination with 5-fluorouracil/leucovorin to treat advanced colorectal cancer, but recent reports have suggested the use of this drug in metastatic breast cancer. In fact, clinical trials have shown promising results for oxaliplatin in breast cancer, either in monotherapy [29] or in combination protocols [30-35], especially in anthracycline- and taxane-pretreated metastatic breast cancer patients. Although the mechanism of action of oxaliplatin is mostly at the DNA level, this drug can also increase oxidative stress. Kim *et al* [36] have shown an intracellular accumulation of ROS in human renal carcinoma cells treated with oxaliplatin, using the fluorescent probe 2',7'-dichlorodihydrofluorescein diacetate. Laurent *et al* [12] demonstrated that, in mouse colon carcinoma cells treated

with oxaliplatin, $O_2^{\bullet-}$ markedly increased in a dose-dependent way. Also, a small increase in $H_2O_2$ and a decrease in GSH were reported. An increase in $O_2^{\bullet-}$ and $H_2O_2$ was also described in normal leukocytes and in CT26 colon carcinoma cells upon treatment with oxaliplatin [19]. The involvement of $O_2^{\bullet-}$ in oxaliplatin toxicity justifies the study of SODm as possible chemotherapy adjuvants. The rational basis underlying this hypothesis is analogous to that aforementioned for Dox, and is schematized in Fig. 6.1. In fact, Laurent *et al* [12] have previously shown that in oxaliplatin-treated tumor cells, an increase in ROS production associated with a decrease in proliferation was observed upon addition of the catalytic antioxidants MnTBAP and CuDIPS. These authors also demonstrated that the DNA damage caused by oxaliplatin *in vitro* was increased by the $H_2O_2$ generated by the SODm [12]. Alexandre *et al* [19] have also reported a potentiation of oxaliplatin cytotoxicity by mangafodipir, MnTBAP and CuDIPS in colon carcinoma cells. Furthermore, the SODm mangafodipir protected normal leukocytes from the cytotoxicity of oxaliplatin, while CuDIPS and MnTBAP enhanced the toxicity of the drug.

## 6.2. Materials and Methods

### *6.2.1 Chemicals*

The starting compounds used for the synthesis of the macrocycles were purchased from Aldrich. 2,6-Pyridinedicarbaldehyde was prepared by published methods [37]. All the commercially available chemicals were of reagent grade and used as supplied without further purification. Organic solvents were purified or dried by standard procedures [38]. PBS, xanthine, xanthine oxidase, NBT, caffeic acid, trypsin, DMEM, DMEM/Nutrient Mixture F-12 Ham (DMEM/F12), penicillin-streptomycin solution, foetal bovine serum, horse serum, insulin solution from bovine pancreas, hydrocortisone, cholera toxin, human epidermal growth factor, Dox, oxaliplatin, MTT, and Cu,Zn-SOD from human erythrocytes were obtained from Sigma-Aldrich. Copper(II) nitrate-trihydrate and DHE were purchased from Fluka. DMSO was obtained from Merck. Chelex 100 resin was acquired to Biorad.

### *6.2.2. Synthesis of the macrocycles*

The macrocyclic ligands used for the preparation of the copper(II) complexes studied in the present work are shown in Scheme 6.1.

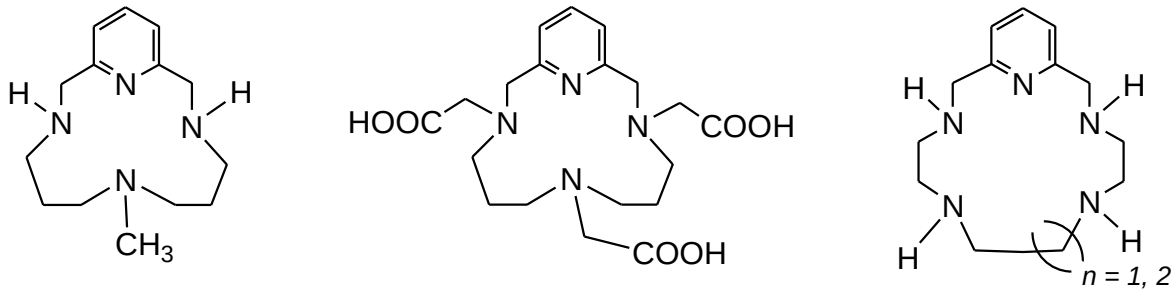


**L6** **L7** **L8** - *n = 1*
**L9** - *n = 2*

**Scheme 6.1**

All the compounds were obtained in good yield and were characterized by melting points and $^{1}H$ and $^{13}C$ NMR spectroscopy. The NMR spectra were recorded on a Bruker Avance-400 spectrometer and were performed in $CDCl_3$ or $D_2O$. The reference used for the $^{1}H$ NMR measurements in $D_2O$ was 3-(trimethylsilyl)propionic acid-$d_4$-sodium salt and in $CDCl_3$ the solvent itself. For $^{13}C$ NMR spectra 1,4-dioxane was used as internal reference.

L6 was synthesized by previously reported procedures [37], using Cu(II) as the template metal ion (Fig. 6.2). Briefly, 3,3‘-diamino-*N*-methyldipropylamine was added to a solution of 2,6-pyridinedicarbaldehyde and copper nitrate (in a mixture of ethanol/water, 1:l v/v). The copper(II) diimine complex formed was reduced by sodium borohydride, and the copper was removed by precipitation of its sulfide [37]. Yield: 75%. Mp 79-80 $^{o}C$. $^{1}H$ NMR ($CDCl_3$): $\delta$ (ppm) 1.63 (m, 4H), 1.96 (s, 3H), 2.27 (t, 4H), 2.44 (t, 4H), 3.14 (br s, 2H), 3.77 (s, 4H), 6.90 (d, 2H), 7.43 (t, lH). $^{13}C$ NMR($CDC1_3$): $\delta$ (ppm) 26.89, 40.70, 46.44, 54.30, 56.09, 120.25, 136.21, 159.16.

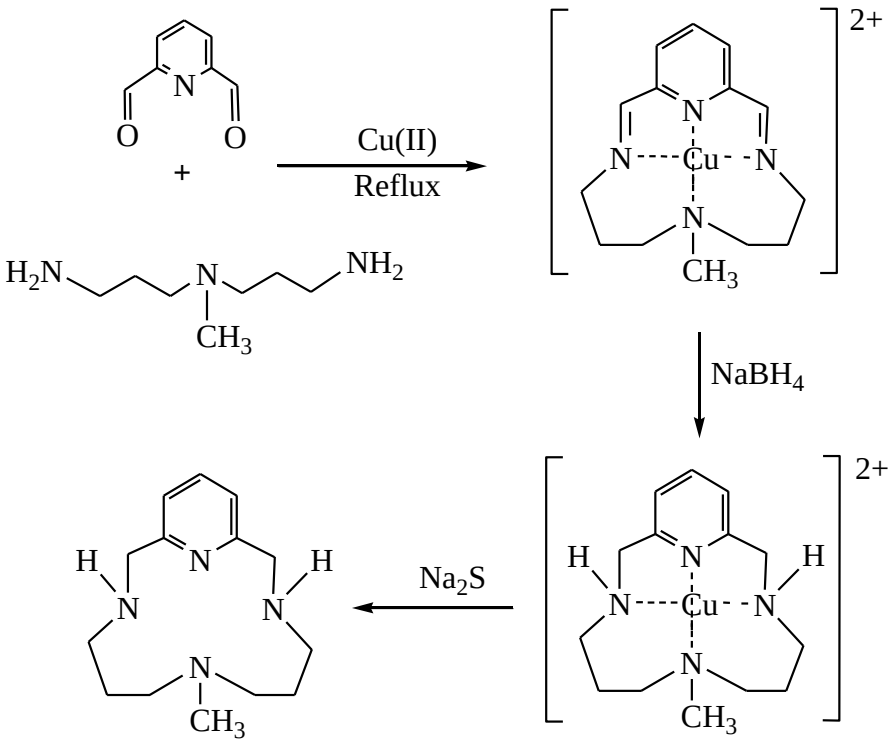


**Fig. 6.2** – Schematic representation of the synthesis of the ligand L6.

L7 as prepared from the parent amine 3,7,11,17-tetraazabicycle[11,3,1]heptadeca-1(17),13,15-triene. This amine was obtained by a templated method similar to L6 but using 3,3'-diaminodipropylamine instead of 3,3'-diamino-N-methyldipropylamine [37]. This amine was then submitted to a condensation of the with ethyl bromoacetate under basic conditions [8]. The resulting ester was hydrolysed under acid conditions (Fig. 6.3). Then the solvent was evaporated and methanol added. The formed inorganic salts were filtered off and the filtrate passed through an anionic resin in the formate form [8]. Yield: 85%. Mp 249–251 ºC. $^{1}$H NMR ($D_2O$, pD 5.0): $\delta$ (ppm) 2.38 (q, 4 H), 3.30 (t, 4 H), 3.45 (t, 4 H), 3.77 (s, 2 H), 3.80 (s, 4 H), 4.64 (s, 4 H), 7.59 (d, 2 H), 7.80 (t, 1 Ht). $^{13}$C NMR ($D_2O$, pD 5.0): $\delta$ (ppm) 18.00, 48.71, 51.28, 56.20, 56.86, 57.63, 126.17, 140.25, 149.41, 169.40, 169.54.

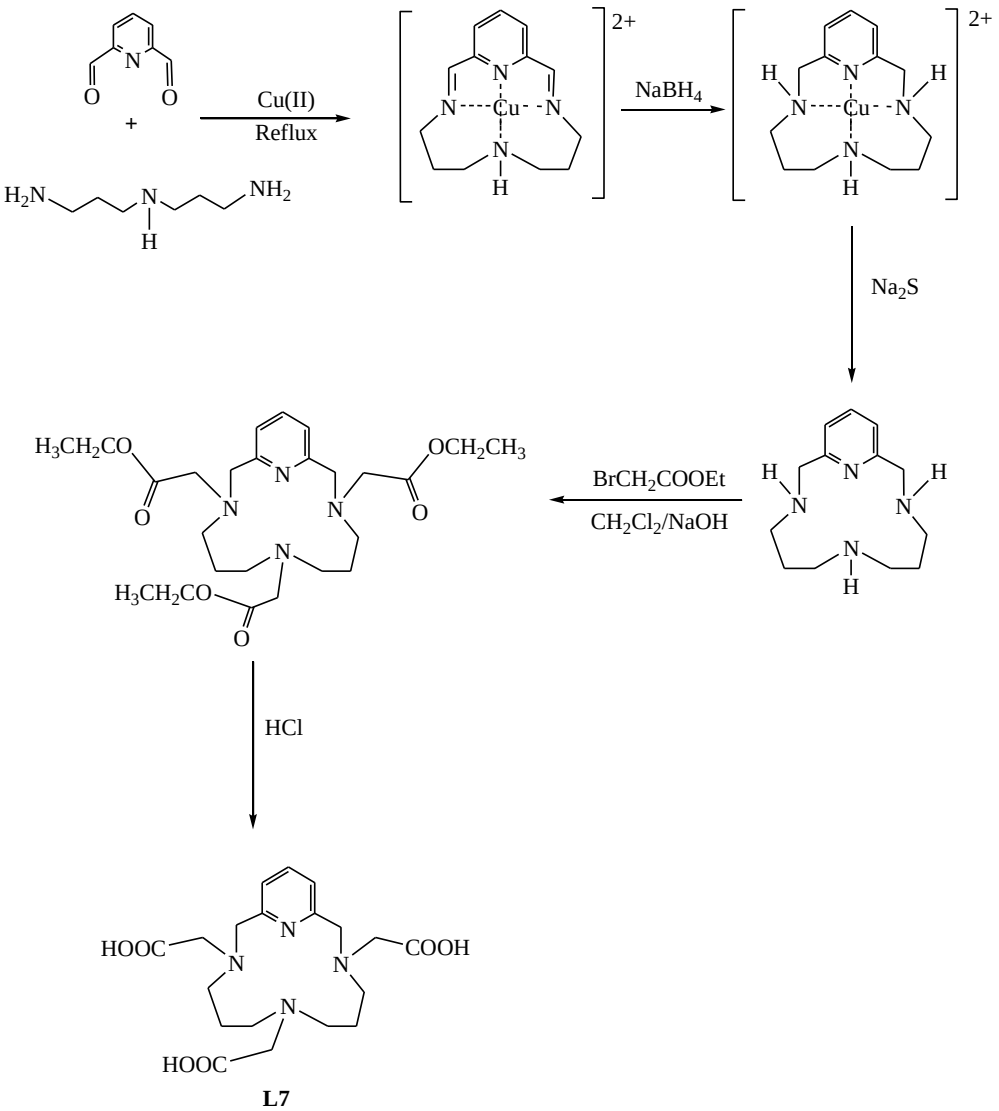


**Fig. 6.3** – Schematic representation of the synthesis of the ligand L7.

L8 was synthesized by [1:1] condensation of 2,6-pyridinedicarboxaldehyde and N,N´-bis(2-aminoethyl)ethane-1,2-diamine (triethylenetetramine), using $Pb^{2+}$ as the template ion, followed by the reduction of the resulting tetraimine with sodium borohydride (Fig. 6.4). The pure product was obtained as a salt by precipitation with HCl 37%. Yield: 85%. Mp 280-2 $^{o}$C (decomp.). $^{1}$H NMR ($D_2O$, pD = 5.10): $\delta$ (ppm) 3.21 (s, 4 H), 3.41 (t, 4 H), 3.51 (t, 4 H), 4.57 (s, 4 H), 7.53 (d, 2 H), 7.99 (t, 1 H) $^{13}$C NMR ($D_2O$, pD = 5.10): $\delta$ (ppm) 43.92, 45.64, 46.33, 49.92, 124.07, 140.33, 150.94.

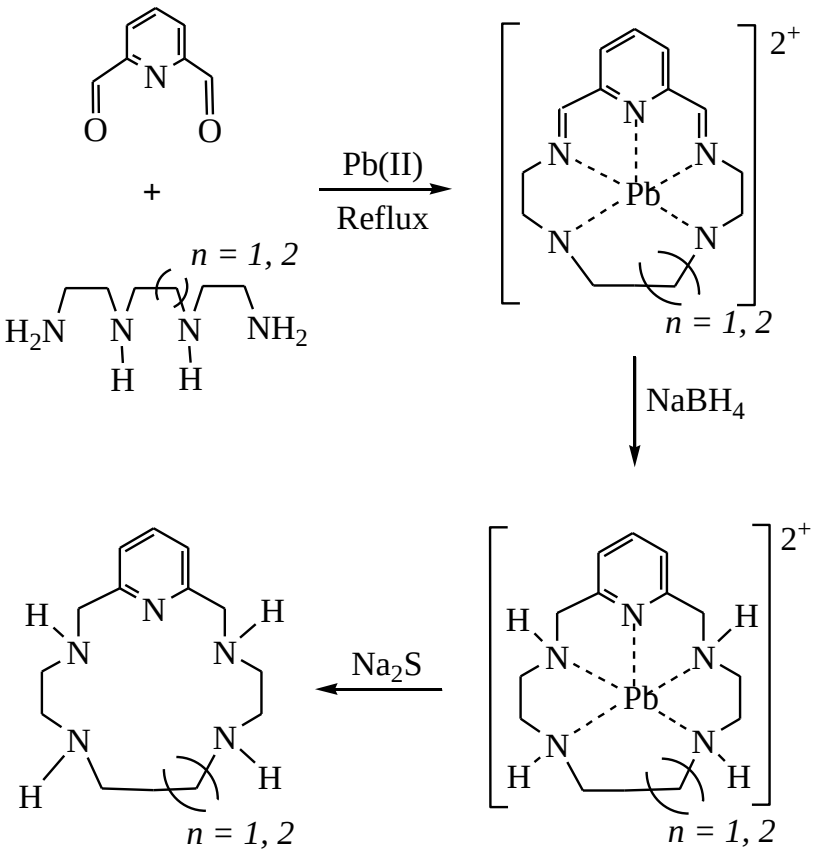


**L8 -** *n = 1*
**L9 -** *n = 2*

**Fig. 6.4** – Schematic representation of the synthesis of the ligands L8 and L9.

L9 was obtained by a procedure analogous to that for L8, replacing the N,N´-bis(2-aminoethyl)ethane-1,2-diamine by N,N´-bis(2-aminoethyl)1,3-propanediamine (Fig. 6.4). Yield: 46%. Mp 266-2 $^{o}$C (decomp.). $^{1}$H NMR ($D_2O$, pD = 2.55): $\delta$ (ppm) 2.21 (q, 2 H), 3.37 (t, 4 H) 3.65 (t, 4 H), 3.71 (t, 4 H), 4.63 (s, 4 H), 7.56 (d, 2 H), 8.00 (t, 1 H). $^{13}$C NMR ($D_2O$, pD = 2.55): $\delta$ (ppm) 21.30, 42.25, 43.20, 44.14, 51.35, 124.50, 140.45, 150.68.

*6.2.3. Synthesis of the macrocyclic copper(II) complexes*

Aqueous macrocycles' solutions were prepared at ~2.5 × $10^{-3}$ M, and their concentrations were determined by potentiometric titrations. Copper(II) complexes were prepared as described in Chapter 5 (5.2.2.2).

The values of the stability constants of Cu(II) with the ligands L6 and L7 were previously determined from potentiometric titrations, performed at 25.0 ± 0.1°C and 0.10 M ionic strength [8, 37]. For L8 and L9, the stability constants for Cu(II) were determined by potentiometric measurements, performed at 25.0 ± 0.1°C and with an ionic strength of 0.10 ± 0.01 mol $dm^{-3}$ with $KNO_3$. For L7, L8 and L9, the ML species were completely formed right from the beginning of the titration and the concentration of the free copper(II) was too small to allow the determination of reliable values for the constants. Therefore, a competition technique using edta as the reference ligand [39] was performed. The constants values were calculated by fitting the potentiometric data obtained using the SUPERQUAD [40] or HYPERQUAD programs [41].

*6.2.4. Species distribution curves*

Species distribution diagrams were plotted from the calculated constants with the HYSS program [42]. These simulations, as well as the pCu values, were determined for the aqueous solutions containing Cu(II) (10 μM) and each ligand (L6-L9; 10.5 μM) at a molar ratio of 1:1, at physiological pH. This concentration was chosen because it is in same order of magnitude of the $IC_{50}$ values of the active superoxide scavenging

complexes. Simulations of the species distribution in the presence of 0.01 M phosphate buffer were also performed, as described in Chapter 5 (5.2.2.2).

### *6.2.5. Structural studies*

#### *6.2.5.1 Spectroscopic studies*

Electronic spectra (visible range) were recorded with a UNICAM model UV-4 spectrophotometer. The aqueous solutions of the Cu(II) complexes (1:1 ratio) were prepared at ~$1 \times 10^{-3}$ mol $dm^{-3}$, at a pH value corresponding to total formation of the metal complex.

EPR spectroscopy measurements were previously recorded for CuL6 (in DMF) [43] and for CuL7 (in a 1 mol $dm^{-3}$ $NaClO_4$ aqueous solution) [8], in a Bruker ESP 380 spectrometer. The EPR spectra of CuL8 and CuL9 were recorded with a Bruker EMX 300 spectrometer, equipped with a continuous-flow cryostat for liquid nitrogen, operating at X-band. These complexes were prepared in a 1 mol $dm^{-3}$ $NaClO_4$ aqueous solution using 1:1 metal-to-ligand ratio, at ~$1 \times 10^{-3}$ mol $dm^{-3}$ (pH 7.23).

#### *6.2.5.2. Electrochemistry*

Cyclic voltammetry experiments were performed for CuL8 and CuL9, according to the procedure described in Chapter 5 (5.2.4.2). Copper(II) complexes of L8 and L9 ($1.63 \times 10^{-3}$ mol $dm^{-3}$; pH = 7.05 and $1.46 \times 10^{-3}$ mol $dm^{-3}$; pH = 7.09, respectively), were prepared in 0.1 mol $dm^{-3}$ $KNO_3$ in water. The solutions were deaerated by an argon stream prior to all measurements, and were kept under argon during the measurements. Cyclic voltammograms with sweep rate ranging from 25 to 1000 mV $s^{-1}$ were recorded in the region from + 1.2 to - 1.2 V.

*6.2.6. Superoxide scavenging activity*

As in Chapter 5, the superoxide scavenging activity of the complexes was determined by two different endpoints: the reduction of NBT and the oxidation of DHE, using the $O_2^{\bullet-}$ generating system XXO.

*6.2.6.1 NBT assay*

The NBT assay was performed as described in Chapter 5 (5.2.3.1.).

*6.2.6.2 DHE assay*

The DHE assay was carried out according to the protocol described in Chapter 5 (5.2.3.2.). For CuL7 and CuL8, since they revealed no activity using the NBT assay (see Results and Discussion section), only the highest concentration (80 μM) was tested.

*6.2.6.3. Xanthine oxidase inhibition assay*

We have evaluated if the generating system XXO could be inhibited by the copper(II) complexes by following the production of uric acid at 293 nm, as described in Chapter 5 (5.2.3.3).

*6.2.7. Cytotoxicity profile of the complexes*

*6.2.7.1. Cell culture*

V79 and MCF7 cells were cultured as described in Chapter 3 (3.2.2) and Chapter 5 (5.2.8.1), respectively. MCF10A cells were purchased from ATCC. These cells were cultured in DMEM/F12 medium, containing 5% horse serum, 1% antibiotic solution, 0.01 mg/mL insulin, 0.5 μg/mL hydrocortisone, 100 ng/mL cholera toxin, and 20 ng/mL

human epidermal growth factor. Cells were kept at 37°C, under an atmosphere containing 5% $CO_2$.

*6.2.7.2. MTT reduction assay*

The toxicity of macrocyclic copper(II) complexes was evaluated in the cell lines V79, MCF10A (non-tumoral human mammary cells) and in MCF7 (human breast cancer cells), using the MTT assay. For V79 and MCF7 cells, the assay was performed as described in Chapter 3 (3.2.3.1) and Chapter 5 (5.2.8.2), respectively. For MCF10A a protocol analogous to that of MCF7 cells was used, but the initial number of cells was ~$4 \times 10^3$. The macrocyclic copper(II) complexes were tested at concentrations of 1, 10, 50 and 100 μM, for a 24 h incubation period. $H_2O_2$ and Dox were used as positive controls. At least two independent experiments were performed and four individual cultures were used for each complex concentration in each independent experiment.

*6.2.8. Evaluation of the potential protective effect of CuL8 against the oxidative injury induced by XXO and by* TBHP

From the results of the previous assays, CuL8 was selected to be further studied in cell-based experiments. The potential antioxidant activity of this complex was studied in V79 cells, by the MTT method, using XXO and TBHP as oxidative stress inducers. These assays were performed as described in Chapter 5 (5.2.6.1). Cells were treated with X (240 μM)/XO (20 U/L) or TBHP (100 μM), in the absence or presence of CuL8 (5, 25, 50, and 100 μM). Two to three independent experiments were performed and eight replicate cultures were used for each complex concentration in each independent experiment.

*6.2.9. DNA strand break analysis*

The generation of $HO^{\bullet}$ radical by the copper(II) complex CuL8 was evaluated by the DNA strand break analysis, according to the procedure described in Chapter 5 (5.2.7).

*6.2.10. Evaluation of the possible role of CuL8 on the modulation of the cytotoxicity of the anticancer drugs Dox and oxaliplatin*

The studies on the modulation of the cytotoxicity of Dox and oxaliplatin were also carried out in MCF7 and MCF10A cells using the MTT protocol described above. Cells were exposed to Dox (0.5, 1 and 5 μM) or to oxaliplatin (20, 50 and 100 μM) in the absence or presence of 100 μM CuL8, for 24 h. Three to eight independent experiments were performed, each comprising four individual cultures.

*6.2.11. Statistical analysis*

The results obtained in points 6.2.8 and 6.2.10 were submitted to a statistical analysis as described in Chapter 3 (3.2.6).

## 6.3. Results and Discussion

As mentioned in the Introduction section (6.1), macrocycles containing a pyridine ring form complexes with copper(II) that appear to have advantages as SODm compounds. Hence, in this Chapter, a set of four pyridine-containing macrocyclic copper(II) complexes was synthesised, characterised and evaluated in cell-based experiments.

### *6.3.1. Chemical characterization and superoxide scavenging activity of the complexes*

The macrocyclic ring sizes (14 - 16 atoms) were chosen so that the ring could encircle the copper(II) ion, taking advantage of the thermodynamic macrocyclic effect and therefore, favouring the complex stability [10]. In fact, as shown in Table VI.1, the four macrocycles present very high stability constants for copper(II) ($\log K_{CuL} > 20$). The direct comparison of stability constants of ligands having different overall basicities can lead to erroneous conclusions, because the different competition of metals with the proton is not taken into account. To overcome this drawback, the pCu values, defined as -log $[Cu^{2+}]$, were calculated for all metal complexes at pH 7.4. All complexes presented high pCu values (Table VI.1). The data on the stability constants and pCu values clearly demonstrate the high thermodynamic stability of the complexes. This is a required feature to avoid the dissociation of the complexes in *in vivo* systems and, therefore, to prevent possible toxic effects and losses of activity.

The simulation of the species distribution in aqueous solution has shown that, for the four ligands, the complexation with copper(II) is complete at pH 7.4 (data not shown). The study of the species distribution is of utmost importance in the evaluation of the SOD-like activity of copper(II) complexes because, since Cu(II) ion is known to be an efficient catalyst of superoxide, its presence would lead to misinterpretation of the results [44]. The species distribution was also calculated for phosphate buffer solutions of the complexes, to consider the possible competition between the phosphate species and the copper(II) complexes. The presence of phosphate did not alter the species in solution. In fact, at physiological pH, the copper in solution was 100% in the form of complexes, both in water and in phosphate buffer.

**Table VI.1 –** Stepwise stability constants (log *K*) [a] and pCu values for copper(II) complexes.

| Equilibrium quotient | L6 | L7 | L8 | L9 |
|---|---|---|---|---|
| [CuL]/[Cu][L] | 20.23(2) [b] | 21.84(4) [c] | 23.31(3) | 20.86(4) |
| [CuHL]/[CuL][H] | - | 3.67(3) [c] | 2.31(4) | 3.59(6) |
| [CuL]/[CuLOH][H] | - | - | 10.06(6) | 11.83(7) |
| **pCu** [d] | 15.30 | 17.05 | 18.49 | 16.27 |

[a] Values in parenthesis are standard deviations on the last significant figure.

[b] $I$ = 0.10 M $KNO_3$; $T$ = 25.0 ºC [37]

[c] $I$ = 0.10 M $N(CH_3)_4NO_3$; $T$ = 25.0 ºC [8]

[d] pCu values calculated for an aqueous solution containing Cu(II) (10 μM) and each ligand (10.5 μM) at pH 7.4. The protonation constants used for the calculations were previously reported for L6 and L7 [8, 37]. For L8 the used values (log units) were: $K_1^H$ = 9.616(8), $K_2^H$ = 8.67(1), $K_3^H$ = 5.33(2), and $K_4^H$ = 1.4(2). For L9 the following values (log units) were used: $K_1^H$ = 9.71(1), $K_2^H$ = 8.32(3), $K_3^H$ = 5.56(5), and $K_4^H$ = 2.37(8).

Spectroscopic studies were performed in order to characterize the copper(II) environment in the complexes, due to the relevance of this information for the understanding of their SOD-like activities [45]. Spectroscopic visible data ($\lambda_{max}$), as well as the hyperfine coupling constants $A_i$ ($i$ = $x$, $y$ and $z$) and $g$ values for the Cu(II) complexes obtained by the simulation of the spectra [46], are collected in Table VI.2. As mentioned in Chapter 5, EPR parameters may be related to the electronic transitions by the factors derived from the ligand field theory [47, 48]: the $g$ values increase and the $A_z$ value decreases as the planar ligand field becomes weaker or as the axial ligand field becomes stronger and this occurs with the simultaneous red-shift of the d-d absorption bands in the electronic spectra. Hence, spectroscopic data provide information on the degree of distortion of the geometry of a complex.

All copper(II) complexes exhibited broad bands in the visible region, due to the copper d-d transitions (Table VI.2). EPR determinations indicated three different $g$ values, that are characteristic of mononuclear Cu(II) complexes in rhombic symmetry with elongation of the axial bonds and a $d_{x^2-y^2}$ ground state. Elongated rhombic-

octahedral, rhombic square-coplanar or distorted square pyramidal stereochemistries would be consistent with these data, but trigonal-bipyramidal or tetragonal geometries involving compression of axial bonds should be excluded [49-51].

**Table VI.2 -** Spectroscopic data for the $Cu^{2+}$ complexes of L6-L9.

| Complex | Visible band | | EPR parameters | | | | | | |
|---|---|---|---|---|---|---|---|---|---|
| | $\lambda_{max}$/nm ($\varepsilon_{molar}$/ $dm^3$ $mol^{-1}$ $cm^{-1}$) | | $A_i \times 10^{-4}$ $cm^{-1}$; $g_{\|\|}/A_{\|\|} \times$ cm | | | | | | |
| | | | $g_x$ | $g_y$ | $g_z$ | $A_x$ | $A_y$ | $A_z$ | $g_{\|\|}/A_{\|\|}$* |
| CuL6 [37] | 550 (119) | | 2.039 | 2.080 | 2.201 | 4.9 | 14.7 | 195.9 | 112 |
| CuL7 [8] | 645 (1560) | A | 2.050 | 2.066 | 2.243 | 2.2 | 17.6 | 192.1 | 117 |
| | | B | 2.229 | 2.110 | 2.010 | 142.5 | 12.1 | 5.8 | 3466 |
| CuL8 | 610 (150) | | 2.035 | 2.070 | 2.210 | 26.9 | 40.0 | 170.6 | 130 |
| CuL9 | 646 (143) | | 2.038 | 2.077 | 2.222 | 23.2 | 33.5 | 163.8 | 136 |

* Considering $g_z$ as $g_{||}$ and $A_z$ as $A_{||}$.

The redox behaviour of CuL8 and CuL9 was investigated by cyclic voltammetry. Since under similar experimental conditions the free ligands revealed no electrochemical activity within the scanned potential window, the redox processes are assigned to the metal centers only. The electrochemical data obtained for the copper(II) complexes are shown in Table VI.3. The complexes exhibited analogous electrochemical behaviour showing a single quasi-reversible one-electron transfer reduction process at half wave potential values, $E_{1/2}$, (*vs*. Ag/AgCl) of –711 mV ($E_{pa}$-$E_{pc}$= 76 mV) and –609 mV ($E_{pa}$–$E_{pc}$= 80 mV), respectively, that can be assigned to the $Cu^{II}/Cu^{I}$ couple. Upon repetitive cycling the potential scan, the voltammetric response remained essentially unchanged. This feature indicates that the initial copper complexes are regenerated during the potential scan. This reversibility is important when a SOD-like activity is sought, since it means that the complexes may be able to act as catalytic

antioxidants rather than stoichiometric scavengers. Despite the redox potentials of CuL8 and CuL9 are not within the optimal range of values reported for SODm, other authors have referred that the redox potentials of the copper(II) complexes are not essentially associated with their SOD activities [3, 45]. Furthermore, other electroactive species are present in biological milieus, influencing the cellular redox processes. CuL9 yielded a $E_{1/2}$ value that is shifted to less negative (easier reduction to Cu(I)) than the corresponding value observed for CuL8. This difference can be rationalized in terms of flexibility and the size of the coordination cavity in the complexes, and the geometric requirements and the size of the metal ion in different oxidation states. The reduction of Cu(II) to Cu(I) involves a drastic increase in the metal radius and a configuration change from square planar to tetrahedral. Obviously, the larger and more flexible 16-membered coordination cavity in L9, compared with the 15-membered one in L8, tends to stabilize the copper(I) complex.

**Table VI.3 -** Cyclic voltammetric data for the copper(II) complexes of L8 and L9[a]

| Complex | $E_{pc}$/mV | $E_{pa}$/mV | $\Delta E_p$/mV | $E_{1/2}$/mV |
|---|---|---|---|---|
| CuL8 | -749 | -673 | 76 | -711 |
| CuL9 | -649 | -569 | 80 | -609 |

[a] Scan rate = 100 mV $s^{-1}$. $E_{1/2}$ values (*vs.* Ag/AgCl) were taken as the averages of the anodic peak potentials ($E_{pa}$) and the cathodic peak potentials ($E_{pc}$). $\Delta E_p = \left| E_{pa} - E_{pc} \right|$.

The superoxide scavenging activity of the four macrocyclic copper(II) complexes was assessed using two different methods: the NBT reduction and the DHE oxidation. The results obtained in these assays are depicted in Fig. 6.5. The $IC_{50}$ values calculated for the complexes are presented in Table VI.4.

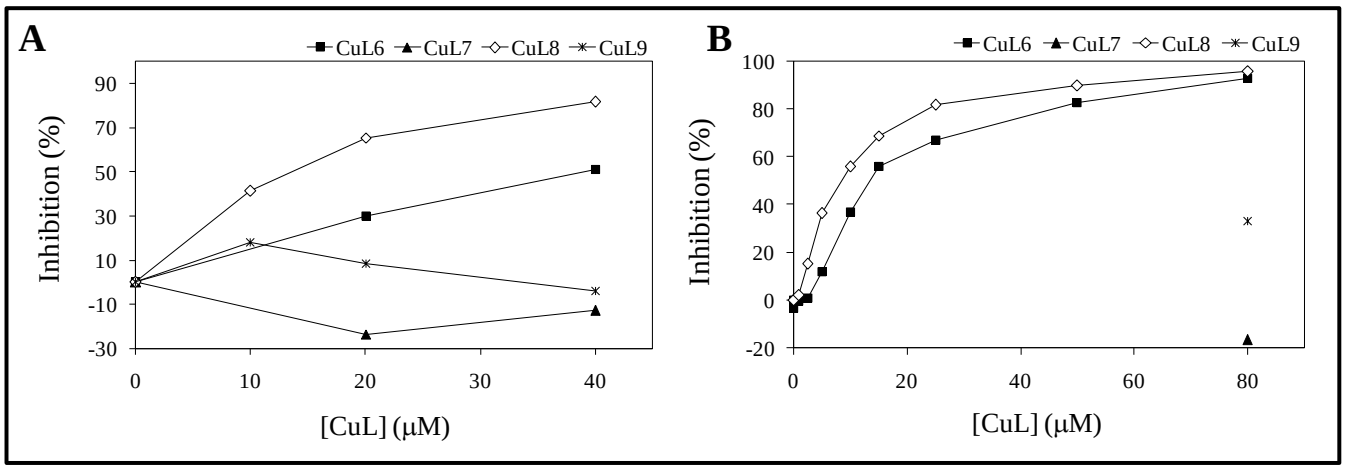


**Fig. 6.5** –Effect of the macrocyclic copper(II) complexes CuL6-CuL9 on the inhibition of NBT reduction (A) and DHE oxidation (B) by the XXO generated superoxide.

**Table VI.4 -** Superoxide scavenging activity for the copper(II) compounds and native Cu,Zn-SOD.

| **Compound** | **$IC_{50}$ (μM)** | |
|---|---|---|
| | **NBT assay** | **DHE assay** |
| CuL6 | 38.07 | 13.46 |
| CuL7 | N.D. | N.D. |
| CuL8 | 14.41 | 6.56 |
| CuL9 | N.D. | N.D. |
| $Cu(NO_3)_2$ | 0.28 | 0.11 |
| Cu,Zn-SOD | 0.017 | 0.001 |

N.D., Not Determined

Two out of four complexes (CuL6 and CuL8) have shown an effective superoxide scavenging effect. In agreement to the results of Chapter 5, the $IC_{50}$ values obtained using both assays were correlated, being the values found using the NBT assay approximately 3-fold higher than those obtained with the DHE assay.

Some copper(II) complexes of 14-membered pyridine-containing macrocycles were previously tested for the SOD-like activity by Autzen *et al* [3]. However, those compounds did not show remarkable activities. In this Chapter, other two 14-membered pyridine-containing macrocyclic copper(II) complexes were studied for their $O_2^{\bullet-}$ scavenging activity. It has been reported that non-coordinating *n*-alkyl pendant arms may participate in various equilibria and may have practical applications on the modulation of the hydrophobic properties, metal selectivity and redox properties [1, 10, 11]. Furthermore, the alkylation on secondary amino groups of a 14-membered tetraaza macrocyclic copper(II) complex was previously shown to made the reduction to Cu(I) easier [11]. The study of CuL6 aimed to test whether the *N*-methylation of Py[14]ane$N_4$ could enhance the activity of the correspondent copper(II) complex. CuL6 has indeed shown $O_2^{\bullet-}$ scavenging activity, having an $IC_{50}$ value in the micromolar range. However, when the production of uric acid by the XXO system was assayed in the presence of CuL6, an inhibitory effect was observed. In fact, CuL6 reduced the production of uric acid in about 30% at t = 180 sec, although at t = 290 sec there was not a statistically significant inhibitory effect. The moderate decrease in urate production by CuL6 was, however, far from being comparable to the exceedingly efficacy on the extent of the inhibition of NBT reduction seen in Fig. 6.5. CuL6 can thus be classified as a mild superoxide scavenger. The EPR data of this complex (Table VI.2) indicate a square-planar structure that does not favour SOD-like activity. Also the distortion factor ($g_{||}/A_{||}$) of CuL6 (112 cm) is far from the value reported for the active center of the native Cu,Zn-SOD (162 cm) [52], what can contribute to the mild $O_2^{\bullet-}$ scavenging activity exhibited by this complex.

Another modification on the Py[14]ane$N_4$ ligand studied in the present Chapter was the introduction of carboxymethyl groups in the *N* atoms. The *N*-functionalization of aza-macrocycles with coordinating groups may change the geometry of the complex and its redox properties [9]. In Chapter 5, the functionalization of CuL3 with $CH_2COOH$ pendant arms resulted in a complex (CuL4) more efficient in terms of superoxide scavenging activity (lower $IC_{50}$ value). However, in this Chapter, no scavenging effect was detected for CuL7 neither using the NBT assay nor by the DHE method. The EPR spectrum of CuL7 presents two isomers for this complex. The data of the A isomer is consistent with elongated rhombic octahedral or distorted square-based pyramidal stereochemistries. The B isomer is typical of either trigonal-bipyramidal,

tetragonal or square pyramidal axially compressed stereochemistries. For both isomers, the empirical distortion factor $g_{\|}/A_{\|}$ is far from that reported for Cu,Zn-SOD. This structural difference may contribute to the absence of SOD-like activity of this complex. The geometry of CuL7 was previously proposed by Costa *et al* [53]. In this complex, Cu(II) is encapsulated by the macrocycle in a distorted octahedral environment and the four *N* atoms of the tetraaza ring define the equatorial plan. The six-coordination is completed with two oxygen atoms of the appended carboxymethyl arms, one adjacent to the pyridine ring and the other opposite to the pyridine moiety. The remaining carboxymethyl group is further away from the metal center. It is possible that the geometry of this complex does not provide the flexibility of the copper(II) arrangement that is required for the $O_2^{\bullet-}$ dismutation reaction [7, 44]. Furthermore, the presence of three carboxymethyl arms may cause steric hindrance and electrostatic repulsion to the approach of superoxide anion.

The complex of L8 with Mn(II) was previously studied by Riley *et al* [54] and has shown an effective SOD-like activity. However, the thermodynamic stability of the Cu(II) complex is much higher than that of the Mn(II) complex (log $K_{MnL}$ = 11.64 [54] *vs* log $K_{CuL}$ = 23.31). In the present work CuL8 has shown the highest $O_2^{\bullet-}$ scavenging activity, presenting an $IC_{50}$ value in the low micromolar range (Fig. 6.5, Table VI.4). By monitoring the production of uric acid, the possibility of inhibition of xanthine oxidase by CuL8 was excluded (data not shown). The EPR parameters of this complex (Table VI.2) are consistent with a distorted square pyramidal five-coordinated geometry, as also observed in the solid state by crystallography (data not shown). The slightly distorted structure of CuL8, along with its quasi-reversible redox behavior (Table VI.3) may justify the $O_2^{\bullet-}$ scavenging activity observed.

As described above, CuL8 and CuL9 are quite similar in terms of chemical properties. However, in a previous study performed by Kimura *et al* [5], no SOD-like activity was found for CuL9. In the present Chapter, the superoxide scavenging activities of CuL8 and CuL9 were evaluated under the same circumstances. In fact, no activity was found for CuL9 using the NBT assay (Fig. 6.5A). Using the DHE method, only a slight effect (< 40% of inhibition) was observed for CuL9 at 80 μM (Fig. 6.5B). The redox behaviour of CuL9, as well as the proposed complex geometry, is close to that of CuL8. Since the difference of the two complexes remains in the extra methylenic

group in the backbone of L9, it seems possible that this group causes steric hindrance, blocking the access of superoxide anion to the Cu(II) center.

*6.3.2. Cytotoxicity profile of the complexes*

The cytotoxicity pattern of the four macrocycles was studied using the MTT assay, in three different cell lines. One of them was the V79 cell line, which was also used in the previous Chapters and is widely used in cytotoxicity evaluations. The MCF7 cells, described in Chapter 5, were used as a breast cancer cell line. The MCF 10A cell line (human breast epithelial cells) was used as a model of non-tumoral mammary cells. The complexes were evaluated in concentrations from 1 to 100 μM, which are in the same range of those tested in the SOD-like assays.

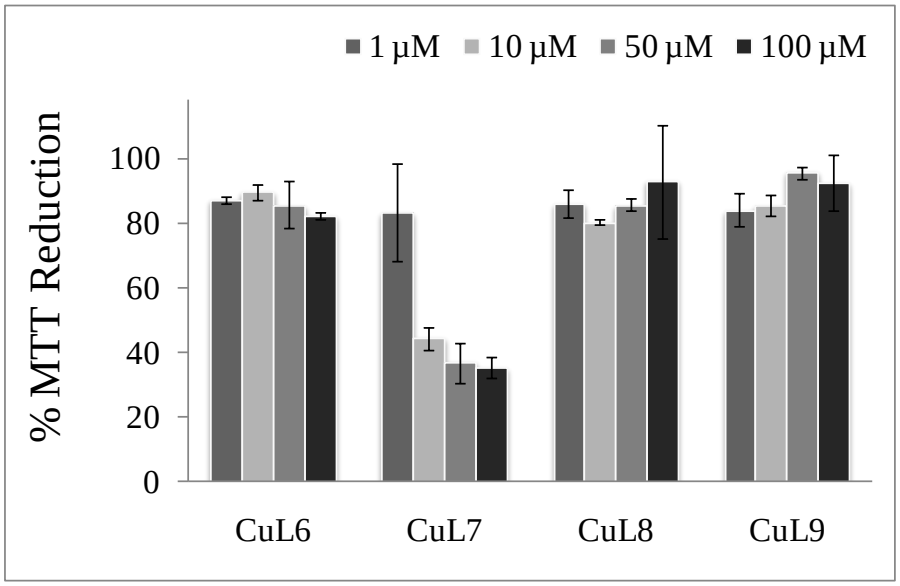


**Fig. 6.6** – Cell viability of V79 cells treated with different concentrations of the complexes CuL6-CuL9, as evaluated by the MTT assay. Values (mean ± SD) are percentages relative to non-treated control cells (100%).

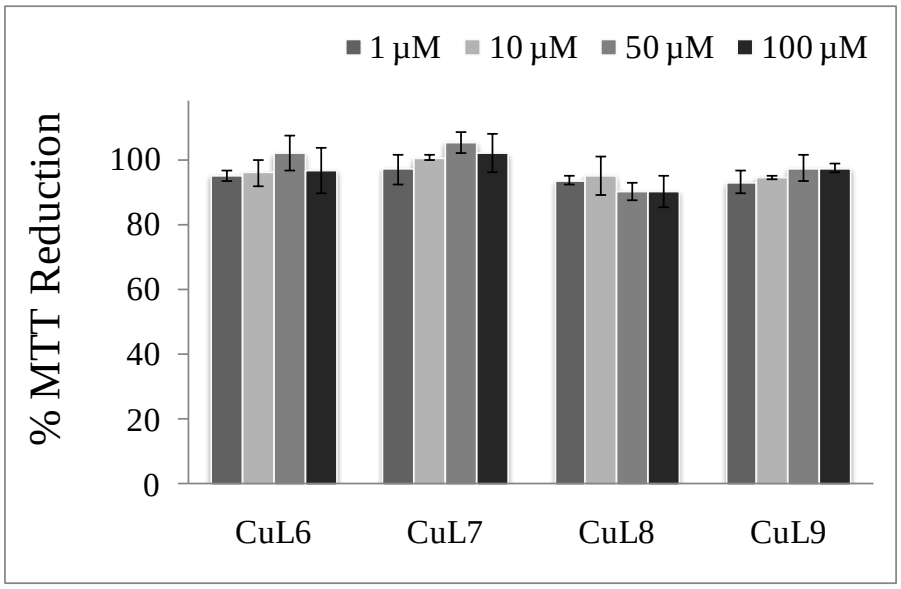


**Fig. 6.7** – Cell viability of MCF10A cells treated with different concentrations of the complexes CuL6-CuL9, as evaluated by the MTT assay. Values (mean ± SD) are percentages relative to non-treated control cells (100%).

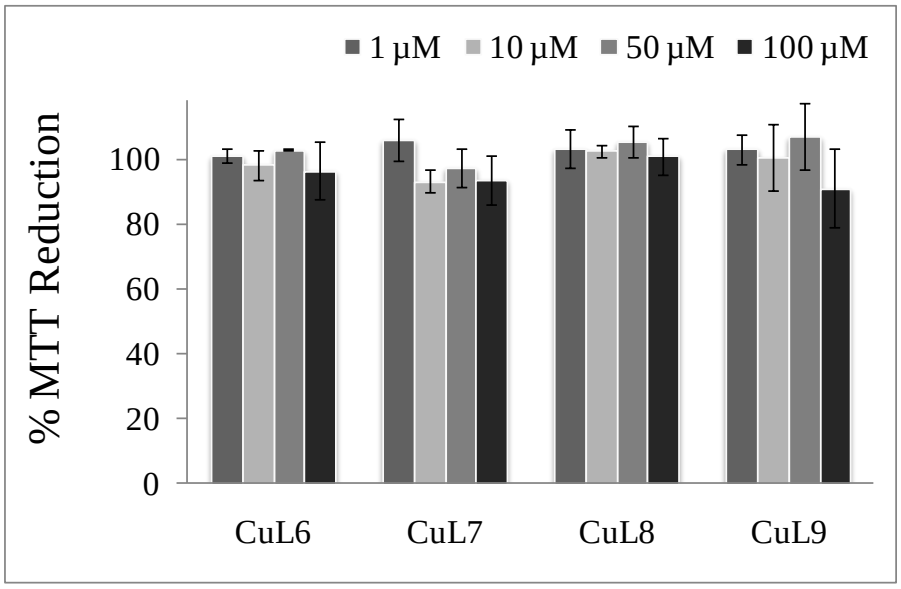


**Fig. 6.8** – Cell viability of MCF7 cells treated with different concentrations of the complexes CuL6-CuL9, as evaluated by the MTT assay. Values (mean ± SD) are percentages relative to non-treated control cells (100%).

As can be seen in Fig. 6.6, the complexes CuL6, CuL8 and CuL9 did not show marked cytotoxic effects up to 100 µM in V79 cells. Conversely, CuL7 exhibited

notorious toxic effects, decreasing the % MTT reduction to ~35% of that of control cells at a concentration of 100 μM. In MCF10A and MCF7 cells (Fig. 6.7 and 6.8), the four complexes exhibited only slight decreases in cell survival (up to 10% loss of viability). The differences observed for CuL7 may be ascribed to a different sensitivity between V79 fibroblasts and mammary cells. Differences in the cellular uptake of this complex may also be involved, since V79 cells were previously reported to have endocytic activity [55]. Based on these results, toxicity does not seem to be a limiting factor of the biological use of the macrocyclic complexes CuL6, CuL8 and CuL9.

### *6.3.3. Studies on CuL8 as a potential antioxidant*

From the aforementioned studies, CuL8 was selected to be further evaluated in cell-based experiments. This complex gathers a number of properties that a SODm should present: water solubility, thermodynamic stability (even in the acid region), quasi-reversible redox behavior, an effective SOD-like activity with low $IC_{50}$, and the absence of considerable cytotoxicity. The antioxidant properties of CuL8 were therefore evaluated in the models XXO and TBHP, validated in Chapter 3. The obtained results are depicted in Fig. 6.9.

As depicted in Fig. 6.9A, when V79 cells were exposed to the $O_2^{\bullet-}$ generator XXO, a significant decrease in cell survival was observed ($P < 0.05$). The addition of CuL8 (up to 100 μM) did not considerably alter the viability of XXO-exposed cells. The exposure of V79 cells to the short chain hydroperoxide TBHP (100 μM) also resulted in a considerable decrease in cell viability (Fig. 6.9B). CuL8 did not afford protection to TBHP-treated cells. On the contrary, a slight and not statistically significant pro-oxidant effect was observed in V79 cells simultaneously exposed to TBHP and to the highest concentrations of CuL8 (Fig. 6.9B). Although CuL8 is an efficient $O_2^{\bullet-}$ scavenger *in vitro*, it did not protect cells exposed to the oxidants XXO and TBHP. The lack of antioxidant activity in these cell-based experiments may be ascribed to a possible insufficient intracellular concentration of the complex or to an inadequate catalytic rate of the reaction between the CuL8 and $O_2^{\bullet-}$.

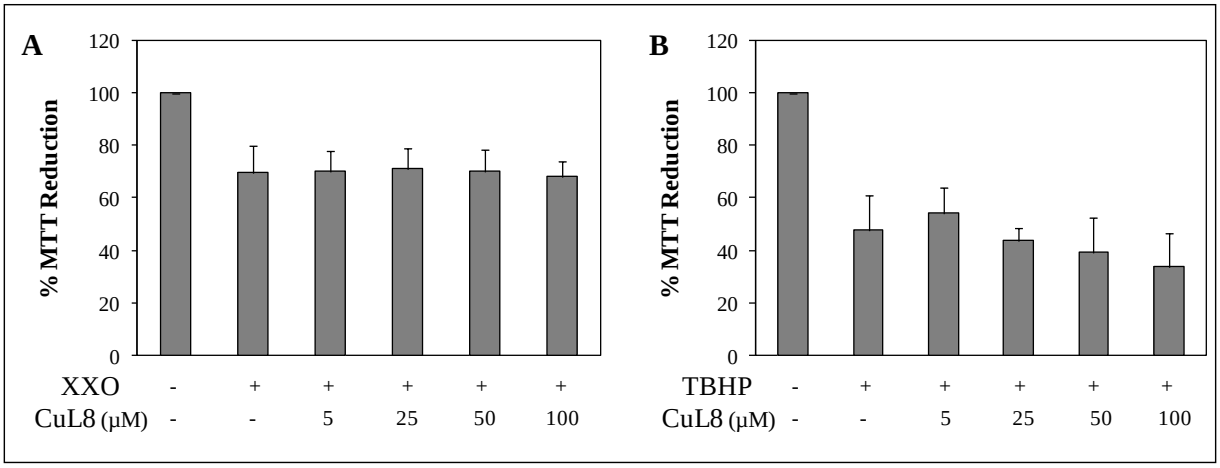


**Fig. 6.9 -** Effect of CuL8 on the cytotoxicity induced by xanthine (240 μM) plus xanthine oxidase (20 U/L) (A) or by TBHP (100 μM) (B), in V79 cells. Cells were incubated with increasing concentrations of the complex in the presence of the oxidants for 24 h, and then submitted to the MTT assay.

*6.3.4. Studies on CuL8 as a potential anticancer agent*

As mentioned in the Introduction section, SODm may be useful in chemotherapy, either protecting non-tumoral tissues from the oxidative damage induced by anticancer agents, or potentiating its toxic effects in tumoral cells. In this later case, the increase in intracellular $H_2O_2$ seems to be a critical factor [12, 18]. If the complex reacts with $H_2O_2$ originating $HO^{\bullet}$, this could be advantageous to induce cancer cells' death [12, 27]. In view of this, the possibility of hydroxyl radical generation by CuL8 was evaluated using the DNA strand break analysis. This assay was validated using a set of controls as shown in Chapter 5 (Fig. 5.17). The results obtained for CuL8 are depicted in Fig. 6.10.

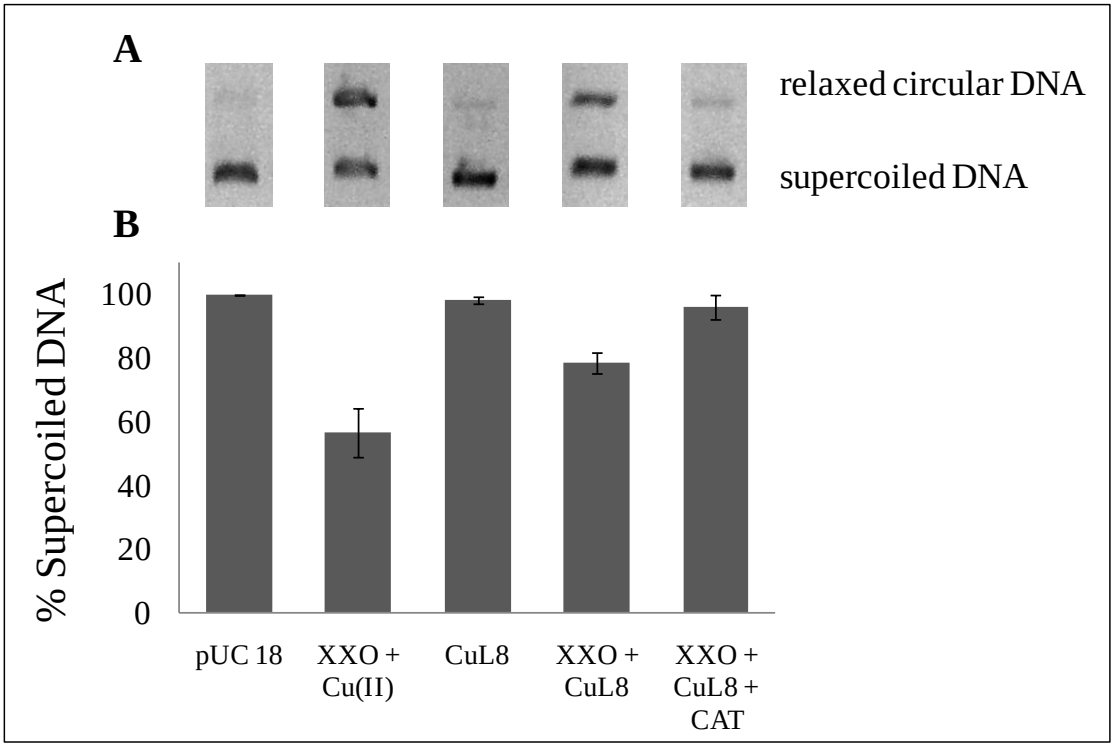


**Fig. 6.10 –** Evaluation of $HO^{\bullet}$ generation by CuL8, by the DNA strand break analysis. (A) Representative lanes of one electrophoretic separation showing the cleavages of pUC18. (B) Percentages (mean ± SD) of DNA in the supercoiled form. Two independent experiments were performed, each comprising three lanes per sample. (XXO, xanthine-xanthine oxidase; CAT, catalase).

As can be seen in Fig. 6.10, CuL8 *per se* does not attack DNA. Although some copper(II) complexes have chemical nuclease activity [56], this is not the case of CuL8. However, in the presence of superoxide anion generated by XXO, CuL8 led to a considerable decrease in the supercoiled DNA and an increase in the relaxed circular form (Fig. 6.10). This data show that CuL8 is devoid of catalase-like activity. Moreover, CuL8 reacts with $H_2O_2$ to generate hydroxyl radical, which attacks DNA. The reversion of the DNA cleavage in the presence of CAT confirms that $H_2O_2$ is an intermediate in the process. In addition, this reversion suggests that, in the cellular environment, the production of $HO^{\bullet}$ by CuL8 could be relevant only if the cellular antioxidant defences are not enough to degrade the intermediate $H_2O_2$. This could be an important approach to induce selective cell death between cancer and normal cells, since cancer cells usually have lower antioxidant defences [17].

To have some insight on the potential application of CuL8 in chemotherapy, studies were performed in human mammary cell lines MCF7 and MCF10A, which represent respectively tumor and non-tumor cells. These cell lines vary in their inherent antioxidant defences. Weydert *et al* [22] have reported that MCF-7 cells have lower total SOD and MnSOD activities than MCF10A. Catalase activities are similar between the two cell lines, but MCF10A contains higher activity of GPx. In terms of total antioxidant capacity, MCF-7 cells present a much lower level than MCF-10A cells [20]. This pair of cell lines provides thus a useful model to anticipate the effects of CuL8 in tumoral and non-tumoral breast tissue. The effects of CuL8 on the modulation of Dox-induced toxicity were therefore evaluated in MCF10A and MCF7 cells, and the results are shown in Fig. 6.11.

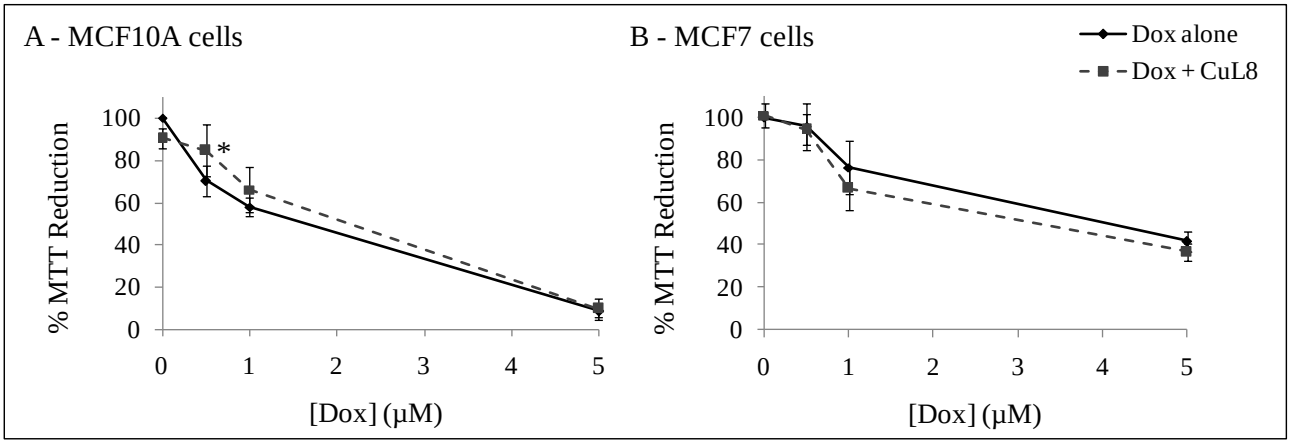


**Fig. 6.11 –** Effect of CuL8 on the cell viability of human mammary cells treated with doxorubicin (Dox), as evaluated by the MTT assay. Cells were incubated with increasing concentrations of Dox in the absence (solid line) or presence (dashed line) of 100 µM CuL8. (A) Non-tumoral MCF10A cells. (B) Breast carcinoma MCF7 cells. (* $P < 0.05$, when compared with Dox-treated cells without CuL8).

As depicted in Fig. 6.11A, the addition of CuL8 to Dox-treated MCF10A cells resulted in a small increase in cell viability. This protective effect was statistically significant ($P < 0.05$) for the concentration of 0.5 µM of Dox, in which the presence of CuL8 led to an increase in cell viability of ~14%. On the other hand, CuL8 potentiated the toxicity of Dox in MCF7 cancer cells (Fig. 6.11B). The % viabilities of cells co-

treated with CuL8 and Dox were consistently lower than those exhibited by cells treated only with Dox, although these differences were not statistically significant.

Since CuL8 has shown a trend to protect non-tumoral breast cells form Dox-toxicity, while it slightly potentiated the anticancer drug in tumoral cells, a second cytotoxic drug was studied. The platinum-based drug oxaliplatin was chosen, since this drug was previously shown to increase intracellular ROS, namely superoxide anion [12, 19]. The effects of CuL8 on the modulation of oxaliplatin were also evaluated in MCF10A and MCF7 cells, as shown in Fig. 6.12.

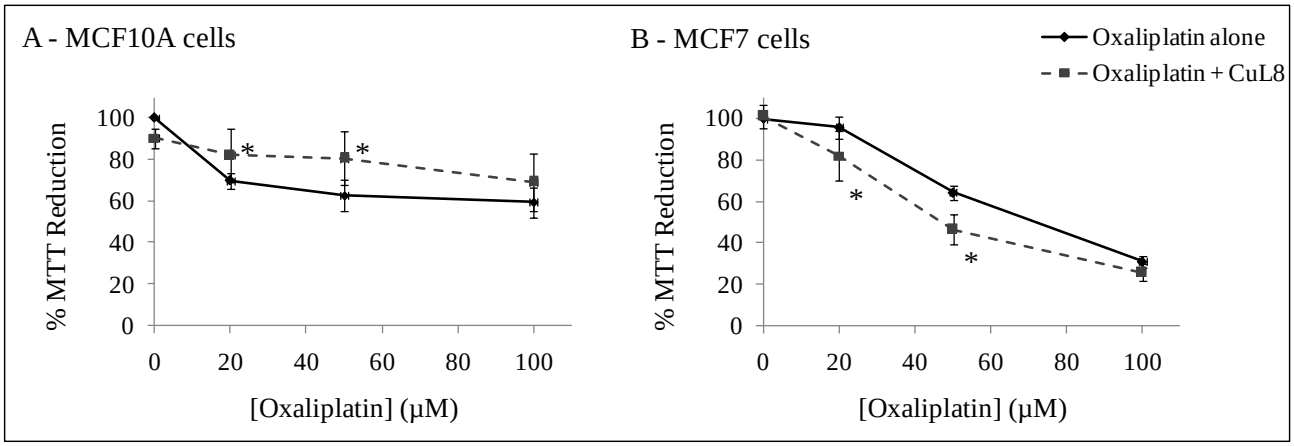


**Fig. 6.12 –** Effect of CuL8 on the cell viability of human mammary cells treated with oxaliplatin, as evaluated by the MTT assay. Cells were incubated with increasing concentrations of oxaliplatin in the absence (solid line) or presence (dashed line) of 100 µM CuL8. (A) Non-tumoral MCF10A cells. (B) Breast carcinoma MCF7 cells. (* $P < 0.05$, when compared with oxaliplatin-treated cells without CuL8).

In non-tumoral MCF10A cells, CuL8 reduced the cytotoxicity of oxaliplatin (Fig. 6.12A). A protective effect was observed for all concentrations of oxaliplatin tested and was statistically significant ($P<0.05$) at 20 and 50 µM. A maximum protection was observed for 50 µM of oxaliplatin, where the co-treatment with CuL8 increased the absolute cell viability in ~18%. On the other hand, in MCF7 tumor cells the incubation of oxaliplatin with 100 µM CuL8 resulted in a considerable potentiation of the cytotoxicity of the drug (Fig. 6.12B). This effect was consistent in the three concentrations of oxaliplatin tested and was statistically significant for 20 and 50 µM

($P$<0.05). At these concentrations, decreases in absolute cell viability of 14% and 18%, respectively, were found in the presence of CuL8.

The opposite effects of CuL8 in normal and cancer cells are probably related to the differences in basal concentration of ROS and in antioxidant defenses. In MCF10A cells, CuL8 presented protective effects against Dox and oxaliplatin. Although different mechanisms may be involved in this protection, the results suggest that $O_2^{\bullet-}$ production is involved in the cytotoxicity induced by the drugs. CuL8 may be dismutating $O_2^{\bullet-}$ and the generated $H_2O_2$ should be efficiently degraded by cellular CAT and peroxidases. Since the threshold of toxicity is reached more easily in cancer cells than in non-tumoral cells, a further increase in $H_2O_2$ due to a combined treatment with $O_2^{\bullet-}$-generating drugs and CuL8 can induce differential effects in MCF10A and MCF7 cells. While $H_2O_2$ seems to be efficiently degraded in MCF10A cells, it can accumulate in MCF7 cells. The subsequent reaction of $H_2O_2$ with CuL8 via Fenton reaction may be occurring, originating the highly toxic hydroxyl radical. This radical is known to attack cell biomolecules like DNA, proteins or lipids [57], promoting MCF7 cells' death.

### *6.3.5. Conclusion*

In the present Chapter four pyridine-containing macrocyclic copper(II) complexes were prepared and chemically characterized. These complexes were studied for their superoxide scavenging activity, as well as for their cytotoxicity profile. Among the four complexes, CuL8 was the most active as a superoxide scavenger. In the absence of catalase, CuL8 can also react with the $H_2O_2$ generated in the $O_2^{\bullet-}$ dismutation, leading to $HO^{\bullet}$. Compounds showing SOD-like activity and Fenton-like reaction were previously proposed as a new class of anticancer drugs to induce selective cell death between cancer and normal cells [27]. Our results show that CuL8 can indeed enhance the therapeutic index of Dox and oxaliplatin in mammary cells, by both protecting normal cells and increasing its antitumoral effect in cancer cells. CuL8 is thus a promising compound to be further studied as a chemotherapy sensitizer. Moreover, it can be a lead compound for the design and optimization of bioactive macrocyclic copper(II) complexes.

## 6.4. References


[1] Costamagna, J.; Ferraudi, G.; Matsuhiro, B.; Campos-Vallette, M.; Canales, J.; Villagrán, M.; Vargas, J.; Aguirre, M. J. Complexes of macrocycles with pendant arms as models for biological molecules. *Coord Chem Rev* **196:**125-164; 2000.

[2] Riley, D. P. Functional mimics of superoxide dismutase enzymes as therapeutic agents. *Chem Rev* **99:**2573-2588; 1999.

[3] Autzen, S.; Korth, H.-G.; Boese, R.; de Groot, H.; Sustmann, R. Studies of pyridinyl-containing 14-membered macrocyclic copper(II) complexes. *Eur J Inorg Chem***:**1401-1410; 2003.

[4] Bienvenue, E.; Choua, S.; Lobo-Recio, M.-A.; Marzin, C.; Pacheco, P.; Seta, P.; Tarrago, G. Structure and superoxide dismutase activity of Ru(II), Cu(II), and Mn(II) macrocyclic complexes. *J Inorg Biochem* **57:**157-168; 1995.

[5] Kimura, E.; Sakonaka, A.; Nakamoto, M. Superoxide dismutase activity of macrocyclic polyamine complexes. *Biochim Biophys Acta* **678:**172-179; 1981.

[6] Kimura, E.; Yatsunami, A.; Watanabe, A.; Machida, R.; Koike, T.; Fujioka, H.; Kuramoto, Y.; Sumomogi, M.; Kunimitsu, K.; Yamashita, A. Further studies on superoxide dismutase activities of macrocyclic polyamine complexes of copper(II). *Biochim Biophys Acta* **745:**37-43; 1983.

[7] Gonzalez-Alvarez, M.; Alzuet, G.; Borras, J.; Castillo Agudo, L.; Montejo-Bernardo, J. M.; Garcia-Granda, S. Development of novel copper(II) complexes of benzothiazole- N-sulfonamides as protective agents against superoxide anion. Crystal structures of [Cu( N-2-(4-methylbenzothiazole)benzenesulfonamidate)(2)(py)(2)] and [Cu( N-2-(6-nitrobenzothiazole)naphthalenesulfonamidate)(2)(py)(2)]. *J Biol Inorg Chem* **8:**112-120; 2003.

[8] Costa, J.; Delgado, R.; Drew, M. G. B.; Félix, V. Design of selective macrocyclic ligands for the divalent first-row transition-metal ions. *J Chem Soc Dalton Trans***:**1063 - 1072; 1998.

[9] Elias, H. Kinetics and mechanism of metal complex formation with N,-donor macrocycles of the cyclam type. *Coord Chem Rev* **187:**37-73; 1999.

[10] Lindoy, L. F. Tailoring macrocycles for metal ion binding. *Pure & Appl Chem* **69:**2179-2186; 1997.

[11] Kang, S.-G.; Kim, M.-S.; Choi, J.-S.; Cho, M. H. Synthesis, characterization and properties of new fully *N*-alkylated 14-membered tetraaza macrocycles and their copper(II) complexes. *Polyhedron* **14:**781-786; 1995.

[12] Laurent, A.; Nicco, C.; Chereau, C.; Goulvestre, C.; Alexandre, J.; Alves, A.; Levy, E.; Goldwasser, F.; Panis, Y.; Soubrane, O.; Weill, B.; Batteux, F. Controlling tumor growth by modulating endogenous production of reactive oxygen species. *Cancer Res* **65:**948-956; 2005.

[13] Kaiserova, H.; den Hartog, G. J.; Simunek, T.; Schroterova, L.; Kvasnickova, E.; Bast, A. Iron is not involved in oxidative stress-mediated cytotoxicity of doxorubicin and bleomycin. *Br J Pharmacol* **149:**920-930; 2006.

[14] Oury, T. D.; Thakker, K.; Menache, M.; Chang, L. Y.; Crapo, J. D.; Day, B. J. Attenuation of bleomycin-induced pulmonary fibrosis by a catalytic antioxidant metalloporphyrin. *Am J Respir Cell Mol Biol* **25:**164-169; 2001.

[15] Ramos, D. L.; Oliveira, N. G.; Pingarilho, M.; Gil, O. M.; Fernandes, A. S.; Rueff, J.; Gaspar, J. F. Modulation of doxorubicin genotoxicity in human lymphocytes by GSTs polymorphisms: possible role of *GSTp1* Ile105Val polymorphism. **in preparation**; 2010.

[16] Singal, P. K.; Li, T.; Kumar, D.; Danelisen, I.; Iliskovic, N. Adriamycin-induced heart failure: mechanism and modulation. *Mol Cell Biochem* **207:**77-86; 2000.

[17] Oberley, L. W. Mechanism of the tumor suppressive effect of MnSOD overexpression. *Biomed Pharmacother* **59:**143-148; 2005.

[18] Nicco, C.; Laurent, A.; Chereau, C.; Weill, B.; Batteux, F. Differential modulation of normal and tumor cell proliferation by reactive oxygen species. *Biomed Pharmacother* **59:**169-174; 2005.

[19] Alexandre, J.; Nicco, C.; Chereau, C.; Laurent, A.; Weill, B.; Goldwasser, F.; Batteux, F. Improvement of the therapeutic index of anticancer drugs by the superoxide dismutase mimic mangafodipir. *J Natl Cancer Inst* **98:**236-244; 2006.

[20] Francisco, D. C.; Peddi, P.; Hair, J. M.; Flood, B. A.; Cecil, A. M.; Kalogerinis, P. T.; Sigounas, G.; Georgakilas, A. G. Induction and processing of complex DNA damage in human breast cancer cells MCF-7 and nonmalignant MCF-10A cells. *Free Radic Biol Med* **44:**558-569; 2008.

[21] Li, J. J.; Oberley, L. W.; St Clair, D. K.; Ridnour, L. A.; Oberley, T. D. Phenotypic changes induced in human breast cancer cells by overexpression of manganese-containing superoxide dismutase. *Oncogene* **10:**1989-2000; 1995.

[22] Weydert, C. J.; Waugh, T. A.; Ritchie, J. M.; Iyer, K. S.; Smith, J. L.; Li, L.; Spitz, D. R.; Oberley, L. W. Overexpression of manganese or copper-zinc superoxide dismutase inhibits breast cancer growth. *Free Radic Biol Med* **41:**226-237; 2006.

[23] Berthiaume, J. M.; Wallace, K. B. Adriamycin-induced oxidative mitochondrial cardiotoxicity. *Cell Biol Toxicol* **23:**15-25; 2007.

[24] Minotti, G.; Menna, P.; Salvatorelli, E.; Cairo, G.; Gianni, L. Anthracyclines: molecular advances and pharmacologic developments in antitumor activity and cardiotoxicity. *Pharmacol Rev* **56:**185-229; 2004.

[25] Keizer, H. G.; Pinedo, H. M.; Schuurhuis, G. J.; Joenje, H. Doxorubicin (adriamycin): a critical review of free radical-dependent mechanisms of cytotoxicity. *Pharmacol Ther* **47:**219-231; 1990.

[26] Kiyomiya, K.; Matsuo, S.; Kurebe, M. Differences in intracellular sites of action of Adriamycin in neoplastic and normal differentiated cells. *Cancer Chemother Pharmacol* **47:**51-56; 2001.

[27] Ohse, T.; Nagaoka, S.; Arakawa, Y.; Kawakami, H.; Nakamura, K. Cell death by reactive oxygen species generated from water-soluble cationic metalloporphyrins as superoxide dismutase mimics. *J Inorg Biochem* **85:**201-208; 2001.

[28] Di Francesco, A. M.; Ruggiero, A.; Riccardi, R. Cellular and molecular aspects of drugs of the future: oxaliplatin. *Cell Mol Life Sci* **59:**1914-1927; 2002.

[29] Garufi, C.; Nistico, C.; Brienza, S.; Vaccaro, A.; D'Ottavio, A.; Zappala, A. R.; Aschelter, A. M.; Terzoli, E. Single-agent oxaliplatin in pretreated advanced breast cancer patients: a phase II study. *Ann Oncol* **12:**179-182; 2001.

[30] Caruba, T.; Cottu, P. H.; Madelaine-Chambrin, I.; Espie, M.; Misset, J. L.; Gross-Goupil, M. Gemcitabine-oxaliplatin combination in heavily pretreated metastatic breast cancer: a pilot study on 43 patients. *Breast J* **13:**165-171; 2007.

[31] Zelek, L.; Cottu, P.; Tubiana-Hulin, M.; Vannetzel, J. M.; Chollet, P.; Misset, J. L.; Chouaki, N.; Marty, M.; Gamelin, E.; Culine, S.; Dieras, V.; Mackenzie, S.; Spielmann, M. Phase II study of oxaliplatin and fluorouracil in taxane- and anthracycline-pretreated breast cancer patients. *J Clin Oncol* **20:**2551-2558; 2002.

[32] Delozier, T.; Guastalla, J. P.; Yovine, A.; Levy, C.; Chollet, P.; Mousseau, M.; Delva, R.; Coeffic, D.; Vannetzel, J. M.; Zazzi, E. S.; Brienza, S.; Cvitkovic, E. A phase II study of an oxaliplatin/vinorelbine/5-fluorouracil combination in patients with anthracycline-pretreated and taxane-pretreated metastatic breast cancer. *Anticancer Drugs* **17:**1067-1073; 2006.

[33] Kakolyris, S.; Kalbakis, K.; Potamianou, A.; Malamos, N.; Vamvakas, L.; Christophillakis, C.; Tselepatiotis, E.; Giassas, S.; Mavroudis, D.; Amarantidis, K.; Georgoulias, V. Salvage chemotherapy with gemcitabine and oxaliplatin in heavily pretreated patients with metastatic breast cancer: a multicenter phase II study. *Oncology* **70:**273-279; 2006.

[34] Polyzos, A.; Gogas, H.; Markopoulos, C.; Tsavaris, N.; Papadopoulos, O.; Polyzos, K.; Giannopoulos, A. Salvage chemotherapy with oxaliplatin and capecitabine for breast cancer patients pretreated with anthracyclines and taxanes. *Anticancer Res* **29:**2851-2856; 2009.

[35] Decatris, M. P.; Sundar, S.; O'Byrne, K. J. Platinum-based chemotherapy in metastatic breast cancer: current status. *Cancer Treat Rev* **30:**53-81; 2004.

[36] Kim, S.; Lee, T. J.; Park, J. W.; Kwon, T. K. Overexpression of cFLIPs inhibits oxaliplatin-mediated apoptosis through enhanced XIAP stability and Akt activation in human renal cancer cells. *J Cell Biochem* **105:**971-979; 2008.

[37] Costa, J.; Delgado, R. Metal complexes of macrocyclic ligands containing pyridine. *Inorg Chem* **32:**5257-5265; 1993.

[38] Perrin, D. D.; Armarego, W. L. F. *Purification of Laboratory Chemicals.* Oxford: Pergamon; 1988.

[39] Delgado, R.; Figueira, M. d. C.; Quintino, S. Redox method for the determination of stability constants of some trivalent metal complexes. *Talanta* **45:**451-462 1997.

[40] Gans, P.; Sabatini, A.; Vacca, A. SUPERQUAD: an improved general program for computation of formation constants from potentiometric data. *J Chem Soc, Dalton Trans***:**1195-1200; 1985.

[41] Gans, P.; Sabatini, A.; Vacca, A. Investigation of equilibria in solution. Determination of equilibrium constants with the HYPERQUAD suite of programs. *Talanta* **43:**1739-1753; 1996.

[42] Alderighi, L.; Gans, P.; Ienco, A.; Peters, D.; Sabatini, A.; Vacca, A. Hyperquad simulation and speciation (HySS): a utility program for the investigation of equilibria involving soluble and partially soluble species *Coord Chem Rev* **184:**311-318 1999.

[43] Costa, J.; Delgado, R.; Drew, M. G. B.; Félix, V.; Saint-Maurice, A. A new redox-responsive 14-membered tetraazamacrocycle with ferrocenylmethyl arms as receptor for sensing transition-metal ions. *J Chem Soc, Dalton Trans***:**1907-1916; 2000.

[44] Pogni, R.; Baratto, M. C.; Busi, E.; Basosi, R. EPR and O2.- scavenger activity: Cu(II)-peptide complexes as superoxide dismutase models. *J Inorg Biochem* **73:**157-165; 1999.

[45] Palivan, C. G.; Balasubramanian, V.; Goodman, B. A. Global structure-activity analysis in drug development illustrated for active Cu/Zn superoxide dismutase mimics. *Eur J Inorg Chem***:**4634-4639; 2009.

[46] Neese, F. Diploma thesis. Germany: University of Konstanz; 1993.

[47] Lau, P. W.; Lin, W. C. Electron spin resonance and electronic structure of some metalloporphyrins *J Inorg Nucl Chem* **37:**2389-2398; 1975.

[48] Yokoi, H.; Sai, M.; Isobe, T.; Ohsawa, S. ESR studies of the copper(II) complexes of amino acids. *Bull Chem Soc Jpn* **45:**2189-2195; 1972.

[49] Hathaway, B. J. Copper. *Coord Chem Rev* **52:**87-169; 1983.

[50] Costa, J.; Delgado, R.; Figueira, M. d. C.; Henriques, R. T.; Teixeira, M. Metal complexes of a tetraaza macrocycle with N-carboxymethyl groups as pendant arms. *J Chem Soc, Dalton Trans***:**65-73; 1997.

[51] Styka, M. C.; Smierciak, R. C.; Blinn, E. L.; DeSimone, R. E.; Passariello, J. V. Copper(II) complexes containing a 12-membered macrocyclic ligand. *Inorg Chem* **17:**82-86; 1978.

[52] Müller, J.; Schübl, D.; Maichle-Mössmer, C.; Strähle, J.; Weser, U. Structure-function correlation of Cu(II)-and Cu(I)-di-Schiff-base complexes during the catalysis of superoxide dismutation *J Inorg Biochem* **75:**63-69; 1999.

[53] Costa, J.; Delgado, R.; Drew, M. G. B.; Félix, V.; Henriques, R. T.; Waerenborgh, J. C. Structural characterization of cobalt(III), nickel(II), copper(II) and iron(III) complexes of tetraazamacrocycles with N-carboxymethyl arms. *J Chem Soc, Dalton Trans***:**3253-3265; 1999.

[54] Riley, D. P.; Henke, S. L.; Lennon, P. J.; Weiss, R. H.; Neumann, W. L.; Willie J. Rivers, J.; Aston, K. W.; Sample, K. R.; Rahman, H.; Ling, C.-S.; Shieh, J.-J.; Busch, D. H.; Szulbinski, W. Synthesis, characterization, and stability of manganese(II) C-substituted 1,4,7,10,13-pentaazacyclopentadecane complexes exhibiting superoxide dismutase activity *Inorg Chem* **35:**5213-5231; 1996.

[55] Muller, L.; Kikuchi, Y.; Probst, G.; Schechtman, L.; Shimada, H.; Sofuni, T.; Tweats, D. ICH-harmonised guidances on genotoxicity testing of pharmaceuticals: evolution, reasoning and impact. *Mutat Res* **436:**195-225; 1999.

[56] Liu, J.; Zhang, H.; Chen, C.; Deng, H.; Lu, T.; Ji, L. Interaction of macrocyclic copper(II) complexes with calf thymus DNA: effects of the side chains of the ligands on the DNA-binding behaviors. *Dalton Trans***:**114-119; 2003.

[57] Halliwell, B.; Gutterdige, J. M. C. *Free Radicals in Biology and Medicine.* New York: Oxford University Press; 2007.

# Chapter 7

## CONCLUDING REMARKS AND FUTURE PROSPECTS

Free radical toxicology is a multidisciplinary field that underwent a remarkable surge in interest during the past three decades, driven by the flood of new data associating ROS with the mechanisms of toxicity of several xenobiotics, as well as with an ever-expanding list of pathological processes. Superoxide anion is known to be implicated in tissue injury and different inflammation processes. By catalyzing the conversion of $O_2^{\bullet-}$ to $H_2O_2$ and $O_2$, SOD enzymes represent the first line of defense against the harmful effects of $O_2^{\bullet-}$. Although preclinical and clinical studies have demonstrated a beneficial role for SOD in a variety of pathological conditions, the clinical use of the native enzyme has several drawbacks, as mentioned in Chapter 1.

Synthetic SOD mimetics with drug-like properties have thus emerged as pharmaceutical candidates affording a new and promising approach to treat a variety of diseases in which superoxide plays a deleterious role. Moreover, these compounds are useful research tools to understand the mechanisms of action of toxic compounds, namely to establish whether oxidative stress is involved. A number of researchers and companies have been pursuing the development of compounds with SOD-like activity in recent years. The relevance of this emergent field is also revealed by the increasingly number of publications in the last few years. Complexes of transition metal ions, namely complexes of Mn(II), Mn(III), Cu(II) and Fe(III), have shown notable SODm activities. Among the metal containing SODm more extensively studied are manganese macrocyclic complexes (manganese(III) porphyrins and manganese(II) cyclic polyamines), manganese(III) salens, and copper(II) macrocyclic complexes. This thesis aims to contribute to the development of the SODm field, especially in two classes of macrocyclic complexes: the MnPs and the macrocyclic copper(II) complexes.

The choice of studying MnPs was based on the fact that this class contains the most stable and active SODm developed so far. As described in Chapter 1, several studies have been performed on MnPs, showing remarkable protective effects in a variety of oxidative stress models. However, a thorough knowledge on the effects of MnPs at the cellular level is still lacking. Three MnPs were therefore studied in order to contribute to fill this gap.

In this work, studies on antioxidant protection were performed using the systems XXO, TBHP and Dox as oxidative stress inducers. This strategic approach based on different types of oxidants was relevant because these systems vary in terms of the ROS

involved and in the site of formation of those species, being therefore somehow representative of different pathological and toxicological conditions. Increased levels of extracellular $O_2^{\bullet-}$, along with a reduction in EC-SOD expression, have been reported in a variety of pathological conditions. An imbalance of extracellular $O_2^{\bullet-}$/EC-SOD in the cerebral spinal fluid have been reported in traumatic brain injury, cognitive function impairment, and cellular injury following cerebral ischemia. Increased production of $O_2^{\bullet-}$ and decreased EC-SOD activity in vascular spaces were found in atherosclerosis, hypertension, and myocardial infarct. Accumulation of $O_2^{\bullet-}$ in the synovial fluid is implicated in inflammatory joint diseases. Also, a disequilibrium between $O_2^{\bullet-}$ and EC-SOD in pulmonary extracellular spaces seems to be involved in acute lung injury and bleomycin-induced pulmonary fibrosis. The clinical relevance of extracellular $O_2^{\bullet-}$ justifies the choice of an extracellular $O_2^{\bullet-}$ generator, such as the XXO system. The protective effects observed with MnTM-4-PyP against XXO-induced toxicity suggest that this MnP may have a therapeutic role in the aforementioned disorders.

Many studies carried out in this thesis used TBHP as an oxidative stress model. This short chain analogue of lipid hydroperoxides is a convenient model of acute oxidative stress, which injuries cells by different mechanisms including lipid peroxidation, free radicals generation, and glutathione depletion. The protective effects of the three studied MnPs, and in a much lesser extent of CuL3, against this peroxide, suggest a potential role of these compounds in pathological conditions in which lipid peroxidation is involved. In fact, lipid peroxides have been increasingly shown to be associated with inflammation, being implicated in a variety of human diseases such as Alzheimer disease, chronic obstructive pulmonary disease, spongiform encephalopathies, thalassaemia, sickle-cell anemia, ageing, and carcinogenesis processes. Furthermore, lipid peroxidation is an important mechanism that contributes to the toxicity of a number of xenobiotics (e.g. carbon tetrachloride, aniline, asbestos fibres, gentamicin, and nickel).

The anticancer drug Dox was used as a third oxidative stress inducer. The mechanisms of cytotoxicity of Dox are very complex and include, among others, hindering of DNA synthesis and ROS generation. Dox is a $O_2^{\bullet-}$ generator and was chosen mainly due to its clinical relevance. In fact, Dox is commonly used to treat a variety of solid tumors and hematological malignancies. However, the occurrence of

severe cardiotoxic effects, which are mostly ascribed to oxidative stress phenomena, is a major limitation of the clinical use of Dox.

V79 cells represent a well-established mammalian fibroblast cell line widely used in antioxidant research, as shown by the large number of studies published in the field that use this cell model. In the present work, V79 cells also showed to be a convenient model to assess antioxidant protection against XXO and TBHP. Although these cells can also be used to evaluate the role of SODm against Dox-induced damage, due to the cell specificity of Dox cardiotoxicity, cell type limitations can not be ruled out. In fact, the contribution of the different mechanisms of toxicity of Dox depends largely on the cell type and has not yet been completely established for V79 cells. Hence, it was not possible to identify whether the absence of considerable protection by MnTM-4-PyP is ascribed to an insufficient antioxidant activity of this MnP, or to the possibility that $O_2^{\bullet-}$ generation is not the limiting mechanism for Dox toxicity in V79 cells. To clarify this issue, and to better mimic the clinical pitfalls of Dox, future studies should be performed in cardiomyocytes. The role of oxidative damage inflicted by Dox in these cells is well recognized, what makes cardiomyocytes a more suitable model to evaluate the potential protective role of SODm against Dox-induced cardiotoxicity.

The endpoints used in the studies of antioxidant protection were adequate to give more insights on the cellular effects of the MnPs. Two mechanistically different methods were used to evaluate cell viability. The assessment of the intracellular levels of $O_2^{\bullet-}$ was useful to give information on whether the results were related to the $O_2^{\bullet-}$ scavenging activity of the compounds. In what concerns to the MI analysis, MnTM-4-PyP did not counteract the cell cycle arrest induced by the oxidants, indicating that the effects of this recognized SODm are not observed at the cell division level. Therefore, the MI analysis was not included in the subsequent Chapters of this thesis.

The three MnPs were studied in TBHP-treated V79 cells. As expected, in the cell viability assays the *ortho*-substituted MnPs exhibited notorious protective effects with statistical significance at lower concentrations than MnTM-4-PyP. In cells treated with high concentrations of TBHP (1 and 2 mM), the *ortho*-substituted MnPs also revealed higher potency in decreasing the intracellular $O_2^{\bullet-}$ levels than the *para* analogue. These differences may be ascribed to the higher antioxidant potency of the *ortho*-substituted MnPs. The two *ortho* analogues, MnTE-2-PyP and MnTnHex-2-PyP,

possess identical antioxidant potencies. Since MnTnHex-2-PyP is more lipophilic and hence more prone to enter the cell and the mitochondria, it was expected to be more efficient than the ethyl analogue at lower concentrations. However, the MnPs presented comparable protective effects in the cell viability assays, being MnTE-2-PyP slightly more effective. It is possible that, despite the higher lipophilicity of MnTnHex-2-PyP, both MnPs have been uptaken by V79 cells in a similar way due to the endocytic activity of these cells. Other hypothesis is that the protective effects occurred in extracellular millieu, plasma membrane or cytosolic space, rather than in mitochondria.

Since thiol homeostasis determines critical aspects of cell function and response, the effects of the MnPs on the glutathione status were evaluated. The three MnPs have shown a remarkable capacity to abrogate the GSHt depletion in TBHP-treated cells, what can be very relevant in therapeutics. Glutathione deficiencies have been documented in many disorders, namely neurodegenerative conditions (e.g. Parkinson's disease) and respiratory diseases (e.g. chronic obstructive pulmonary disease, idiopathic pulmonary fibrosis, acute respiratory distress syndrome, asthma). Moreover, glutathione plays a major role in the removal and detoxification of toxicants and carcinogens. The reasons underlying the notorious increase in GSHt in cells simultaneously exposed to TBHP and MnPs should be explored in futures studies. The observed increases may be related, at least partially, to an enhancement of the *de novo* GSH synthesis. To assess this hypothesis, studies on a possible stimulation of the expression and activity of γ-GCS, the rate-limiting enzyme in glutathione synthesis, should be performed. MnPs may also play a role in providing NADPH to the cell, assuring the function of glutathione reductase. This would explain the reduction of GSSG back to GSH and the prevention of GSSG release from the cell. The potential effect of MnPs on the activity of the enzymes that provide NADPH to the cell, as well as in the cellular pool of this cofactor, should also be evaluated.

The results obtained in this thesis provide a better comprehension of the cellular effects of the MnPs. However, there is still very limited data on the protective effects of these compounds at the genome level. Previous studies have pointed out a possible application of *ortho*-substituted MnPs in cancer therapy, as radiation protectors. Our next step in terms of MnPs research will focus the role of MnTE-2-PyP and MnTnHex-2-PyP on the protection of human lymphocytes from radiation-induced

genotoxicity. These studies are already ongoing. Human lymphocytes from healthy donors have been submitted to low LET radiation ($^{60}$Co-γ rays), in the presence or absence of the MnPs under study, and genotoxicity is being evaluated using the Cytokinesis-Blocked Micronucleus assay. These studies will provide data on the usefulness of MnPs as radioprotectors, and will give additional information on the genotoxicity of the MnPs *per se*, which is an issue of utmost importance since these SODm have high therapeutical potential.

The present thesis was also devoted to the development of macrocyclic copper(II) complexes. Most of the Cu(II) compounds developed so far are not thermodynamically stable or highly active in physiological conditions, and the use of macrocyclic ligands has been pointed out as a strategy to overcome these limitations. One of the aims of the research group in which this work is integrated has been the synthesis and chemical evaluation of macrocyclic compounds. Some of these presented thermodynamic and structural properties that could anticipate a possible SOD-like activity. As a result of this previous experience, a number of synthetic procedures were already optimized, allowing the synthesis of a battery of nine macrocycles within the course of this thesis.

Copper(II) was chosen as the redox active metal ion, since an application of the compounds in cancer therapy was sought. Due to its capacity to undergo Fenton chemistry, copper has advantages over manganese in boosting anticancer drugs. Moreover, the macrocyclic ligands of this thesis are expected to form Mn(II) complexes with low thermodynamic stability. In fact, the stability constants of CuL6 and CuL8 for Mn(II) were previously reported and are relatively low. As the structures of these ligands do not present a considerable hindrance, the kinetic stability of the complexes is not expected to compensate the low thermodynamic stability. Conversely, the copper(II) complexes are thermodynamically stable, as shown by their stability constants and pCu values.

MnPs and macrocyclic copper(II) complexes cannot be compared straightforwardly, since both the ligands and the metal center of the complexes exhibit very distinct chemical properties. However, pulling together the data on chemical properties and $O_2^{\bullet -}$ scavenging activities of the nine macrocyclic copper(II) complexes studied, some conclusions may be drawn. In fact, although a number of macrocyclic

copper(II) complexes has been previously developed as SODm, few studies have tried to correlate the biological activity with electrochemical or spectroscopic data. Therefore, this thesis aimed to relate this activity with chemical properties, namely thermodynamic stability, structural features and redox potentials.

The characterization of the thermodynamic stability of the complexes is an issue of utmost importance in SODm research. In complexes with low thermodynamic stability, the chelation with copper(II) may not be fulfilled at physiological pH, leading to erroneous conclusions in the evaluation of their SOD-like activity. Furthermore, the release of copper(II) in biological milieus would lead to a loss of activity of the complex and to cytotoxicity due to the indiscriminate redox chemistry by free copper(II). The size of the macrocyclic cavity deeply influences the thermodynamic stability of the complexes. Too small cavities may not properly accommodate copper(II). This was observed for CuL1 and CuL2, precluding the interest of these complexes as SODm compounds. The effect of the introduction of substituents in the macrocyclic backbone was evaluated. Macrocycles with carboxymethyl pendant arms (L2, L4 and L7) were studied, since these substituents provide a flexible arrangement of the donor atoms around the copper(II) ion. However, differential effects were observed in the SOD-like activity of the complexes. Steric hindrance was shown to have profound effects on $O_2^{\bullet-}$ scavenging activity. In fact, the absence of activity of CuL5, CuL7 and CuL9 could be, at least partially, attributed to geometries with steric hindrance that would block the access of $O_2^{\bullet-}$ to the copper(II) center of the complexes.

Taking into account the data on thermodynamic stability, $O_2^{\bullet-}$ scavenging activity and cytotoxicity, CuL3, CuL4 and CuL8 were selected to be evaluated in cell-based assays. The potential of these complexes as antioxidants was studied in the cellular models of oxidative stress validated for MnTM-4-PyP (XXO and TBHP). However, despite of the promising chemical and biochemical properties of the complexes, no relevant antioxidant effects were observed. One hypothesis that may contribute to explain this lack of antioxidant activity is that the intracellular concentration of the complexes may not be sufficient to afford an extra SOD activity to the cell. In addition, it is possible that the catalytic rate of reaction between the complexes and $O_2^{\bullet-}$ is not high enough. If this is the case, $O_2^{\bullet-}$ will react with biological targets instead of being dismutated by the complexes, and oxidative damage still occurs.

Nevertheless, before excluding a potential role for these complexes as antioxidants, they should be evaluated in other oxidative stress models.

The potential role of CuL3, CuL4 and CuL8 in chemotherapy was also evaluated. The three complexes were shown to undergo Fenton chemistry, what can be an advantage to promote cancer cells' death. The studies on the potential effect of the complexes as potential chemotherapy sensitizers were performed in breast cell lines, since it has been reported that breast cancer tissue has higher levels of oxidative stress than normal breast tissue. Furthermore, the overexpression of MnSOD, as well as of Cu,Zn-SOD, was previously shown to suppress the proliferation of breast carcinoma cells. Human mammary MCF7 and MCF10A cell lines, that represent respectively tumor and non-tumor cells, vary in their inherent oxidative stress levels and antioxidant defences, being therefore appropriate models to mimic the *in vivo* situation.

CuL3 and CuL4 were not toxic to MCF7 carcinoma cells, and failed to potentiate the cytotoxicity of Dox. This lack of activity can be related to the intracellular concentration of the complexes or to their catalytic rate, as aforementioned. Other hypothesis is that, although the complexes may be dismutating $O_2^{\bullet-}$ into $H_2O_2$, the increase in $H_2O_2$ concentration is not high enough to overwhelm the detoxification capacities of CAT and GPx enzymes. If this is the case, the $H_2O_2$ concentration will not significantly increase and the threshold of toxicity will not be achieved. Furthermore, if cells can efficiently detoxify $H_2O_2$, no Fenton chemistry is likely to occur.

CuL8 has shown a trend to potentiate Dox cytotoxicity in MCF7 cancer cells, while it exhibited some protection in Dox-treated MCF10A cells. Due to these interesting results, oxaliplatin, other anticancer drug known to generate $O_2^{\bullet-}$, was studied. Again, CuL8 boosted the anticancer properties of oxaliplatin, while it protected non-tumoral cells from the toxicity of this drug. The differential effect of CuL8 in normal and cancer cells is probably related to the differences in the basal ROS and antioxidant defenses of the two cell lines. Chemotherapy regimens commonly use high doses to achieve a substantial reduction in the number of tumor cells, what leads to considerable side effects. Novel strategies to allow an effective treatment without the side effects of high-dose chemotherapy are thus needed. One such strategy is the potentiation of chemotherapy with well tolerated agents that are capable of lowering the threshold for chemotherapy-induced cell death in cancer cells. The results obtained for

CuL8 suggest a potential role of this complex as a chemotherapy sensitizer for breast cancer. By improving the efficacy of a given anticancer drug, CuL8 could eventually allow a reduction of its doses and, therefore, a decrease in the occurrence of side effects. Furthermore, the sensitization of cancer cells by CuL8 can be an advantageous strategy to overcome drug resistance. On the other hand, CuL8 exhibited protective effects in non-tumoral mammary epithelial MCF10A cells, what may be a benefit in the reduction of chemotherapy side effects. These notable results highlight the therapeutic opportunities of copper(II) complexes with SOD-like activity in oncology and support the future evaluation of CuL8 and related compounds in cell-based protocols and/or in animal experiments, towards an application as chemotherapy sensitizers. Chemotherapy will certainly be an area of future research in the SODm field. The rational design of novel compounds for this purpose, targeting specific organs and cellular compartments, is a pertinent issue. In addition, it is crucial to better understand the mechanisms underlying anticancer effects, namely in what concerns to the redox modulation of transcription factors that may be involved.

The understanding the molecular mechanisms related with the effects of SODm is a challenging issue not only in chemotherapy, but also in the broad variety of diseases in which SODm may have clinical applications. One emergent field in oxidative stress research is the unraveling of the signal transduction mechanisms used by $O_2^{\bullet-}$ and other ROS to modify key components of the inflammatory response. This will undoubtedly elucidate on molecular targets that may be modulated by SODm, being crucial to propose and clarify pharmacological interventions using these compounds.

Other area of major interest in SODm research is the rational drug design of optimized SODm compounds. In the case of the copper(II) complexes studied in this thesis, a number of chemical modifications could be endeavored in order to increase the $O_2^{\bullet-}$ scavenging activity of the complexes. These would include changes in the macrocyclic backbone and/or in the substituents to obtain copper(II) complexes with more suitable geometries and redox potentials. In addition, the functionalization of the compounds with positively charged pendant arms would provide electrostatic facilitation to guide the negatively charged $O_2^{\bullet-}$ to the metal center of the complex. Along with the catalytic activity, also the pharmacokinetic properties of the complexes could be improved. The compounds prepared in this thesis are water soluble, which is

advantageous in terms of biopharmaceutical attributes. However, an increase in lipophilicity would enhance cellular uptake, and therefore the biological effectiveness of the complexes. Other interesting strategy that could be tested in future studies is the attachment of lipophilic groups (e.g. triphenylphosphonium cation) to obtain mitochondria-targeted copper(II) complexes. For the generality of the SODm under development, the optimization of structures tailored to meet the needs of a particular disease would be a plus. By adapting a promising core catalyst structure and/or varying functional substituents, it is possible to design a SODm targeting a specific organ or subcellular compartment. This strategy will provide compounds with minimal toxicity and maximal efficacy, more appropriate for pharmaceutical applications.

In summary, the broad array of pathological conditions that are, at least partially, related to oxidative stress has drawn increasing attention to the therapeutic use of antioxidants. Among those, metal macrocyclic complexes with SOD-like activity bring promising perspectives that have not been fully explored yet. The original findings presented herein add important data to the global scenario of the SODm field. Although many questions were raised and dealt along this thesis, additional issues remain unsolved. Even so, SODm compounds have already proven their high therapeutical potential and future research in this field will certainly push it fast towards their clinical use.